TE
662
.A3
no.
FHWA-
RD-
73-91

PB 228 154

ort No. FHWA-RD-73-91

RIFICATION OF FRACTURE MECHANICS CONCEPTS PREDICT CRACKING OF FLEXIBLE PAVEMENTS

K. Majidzadeh, E. M. Kauffmann, and C. W. Chang

DEPARTMENT OF
TRANSPORTATION
FEB 12 1974
LIBRARY

June 1973
Final Report

This document is available to the public through the National Technical Information Service, Springfield, Virginia 22151

Prepared for
FEDERAL HIGHWAY ADMINISTRATION
Offices of Research & Development
Washington, D.C. 20590

NOTICE

This document is disseminated under the sponsorship of the Department of Transportation in the interest of information exchange. The United States Government assumes no liability for its contents or use thereof.

The contents of this report reflect the views of the contracting organization, which is responsible for the facts and the accuracy of the data presented herein. The contents do not necessarily reflect the official views or policy of the Department of Transportation. This report does not constitute a standard, specification, or regulation.

TF
662
.A3
no.
FHWA
RD-
73-91

TECHNICAL REPORT STANDARD TITLE PAGE

1. Report No. FHWA-RD-73-91	2. Government Accession No.	3. Recipient's Catalog No.
4. Title and Subtitle Verification of Fracture Mechanics Concepts to Predict Cracking of Flexible Pavements		5. Report Date June 1973
		6. Performing Organization Code
7. Author(s) K. Majidzadeh, E.M. Kauffmann and C. W. Chang		8. Performing Organization Report No. RF 3200
9. Performing Organization Name and Address Ohio State University Research Foundation Dept. of Civil Engineering Columbus, Ohio 43210		10. Work Unit No. FCP 35C3-051
		11. Contract or Grant No. FH-11-7703
12. Sponsoring Agency Name and Address Offices of Research and Development Federal Highway Administration Department of Transportation Washington, D. C. 20590		13. Type of Report and Period Covered Final
		14. Sponsoring Agency Code SØ 202

15. Supplementary Notes
FHWA Contract Manager: R. A. McComb (HRS-14)

16. Abstract A review of the state of art of application of fracture mechanics concepts to the prediction of fatigue cracking of bituminous mixtures is presented. The basic principles of fracture mechanics and the methods of analysis of cracked plates resting on elastic foundation are discussed. Analytical and experimental methods of determination of stress-intensity factor for two-dimensional and three-dimensional systems using plate bending analysis, finite element and boundary collocation programs are presented.

The experimental works consisting of testing of sand asphalt beams and slabs resting on elastic foundation are presented. The experiments were conducted to verify the applicability of fracture mechanics to estimate the fatigue life of asphaltic mixtures subjected to loads of variable amplitude, pattern, high stress levels, and various temperature conditions.

The experimental results indicate that cracking propagation process of asphaltic mixtures can be predicted using the power law relation between the crack growth rate and the stress-intensity factor.

A framework for the rational method of analysis of pavement fatigue using fracture mechanics principles is presented. Available experimental data on full-scale pavement is used to show the applicability of the concepts developed to analysis in-service pavement structures.

17. Key Words fracture mechanics, crack growth rate, fatigue, stress-intensity factor, random loading, temperature, elastic-plastic, design	18. Distribution Statement No restrictions. This document is available to the public through the National Technical Information Service, Springfield, Virginia 22151.

19. Security Classif. (of this report) Unclassified	20. Security Classif. (of this page) Unclassified	21. No. of Pages 358	22. Price

Form DOT F 1700.7 (8-69)

PREFACE

This is the final report on research project RF 3200, "Verification of Fracture Mechanics Concepts to Predict Cracking of Flexible Pavements," conducted by the Department of Civil Engineering, Materials Division, The Ohio State University Research Foundation. The financial support for this study was provided by the U.S. Department of Transportation under contract no. FH-11-7703.

A number of graduate and undergraduate students plus the staff of the Materials Division have assisted in this investigation. Messrs. C. Bentz, M. Bishara, R. Halprin and S. Gallagher are acknowledged for their help to the study.

Above all, Mr. E. M. Kauffmann has contributed the most to this investigation. This report is comprised of a major part of his doctoral dissertation entitled, "The Application of Fracture Mechanics Concepts to Predict Cracking of Flexible Pavements." Messrs. G. Bokowski and C. W. Chang are also acknowledged for their contribution to the development of computer programs. Special thanks is due to Mrs. Carole Painter for typing the manuscript.

TABLE OF CONTENTS

DEPARTMENT OF TRANSPORTATION
FEB 12 1974
LIBRARY

	Page
ABSTRACT	i
PREFACE	ii
TABLE OF CONTENTS	iii
CHAPTER I. INTRODUCTION	1
CHAPTER II. THE MECHANISTIC APPROACH TO THE SOLUTION OF CRACKING IN PAVEMENTS	5
A. Fracture Mechanics Concepts	5
B. The Mechanistic Approach	12
C. Determination of the Stress-Intensity Factor	16
CHAPTER III. THE INFLUENCE OF LOADING FUNCTIONS ON CRACK PROPAGATION	33
A. Introduction	33
B. Review of State of the Art	34
C. Experimentation of Two-Dimensional Systems	47
(1) Loading Function	47
(2) Method of Analysis	48
(3) Summary of Research Findings	55
D. Experimentation on Slabs Supported on an Elastic Foundation	69
(1) Loading Function	69
(2) Analysis and Discussion of Results	77
(3) Significance of Results	90
CHAPTER IV. THE EFFECT OF TEMPERATURE ON FATIGUE CRACK PROPAGATION	94
A. Introduction	94
B. Verification of the Proposed Model at 77.5°F	96

(Table of Contents Continued) Page

C. Verification of Distress Model at 41° and 90°F 107

(1) Experimentation on Slabs Resting on an Elastic Foundation 107
(2) Analysis and Discussion of Results for Tests at 41°F 111
(3) Analysis and Discussion of Results for Tests at 90°F 116

D. Conclusions 124

CHAPTER V. EFFECT OF HIGH STRESS LEVELS ON FATIGUE CRACK PROPAGATION 126

A. Introduction 126

B. A Review of Mathematical Formulations 127

C. Experimental Procedures for Slabs Resting on An Elastic Foundation 139

D. Analysis and Discussion of Results 140

E. Conclusions 146

CHAPTER VI. APPLICATION OF THE PROPOSED MODEL TO ANALYSIS AND DESIGN OF FLEXIBLE PAVEMENTS 152

A. Introduction 152

B. Verification of the Model for a Pavement Resting on Subgrade Soil 152

C. An Outline of Method of Design 168

(1) Material Characteristics 169
(2) Traffic Loading 175
(3) Analysis and Evaluation 180
(4) Design Example 188

CHAPTER VII. SUMMARY AND CONCLUSIONS 196

BIBLIOGRAPHY 200

(Table of Contents Continued)

		Page
APPENDIX A.	EXPERIMENTAL PROCEDUES	A-1
APPENDIX B.	PRISMATIC FINITE ELEMENT PROGRAM	B-1
APPENDIX C.	RESULTS OF THREE-DIMENSIONAL AND PRISMATIC FINITE ELEMENT PROGRAMS	C-1
APPENDIX D.	DESCRIPTION AND USE OF PROGRAM FOR CALCULATION OF STRESS-INTENSITY FACTORS K_1 and K_2 UNDER MOVING LOAD	D-1
APPENDIX E.	DESCRIPTION AND USE OF THE PROGRAM COLLOCATION WHICH CALCULATES THE STRESS-INTENSITY FACTOR K FOR FINITE CRACKED PAVEMENTS	E-1
APPENDIX F.	FINITE ELEMENT PROGRAM FOR BEAM ON ELASTIC ANALYSIS	F-1
APPENDIX G.	c_o PROGRAM DETERMINATION OF THE STARTER FLAW FROM EXTRAPOLATION OF THE CRACK GROWTH LAW	G-1

CHAPTER I

INTRODUCTION

Pavements are complex structural systems involving many variables such as load combinations, materials, geometric configurations, construction, environment and performance. The rational design of these structures must lead to the prediction of their performance during their service life as well as the prevention of catastrophic failures.

Due to destructive action of traffic and environment, the structural integrity of a pavement is damaged by serveral distress mechanisms developed within the structure and which propagate either independently or interacting to finally produce disintegration, distorion and/or fracture.

The structural damage in flexible pavements appears in two main forms: cracking and permanent deformation (1)*, both of which are due to load repetitions or environmental factors. Damage associated with permanent deformation is believed to be due to shear distortion or volumetric changes. Cracking due to load repetitions occurs primarily as a result of bending deflections and this type of distress is often referred to as fatigue failure (2).

The problem of failures resulting from repeated flexure, i.e., fatigue failures have been under intensive study in the past decades. These studies

---

*Numbers in parentheses refer to the reference numbers at the end of the text.

have led to the development of two independent methods of analysis (3)--the phenomenological and the mechanistic approaches.

The phenomenological approach, credited to Monismith (4, 5, 6), Pell (7, 8) and other (9,10) relates the fatigue life of a flexible pavement, N_f, to the maximum tensile stress, σ, or tensile strain, ε, developed in the underside of the bituminous layer by semi-empirical relations of the form:

$$N_f = c_1 \left(\frac{1}{\sigma}\right)^{m_1} \quad \text{for controlled stress tests,}$$

and

$$N_f = c_2 \left(\frac{1}{\sigma}\right)^{m_2} \quad \text{for controlled strain tests,}$$

where c_1, c_2, m_1, m_2, are constants to be determined experimentally on simply-supported or cantilever beams.

The method was developed as a laboratory investigation that followed field observations and although it is reasonabley simple, it has serious limitations. Firstly, the load and boundary conditions of a simply-supported or cantilever beams are quite different from those of a full-scale pavement. Secondly, the interpretations of the test results is influenced by the mode of loading. Finally, and most important, the method fails to recognize the role played by crack propagation and the consequent redistribution of stresses in the fatigue of pavements.

The mechanistic approach utilizes the principles of fracture mechanics to explain the mechanism of damage and the prediction of the fatigue life of pavements. This method, which was developed at the Ohio State University (11, 12,13, 14, 15, 16), considers fatigue of asphaltic mixtures as a process of

damage where under a given state of stresses damage grows according to a crack propagation law from an initial stage to a critical and final level.

Basically, it has been shown that for three different systems, simply-supported beams, beams on an elastic foundation and slabs resting on an elastic foundation, subjected to repeated loads of constant magnitude, the rate of crack propagation, $\frac{dc}{dN}$, follows the theoretical relation (17, 18,19,20)

$$\frac{dc}{dN} = A\,K^n$$

where $n = 4$, for mixtures reported in this study

K = stress-intensity-factor

A = constant of the material,

and that the critical value of the stress-intensity factor, K_{1c}, a materials constant, is the failure criterion for both fracture and fatigue.

In this method, the prediction of the fatigue life of pavements from laboratory tests is independent of mode of loading or specimen geometry. Failure by cracking is defined in terms of the stress-intensity factor and catastrophic failure by the critical stress-intensity factor.

The research work at Ohio State University, which has led to the proposal of a method of analysis and design of multi-layered pavement systems (15,16), was basically done for repeated loads of constant amptitude and at room temperature. It is the purpose of this report, however, to investigate the applicability of fracture mechanics concepts to explain the fatigue behavior of flexible pavements subjected to loads of variable amptitude, high stress levels that produce

permanent deformation, and temperatures different than room temperature.

The specific objectives of this study can be summarized as:

(i) review of literature

(ii) development of mathematical relations for;

(a) crack problems in bonded slabs
(b) crack propagation problem when accompanied with permanent deformation
(c) crack propagation at different temperatures

(iii) experimental verification of developed concepts,

(iv) development of design guidelines and recommendations for prediction of pavement cracking.

CHAPTER II

THE MECHANISTIC APPROACH TO THE SOLUTION OF CRACKING IN PAVEMENTS

A. Fracture Mechanics Concepts

The pheomeonon of fatigue tackled from a fracture mechanics viewpoint is associated with the concept of damage or those internal changes in the material that lead to formation of macroscopic cracks. The fatigue life is defined as the time period during which damage, i.e., cracking in a material body subjected to a given state of stresses, grows from an initial level, to a critical and final level. So, the occurrence of fatigue failure is a result of two separate processes; damage initiation and damage growth.

In paving mixtures the initial state of damage can be represented by those surface and internal flaws and microcracks which vary statistically within the material. The final state can be described by one or a number of cracks of critical dimensions and patterns. However, knowledge of the initial and final states are not sufficient for determining the fatigue life. It is essential that the law governing the damage growth is known in terms of the material properties, stress level and boundary conditions.

The processes of crack initiation and growth differ among various materials. In materials that have inherent flaws such as polymers, certain alloys and bituminous mixtures, the fatigue cracks initiate at the first few cycles of load applications (21). The inhomogeneities and flaws, which serve as stress

concentrators, vary statistically in size and distribution and this can, in fact, account for statistical variation in the fatigue life.

The mechanism of the fatigue crack growth can be explained in terms of the energy balance at the tip of the discontinuities. The work of external forces at the crack tip is divided into stored elastic energy, surface energy required to form cracks, and deformation energy required for irreversible changes in the material body as plastic and viscous flow.

During a cyclic deformation, a crack will undergo a phenomenon of blunting and resharpening, resulting in crack growth through the body. In tensile loading cycles, the crack tip tends to open first and then becomes blunted as the plastic zone forms ahead of the crack tip. During the unloading cycle, the elastic contraction of the material surrounding the crack imposes residual compressive stress on the plastically deformed material at the crack tip. This reduces ductility and resharpens the crack which aids the growth in the next loading cycle. This process leads to slow crack growth until the crack reaches a critical size, and the induced state of stress results in structural instability of the terminal event of fracture.

The fundamentals of fracture mechanics were developed from Griffith's classical theory of brittle fracture. Irwin and Kies extended Griffith's theory for the fracture-strength analysis for materials having substantial amounts of plastic strain, as long as fracture occurred in advance of yielding. Most of

the development of fracture mechanics is due to Irwin who invented the concept of the stress-intensity factor, to define the stress field near a crack tip.

All linear elastic solutions to problems involving cracks in homogeneous isotropic materials shown an inverse square root dependency of the crack tip stress singularity (22). The stress distribution of the end of a crack has been shown by Irwin to take the form:

$$\sigma_{ij} = r^{-\frac{1}{2}} \left[K_{I} f_{ij}^{I}(\theta) + K_{II} f_{ij}^{II}(\theta) + K_{III} f_{ij}^{III}(\theta) \right]$$
$$+ \text{ other terms nonsingular at the crack tip} \qquad (2.1)$$

where r and θ are polar coordinates introduced at the crack tip (Figure 2.1). The symbols I, II, III, pertain to three distinct modes according to whether the resulting displacements at the crack tip contribute to opening (Mode I), in-plane sliding (Mode II), or tearing (Mode III), or modes of relative displacement of the crack surfaces (Figure 2.1). The dimensionless functions f_{ij}^{I}, f_{ij}^{II}, and f_{ij}^{III} depend on the orientation of the angle θ only, and K_{I}, K_{II}, and K_{III} are the stress-intensity factors related to the three modes of crack tip deformation.

Hence, the elastic stress field surrounding the tip of a crack, where the crack plane is a plane of symmetry, and for small scale yielding, can be expressed as follows:

For Mode I:

$$\begin{Bmatrix} \sigma_x \\ \sigma_y \\ \tau_{xy} \end{Bmatrix} = K_{I} (2\pi r)^{-\frac{1}{2}} \cos\frac{\theta}{2} \begin{Bmatrix} 1 - \sin\frac{\theta}{2} \quad \sin\frac{3\theta}{2} \\ 1 + \sin\frac{\theta}{2} \quad \sin\frac{3\theta}{2} \\ \sin\frac{\theta}{2} \quad \cos\frac{3\theta}{2} \end{Bmatrix} \qquad (2.2)$$

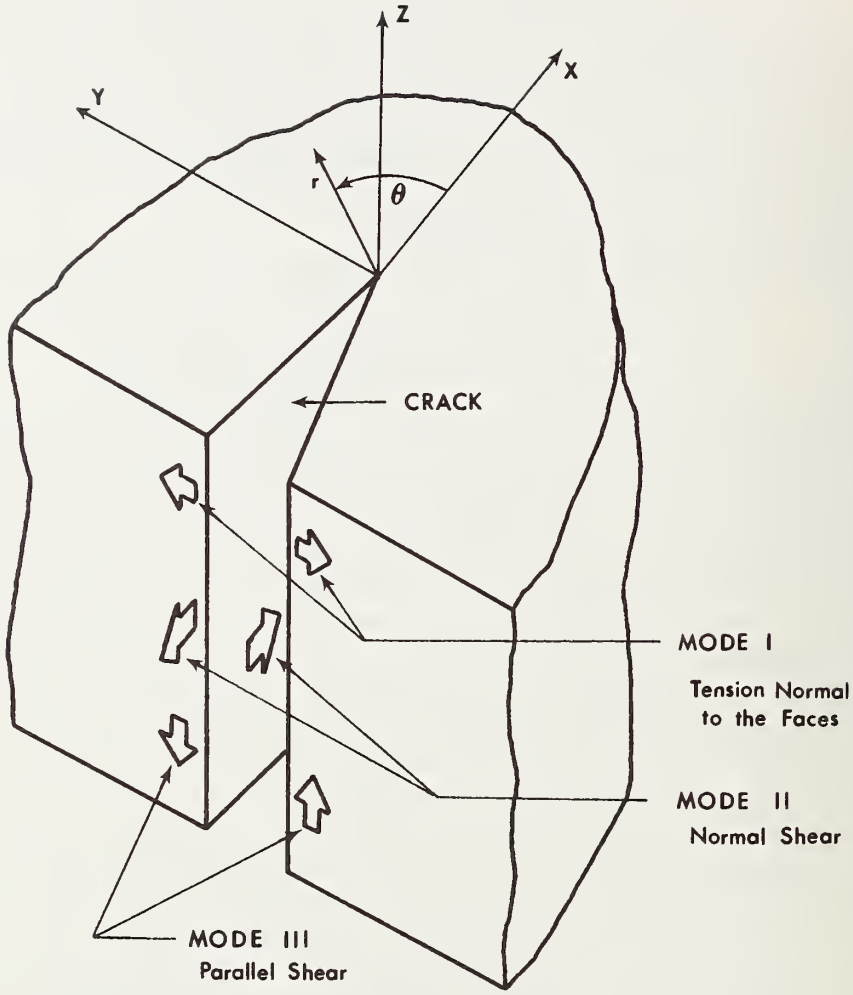

Figure 2.1. Modes of Deformation of a Crack

For Mode II fracture, the elastic stress field at the crack tip can be written as:

$$\begin{Bmatrix} \sigma_{xx} \\ \sigma_{yy} \\ \tau_{xy} \end{Bmatrix} = K_2 (2\pi r)^{-\frac{1}{2}} \begin{Bmatrix} -\sin\frac{\theta}{2} \quad (2 + \cos\frac{\theta}{2} \cos\frac{3\theta}{2}) \\ \sin\frac{\theta}{2} \cos\frac{\theta}{2} \quad \cos\frac{3\theta}{2} \\ \cos\frac{\theta}{2} \ (1 - \sin\frac{\theta}{2} \sin\frac{3\theta}{2}) \end{Bmatrix} \tag{2.3}$$

The stress-intensity-factor, K, has also been shown to be related to the strain energy release rate, G, which was introduced by Griffith, according to the following equations:

$$\begin{aligned} K^2 &= \frac{G\,E}{(1 - \mu^2)} \qquad \text{for plane strain} \\ K^2 &= G\,E \qquad \text{for plane stress} \end{aligned} \tag{2.4}$$

where E is the Young modulus, μ the Poisson's ratio and $G = \frac{\delta W}{\delta c}$, the strain energy release rate, which may also be considered as the crack extension force. Therefore, K is a very important parameter since it not only defines the stress field at the vicinity of the crack tip in accordance with load, geometry and boundary conditions, but is also proportional to the force that causes crack growth. And when the crack reaches a critical size, at the onset of rapid growth, the critical value of K, designated as the critical stress-intensity factor, K_c was found to be a materials property.

It should be noted that the use of Mode I fracture concept is applicable only when the crack propagation direction remains perpendicular to the direction

of the principle stress responsible for the crack opening. It has been shown that for mixtures with large size aggregate, when tested as a beam on elastic foundation, the crack surface follows a zig-zag pattern and as a result, the stress component σ_{yy} responsible for the crack growth would no longer remain perpendicular to the crack surface.

Under such conditions, the stress state ahead of the crack will be governed by two stress-intensity factors (K_I and K_{II}) instead of a simple parameter K. The elastic stress distribution at the crack tip can be written as:

$$\sigma_{xx} = \frac{K_1}{\sqrt{2r}} \cos\frac{\theta}{2} \left(1 - \sin\frac{\theta}{2} \sin\frac{3\theta}{2}\right) - \frac{K_2}{\sqrt{2r}} \sin\frac{\theta}{2} \left(2 + \cos\frac{\theta}{2} \cos\frac{3\theta}{2}\right)$$

$$\sigma_{yy} = \frac{K_1}{\sqrt{2r}} \cos\frac{\theta}{2} \left(1 + \sin\frac{\theta}{2} \sin\frac{3\theta}{2}\right) + \frac{K_2}{\sqrt{2r}} \sin\frac{\theta}{2} \cos\frac{\theta}{2} \cos\frac{3\theta}{2} \tag{2.5}$$

$$\tau_{xy} = \frac{K_1}{\sqrt{2r}} \cos\frac{\theta}{2} \sin\frac{\theta}{2} \cos\frac{3\theta}{2} + \frac{K_2}{\sqrt{2r}} \cos\frac{\theta}{2} \left(1 - \sin\frac{\theta}{2} \sin\frac{3\theta}{2}\right)$$

where $K_1 = \sqrt{\pi}\, K_I$, $K_2 = \sqrt{\pi}\, K_{II}$.

Under such a state of stress, the failure condition can be evaluated using the energy concept. Considering that strain energy of the system in the crack vicinity, ϕ, can be expressed in terms of stresses, for an element $r \triangle \theta$, $\triangle r$ ahead of the crack tip the strain energy function is:

$$\frac{d\phi}{dA} = \frac{1+\mu}{2E} \left[\sigma_{xx}^2 + \sigma_{yy}^2 - \mu (\sigma_{xx} + \sigma_{yy})^2 + 2\tau_{xy}^2 \right] \tag{2.6}$$

then by inserting the stress components from the previous equation (2.5)

$$\frac{d\phi}{dA} = \frac{1}{r} \left[A_{11} K_1^2 + A_{22} K_2^2 + 2 A_{12} K_1 K_2 \right] \tag{2.7}$$

where the term in the bracket is defined as strain energy density factor S,

$$S = A_{11} K_1^2 + A_{22} K_2^2 + 2 A_{12} K_1 K_2 \tag{2.8}$$

A_{11}, A_{22} and A_{12} are constants related to the elastic parameters and element direction as given by

$$\begin{aligned} A_{11} &= \frac{1+\mu}{8E} \left[(3 - 4\mu - \cos\theta)(1 + \cos\theta) \right] \\ A_{12} &= \frac{1+\mu}{4E} \sin\theta \left[\cos\theta - (1 - 2\mu) \right] \\ A_{22} &= \frac{1+\mu}{8E} \left[4(1-\mu)(1-\cos\theta) + (1+\cos\theta)(\cos 3\theta - 1) \right] \end{aligned} \tag{2.9}$$

For the condition that all three modes of fracture are present, S is written as

$$S = A_{11} K_1^2 + A_{22} K_2^2 + A_{33} K_3^2 + 2 A_{12} K_1 K_2 \tag{2.10}$$

where $A_{33} = \frac{1}{4G}$.

If the loading condition and crack propagation is such that mode 1 analysis applies, then

$$S = \frac{1 - 2\mu}{4\pi G} K_1$$

or

$$S = \frac{(1+\mu)(1-2\mu)}{2\pi E} K_1 \tag{2.11}$$

When unstable crack extension or failure occurs, the parameter S approaches its critical value given by S_c,

$$S_c = \frac{(1+\mu)(1-2\mu)}{2\pi E} K_{1c} \tag{2.12}$$

where in this case S_c is a material constant.

It should be pointed out that recent observation on the crack propagation of sand asphalt beams on elastic foundation have shown that the mode 1 fracture analysis

is applicable. On the other hand, for mixtures with large aggregate size, the analysis must incorporate the effect of mode II fracture. For the crack problem related to bending of slabs on elastic foundation, the mode II fracture has been considered when applicable.

B. The Mechanistic Approach

In the mechanistic approach, the fatigue phenomena in pavement materials is presented as a process of damage. It postulates that the fatigue life, N_f, of asphaltic mixtures can be described by three processes; damage initiation, growth and final failure, or it can be represented by the following parametric equation:

$$N_f = F \left[c_o, (A, n, \triangle K), K_c \right] \tag{2.13}$$

The parameter c_o is associated with the process of crack initiation, and may be considered as the "starter flaw" from which the crack will propagate. This parameter cannot be measured directly and should be determined experimentally. It is believed to be principally responsible for the statistical variation in the service life of a mixture.

The second parameter set (A, n, K) expresses the process of crack growth in the material system accordingly. The application of the concept of stress-intensity-factor to study the rate of growth of fatigue cracks was first introduced by Paris, Gomes and Anderson (17). Later Paris and Erdogan (19) found from experimental data that the rate of crack propagation, $\frac{dc}{dN}$, was

proportional to the fourth power of K for a number of materials. This law, known as Paris' law, is expressed as:

$$\frac{dc}{dN} = A\,(\triangle K)^n \tag{2.14}$$

where A is a constant and n = 4 for sand asphalt mixtures.

This fourth power law has also been justified in terms of energy absorption within the plastic zone ahead of the tip of the crack (20), and also Rice (23) derived Paris' expression using a rigid plastic model, which assumes that the plastic deformation is limited to a strip of material ahead of the crack tip.

The terminal event of fracture, when the internal flaws have reached a critical size, c_f, is represented by the critical stress-intensity factor, K_c.

Utilizing the crack growth law presented in equation (2.14) and considering the process explained, the fatigue life can be expressed as:

$$N_f = \int_{c_o}^{c_f} \frac{1}{A \triangle K^n}\, dc \tag{2.15}$$

in which it is assumed that the crack growth law is applicable from the first loading cycle, and continues until failure occurs by brittle fracture at a critical crack, c_f. In order to predict the fatigue life then, it is necessary to determine the crack growth parameters, A, n, $\triangle K$ and c_o.

The applicability of the mechanistic approach involves two important assumptions made in the theoretical concepts. First, the material has to be homogeneous, isotropic and essentially elastic-plastic, and secondly, the size

of the plastic zone at the tip of the crack must be small in comparison to the crack size and specimen dimensions.

The first assumption is generally accepted for asphaltic materials provided that the rate of loading is large and the temperature is not very high.

With respect to the second assumption, Strawley and Roberts (24) established criteria for the crack length, width and depth of the beam to ensure plane strain conditions and the applicability of linear elastic fracture mechanics. Using the estimate of the size of the plastic zone, w, given by the general formula

For Plane Strain:

$$w_y = \frac{1}{2\pi\sigma_y^2} \left\{ K_1^2 \cos^2\frac{\theta}{2} \left[(1-2\mu)^2 + 3\sin^2\frac{\theta}{2}\right] + K_1 K_2 \sin\theta \right. \tag{2.16}$$

$$\left. \left[3\cos\theta - (1-2\mu)\right] + K_2^2 \left[3 + \sin\frac{\theta}{2}\,(1-2\mu) - 9\cos\frac{\theta}{2}\right] + 3K_3^2 \right\}$$

For Plane Stress:

$$w_y = \frac{1}{2\pi\sigma_y^2} \left\{ K_1^2 \cos^2\frac{\theta}{2}\,(1 + 3\sin^2\frac{\theta}{2}) + K_1 K_2 \sin\theta\,(3\cos\theta - 1) \right.$$

$$\left. + K_2^2 \left[3 + \sin^2\frac{\theta}{2}\,(1 - 9\cos\frac{\theta}{2})\right] \right\} \tag{2.17}$$

For a two-dimensional problem where the effect of mode III fracture is neglected and the $\theta = 0$, the following is obtained

For Plane Strain:

$$w_y = \frac{1}{2\pi\sigma_y^2} \left[K_1^2\,(1-2\mu) + 3\,(K_2^2 + K_3^2)\right] \tag{2.18}$$

For Plane Stress:

$$w_y = \frac{1}{2\pi\sigma_y^2} \left[K_1^2 + 3\,K_2^2 \right] \tag{2.19}$$

For mode 1, these fracture equations are reduced to

For Plane Strain:

$$w_y = \frac{(1 - 2\mu)^2}{2\pi} \left(\frac{K_1}{\sigma_y} \right)^2 \tag{2.20}$$

For Plane Stress:

$$w_y = \frac{1}{2\pi} \left(\frac{K_1}{\sigma_y} \right)^2 \tag{2.21}$$

where σ_y is the yield stress in tension. In the fracture toughness evaluation of beam specimens, it has been shown that crack length and the thickness of test specimens must be equal or greater than $2.5 \left(\frac{K_1}{\sigma_y} \right)^2$.

With respect to the effect of plastic zone on the stress intensity factor, Irwin has presented a semi-empirical adjustment to the elastic stress intensity factor. It is assumed that the effective crack length is increased by an amount comparable to the size of the plastic zone.

The modified elastic stress intensity factor can be written as:

$$K_{modified} = \frac{K_{elastic}}{\left[1 - \frac{1}{2} \left(\frac{\sigma_{yy}}{\sigma_y} \right)^2 \right]^{\frac{1}{2}}} \tag{2.22}$$

where σ_{yy} is applied tensile stress and σ_y is yield stress for the material. The analysis by Hilton and Hutchinson (25) has indicated that at an applied

tensile stress level of half the yield stress, the elastic-plastic boundary is already exceeding 40% of the crack length. Even with such a limitation, the elastic fracture mechanics gives a rather accurate prediction of crack initiation.

C. Determination of the Stress-Intensity Factor

Throughout the available literature on fracture mechanics, one finds various analytical methods that have been developed to determine the stress-intensity-factor, K, for a given geometric configuration, crack size and boundary condition. In this section, a brief review of the methods available to determine K for various test configurations is presented.

The K value for a simply-supported beam with a central load can be determined experimentally from tests using Winne and Wundt's equation (26)

$$K_1^2 = \sigma_n^2 (1 - \nu^2) h \; f(c/d) \tag{2.23}$$

where σ_n = nominal bending stress at the root of the notch = $\frac{6M}{b(d-c)^2}$

M = bending moment = $\frac{Pl}{4}$

ν = Poisson's ratio

P = Load

l = Span

b = Width of the beam

c = Crack depth

$f(c/d)$ = a function of the geometry given in reference (26)

Experimentally, the stress-intensity factor, K, for any type of loading configuration, crack pattern and geometry can be determined by a very simple procedure. This is done by measuring the change in deflection as the cracks grow and applying the formula,

$$K^2 = \frac{P^2 E}{2 (1 - \nu^2)} \quad \frac{\delta L}{\delta c} \tag{2.24}$$

where P = load

E = Young's modulus

ν = Poisson's ratio

L = compliance, or th inverse slope in the load/deflection diagram

c = crack length.

Similarly, K, can be determined from Strawley's (27) approach in which the square of dimensionless stress-intensity factor, Y^2, is determined in terms of c/d ratio using the boundary collocation method:

$$Y^2 = \frac{K^2 d^3 b^2}{M^2} = \frac{16 K^2 d^3 b^2}{P^2 l^2} \tag{2.25}$$

The results of this analysis are presented graphically in Figure 2.2. Finite element method has been used to develop a similar non-dimensionalized relation between the stress-intensity-factor, K, load and beam geometries.

The stress-intensity factor, K-value, for a beam on an elastic foundation with a central load was obtained by Ramsamooj (14), using the boundary collocation method. Similarly, a finite element program has been developed to calculate K for any crack size, and it is presented in reference (15).

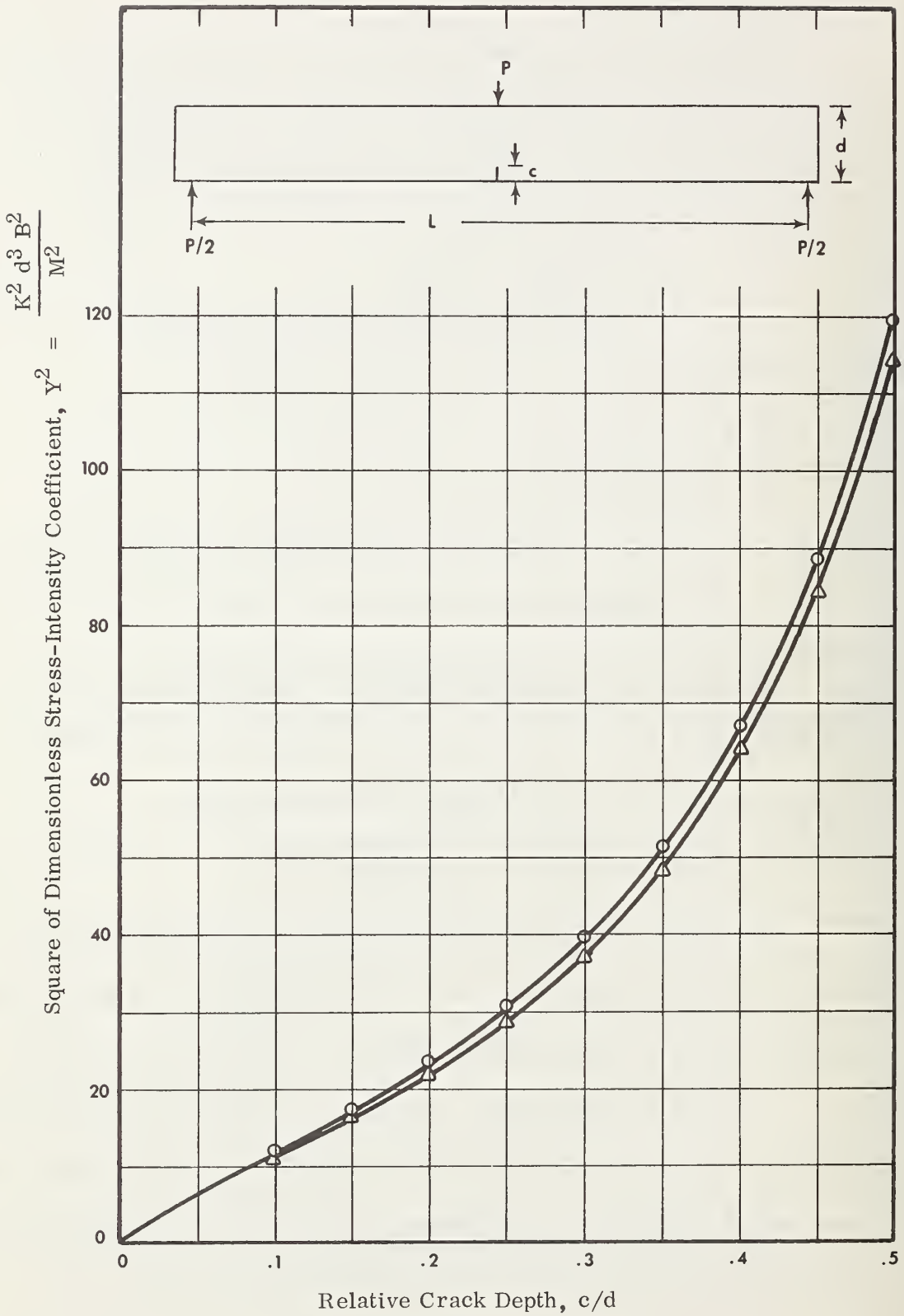

Figure 2.2. Dimensionless Stress-Intensity Factor for a Simply-Supported Beam

The stresses in a slab with a semi-infinite crack resting on an elastic foundation are obtained using the solution developed by Williams, Ang and Folias (28). Ramsamooj (14) obtained a solution for the K-values under a moving load. The computer program that performs such calculations was recently revised by Bokowski (39) and in its new version is presented in Appendix D.

The revised computer program incorporates the improvements made on the development of mathematical expressions for moment function and stresses at the bottom and top surfaces of the slab. As has been shown in references (14,15), the deflection $w(r)$, bending moment $M_y(x,o)$ and equivalent shear $V_y(x,o)$, for a slab supported on an elastic foundation of modulus, k, loaded by a uniform distributed load of radius a, are:

$$w(r) = \frac{P}{\pi k a} \int_0^{\infty} \frac{J_1(ma)\, J_o(mr)}{1 + m^4 l^4} \, dm \tag{2.26}$$

$$M_y(x,o) = -D \left(\frac{\partial^2 w}{\partial y^2} + \nu \frac{\partial^2 w}{\partial x^2} \right), \quad y = 0 \tag{2.27}$$

$$V_y(x,o) = -D \left(\frac{\partial^3 w}{\partial y^3} + (2-\nu) \frac{\partial^3 w}{\partial x^2 \partial y} \right), \quad y = 0 \tag{2.28}$$

where $x - x = r \cos\theta$; $y - y = r \sin\theta$, as shown in Figure

Equations (2.26) and (2.27) give the moment $M_y(x,o)$ and shear $V_y(x,o)$ along the crack surface as the load moves in a longitudinal direction from -00 to +00. To improve the results of the analysis, the following improvement

has been recently recommended (30). The moment function can be expanded in an even Fourier expansion given by:

$$M_y(x,o) = -D \left\{ \frac{m_o}{2} + \sum_{n=1} \left[\frac{m_n}{2} e^{\frac{in\pi x}{p}} + \frac{m_{-n}}{2} e^{\frac{-in\pi x}{p}} \right] \right\} \quad (2.29)$$

The stresses at the top and bottom surfaces of the slab are given in reference (15) as:

$$\sigma_{xx} = \frac{-\Gamma(3/2)\, Eh\, \nu_o(1+i)\, \lambda^2 P_o}{2i(1+\nu)\quad \lambda r} \left[2\left(\cos\frac{\phi}{2} + \sin\frac{\phi}{2}\right) - \cos\phi \left(\cos\frac{3\phi}{2} + \sin\frac{3\phi}{2}\right) \right] \quad (2.30)$$

$$\pm \frac{\Gamma(3/2)\, Eh(1-i)\, \lambda^2 Q_o}{2i(1+\nu)\quad \lambda r} \left[4(2-\nu_o)\left(\cos\frac{\phi}{2} - \sin\frac{\phi}{2}\right) + \nu_o \cos\phi \left(\cos\frac{3\phi}{2} - \sin\frac{3\phi}{2}\right) \right] + \ldots\ldots$$

$$\sigma_{yy} = \frac{\Gamma(3/2)\, Eh(1+i)\, \lambda^2 P_o}{2i(1+\nu)\quad \lambda r} \left[2(4-\nu_o)\left(\cos\frac{\phi}{2} + \sin\frac{\phi}{2}\right) - \nu_o \cos\phi \left(\cos\frac{3\phi}{2} + \sin\frac{3\phi}{2}\right) \right. \quad (2.31)$$

$$\mp \frac{\Gamma(3/2)\, Eh(1-i)\, \nu_o\, \lambda^2 Q_o}{i(1+\nu)\sqrt{\lambda r}} \left[\cos\phi \left(\cos\frac{3\phi}{2} - \sin\frac{3\phi}{2}\right) \right] + \ldots\ldots$$

where E = Young's modulus

ν = Poisson's ratio

$\nu_o = 1 - \nu$

$$\lambda = \sqrt[4]{\frac{K}{D}}$$

K = modulus of subgrade reaction

$$D = \frac{E\,h^3}{12\,(1 - \nu^2)}$$

h = thickness of the slab

$$\phi = 90 - \theta$$

and according to Ramsamooj (30), P_o and Q_o are given by:

$$P_o = \sum_{n=-\infty}^{\infty} \left\{ \left[- \frac{\frac{m_n}{2}}{2\,\pi\,(4 - \nu_o)\,\nu_o\,\lambda^{3/2}} \frac{1}{\sqrt{\frac{n\pi}{p}}} (1 + i) \right] + \left[- \frac{\left(\frac{(4-\nu_o)\,\nu_o}{\sqrt{2}}\right)^{\frac{1}{2}}}{2\,\pi\,(4-\nu_o)\nu_o\,\lambda^2} \sqrt{2}\,\frac{m_n}{2}\,(1 + i) \right] \right\} \tag{2.32}$$

and

$$Q_o = \sum_{n=-\infty}^{\infty} \left\{ \left[- \frac{\frac{m_n}{2}}{2\,\pi\,(4-\nu_o)\,\nu_o\,\lambda^{3/2} \left(\frac{n\pi}{p}\right)^{3/2}} (1 - i) \right] + \left[- \frac{\left(\frac{(4-\nu_o)\,\nu_o}{\sqrt{2}}\right)^{\frac{1}{2}}}{2\,\pi\,(4-\nu_o)\,\nu_o\,\lambda^3} \sqrt{2}\sqrt{\frac{n}{2}}\,(1 - i) \right] \right\} \tag{2.33}$$

when $\frac{n\pi}{p\lambda} > 1$ only the first terms of P_o and Q_o are applicable, and when $\frac{n\pi}{p\lambda} < 1$ only the second terms are applicable.

The stress-intensity factors, K_{1B} and K_{2B} for the bending of the slab, may be determined from the relationship:

$$\sigma_{xx} + \sigma_{yy} = \sqrt{2}\,\frac{(1+\nu)}{(3+\nu)} \left[\frac{K_{1B}}{\sqrt{\pi r}} \cos\frac{\theta}{2} - \frac{K_{2B}}{\sqrt{\pi r}} \sin\frac{\theta}{2} \right], \quad (z = h/2) \tag{2.34}$$

Therefore:

$$K_1 = \pi \; Eh \frac{(3+\nu)}{(1+\nu)} \; \lambda^{3/2} \; (1-i) \; P_o$$

$$K_2 = \pi \; Eh \frac{(3+\nu)}{(1+\nu)} \; \lambda^{3/2} \; (1+i) \; Q_o \qquad (2.35)$$

It should be noted that these analyses are concerned with the determination of stress-intensity factor for a semi-infinite crack. However, the result of previous research (15) has indicated that during fatigue experiments, usually four radial cracks of equal length are developed. In the analysis of crack propagation presented by Ramsamooj (14), it was assumed that the crack tip stress fields are independent. It has also been considered that the stress field of each crack is confined to a zone of radius much smaller than the crack itself. With more generality, it has been stated that the crack tip stress fields are independent providing the cracks are at least one radian apart. Westmann (31) has presented an analytical approach for calculation of stress-intensity-factor as affected by multiple equi-length cracks.

In Westmann's analysis, it is assumed that the elastic plate contains n-line cracks of length c radiating from a common point and having angles of $\frac{2\pi}{n}$ between adjacent crack flanks. The crack faces are taken to be shear free, and it is assumed that the stress field vanishes at large distances from the crack. Utilizing Mellin's transform and its inversion formula, integral expressions for the stress and displacement fields, satisfying the condition of symmetry and

shear free boundaries, are obtained. The crack tip stress intensity factor in terms of numbers of cracks is given by:

$$K(n) = \frac{2\,\Gamma(3/4)\;G(n)}{n^{\frac{1}{2}}\;\Gamma(1+n^{-1})\;\;\Gamma(1-n^{-1})\;\;\Gamma(\frac{1}{2})} \tag{2.36}$$

where G(n) is an expression related to n and integration variables.

The numerical evaluation of the crack tip stress-intensity factors for various numbers of equi-length cracks is shown in Figure (2.3). For large values of n, an asymptotic expansion of K(n) function leads to the following approximation:

$$K(n) \approx \sqrt{\frac{2}{n}} \qquad n \longrightarrow \infty \tag{2.37}$$

For the number of cracks exceeding six, this asymptotic expansion compares very accurately with the values calculated numerically. It is noted that using Irwin's correction factor for n = 4, K(n) = 0.71; whereas Westmann's exact solution provides a correction factor of K(n) = 0.62 for four radial cracks of equal length and angle.

As was pointed out previously, finite element method can also be used for determination of stress and displacement fields and the stress-intensity factor. The results of analysis using a two-dimensional method have been shown before to compare rather accurately with the stress-intensity factors determined by boundary collocation and experimental approach. In this study, an attempt was made to utilize a three-dimensional program to determine the

Figure 2.3. Variation of Stress-Intensity Factor with the Number of Radial Cracks

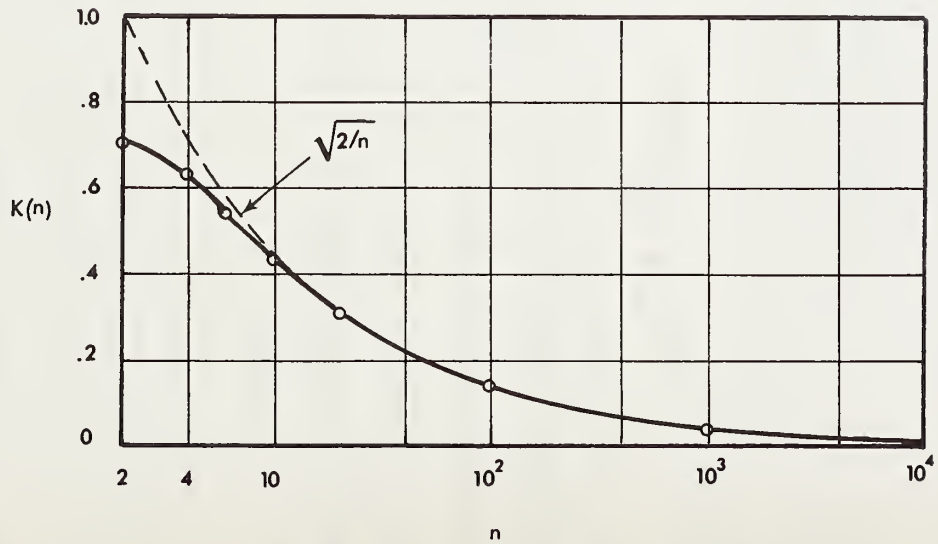

stress and displacement fields in a layered pavement system. A comparison of the stress distribution within a hypothetical pavement using this program and the multi-layered elastic analysis (chevron) have been presented in the Appendix C. Considering the accuracy of results and the operational cost, the use of such a program at this time cannot be fully justified.

However, for the analysis of reflection cracking and the study of upward crack propagation observed directly under the loaded area, a prismatic finite element program has been found to be of great value. This method of analysis has been developed with consideration that in many physical problems, the geometry and material properties do not vary along one of the coordinate directions; whereas, the induced loads exhibit a variation in that direction. In such cases the use of simplified assumptions and a two-dimensional treatment of the problem is prohibited. Therefore, it is possible to consider a "substitute" problem, not involving the particular coordinate (along which the properties do not vary), and to synthesize the true answer from a series of such simplified solutions.

As an example, consider a prismatic space illustrated in Figure 2.4 Let x, y, z be the coordinates describing the domain, while z is the coordinate along which the geometry and material properties do not change. The external load can be expressed as Fourier series with a period length 2L in z direction given by:

$$\left\{P\right\} = \sum_{n=0}^{\infty} \left\{An\right\} \cos \frac{n\pi z}{L} \tag{2.38}$$

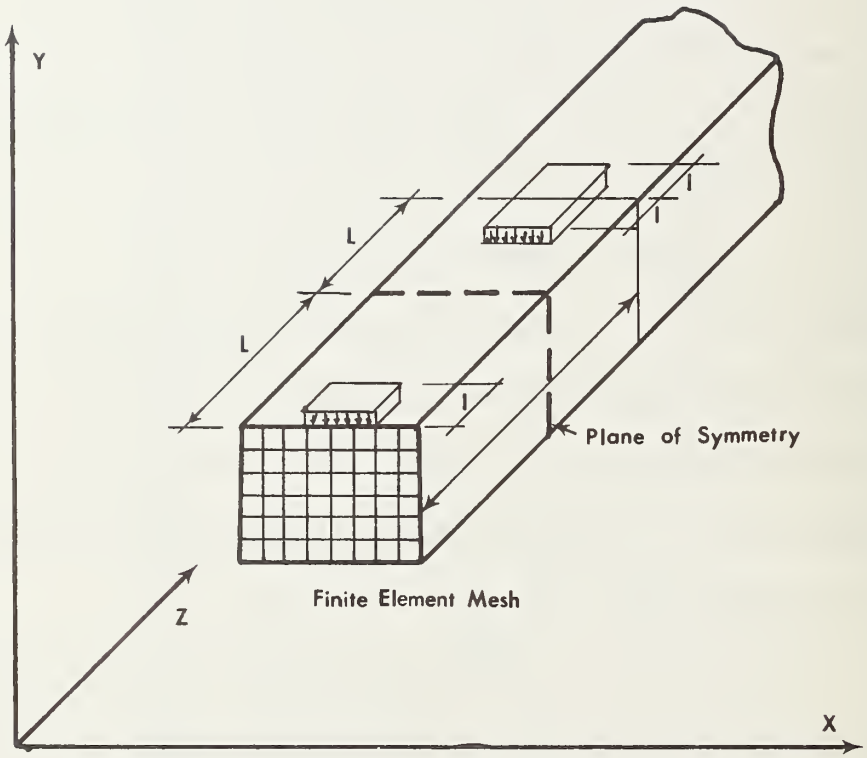

Figure 2.4. A Schematic View of Prismatic Finite Element Model

The analysis is carried out for every Fourier term necessary for adequate representation of the load. Because of symmetry, it can be assumed that the displacements u–in x direction and v–in y direction, have their maximum values and the displacement w–in z direction is equal to zero at planes $z = 0$ and $z = 2L$. It can be further assumed that the x- and y-displacements vary co-sinusoidally and the z-displacement varies sinusoidally. Therefore the displacements or stresses at any desired z-position can be obtained as functions of those components in x-y plane. For analysis purposes, a three-dimensional problem is reduced to a two-dimensional with reduction in computational efforts. The prismatic finite element method used in this study utilizes a displacement method of analysis. To calculate displacements at interior points, consider a triangular prismatic element defined by a set of three nodal points shown in Figure 2.5.

Assuming three degrees of displacement freedom at each nodal point, the displacement vector for any interior point of this element can be written as:

$$\begin{Bmatrix} u \\ v \\ w \end{Bmatrix} = \begin{bmatrix} \xi_1 \cos\frac{n\pi z}{L} & 0 & 0 & \xi_2 \cos\frac{n\pi z}{L} & 0 & 0 & \xi_3 \cos\frac{n\pi z}{L} & 0 & 0 \\ 0 & \xi_1 \cos\frac{n\pi z}{L} & 0 & 0 & \xi_2 \cos\frac{n\pi z}{L} & 0 & 0 & \xi_3 \cos\frac{n\pi z}{L} & 0 \\ 0 & 0 & \xi_1 \sin\frac{n\pi z}{L} & 0 & 0 & \xi_2 \sin\frac{n\pi z}{L} & 0 & 0 & \xi_3 \sin\frac{n\pi z}{L} \end{bmatrix} \begin{Bmatrix} \bar{u} \\ \bar{v} \\ \bar{w} \end{Bmatrix} \tag{2.39}$$

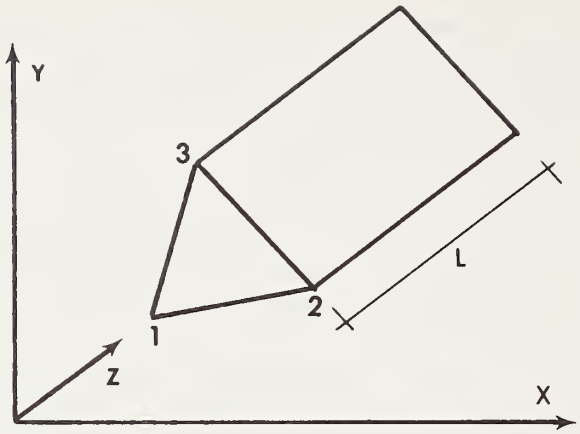

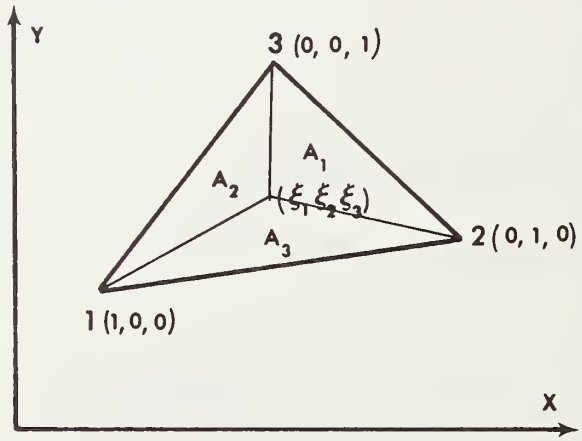

$$\xi_i = \frac{A_i}{A}$$

$$\Sigma\, \xi_i = 1$$

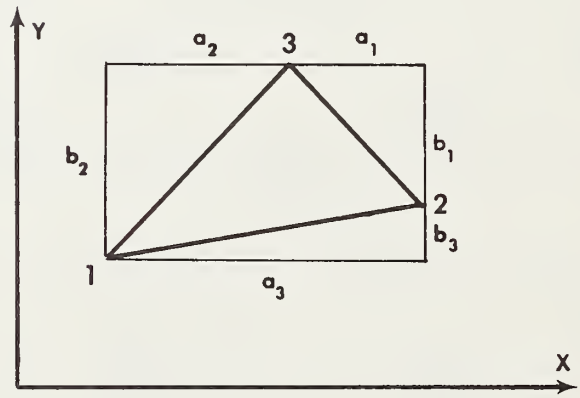

Figure 2.5. Triangular Prismatic Elements and Nodal Points

where $\bar{u}$, $\bar{v}$, $\bar{w}$ are the displacement vectors for nodal points 1, 2, 3 and ξ_1, ξ_2, ξ_3 are the triangular coordintes of this point at x-y plane.

Next, assuming infinitesimal strain state, the strain field in a cartesian system of coordinates is given by:

$$\begin{Bmatrix} \epsilon_x \\ \epsilon_y \\ \gamma_{xy} \\ \epsilon_z \\ \gamma_{yz} \\ \gamma_{zx} \end{Bmatrix} = \begin{Bmatrix} \frac{\partial u}{\partial x} \\ \frac{\partial v}{\partial y} \\ \frac{\partial u}{\partial y} + \frac{\partial v}{\partial x} \\ \frac{\partial w}{\partial z} \\ \frac{\partial v}{\partial z} + \frac{\partial w}{\partial y} \\ \frac{\partial u}{\partial z} + \frac{\partial w}{\partial x} \end{Bmatrix} = \frac{1}{2A} \begin{bmatrix} U_1 & U_2 & U_3 \\ V_1 & V_2 & V_3 \end{bmatrix} \begin{Bmatrix} \bar{u} \\ \bar{v} \\ \bar{w} \end{Bmatrix} \tag{2.40}$$

where

$$\begin{bmatrix} U_i \end{bmatrix} = \begin{bmatrix} b_i \cos\frac{n\pi z}{L} & 0 & 0 \\ 0 & a_i \cos\frac{n\pi z}{L} & 0 \\ a_i \cos\frac{n\pi z}{L} & b_i \cos\frac{n\pi z}{L} & 0 \end{bmatrix} \tag{2.41}$$

and

$$\begin{bmatrix} V_i \end{bmatrix} = \begin{bmatrix} 0 & 0 & 2A\,\xi_i \frac{n\pi}{L} \cos\frac{n\pi z}{L} \\ 0 & -2A\xi_i \frac{n\pi}{L} \sin\frac{n\pi z}{L} & a_i \sin\frac{n\pi z}{L} \\ -2A\xi_i \frac{n\pi}{L} \sin\frac{n\pi z}{L} & 0 & b_i \sin\frac{n\pi z}{L} \end{bmatrix} \tag{2.42}$$

and a_i , b_i are the global dimensions of nodal points 1, 2, 3.

Furthermore, the analysis requires assumption with respect to the stress-strain relation of the material investigated. For the three-dimensional

problem, the linear stress-strain relationship can be represented by:

$$\begin{Bmatrix} \sigma_x \\ \sigma_y \\ \tau_{xy} \\ \sigma_z \\ \tau_{yz} \\ \tau_{zx} \end{Bmatrix} = \begin{bmatrix} C_{11} & C_{12} & C_{13} & C_{14} & C_{15} & C_{16} \\ C_{21} & C_{22} & C_{23} & C_{24} & C_{25} & C_{26} \\ C_{31} & C_{32} & C_{33} & C_{34} & C_{35} & C_{36} \\ C_{41} & C_{42} & C_{43} & C_{44} & C_{45} & C_{46} \\ C_{51} & C_{52} & C_{53} & C_{54} & C_{55} & C_{56} \\ C_{61} & C_{62} & C_{63} & C_{64} & C_{65} & C_{66} \end{bmatrix} \begin{Bmatrix} \epsilon_x \\ \epsilon_y \\ \gamma_{xy} \\ \epsilon_z \\ \gamma_{yz} \\ \gamma_{zx} \end{Bmatrix} = \begin{bmatrix} \overline{C}_{11} & \overline{C}_{12} \\ \overline{C}_{21} & \overline{C}_{22} \end{bmatrix} \begin{Bmatrix} \epsilon_1 \\ \epsilon_2 \end{Bmatrix} \tag{2.43}$$

Utilizing the variational principal of the potential energy for an elastic solids, the element stiffness $\left[K^m\right]$ is determined and can be divided into four parts as given by:

$$\left[K^m\right] = \int_{V_m} \left[B\right]^T \left[C\right]\left[B\right] \, dV_m$$

$$= \int_{V_m} \frac{1}{4A^2} < B_1^{\,T} \; B_2^{\,T} > \begin{bmatrix} \overline{C}_{11} & \overline{C}_{12} \\ \overline{C}_{21} & \overline{C}_{22} \end{bmatrix} \begin{Bmatrix} B_1 \\ B_2 \end{Bmatrix} \, dV_m$$

$$= \left[K_{11}\right] + \left[K_{12}\right] + \left[K_{12}\right]^T + \left[K_{22}\right] \tag{2.44}$$

where K_{11} , K_{12}, $K_{12}^{\,T}$ and K_{22} are four components of element stiffness K_m and

$$\left\{B_1\right\}^T = \begin{Bmatrix} U_1 \\ U_2 \\ U_3 \end{Bmatrix} \qquad \left\{B_2\right\}^T = \begin{Bmatrix} V_1 \\ V_2 \\ V_3 \end{Bmatrix} \tag{2.45}$$

The terms U_i , V_i have been defined previously. The components of element

stiffness can be written as:

$$K_{11} = \frac{1}{4\,A^2} \int_{V_m} \left[B_1\right]^T \left[\overline{C}_{11}\right] \left[B_1\right] d\,V_m$$

$$K_{12} = \frac{1}{4\,A^2} \int_{V_m} \left[B_1\right]^T \left[\overline{C}_{12}\right] \left[B_2\right] d\,V_m \qquad (2.46)$$

$$K_{22} = \frac{1}{4\,A^2} \int_{V_m} \left[B_2\right]^T \left[\overline{C}_{22}\right] \left[B_2\right] d\,V_m$$

Utilizing the basic formulation concepts discussed previously, a computer program has been developed for pavement structural analysis (32). The accuracy of the developed program has been investigated by comparing the calculated stress and strains with the values obtained from the multi-layered elastic program (chevron). The results of comparison are presented in Appendix B. Similarly in a study of cracking of pavement overlay systems (Figure 2.6), Luther (33) has calculated the stress-intensity-factors K_1 and K_{11} using this program. The results of these analyses are also presented in Appendix B.

CHANGE IN STRESS INTENSITY FACTORS WITH POSITION

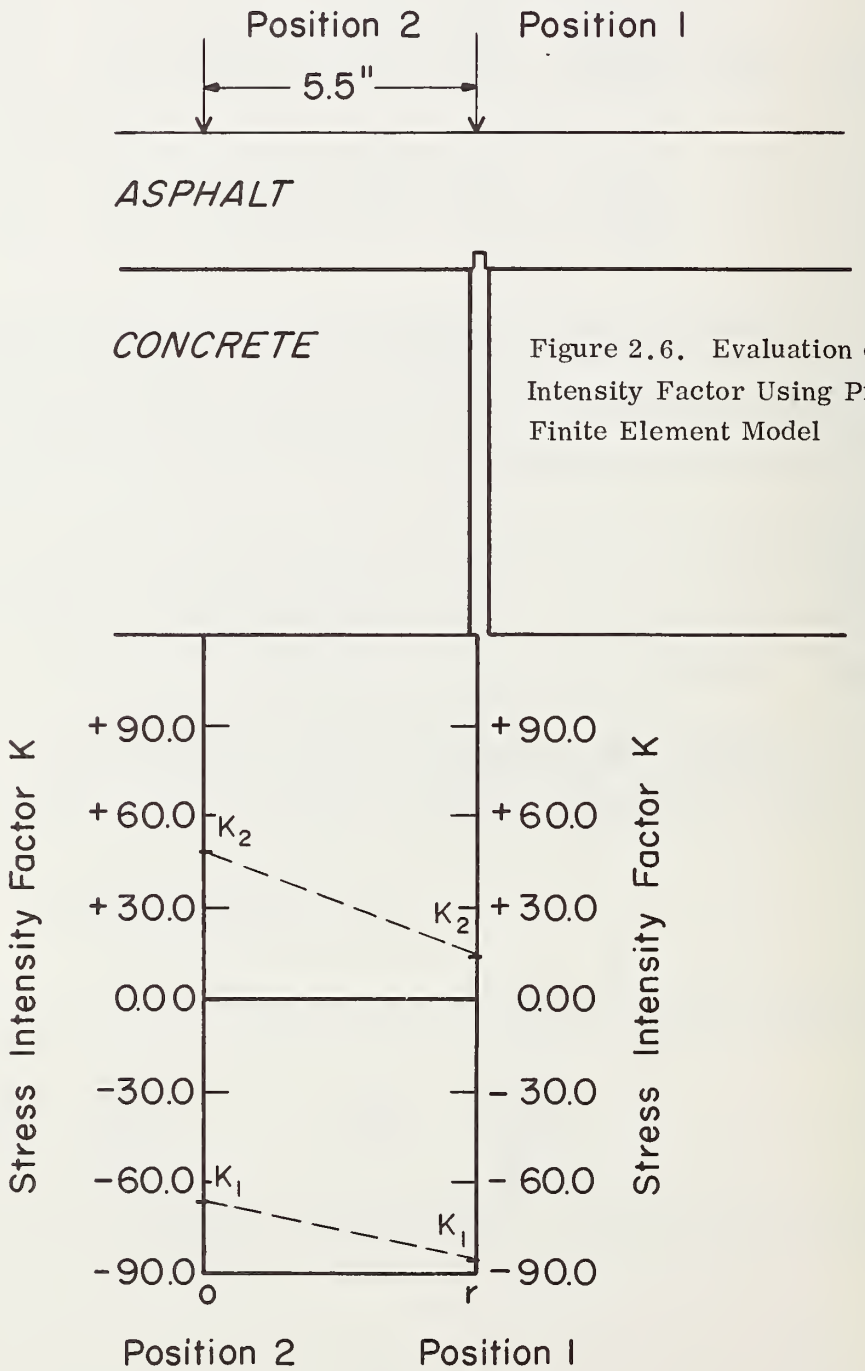

Figure 2.6. Evaluation of Stress-Intensity Factor Using Prismatic Finite Element Model

CHAPTER III

THE INFLUENCE OF LOADING FUNCTIONS ON CRACK PROPAGATION

A. Introduction

In the previous sections of this report, the basic concepts leading to the formulation of fatigue as damage process and the development of a crack propagation law were presented. In the recent research studies conducted for verification of the mechanistic method of fatigue design, idealized loading functions were used to simulate the traffic loading on the pavement's structure. In these studies, sinusoidal loading functions of constant amplitude were utilized as a simplication in the analysis of fatigue data. However it is quite apparent that pavements, similar to most engineering structures, are subjected to loads of variable amplitude, frequency and pattern. Load time histories of periodic form, such as periodic loading of arbitrary wave form, stationary random loads, or superimposed combinations of these are most probably encountered. For highway pavements, however, loads in the form of periodic half-sine function with variable amplitude, frequency and sequence constitutes a realistic approximation.

The development of a fatigue design subsystem using the mechanistic approach requires the evaluation of effect of variable loading functions on the crack propagation and fracture of pavement materials. This design strategy is based, however, upon the successful fulfillment of the following requirements:

(i) the evaluation of fatigue crack propagation interms of loading function of variable amplitude, pattern and frequency.

(ii) the prediction of pavement response under variable loads using simplified laboratory procedures.

In this chapter, the influence of variable loading functions on Paris' crack propagation law is discussed. To demonstrate the predictability of pavement response under variable loads, the results pertaining to two-dimensional and three-dimensional systems subjected to similar loading functions are compared. It should be noted that the results of analysis on two-dimensional problems (beams on elastic foundation) have been presented in the research report of contract no. FH-11-7257, project RF2845 (11). However, in this report to show the similarity of the phenomena observed, the highlights of the findings on the two-dimensional problem are restated and comparison is made with the results of findings on slabs resting on elastic foundation. At the conclusion of this chapter, recommendations pertaining to incorporation of the traffic loading function into the fatigue design subsystem is presented.

B. Review of State of the Art

The analysis of crack growth as presented by Paris (18), recognizes the significance of variation in the load-time history on the damage process. The stress-intensity-factor, K, which appears linearly in equation (2.1), must consequently depend linearly on the intensity of the applied load P, and is also proportional to a function f(c), reflecting the influence of the geometric configu-

ration including the crack size, c. Then, considering P(t) to represent the time variation of the loading function, the time-history of the stress-intensity-factor, K(t), can be expressed as:

$$K(t) = f(c)\ P(t) \tag{3.1}$$

Although during the fatigue crack growth the crack length is a function of time, its change during the interval from one peak load to another is insignificant. Therefore, the function f(c) can be regarded as a slowly changing function of crack size, and momentarily taken as a constant. As a result, the wave form of the local stress field surrounding the crack tip, i.e. the time-history of the stress-intensity-factor, K(t), is proportional to the time-history of the loading function P(t), (18,20).

For sinusoidal loading functions the load parameters affecting the crack growth rate are mean load, load amplitude and frequency of load application. Paris compared the relative effects of load amplitude and frequency and concluded that, for metal alloys, frequency is of minor significance when compared with the effect of load amplitude. He also found that the relative mean load was of secondary importance. Hence, it may be concluded that the primary cause of crack growth is the extend of rises and falls of the load (see Figure 3.1). Another aspect, shown by experimental data is a delay in crack growth following an overload, which indicates that the crack growth process is sensitive to the sequence of load applications.

The above obervations can be regarded as restrictions for the development of a "model" of crack propagation. Such a model should regard damage as occuring

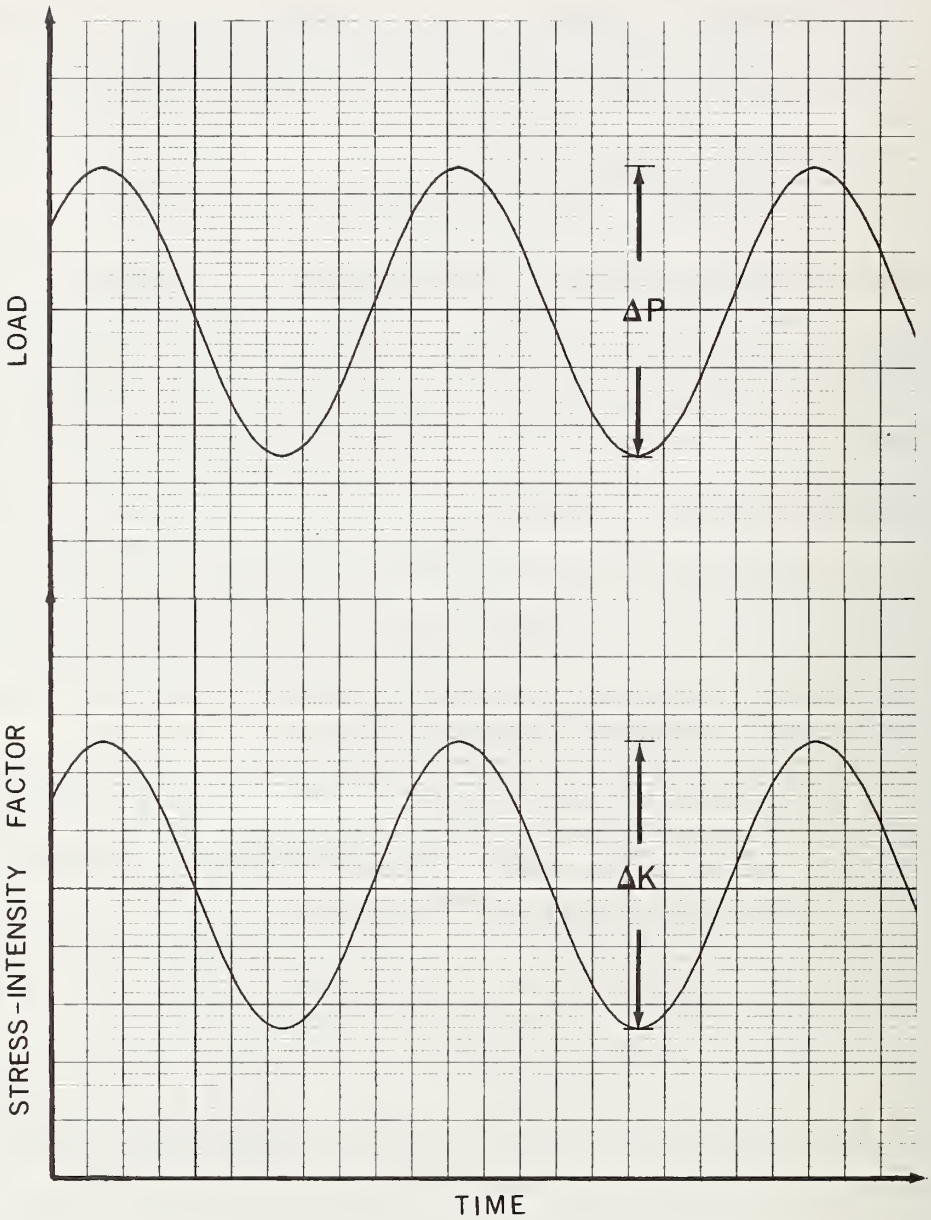

Figure 3.1 Rise and Fall of Load and Stress Intensity Factor With Time

in the plastic zone at the tip of the crack, be sensitive to rises and falls in the load, shown sensitivity to the sequence of rises and falls in the load, be applicable to any configuration using the stress-intensity factor concept, and be capable of incorporating the secondary effects (mean load, frequency of load application, and environmental factors) within its constants. With these restrictions Paris (18) proposed a model resulting in the fourth power dependency on load range.

According to Irwin (34), the size of the plastic zone ahead of the crack tip in a body subjected to a single monotonic loading, can be estimated from equation (2.2), assuming it is valid up to the boundary of the plastic zone. The width, w, of the plastic zone directly ahead of the crack, for $\theta = 0$, is the radius at which the stresses, equation (2.2), violate the yield condition (see Figure 3.3). or

$$w_1 = \frac{K^2}{2\sigma_{yp}^2} \tag{3.2}$$

In fatigue, the load-time history fluctuates through peaks and troughs and the estimate given in equation(3.2) must be modified. Each time the load changes, a reverse plastic flow commences, creating a new plastic zone of reversed deformation imbedded in the original one. Elements of the material within these zones experience alternating plasticity. This concept is best explained by observing Figure (3.2). Figure 3.2a shows the plastic zone induced by the load P. The changes in stress and strain due to load reduction

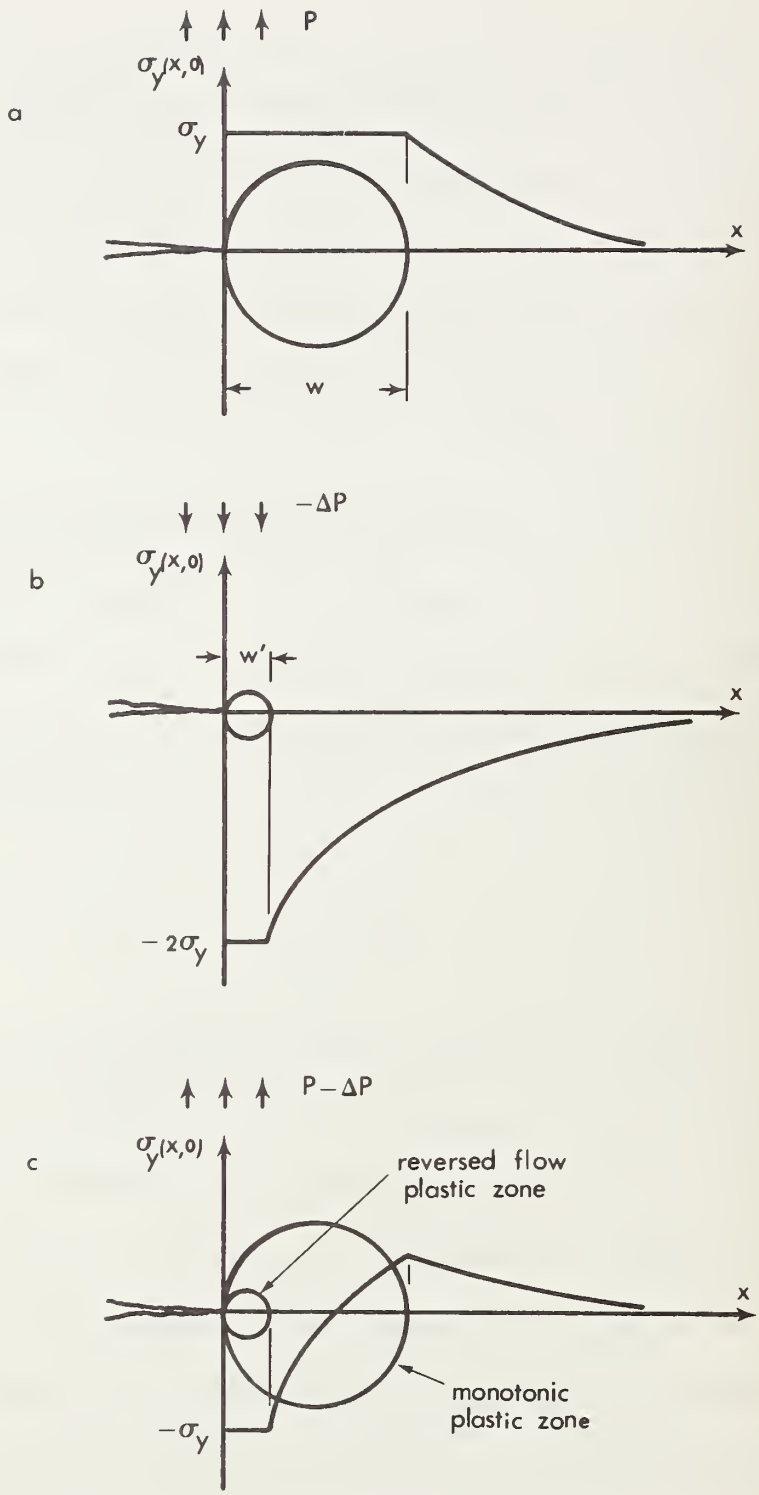

Figure 3.2. Stress-Deformation at the Crack Tip

are then given by a solution identical to that of the original loading, but the yield stress is replaced by twice the value for the original loading (Figure 3.2c). Adding (b) for load $-\triangle P$ with a doubled yield stress, to (a) gives the solution (c) resulting after unloading for P to $P - \triangle P$. Reloading $P - \triangle P$ to P restores (a).

Therefore, for a change in the load of $\triangle P$, the new size of the plastic zone can be estimated by replacing K by h_k, which is the drop in the stress-intensity-factor, and σ_{yp} by $2\sigma_{yp}$ in equation (3.2) giving the result:

$$w_2 = \frac{h_k^2}{8\,\sigma_{yp}^2} \tag{3.3}$$

In this result, the peak-to-peak rises and falls in the K-time history are shown to be of major importance while the relative mean load is of no consequence.

With the assumption that the work absorbed per unit increase in surface area of a crack is constant, the fatigue crack growth can be represented as:

$$\frac{dc}{dN} = \frac{dW}{dN} \quad C_1 \tag{3.4}$$

where $\frac{dW}{dN}$ is the average plastic work per rise in the load-time history. The work done in an excursion of the load will be proportional to the volume of the plastic zone per unit length of the crack front, i.e. proportional to the square of the size of the plastic zone, w_2, and therefore

$$\frac{dW}{dN} = C_2\, w^2 = \frac{C_2\, h_k^4}{64\,\sigma_{yp}^4} \tag{3.5}$$

Substituting this result into equation (3.4):

$$\frac{dc}{dN} = C\ h_k^4 \tag{3.6}$$

which is the same result as the semi-empirical relation expressed in equation (2.14).

The shortcoming of this model is that it "counts" the effects of rises and falls in the load-time history with the same weight regardless of the sequence in which they occur, and a more elaborate model is necessary to account for sequence effects. Such a model would have to consider two phenomena occurring in the vicinity of the crack tip--residual stresses and stress relaxation, because as a result of the interaction of these effects, the sequence of load application has a definite influence on the fatigue life.

Experiments reported (35,36) have shown that under certain loading conditions the material can experience either delay or acceleration of the damage process. Also, there is no single trend showing one particular sequence of stress levels to be the most damaging. The order of application that would result in the lowest life, whether low/high, high/low, high/low/high or random, depends entirely on the exact details of each particular spectrum and the same holds true for block loading conditions.

Recently, the load interaction and load sequence effects on the crack propagation have been investigated by Porter (37). In these experiments, the crack growth data is presented for various base line stresses, σ_1, and overload stresses, σ_2. The analysis of data indicates that the longest fatigue life is

obtained for the highest overload σ_2. It is noted that the crack growth rate decreases as the ratio of σ_2 / σ_1 increases. The results of experiments with various spectrums indicate that when a minimum stress level follows a peak overload, the effect of the overload becomes insignificant.

Finally, Porter has presented a crack growth reduction factor r, to be used in the analysis of fatigue data under variable loading conditions. Using this crack growth reduction factor, the Minor law could be modified as follows:

$$\sum_{i=1}^{k} \frac{r_i n_i}{N_i} = 1.0 \qquad (3.7)$$

where k = number of steps in spectrum

r_i = number of applied cycles at ith stress

N_i = life to growth the crack over the increment at the ith stress

n_i = crack growth reduction factor for the ith stress

This approach requires that the damage rate, i.e. crack growth, is the same function of fractional life n_i / N_f for all stresses. However, it is known that this assumption of stress independency is only approximately true for most materials.

Furthermore, Porter (37) states that a detailed mathematical evaluation of load sequence effect requires elastic-plastic analysis and the study of residual stresses at the crack tip.

To date, such a model is nonexistant (30), which makes the quantitative analysis of fatigue life of materials subjected to random loading a very difficult task.

Wheeler (38) has also proposed an empirical method to take into account the delays in the fatigue life which occur after application of high stress levels in the load sequence. He combined the concepts of fracture mechanics with Minor's idea to sum the damage incurred during each load application to get the damage after the rth load application, i.e.

$$c_r = c_o + \sum_{i=1}^{r} f(\triangle K_i)^n \tag{3.8}$$

where c_r = crack length after the rth load application

c_o = initial crack length

$\triangle K$ = change in the stress-intensity-factor

Based on experimental data, Wheeler proposed that equation (3.8) can be improved by the introduction of a parameter, C_{pi}, which he calles the retardation parameter. Then, equation (3.8)becomes

$$c_r = c_o + \sum_{i=1}^{r} C_{pi} \; f(\triangle K_i)^n \tag{3.9}$$

where

$$C_{pi} = \begin{cases} \left[\dfrac{r_y}{c_p - c}\right]^m & \text{for } c + r_y < c_p \\ 1 & \text{for } c + r_y > c_p \end{cases}$$

in which r_y = size of the plastic zone ahead of the crack tip

$(c_p - c)$ = distance from the crack tip to the elastic-plastic interface, or size of the plastic zone after a high stress application, where c_p and c are defined in Figure 3.3

m = shaping exponent

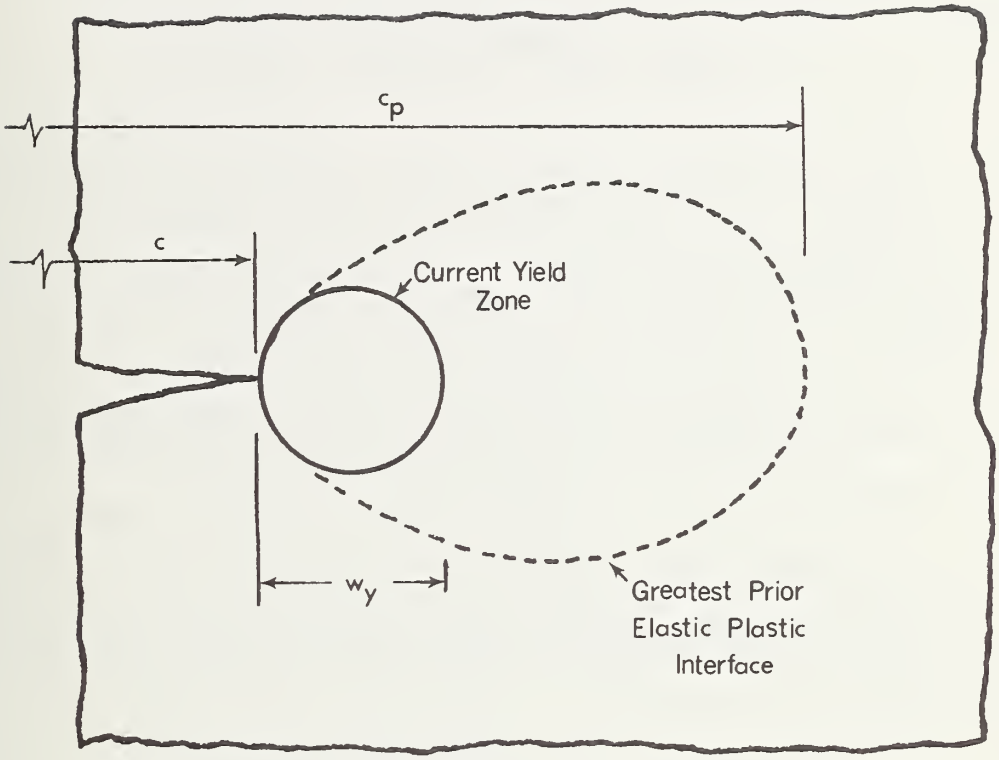

Figure 3.3. Elastic-Plastic Interface at the Crack Tip

With respect to the effect of other test variables, i.e. frequency, mean load and load range, a number of empirical equations have been proposed in the literature. As an example, Mukherejee (39) has presented the following equation:

$$\frac{dc}{dN} = A\,(f)^{-0.43}\,(K_{max})^{3.37}\,(\triangle K)^{1.16} \tag{3.10}$$

where f is frequency, K_{max} and $\triangle K$ are maximum stress intensity factor and $K_{max} - K_{min}$ respectively. This equation indicates that frequency of testing influences the crack growth rate. The effect of rest period has also been investigated by a number of researchers. Kuzamonvic (40) has argued that the mechanism of crack propagation under dynamic loading and static conditions are similar except for the rest period affect. Experimental data are presented to show that in metals, the rest period affects the dislocation motion, polygonization of slip bands and the arrangement of solute foreign atoms.

The effect of mean load and load range has also been incorporated in Pearson (41) and Forman (42) models of crack propagation. The Forman (42) model is expressed in terms of R, load ratio and critical stress intensity factor. This model can be written as:

$$\frac{dc}{dN} = \frac{A\,(\triangle K)^{n}}{(1 - R)\,K_c - \triangle K} \tag{3.11}$$

where $R = \frac{K_{min}}{K_{max}}$ and K_c is the critical stress intensity factor.

Pearson (41) has indicated that for materials with relatively high critical stress intensity factor, the load ratio R does not significantly affect the crack growth rate. However, for conditions where K_{max} approaches K_{1c}, the crack growth data should be modified as follows:

$$\frac{dc}{dN} = \frac{A \; K_c \; (\triangle K)^n}{\left[(1-R) \; K_c - \triangle K\right]^m} \tag{3.12}$$

where m and n are constants.

The most interesting method of analysis of crack growth laws was recently presented by Cherepanov (43). Utilizing the concept of plastic work at the crack tip, a relationship between specific total plastic work γ and the stress intensity factors is derived. This relation can be written as:

$$\gamma = \alpha_2 \frac{K^2}{E} + \alpha_3 \frac{K^3}{\sigma_s^3} \cdot \frac{dK}{dc} \tag{3.13}$$

where α_2 and α_3 are dimensionless functions of yield stress σ_s, applied stress, σ_o, Poisson ratio, μ, and Young modulus E. This equation leads to the development of a crack growth rate function given as:

$$\frac{dc}{dN} = -\beta \left[\frac{(K_{max}^2 - K_{min}^2)}{K_c^2} + \ln \left(\frac{K_c^2 - K_{max}^2}{K_c^2 - K_{min}^2} \right) \right] \tag{3.14}$$

where β is a material constant given by

$$\beta = \alpha_4 \frac{E \, K_c^2}{2 \, \sigma_s^2} \tag{3.15}$$

In this equation, α_4 is a dimensionless parameter related to σ_s, E and μ. σ_s is yield stress of the material. Using a Taylor series expansion, this

equation reduces to the following form:

$$\frac{dc}{dN} = \beta \left(\frac{K_{max}^4 - K_{min}^4}{K_c^4} + \frac{K_{max}^6 - K_{min}^6}{K_c^6} + \ldots\ldots \right) \tag{3.16}$$

if $K_{max} < .5\ K_c$

$$\frac{dc}{dN} = \beta \left(\frac{K_{max}^4 - K_{min}^4}{K_c^4} \right) \tag{3.17}$$

for $K_{min} = 0$, $R = \frac{K_{min}}{K_{max}} = 0$, it is obtained

$$\frac{dc}{dN} = \frac{\beta}{K_c^4} (K_{max})^4 \tag{3.18}$$

or $$\frac{dc}{dN} = A\ (\triangle K)^4 .$$

Utilizing these equations, Cherepanov (43) concludes that both Paris' law and Forman's (42) equations satisfy experimental data available. Most significantly, it is pointed out that the applicability of Paris' law to a large group of materials is not merely a coincidence. Rather, the reason is that the fatigue crack growth is governed by the same mechanism for all materials manifesting plastic properties. The mechanism does not depend on the details of micro-structure at the crack tip, and it is analogous to the K_c concept.

In the discussions presented in this section, the basic concepts of damage and the effect of stress and load interaction were briefly reviewed. It was pointed out that for the theoretical analysis of fatigue under random loading, the present state of the art is deficient in providing a detailed

mathematical model for the effect of load sequence on the crack propagation. Experimental characterization and emperical modeling constitute the primary method of analysis of crack propagation under variable loading functions.

C. Experimentation on Two-Dimensional Systems

(1) Loading Function

The material characteristics and testing procedures used in the evaluation of crack propagation of beams on elastic foundation have been reported previously in References (14, 15). The loading function used in these experiments consisted of a half-sine function with a duration of 0.1 second. This rate of loading corresponds to vehicular speeds of approximately 15-20 miles/hours. The "rest period" or time lapse between successive loads was controlled by an auxilliary function generator and a "data-track" which suppressed the half sine functions appearing in between the successive loads. The rest period, which corresponds to the headway between vehicles in the roadway, was selected as 0, 0.4 and 0.8 seconds. The experimental program consists of the following types of loading conditions:

(a) Monotonic Loading*

Fatigue tests were conducted under a half-sine loading function with a duration of 0.1 second and 0.8 second rest period. The load function of constant amplitude was applied until failure by cracking occurred. Three load ampli-

---

*In this report, the terms constant amplitude and montonic loading are used interchangeably.

tudes of 20, 30 and 40 pounds were utilized (Figure 3.4). To study the effect of the rest period on the process of crack propagation, monotonic loads with different rest periods ranging from 0 to 0.8 seconds were used (Figures 3.5 and 3.6).

(b) Sequential Loading

In these tests, half-sine loading functions with a 0.1 second duration and an 0.8 second rest period were used. The function was programmed by the MTS function generator with the aid of the data track such that the load amplitude was varied in a sequence of 40, 30 and 20 pounds, therefore forming a block of three cycles, each one with a different intensity of load (Figure 3.7). In a second series of tests the sequence of load application was selected as 20, 30 and 40 pounds (Figure 3.8). These blocks of loads were applied to the specimen until failure occurred. A third sequence was used in which the block consisted of eight cycles of 20 pounds and one cycle of 40 pounds (Figure 3.9).

(2) Method of Analysis

The method of analysis of the crack growth rate of asphaltic beams resting on an elastic foundation have been discussed thoroughly in references (11, 14 and 15). These analyses require the calculation of the stress-intensity factor at various crack lengths as well as the experimental determination of the crack size variation with the number of cycles of load application. As mentioned in Chapter II, to determine the stress-intensity-factor, K_1, for a beam

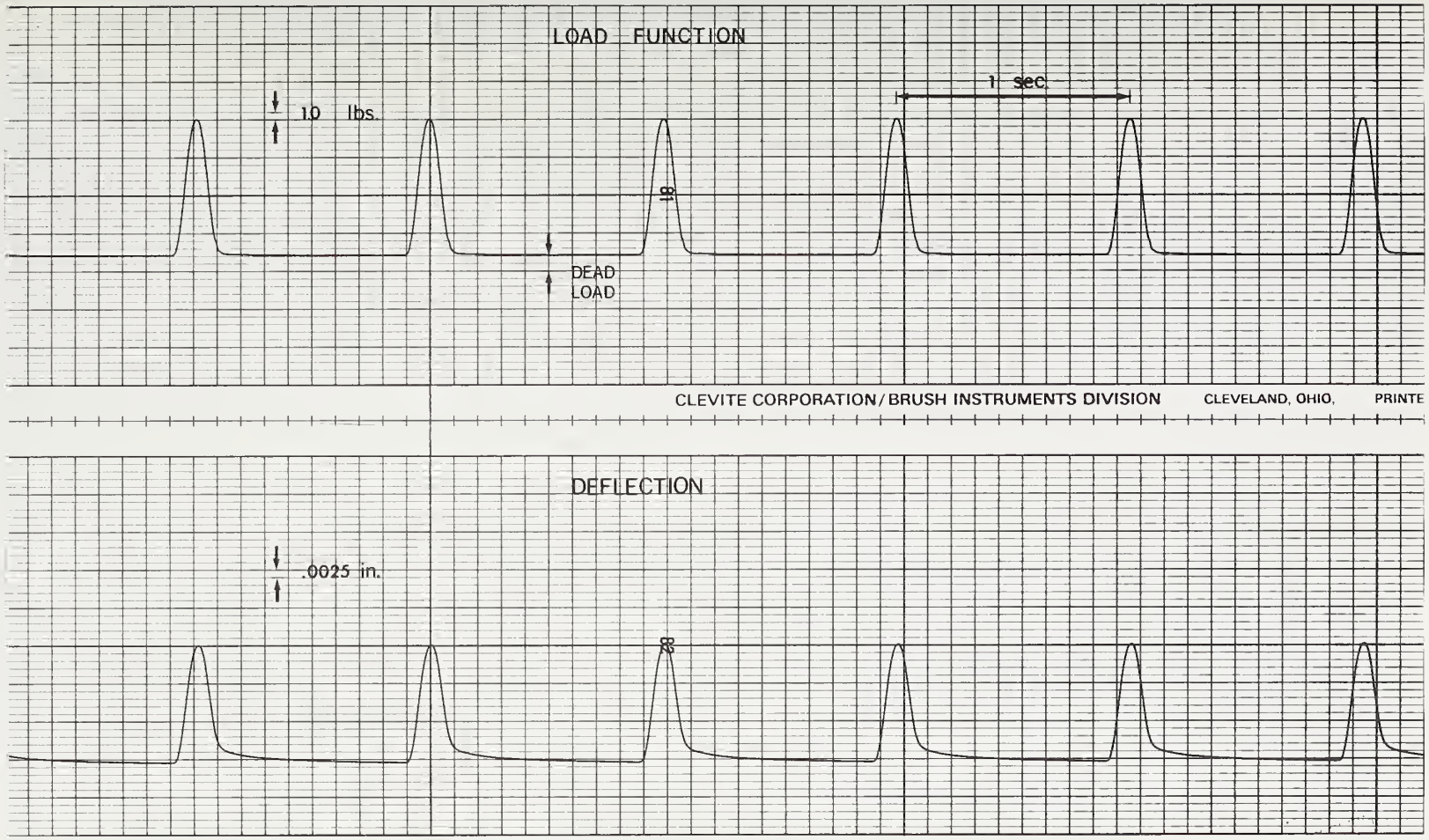

Figure 3.4. Load Function Used in the 20 lbs. Monotonic Tests with 0.8 Second "Rest Period"

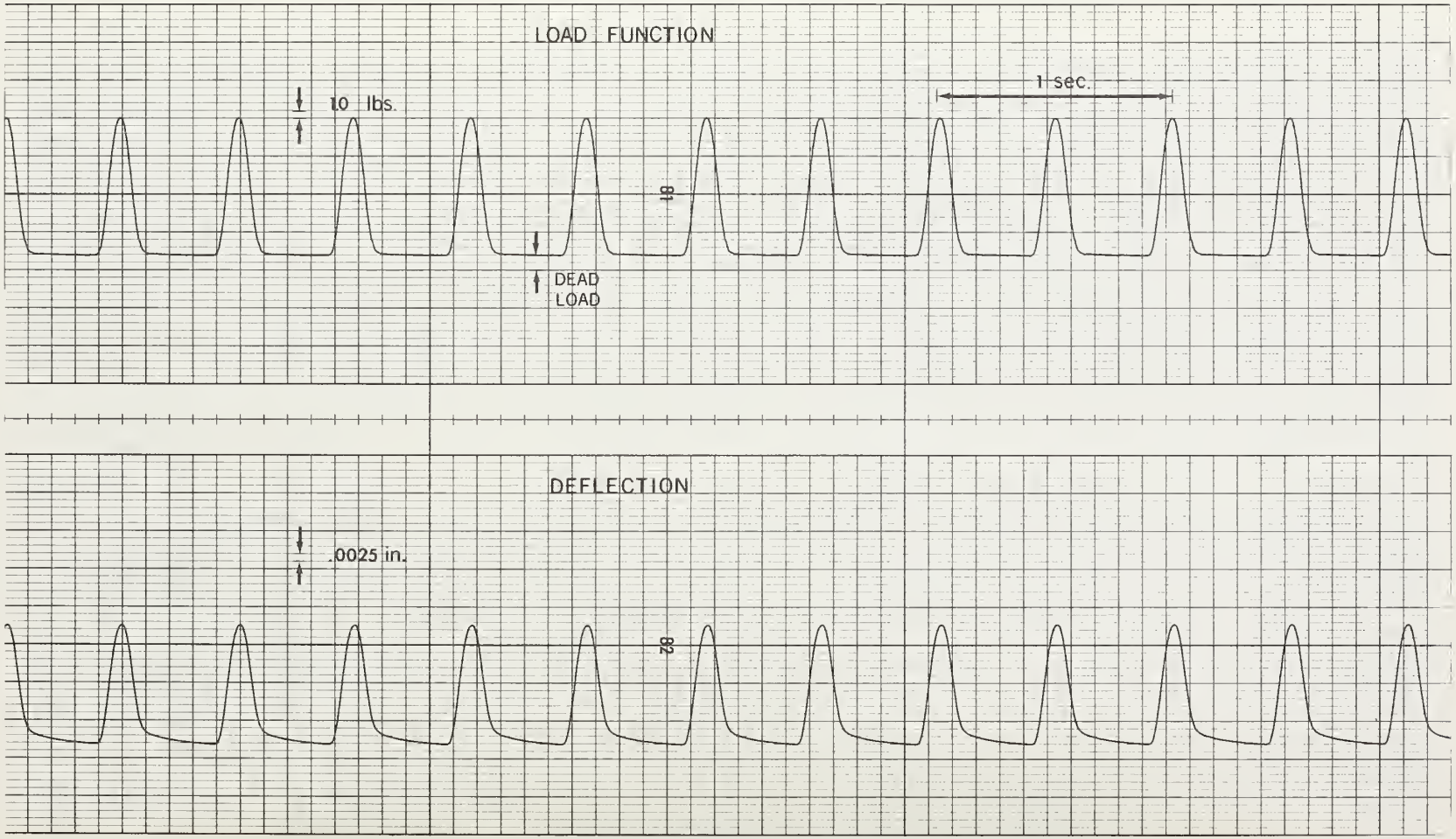

Figure 3.5. Load Function Used in the 20 lbs. Monotonic Tests with 0.4 Second "Rest Period"

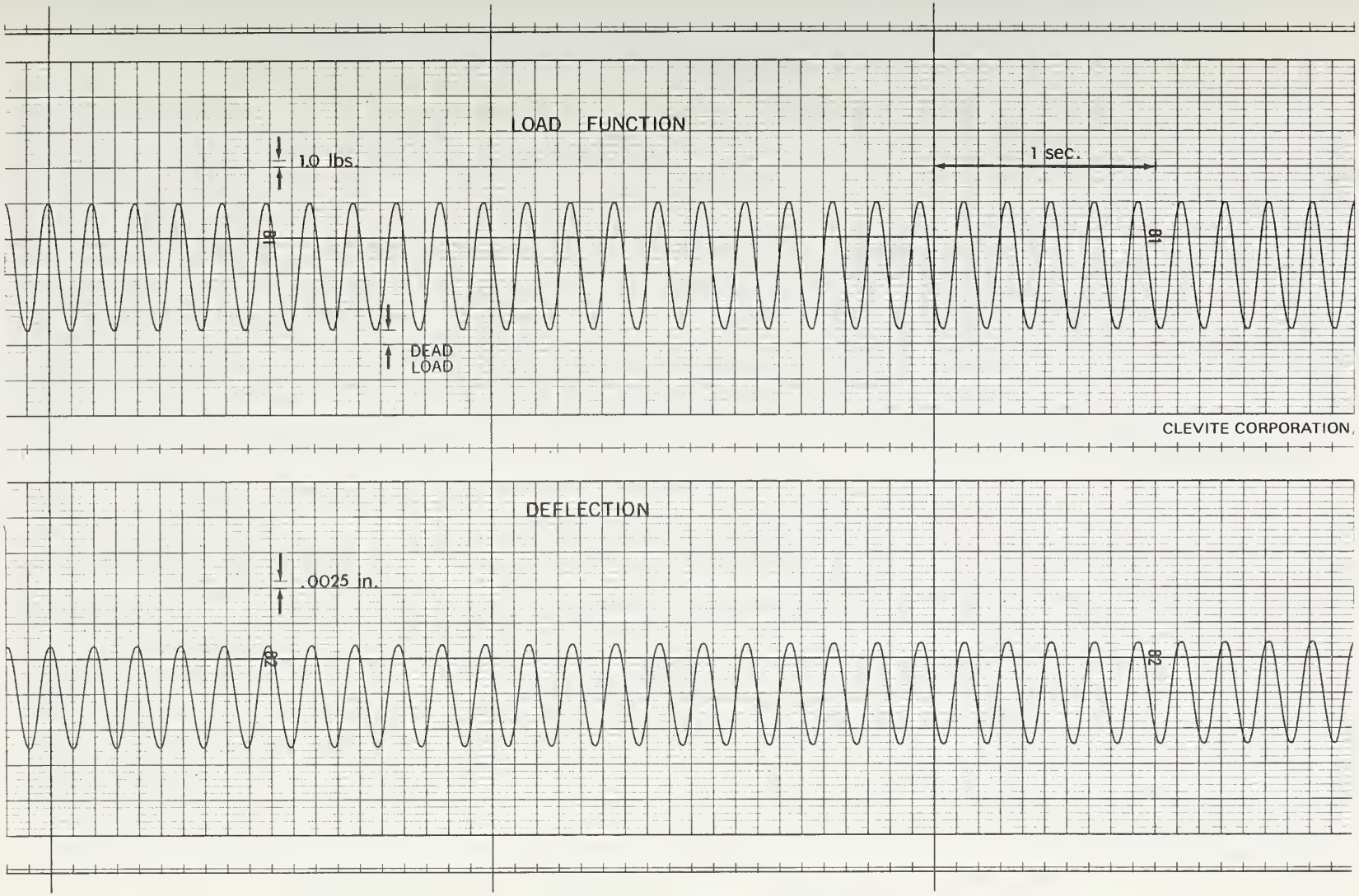

Figure 3.6. Load Function Used in the 20 lbs. Monotonic Tests with Zero "Rest Period"

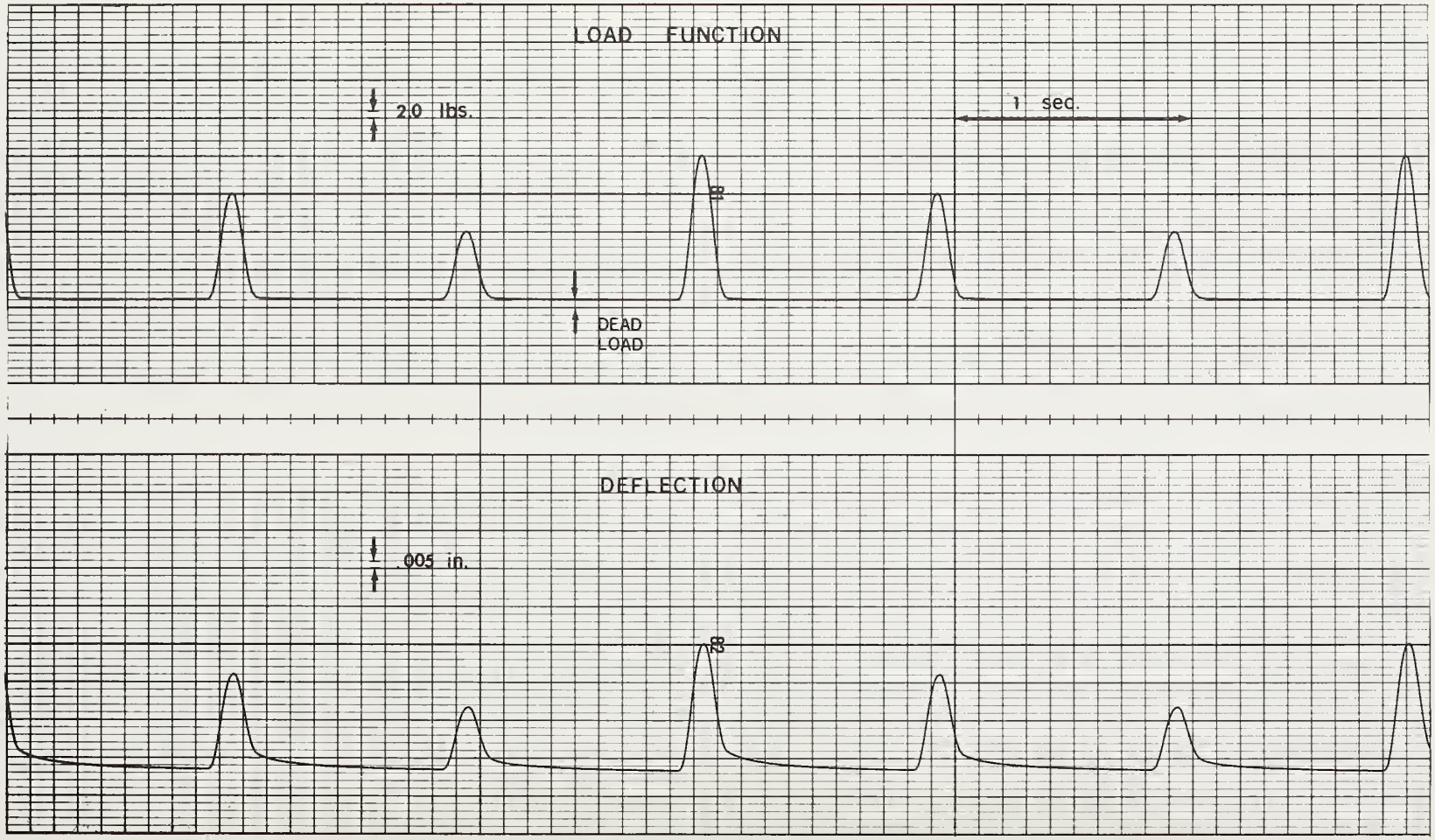

Figure 3.7. Load Function Used in the 40/30/20 lbs. Sequence Tests

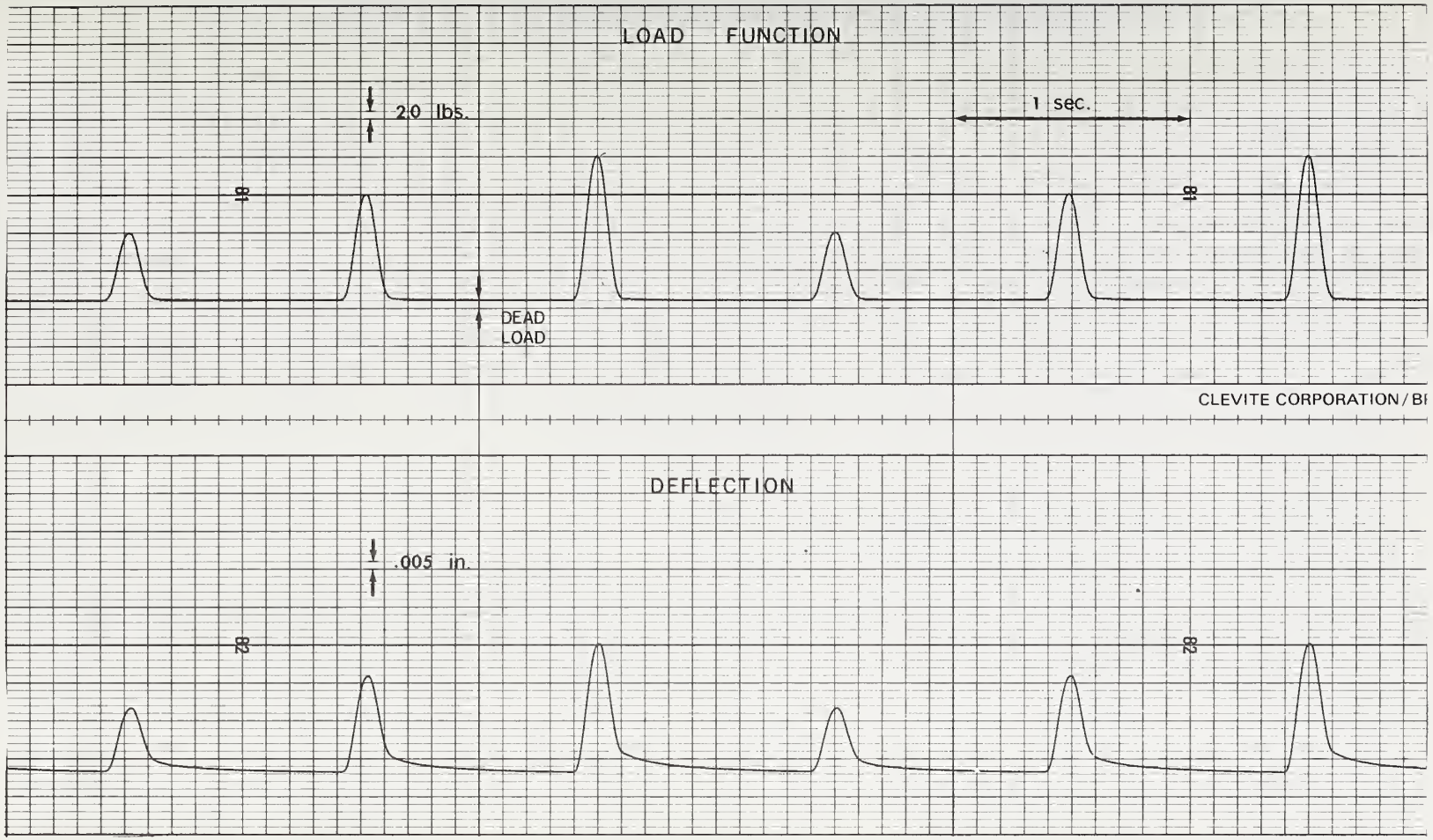

Figure 3.8. Load Function Used in the 20/30/40 lbs. Sequence Tests

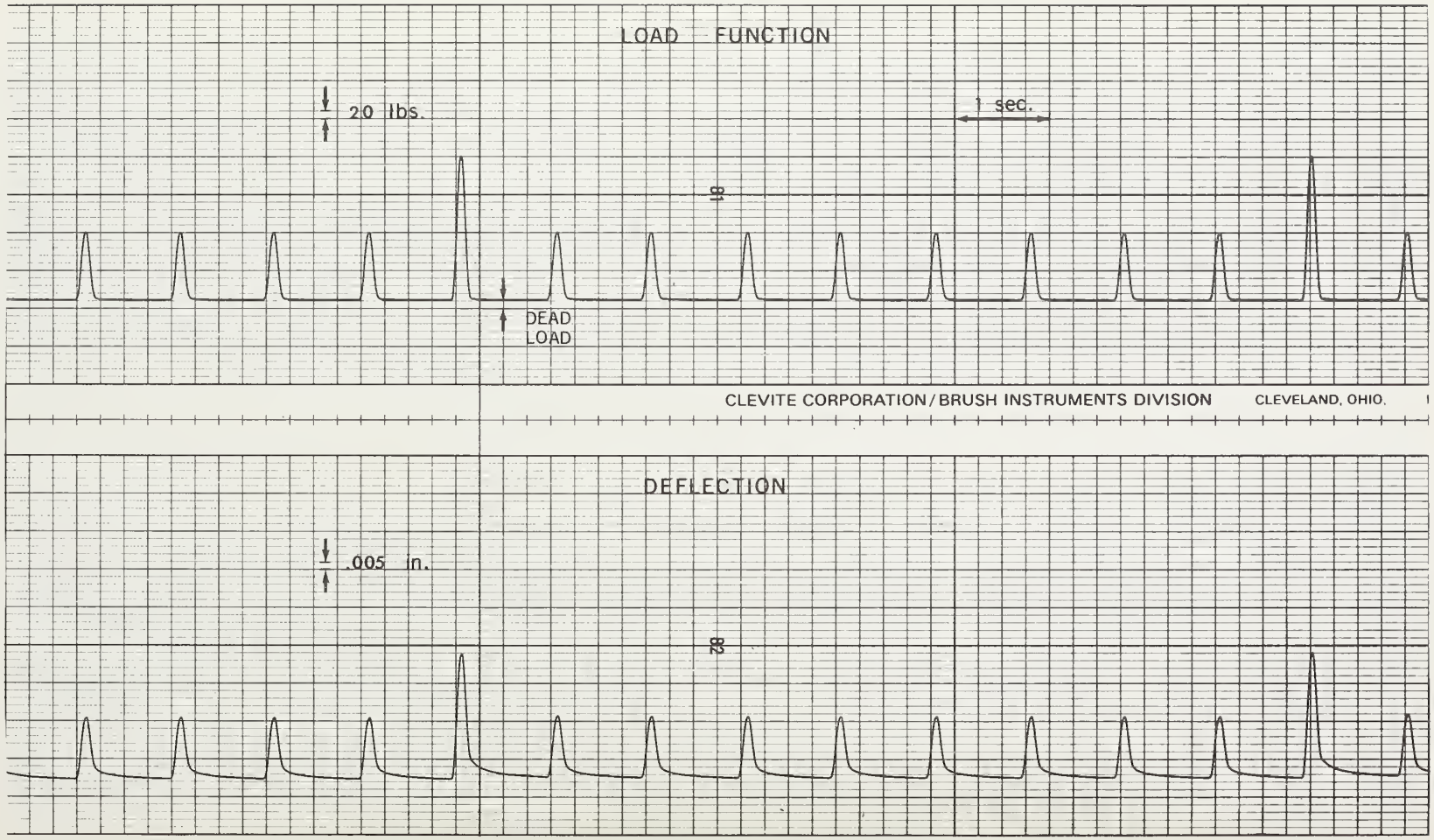

Figure 3.9. Load Function Used in the 20/40 lbs. Sequence Tests

supported on an elastic foundation, three methods are available: boundary collocation, finite elements and experimental methods. The three methods used in this study and the results are presented in Figure 3.10 showing excellent agreement.

To determine the crack size during the fatigue tests, x-ray photographs, visual observation and indirect compliance measurements have been utilized. Since direct measurements have been shown to be more reliable, this was the technique used and a typical x-ray photograph showing the crack at different cycles is presented in Plate 3.1.

(3) Summary of Research Findings

(a) Stress Amplitude Effect

In order to investigate the effect of stress amplitude on the fatigue damage process, sand-asphalt beams resting on an elastic foundation were subjected to three stress levels of constant load amplitude. The crack length - number of cycles of load application relation (c - N) was determined by visual observation and x-ray techniques. Figure 3.11 presents the c - N curves for the three stress levels used, and figure 3.12 shows the variation of crack size for normalized fatigue life N_i / N_f. It is noted that the load amplitude of 20, 30 and 40 pounds result in an identical c - (N_i / N_f) relation. This implies that for monotonic loading (constant amplitude), the crack growth process or "damage" accumulation is independent of the stress levels. In Figure 3.13, the rate of crack propagation is plotted versus the stress-intensity-factor, for

Plate 3.1. X-ray Photograph for a Sand-Asphalt Beam, Showing the Crack at Different Cycles.

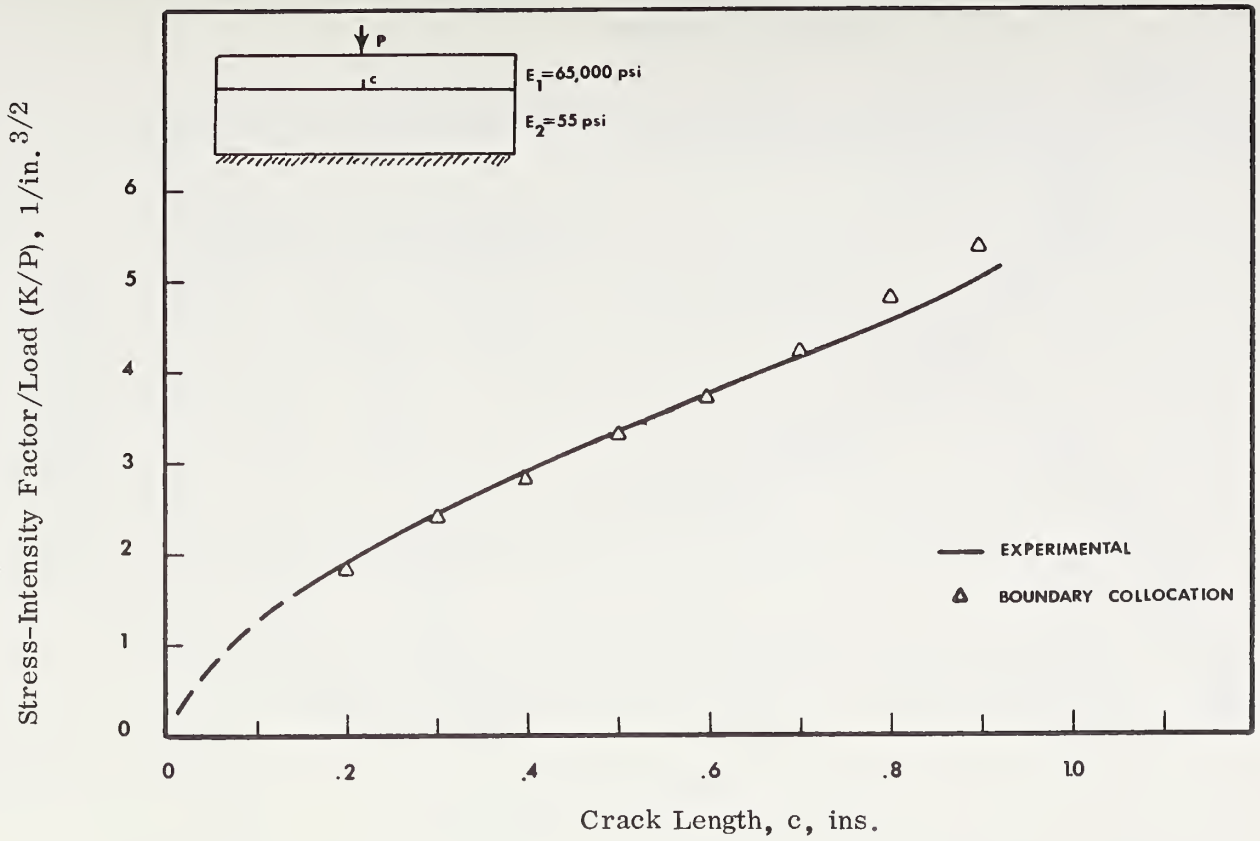

Figure 3.10. Stress-Intensity Factor/Load (K/P) Versus Crack Length (c) for Beams on Elastic Foundation

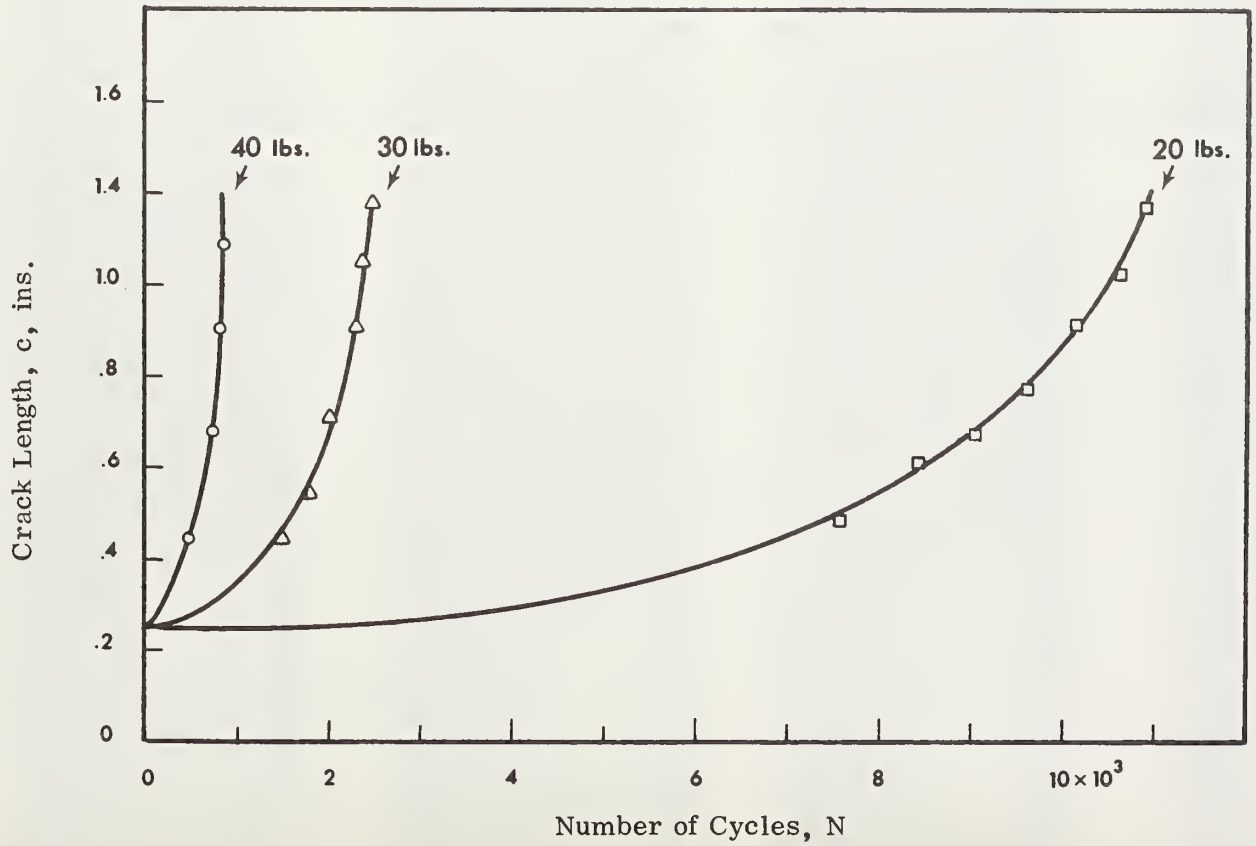

Figure 3.11. Crack Growth Curve for the Tests of 20, 30 and 40 lbs. Monotonic Loading Condition

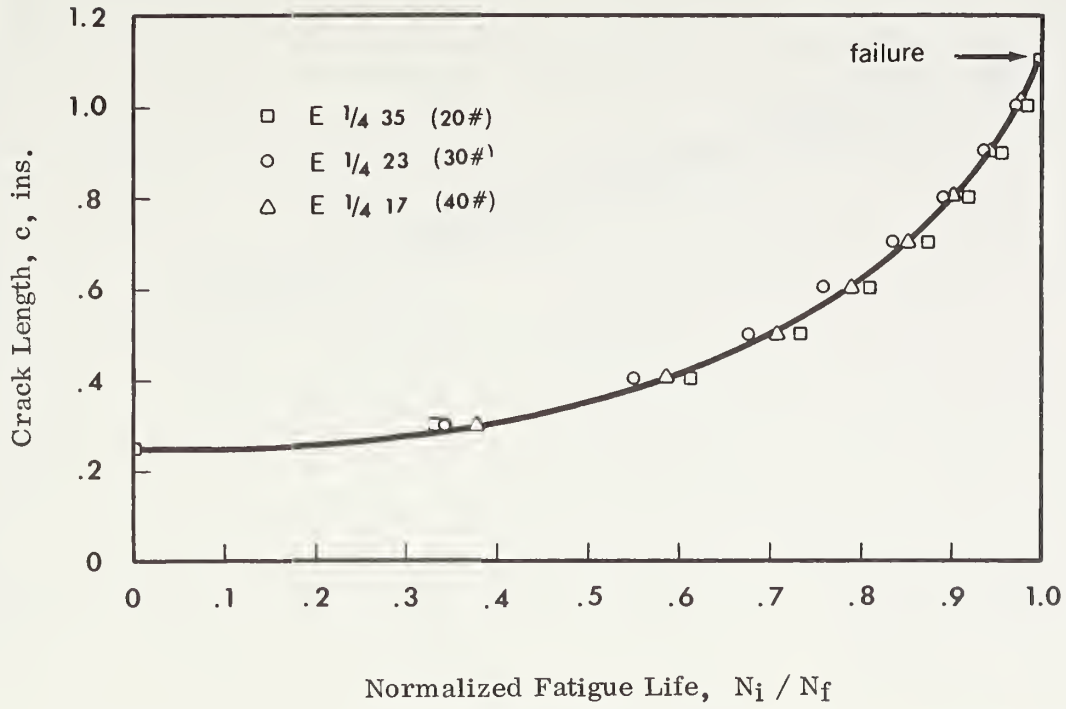

Figure 3.12. Crack Length - Normalized Fatigue Life for Monotonic Loading

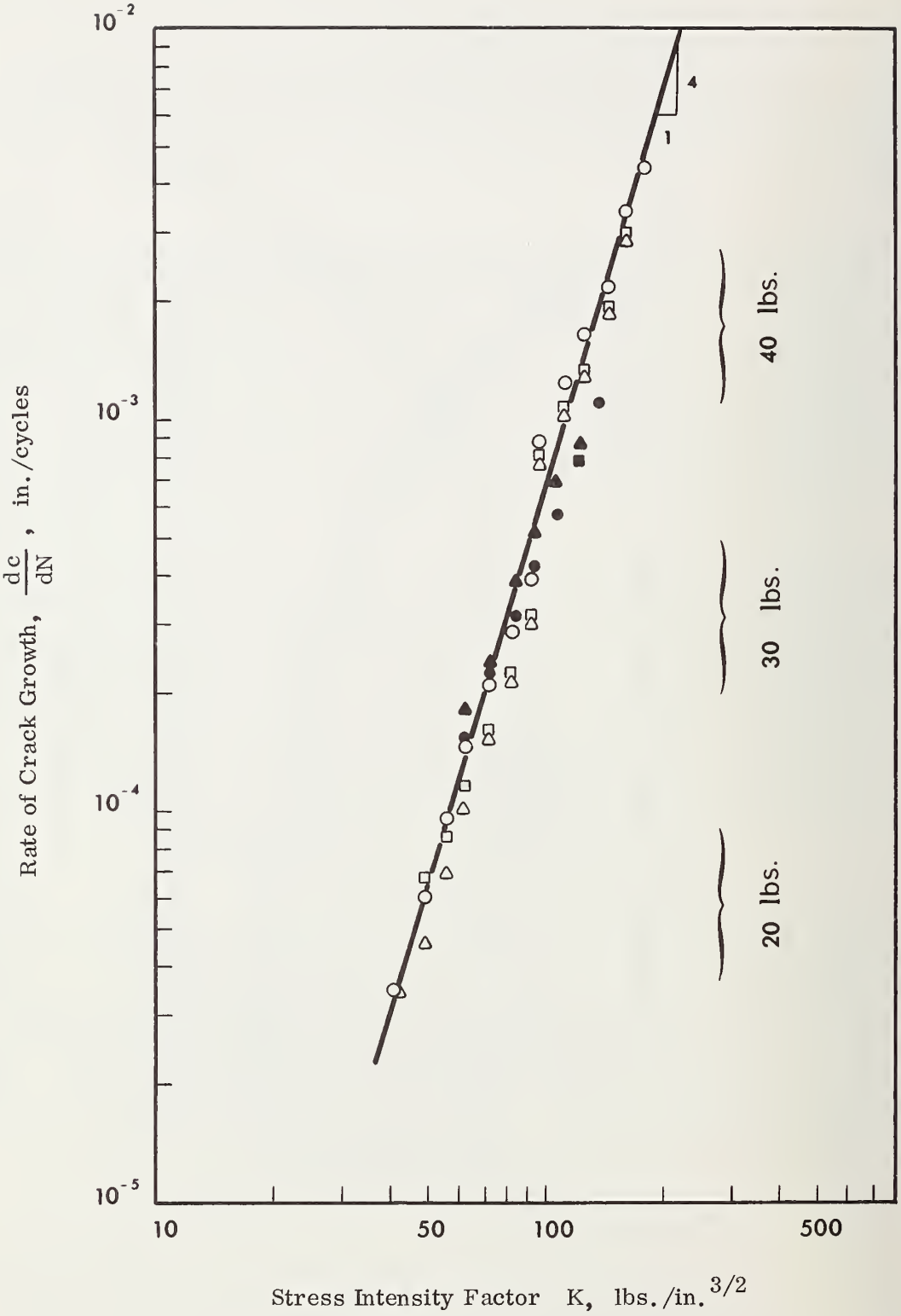

Figure 3.13. K versus $\frac{dc}{dN}$ for Monotonic Loading with Different Amplitudes

load amplitudes of 20, 30 and 40 pounds. It is shown that the crack growth follows Paris' law as $\frac{dc}{dN} = A K^4$.

(b) Effect of Load Sequence

To verify the effect of load sequence and the existance of the "delay effect" in bituminous paving mixtures, a sequential loading condition has been utilized. These loadings are designated as 20/30/40; 40/30/20; and 20/40 corresponding to the amplitude of the loads (in pounds) appearing in the sequence. In the 20/40 loading condition, 8 cycles of 20 pounds succeeded by one cycle of 40 pounds load, forming a block of 9 cycles.

In Figures 3.14, 3.15 and 3.16, the crack length - normalized fatigue life (N_i / N_f) for both monotonic and sequential loadings are shown. It is noted that the rate of change of the crack length with the number of load applications is affected by the sequential loading. However, there is no significant difference between the 20/30/40 and 40/30/20 load sequences. Also, for any given level of damage the normalized fatigue life was greater in the sequential loading than that of the monotonic loading, meaning that the rate of crack growth was delayed whenever sequential loads of variable amplitude were used. These experimental data clearly indicate the existance of the interaction phenomena in the crack growth process.

Referring to equation 3.1, expressing the time variations of the stress-intensity factor in terms of load-time history, the function f(c) can be obtained as the ratio $K(t)/P(t)$. Therefore, a graph of the (dc/dN) - (K/P) relation is a

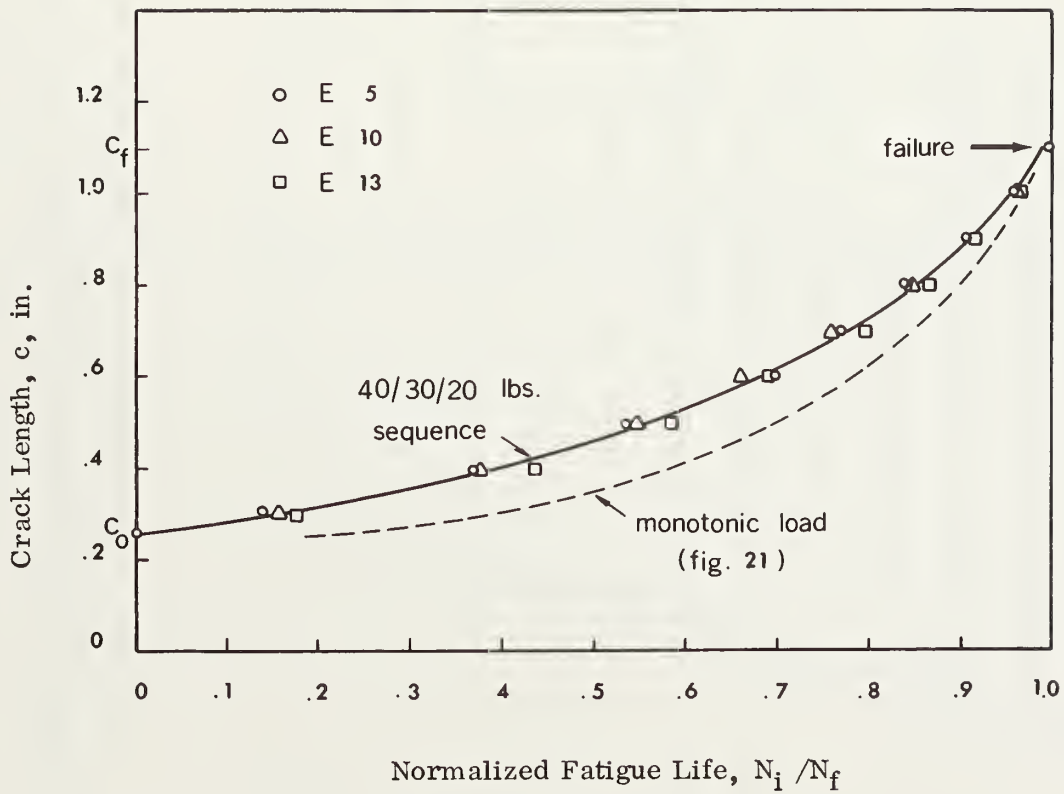

Figure 3.14. Crack Length - Normalized Fatigue Life for 40/30/20 lbs. Load Sequence

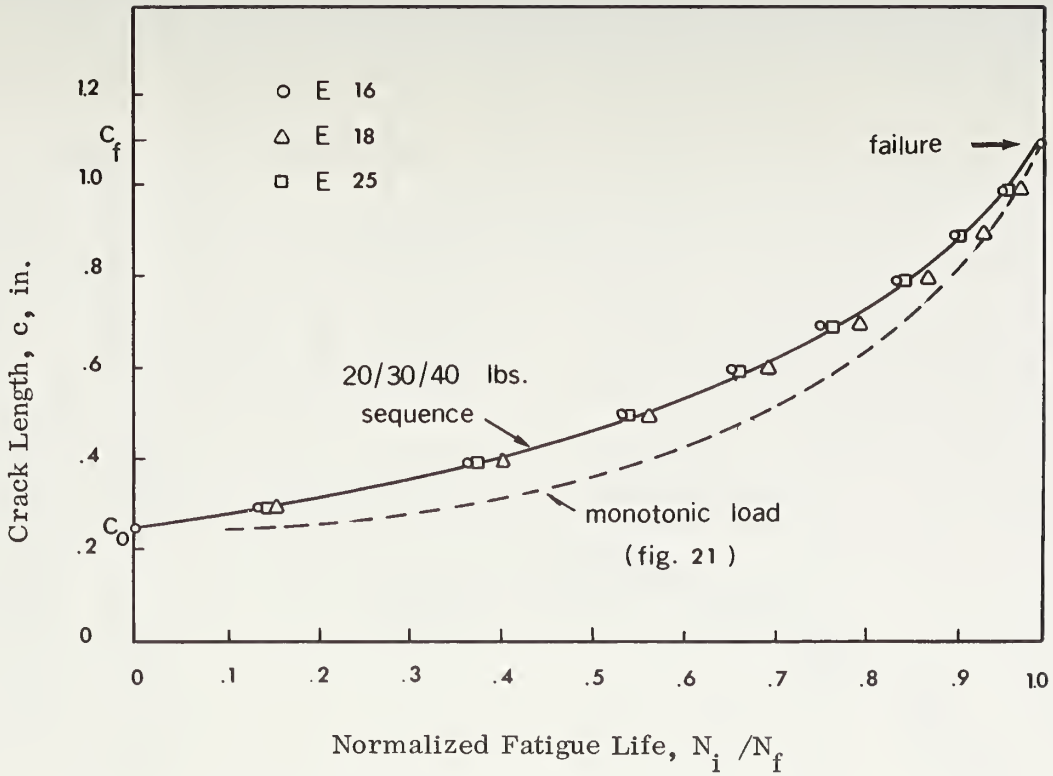

Figure 3.15. Crack Length - Normalized Fatigue Life for 20/30/40 lbs. Load Sequence

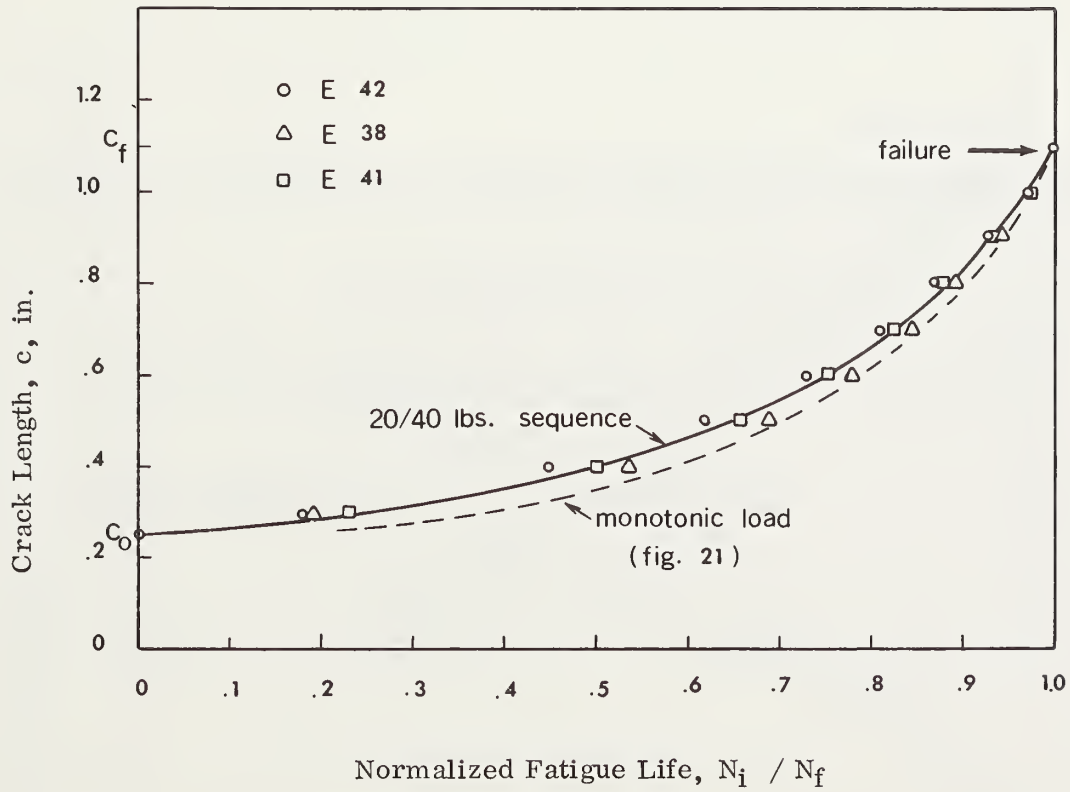

Figure 3.16. Crack Length - Normalized Fatigue Life for 20/40 lbs. Load Sequence

representation of the variation of the damage rate in terms of crack function f(c) (Figure 3.17), The data shown in Figure 3.17 indicate the difference is due to load sequence. It also shows the "delay effect" in terms of Paris' law since the exponent was found to be less than 4, i.e. the cracks grew at a slower rate as compared to the monotonic loading tests.

The observation reported verifies the existance of the interaction effect which is attributed to the interaction of beneficial residual stresses and the stress relaxation phenomena due to periodic stress applications.

(c) Effect of Rest Period

To investigate the effect of the rest period on the crack growth rate, experiments were conducted using a constant amplitude--0.1 second duration, half-sine repeated load function with periods of 0, 0.4 and 0.8 seconds. The effect of rest period on the damage growth process is presented in Figures 3.18 and 3.19.

In the zero-second rest period condition, it is readily observed that the distress due to one load has not fully dissipated before the next load cycle is applied. That is, the required time for the recovery of induced deformation is greater than the rest period. This results in an accumulation of irrecoverable deformations during the fatigue loading, and conditions similar to the creep effect are induced. For this reason, it is noted in Figure 3.18 that the slope of the (dc/dN) - K relation for zero-second rest period is slightly less than 4. However, in general, it can be concluded that with the range of rest

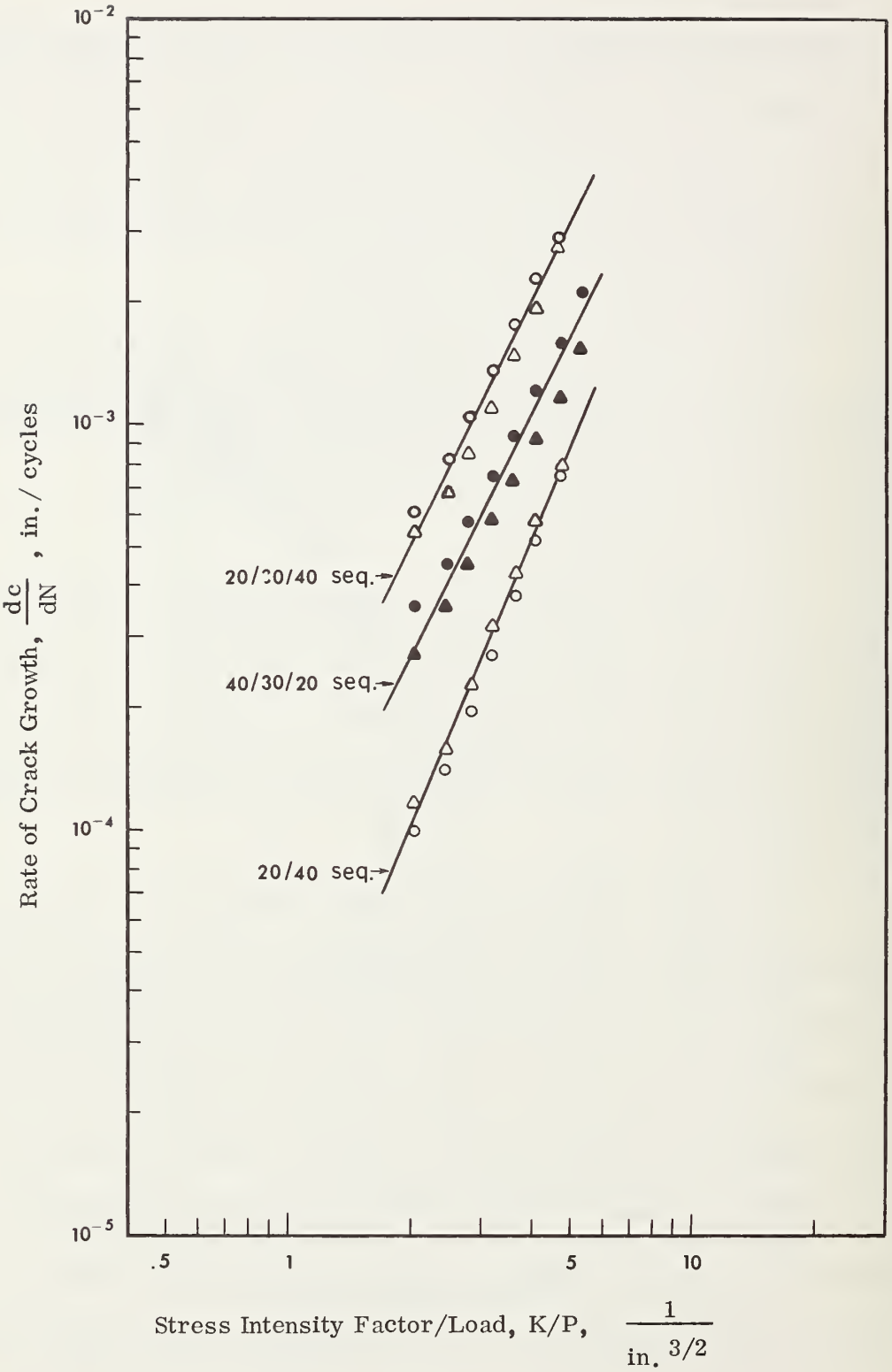

Figure 3.17. $\frac{dc}{dN}$ versus $\frac{K}{P}$ for Sequential Loads

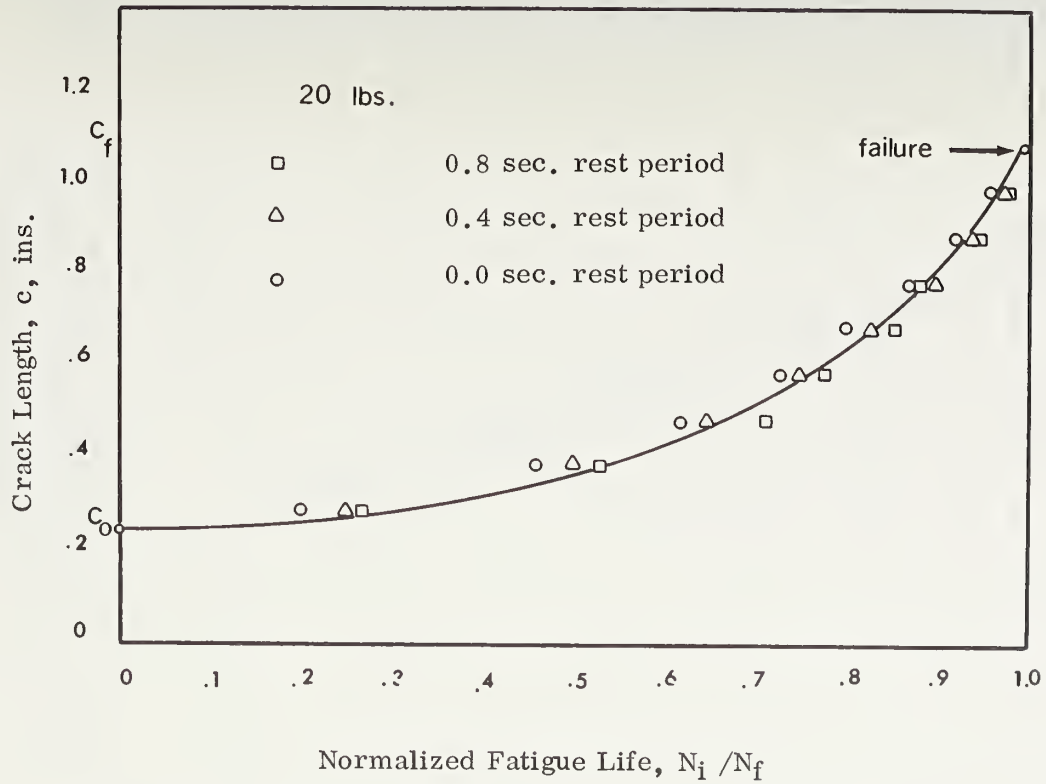

Figure 3.18. Crack-Length-Normalized Fatigue Life for 20 lbs. Load with Different Frequencies

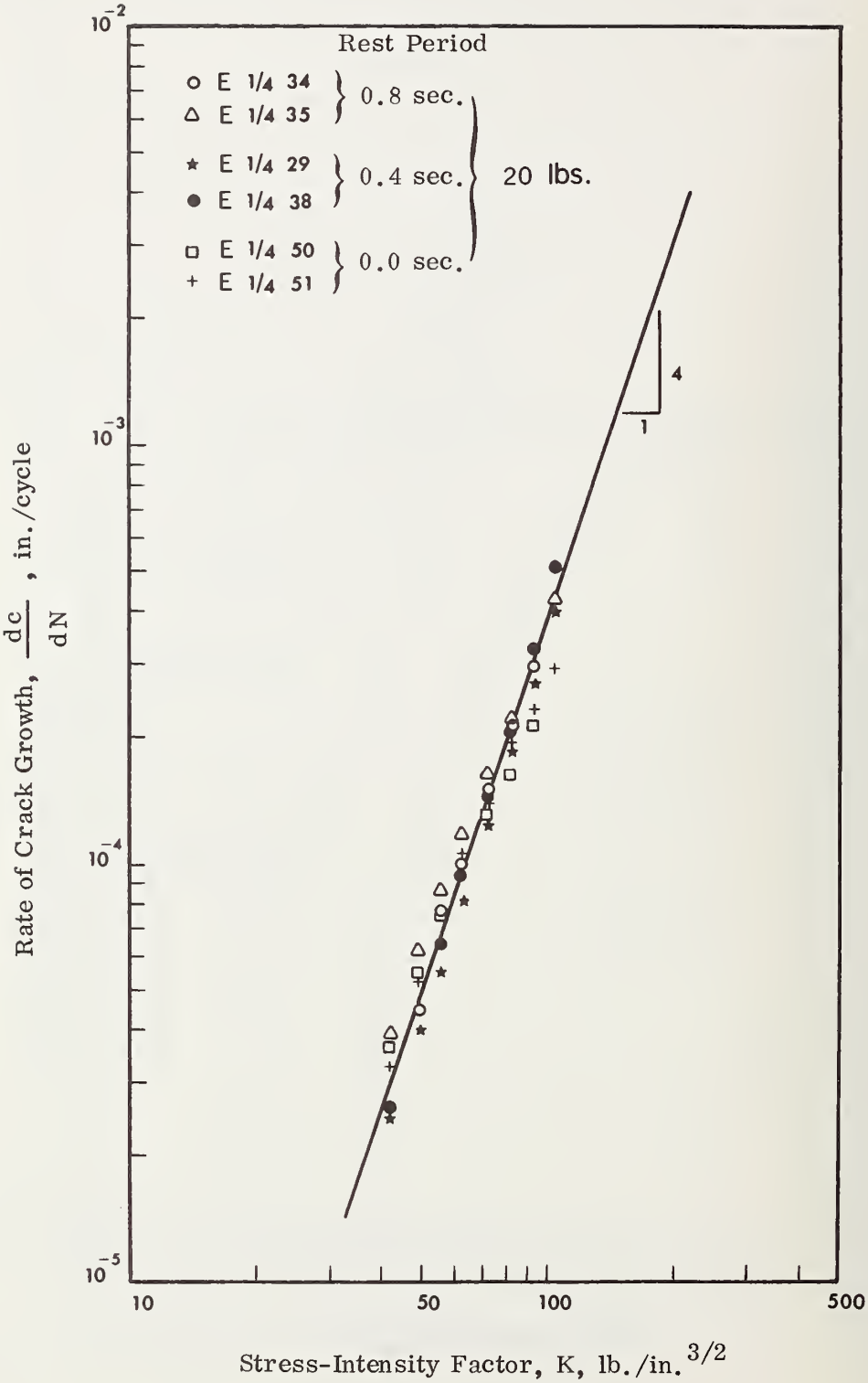

Figure 3.19. K versus $\frac{dc}{dN}$, for 20 lbs. Monotonic Loading with Different Frequencies

periods investigated, this paramter is not of great significance on the crack growth process.

D. Experimentation on Slabs Supported on an Elastic Foundation

Having verified experimentally the effect of loads of variable amplitude on beams on an elastic foundation, and having checked the stress distribution in a cracked slab by means of the determination of the stress-intensity-factor as has been reported previously, it is then possible to proceed with the task of studying the fatigue behavior of slabs supported on an elastic foundation subjected to loads of variable amplitude.*

(1) Loading Function

In this series of tests the slabs were subjected to repetitive loading using the MTS in the load control mode. The loading function used consisted of a half-sine function with a duration of 0.1 second. The magnitude of the loads varied from 200 to 500 pounds, corresponding to a rate of loading of approximately 35 to 50 miles/hours. The rest period or time between two consecutive load pulses, as well as the amplitude of each load pulse was controlled by an auxiliary function generator and a "data-track" connected to the MTS system and capable of suppressing the half-sine functions appearing in between successive loads.

---

*Experimental details are presented in Chapter IV and in Appendix

The experimental program, conducted at room temperature (77.5°F), consisted of the following types of loading conditions:

(a) Constant Loading

Fatigue tests were conducted under a half-sine loading function with an 0.1 second duration and rest periods of 0.8 and 0.4 seconds (Figures 3.20 and 3.20).

(b) Sequential Loading

In these tests, half-sine loading functions with a 0.1 second duration and an 0.8 rest period were used. Four loading sequences were tested. The first sequence consisted of a block of loads of 9 cycles; 3 with amplitude of 200 pounds, then 3 cycles with amplitude of 300 pounds and finally 3 cycles of 400 pounds (Figure 3.22). In the second sequence the loading block was programmed with 3 cycles of 400 pounds, plus 3 cycles of 300 pounds, plus 3 cycles of 200 pounds (Figure 3.23). Both of these sequences were different than those used in the beam tests in that the block of loads consisted of 9 cycles instead of 3. The reason behind this change was to have a larger block of loads, as large as the testing equipment could provide.

The third sequence consisted of a block formed by 8 cycles of 250 pounds and 1 cycle of 500 pounds (Figure 3.24). The final sequence used consisted of testing the asphalt slabs with blocks of loads programmed with 5 cycles of 300 pounds, plus 4 cycles of 400 pounds (Figure 3.25).

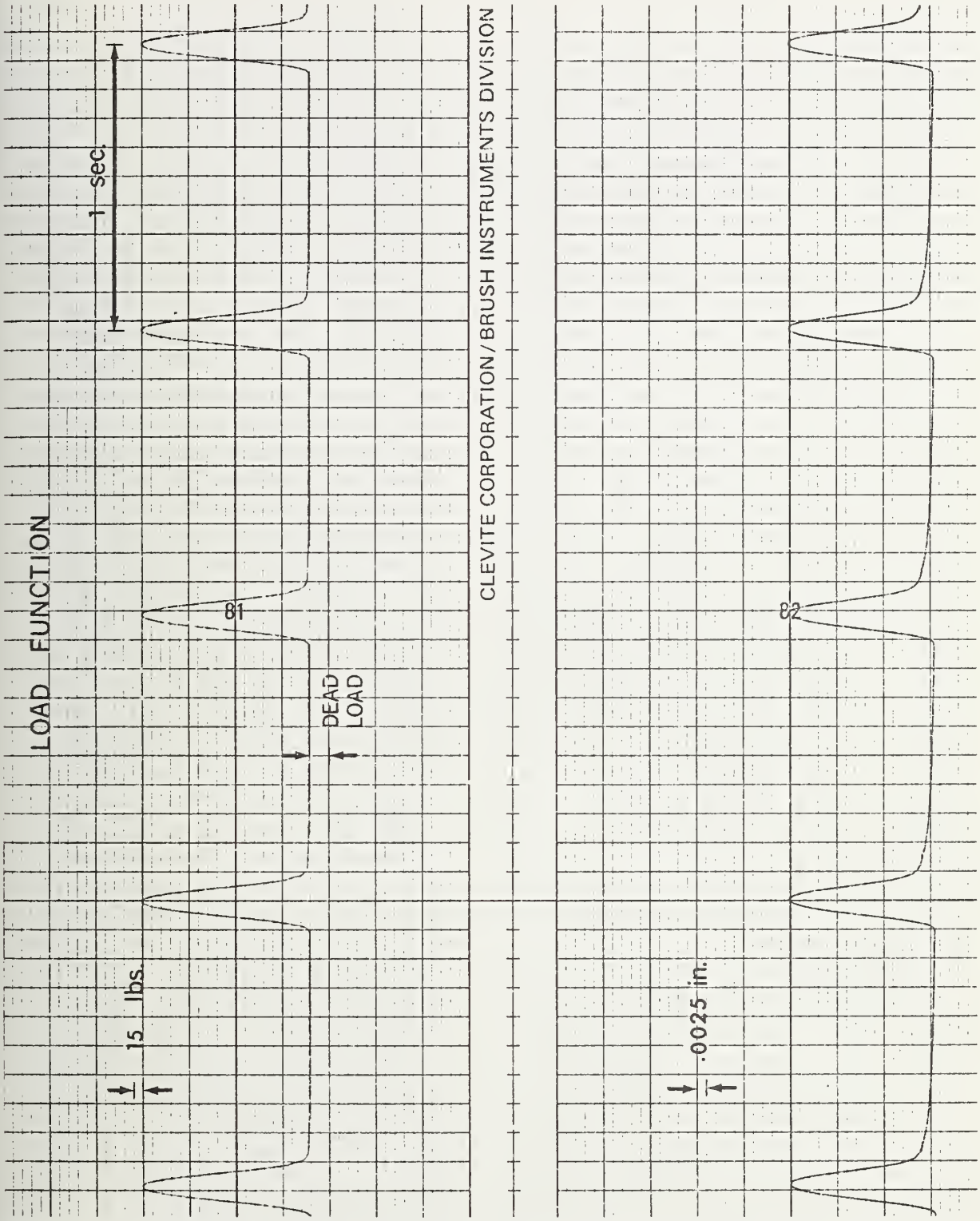

Figure 3.20. Loading Function for 300 lbs. Monotonic Load with Rest Period of 0.8 Second

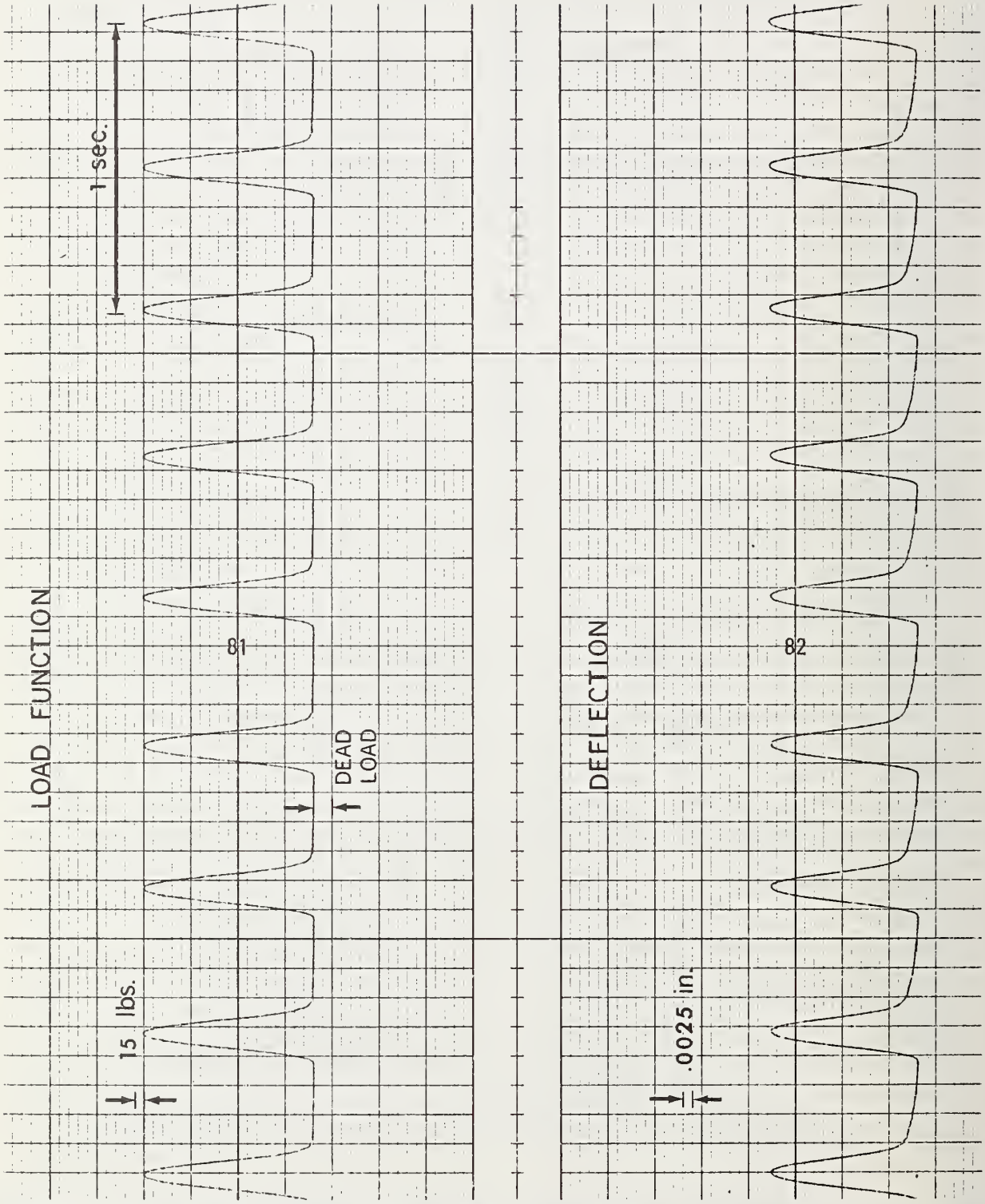

Figure 3.21. Loading Function for 300 lbs. Monotonic Load with Rest Period of 0.4 Second

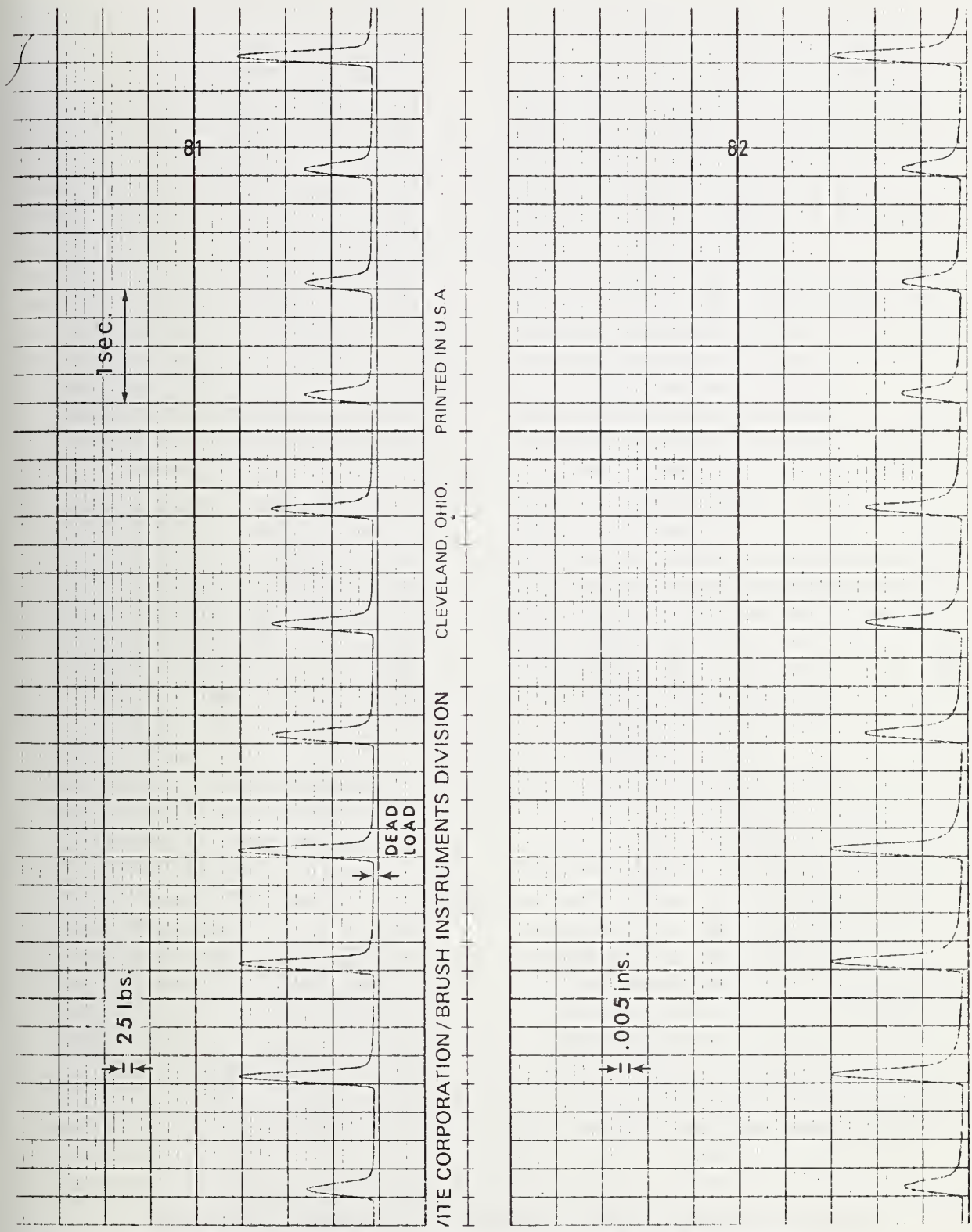

Figure 3.22. Loading Function for 3x400 + 3x300 + 3x200 lbs. Sequence

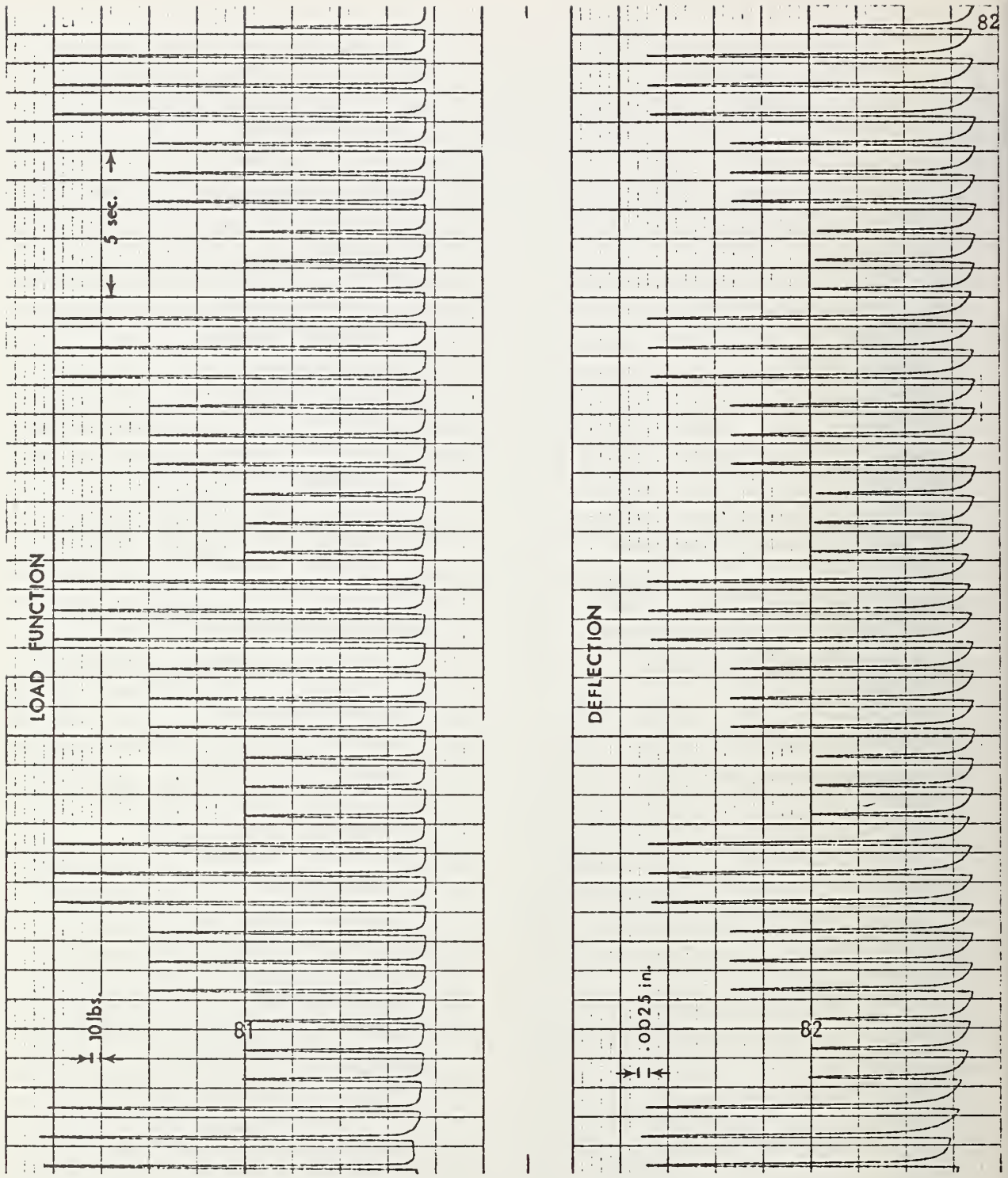

Figure 3.23. Loading Function for 3x200 + 3x300 + 3x400 lbs. Sequence

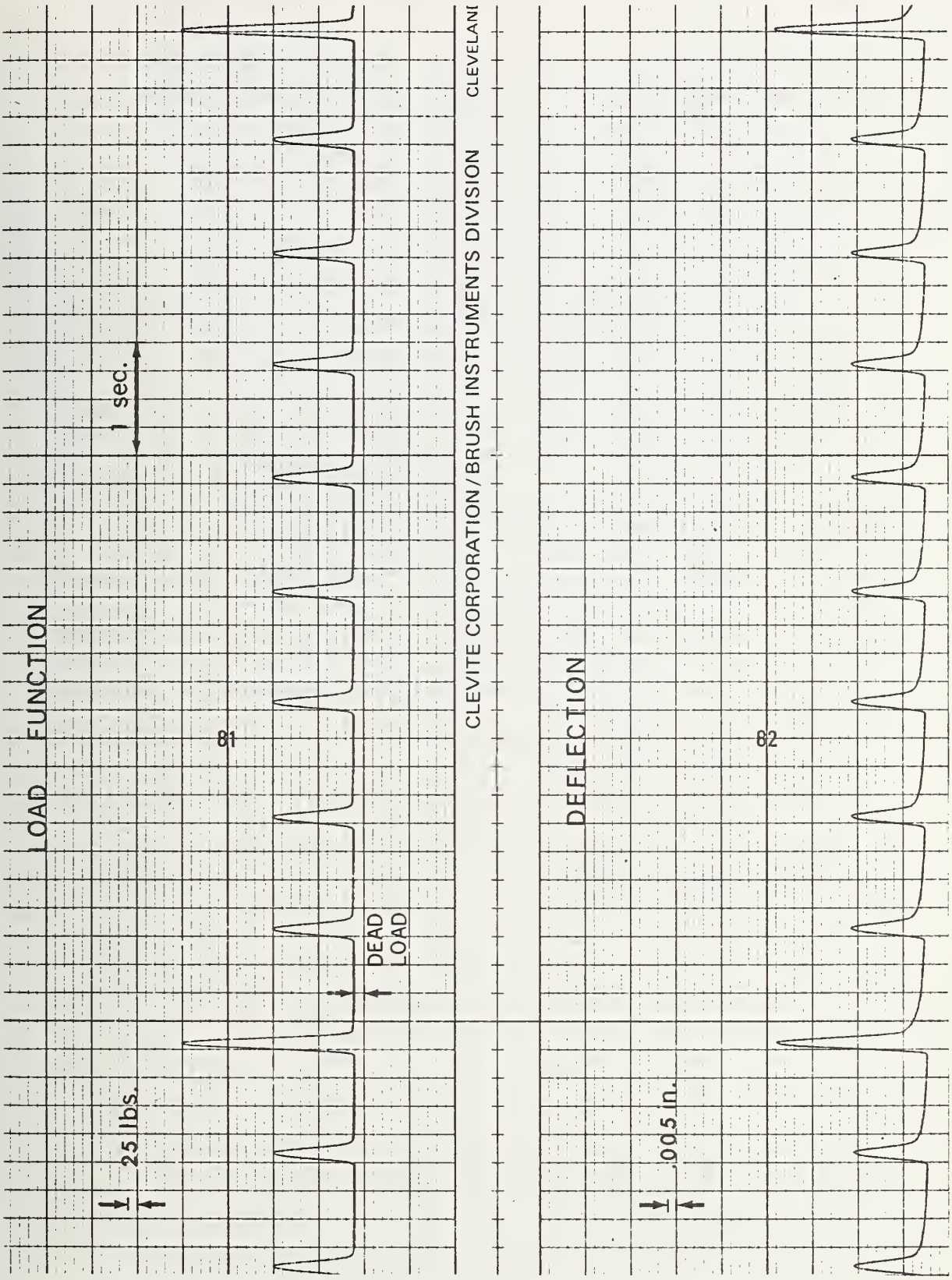

Figure 3.24. Loading Function for 8 x 250 + 1 x 500 lbs. Sequence

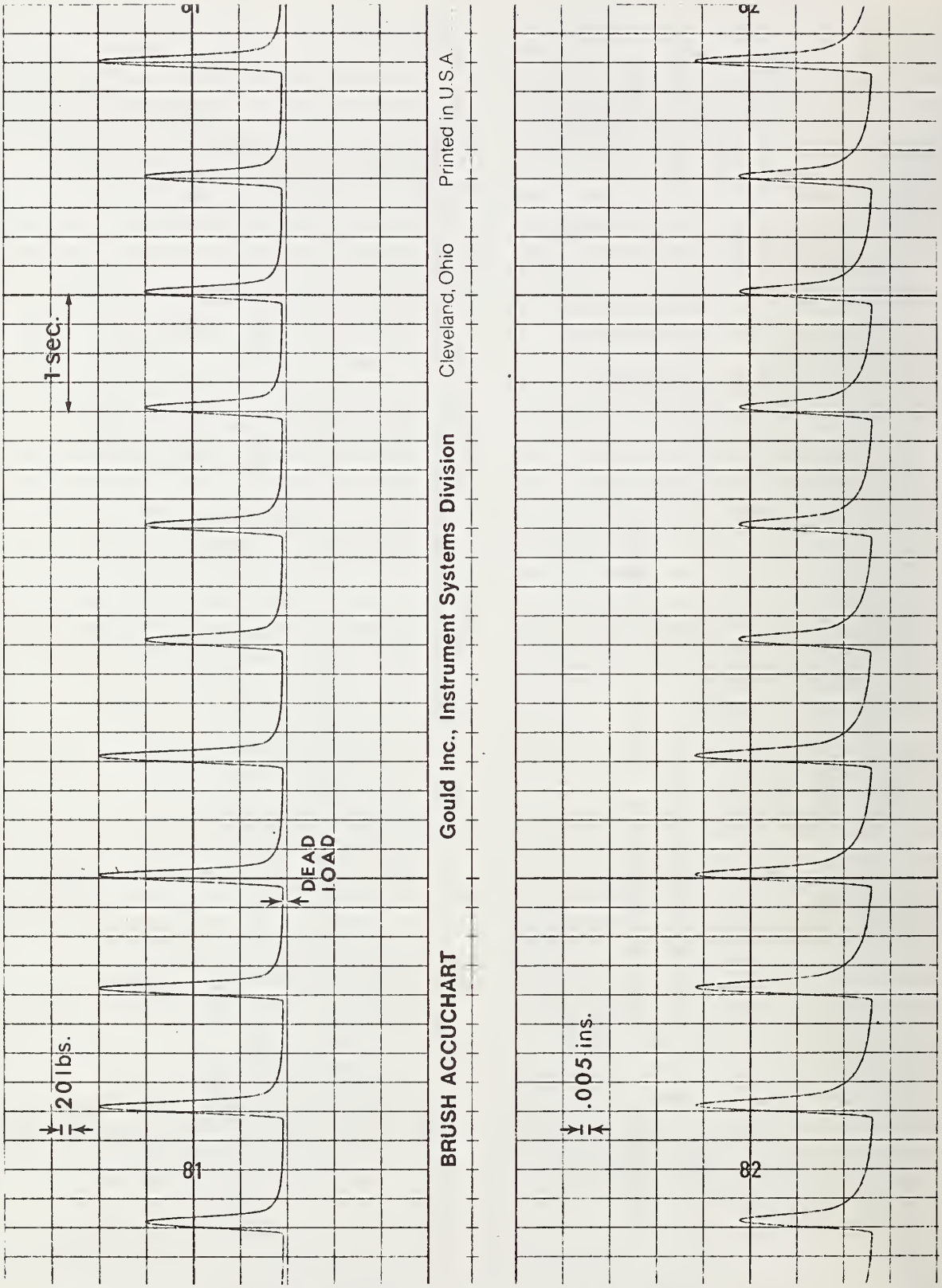

Figure 3.25. Loading Function for 5 x 300 + 4 x 400 lbs. Sequence

(2) Analysis and Discussion of Results

The characteristics of these tests were very similar to those reported in the Final Report of Project RF 2873 (15). Basically, the center deflection, measured by the MTS LVDT, increased steadily throughout the test and with very few changes. In the initial stages of the test there was, however, a rapid change in the deflection amplitude and this fact was probably attributed to some form of damping effect or due to strain hardening of the material under the loaded area.

Crack measurements were made using x-ray photographs to determine the length of the bottom cracks and an ink straining technique and to visually measure the crack length at the top surface of the slabs. To take an x-ray photograph of the slab, the fatigue test was halted for approximately forty-five minutes and the slab was removed from the foundation using a vacuum as has been described previously (15) and placing it under the x-ray machine. The x-ray photographs were taken at intervals of 80,000 to 100,000 cycles, or approximately one a day. Therefore, the rest period introduced by stopping the test for x-rays was not significant when compared with the total length of the test. Also, the center deflection, which became smaller after resumption of the test, recovered fully to its previous value after 2,000 to 3,000 cycles of load application.

The crack pattern observed in all tests was again very similar to that described in references (14, 15). Basically the cracks started at the bottom

surface (tension surface) of the slab and grew upwards through the thickness of the specimen in a semi-circular shape. After a considerable amount of time these cracks appeared at the top surface of the slab and from then on grew radially. The first set of radial cracks, called primary cracks, grew to a length of approximately 4 to 6 inches before the second set of radial cracks, called secondary cracks appeared in between the primary cracks. When both the primary and the secondary cracks stopped growing, a final set of cracks developed forming a circle concentric with the loaded area at a distance of approximately 6 to 8 inches from the center of the slab. This circumferential crack started at the top surface of the slab and grew downwards. At this stage the test was stopped and this condition was considered as the failure of the slab. Figure 3.26 shows a schematic diagram of the crack pattern in the slabs.

The rate of crack growth was studied individually for each crack or collectively as an average crack. This, of course, is a simplification to the problem of multiple cracks, but since the stress field of each crack is confined to a zone of radius much smaller than the crack itself, the analysis of the rate of crack growth can be done independently.

To determine the rate of crack growth, a plot of crack length versus the number of cycles was made for each test. In these plots the bottom cracks measured from the x-ray photographs are shown together with the top cracks, determined by visual measurements. It can be seen that throughout the test

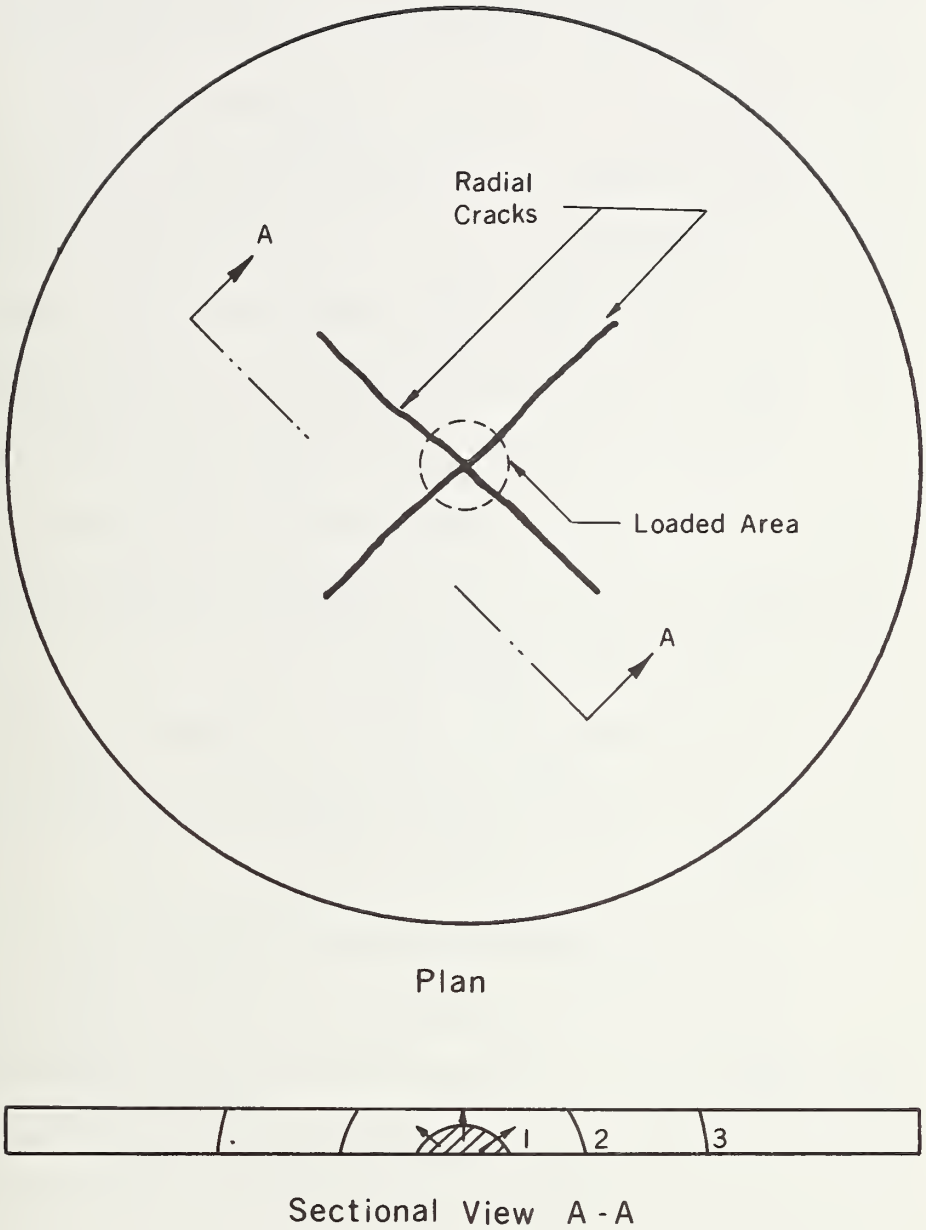

Figure 3.26. Probable Mode of Crack Propagation

the bottom cracks were longer than the top ones, as it would be expected since the bottom surface of the slabs was in tension, while the top surface was in compression. These plots also suggest the equilibrium shape of the cracks, with the bottom cracks being approximately $1\frac{1}{2}$ inches longer than the top cracks in the beginning of the tests. As the tests progressed, the difference in length between top and bottom cracks became smaller, and toward the end of the tests when the radial cracks had stopped growing, both top and bottom cracks had approximately the same length. This approximation of the equilibrium shape was used in a few tests where no x-ray photographs were taken in order to determine the length of the bottom cracks from the known length of the top cracks.

Having determined the rate of crack propagation, the next step was to arrive at a correlation between the stress-intensity-factor and the crack propagation rate.

(a) Effect of Rest Period on Crack Propagation

The rate of crack propagation in tests where the load was applied with a rest period of 0.8 seconds or 0.4 seconds, followed the relation expressed by Paris' law, and it was found that this rate was proportional to the fourth power of the stress-intensity factor.

Figure 3.27 shows the typical crack length versus number of cycles (c - N) curve for a test in which the rest period was 0.4 seconds, and Figure 3.28 presents the rate of crack growth versus the stress-intensity factor (dc/dN - K) relation.

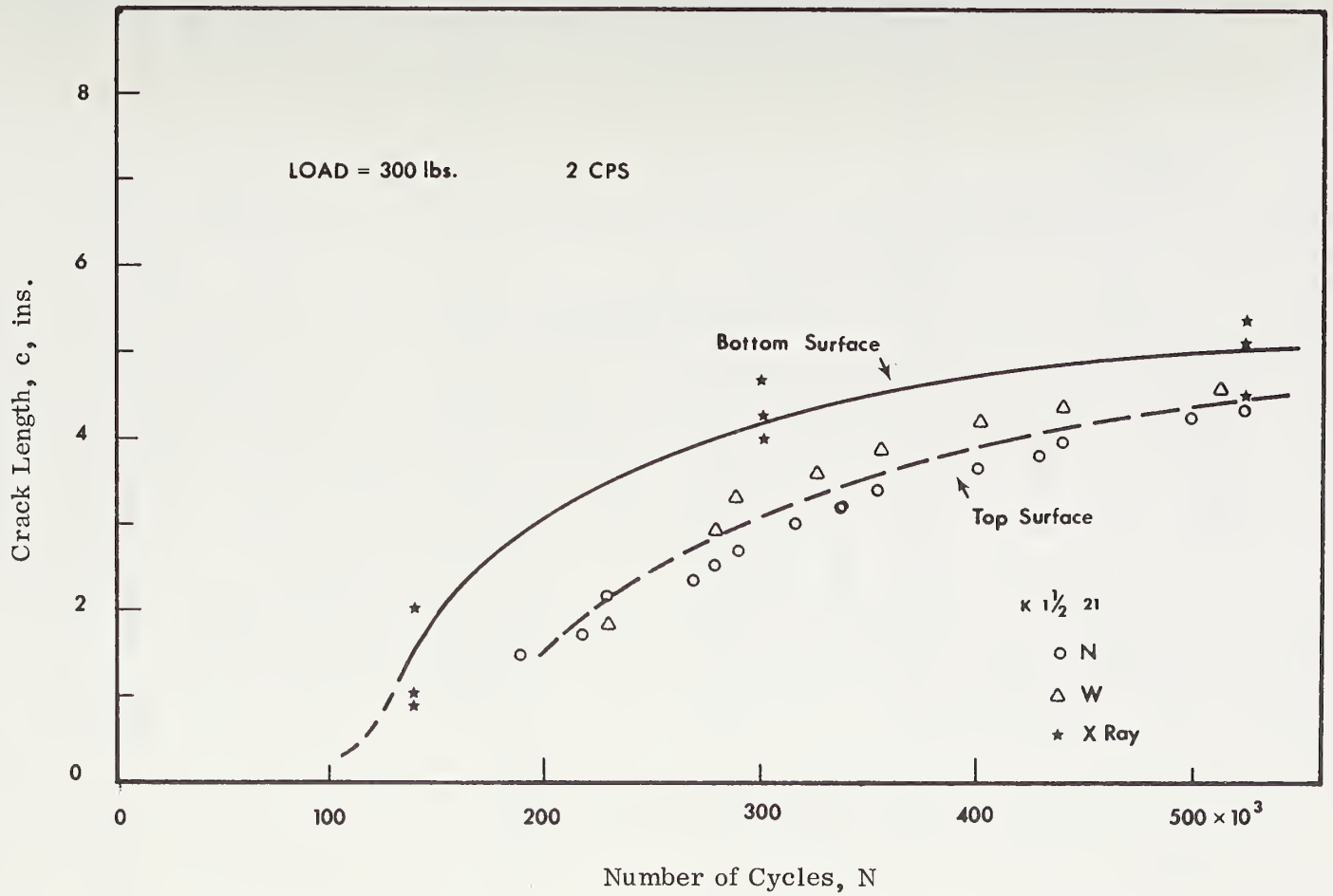

Figure 3.27. Crack Growth Curve Versus Number of Cycles for 300 lbs. Monotonic Load at 2 Cycles/Second

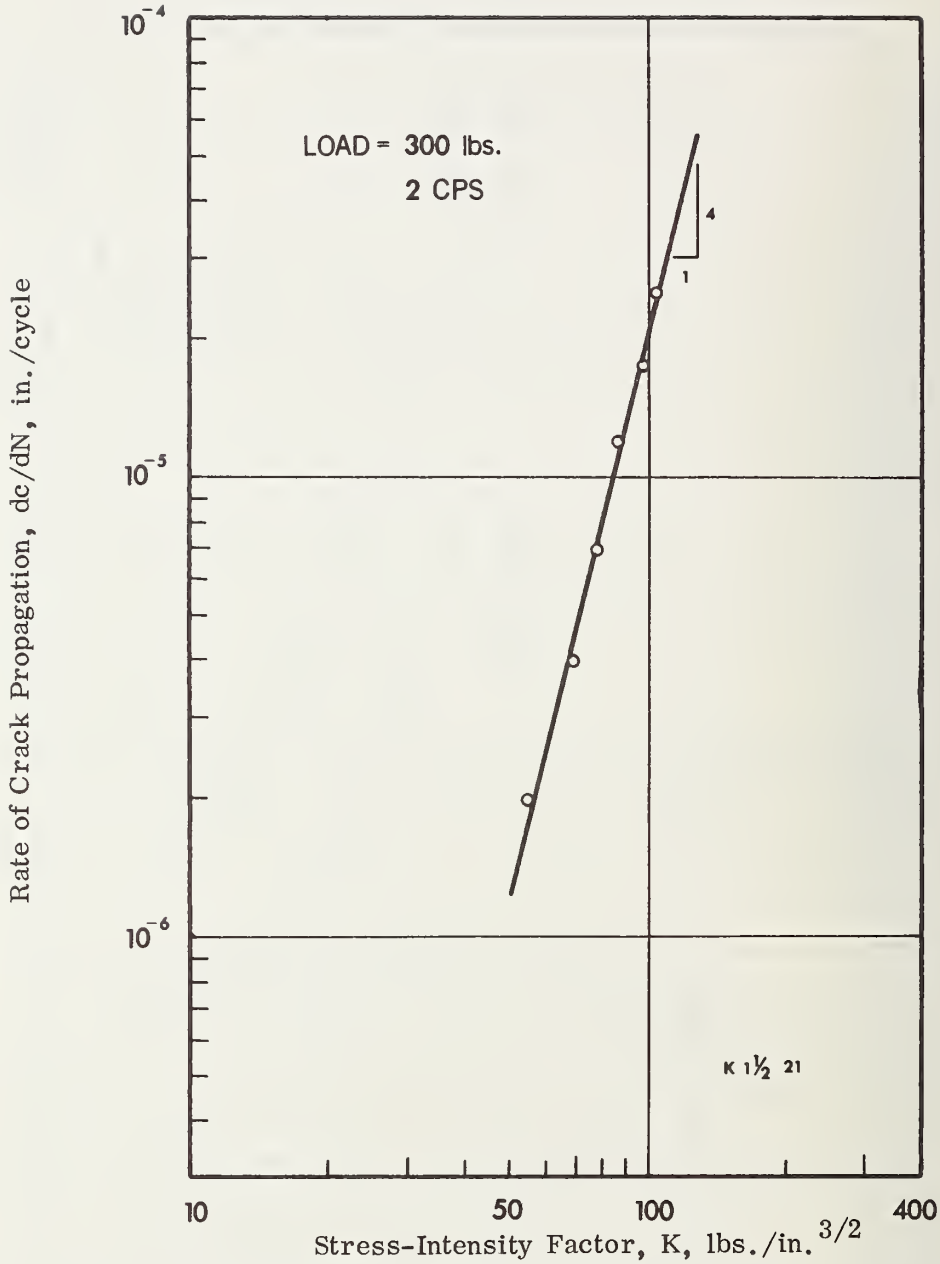

Figure 3.28. $\frac{dc}{dN}$ - K Relationship for 300 lbs. Monotonic Load at 2 Cycles/Second

It is noted that the same conclusion as to the validity of Paris' law of crack growth can be made from the test on a slab resting on an elastic foundation or a beam on elastic foundation. These two experimental systems behave similarly in regards to the effect of rest period on the fatigue crack propagation. Therefore, the rest period or headway between two vehicles using a highway has no major significant effect on the rate of crack propagation. Obviously this conclusion cannot be extrapolated for a wide range of rest periods encountered in the real pavements, which have not been tested. However, as stated by Paris (18), the constant A, in the expression of the rate of crack propagation (Equation 2.14) can take into account the effect of this load variable. Therefore, the effect of rest period can be experimentally evaluated for any desired range.

(b) Effect of Load Sequence

To verify the effect of load sequence and the existance of the delay effect in bituminous paving mixtures, four loading sequences were tested on slabs resting on an elastic foundation. Three of these sequences were equal or similar to those used in the tests on beams on an elastic foundation, and the fourth sequence was programmed with a change in load amplitude no greater than 25%.

Figures 3.29 and 3.30 present the crack growth versus number of cycles (c - N) curve for the sequences of $(3 \times 200 + 3 \times 300 + 3 \times 400)$ pounds forming a block of load and $(3 \times 400 + 3 \times 300 + 3 \times 200)$ pounds respectively. In

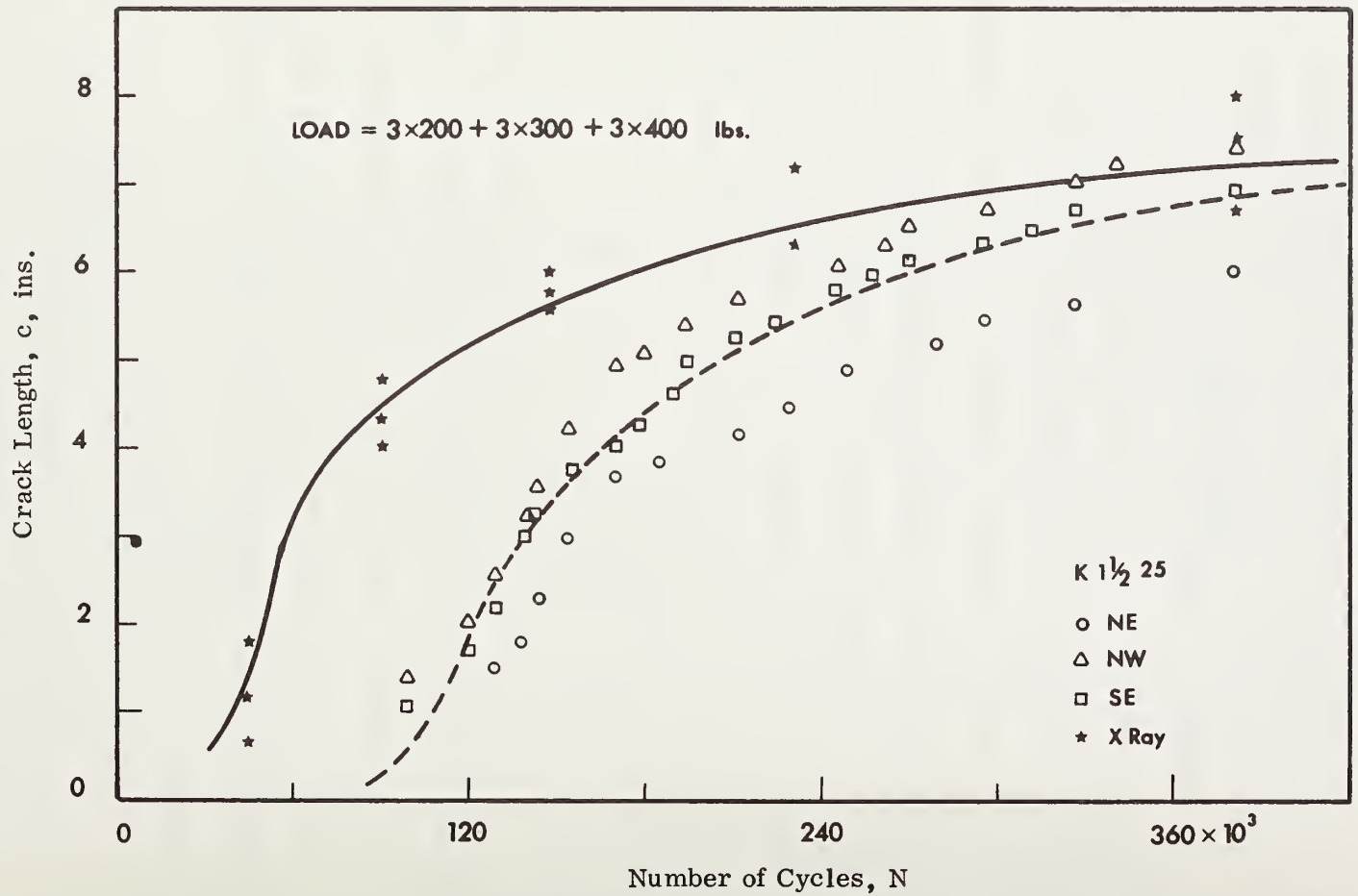

Figure 3.29. Crack Growth Curve Versus Number of Cycles for 3 x 200 + 3 x 300 + 3 x 400 lbs. Sequence

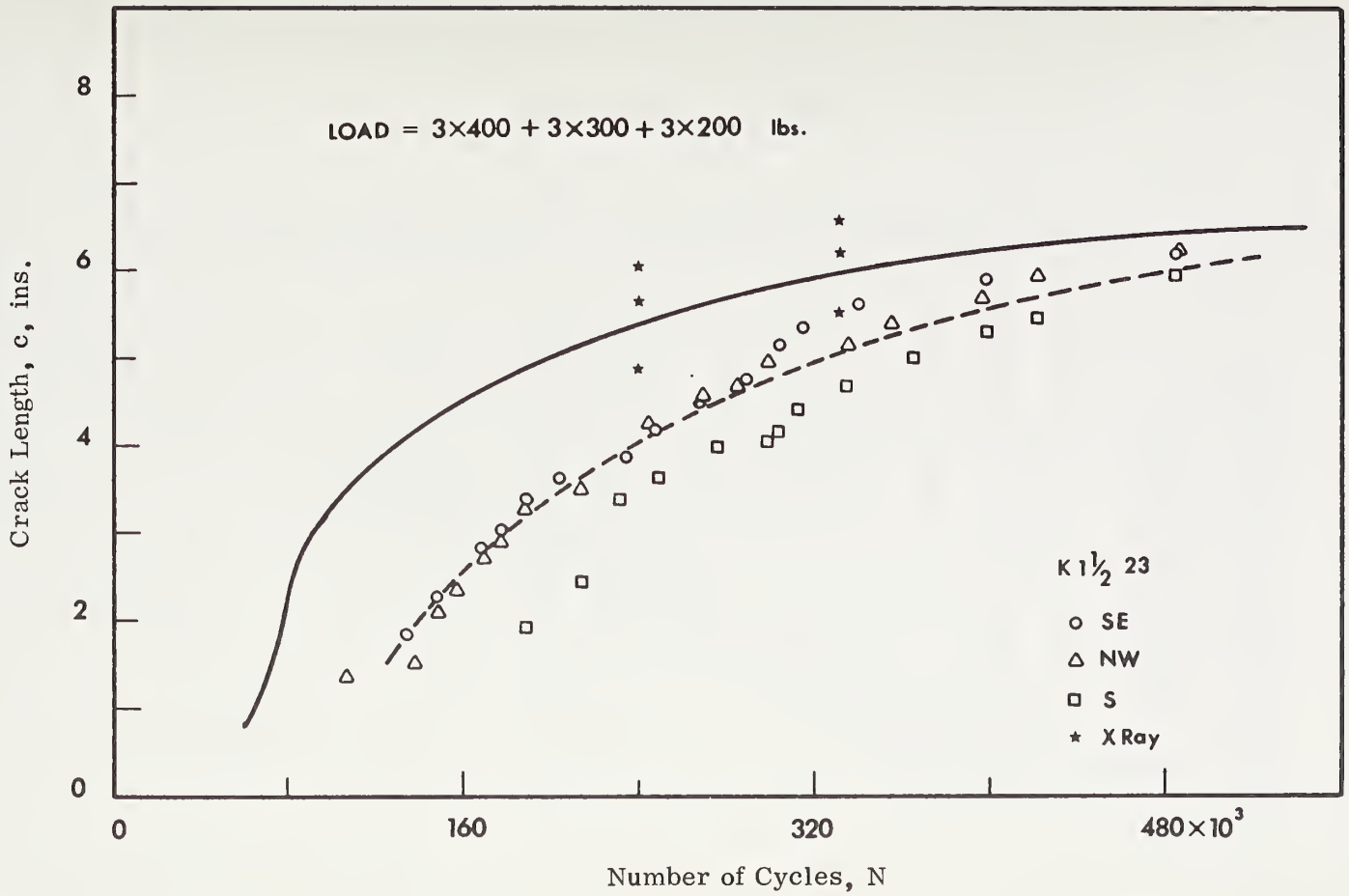

Figure 3.30. Crack Growth Curve Versus Number of Cycles for 3 x 400 + 3 x 300 + 3 x 200 lbs. Sequence

those figures both the top crack measurements made visually and the bottom crack lengths obtained by x-ray photographs are plotted. From these curves the rate of crack growth (dc/dN) was calculated and the results were plotted versus the stress-intensity-factor divided by load (K/P) as was done for the beam tests. The results are presented in the plot of (dc/dN - K/P) (Figure 3.31). It is noted that the delay in the crack propagation rate under similar loading functions are similar when the results of beams and slabs are compared. This again is an indication that the effect of load sequence substanially alters the rate of crack propagation. Secondly, it is significant to note that the same result was obtained from tests on beams on an elastic foundation, despite the fact that the block of loads in the sequences used in the tests on slabs was slightly bigger than that used in the beam tests.

The results from the tests using the sequence of 8 cycles of 250 pounds plus one cycle of 500 pounds are presented in Figures 3.32 and 3.33. The first shows the (c - N) curve with top and bottom cracks, and the second presents the rate of crack propagation versus the stress-intensity-factor divided by load (dc/dN - K/P). For this sequence, also used in the beam on elastic foundation tests, there is again a delay in the rate of crack propagation. This reduction in the crack growth rate has been associated with the effect of residual stresses and the elastic-plastic state formed at the tip of the crack after a high load is applied. From these results presented, it is noted that the rate of crack propagation presented is identical for beams and slabs and the effect

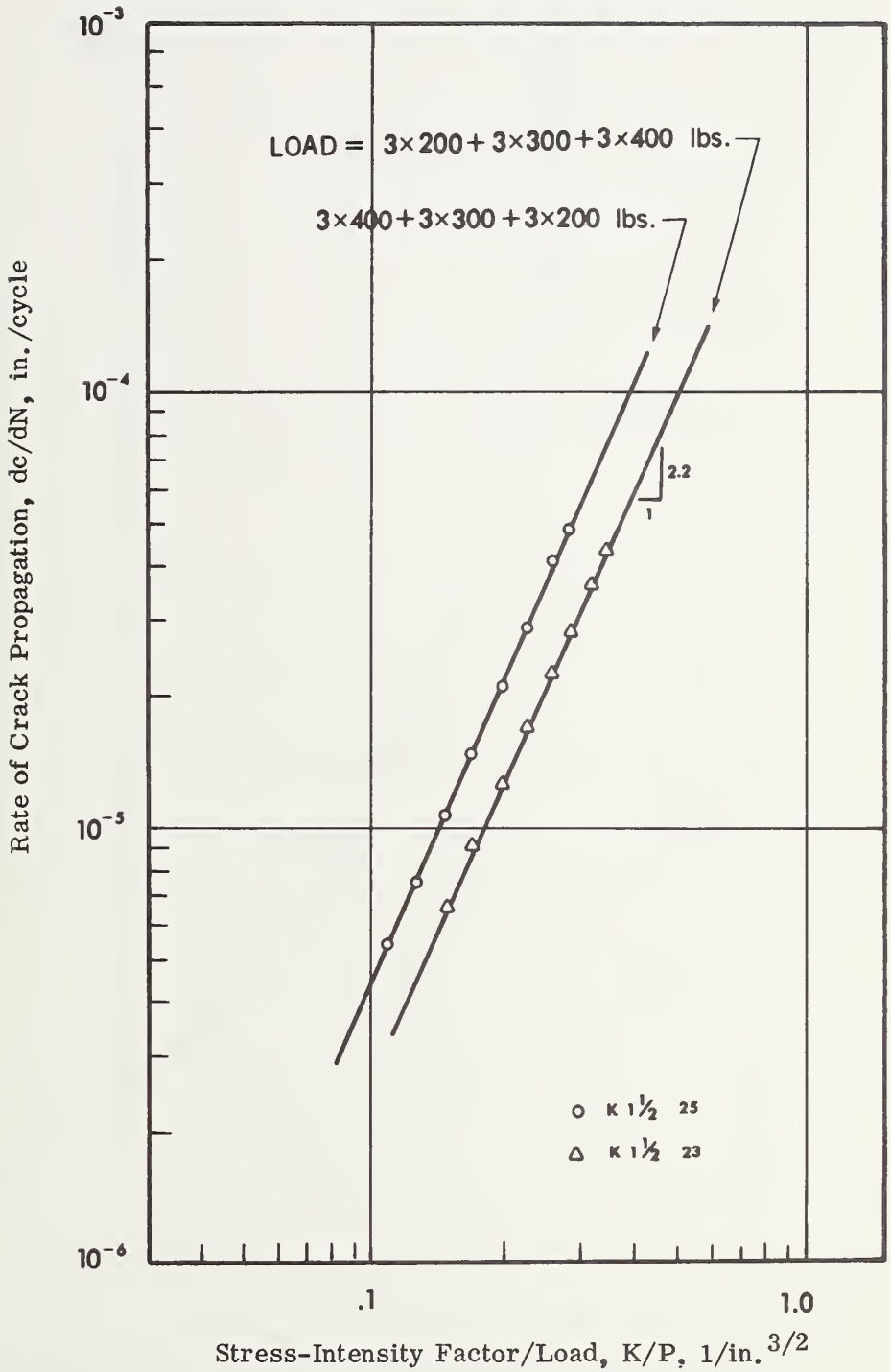

Figure 3.31. $\frac{dc}{dN} - \frac{K}{P}$ Relationship for 3 x 200 + 3 x 300 + 3 x 400 lbs. and 3 x 400 + 3 x 300 + 3 x 200 lbs. Sequence

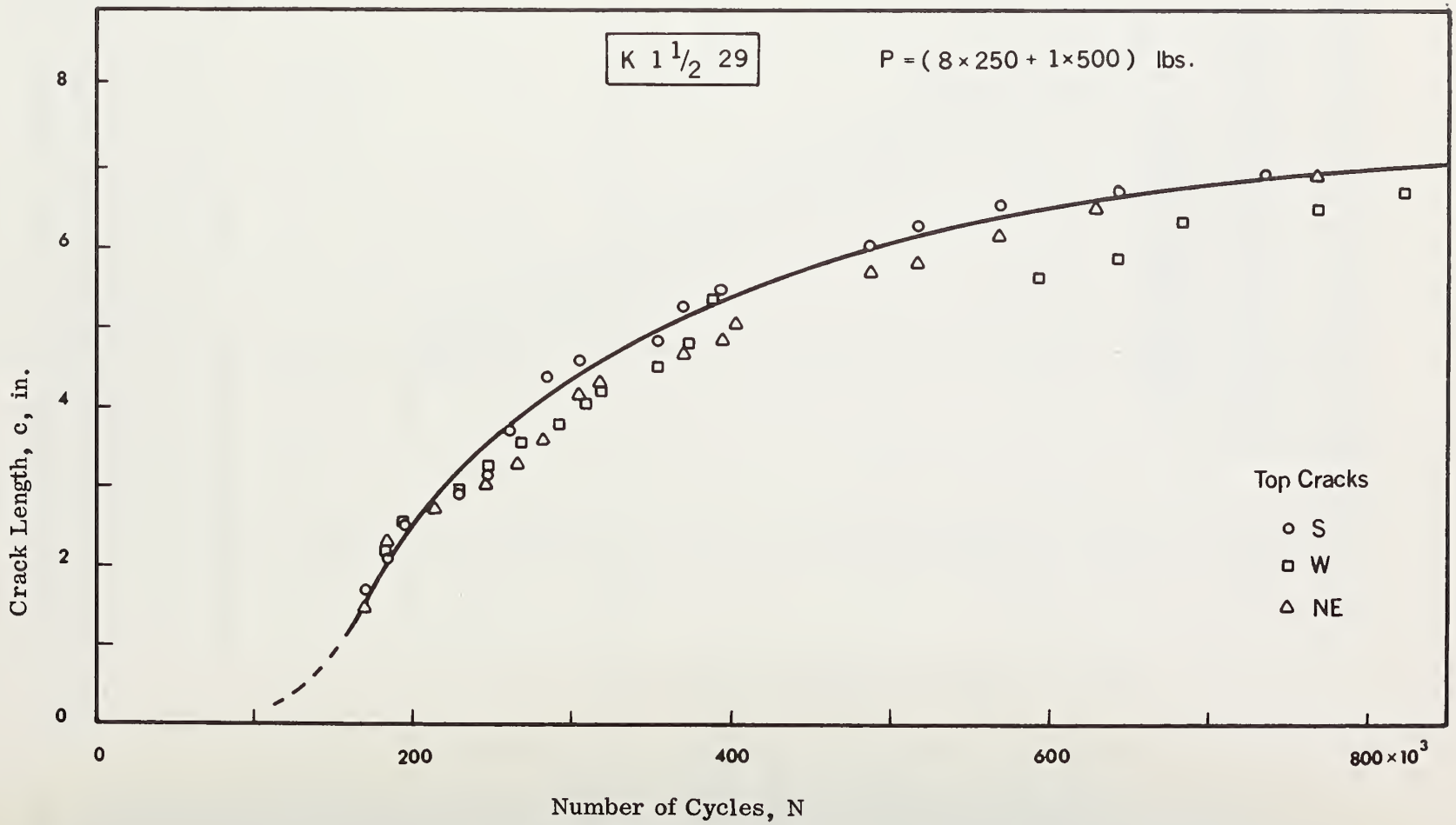

Figure 3.32. Crack Growth (Top Cracks Only) Versus Number of Cycles for 8 x 250 + 1 x 500 lbs. Sequence

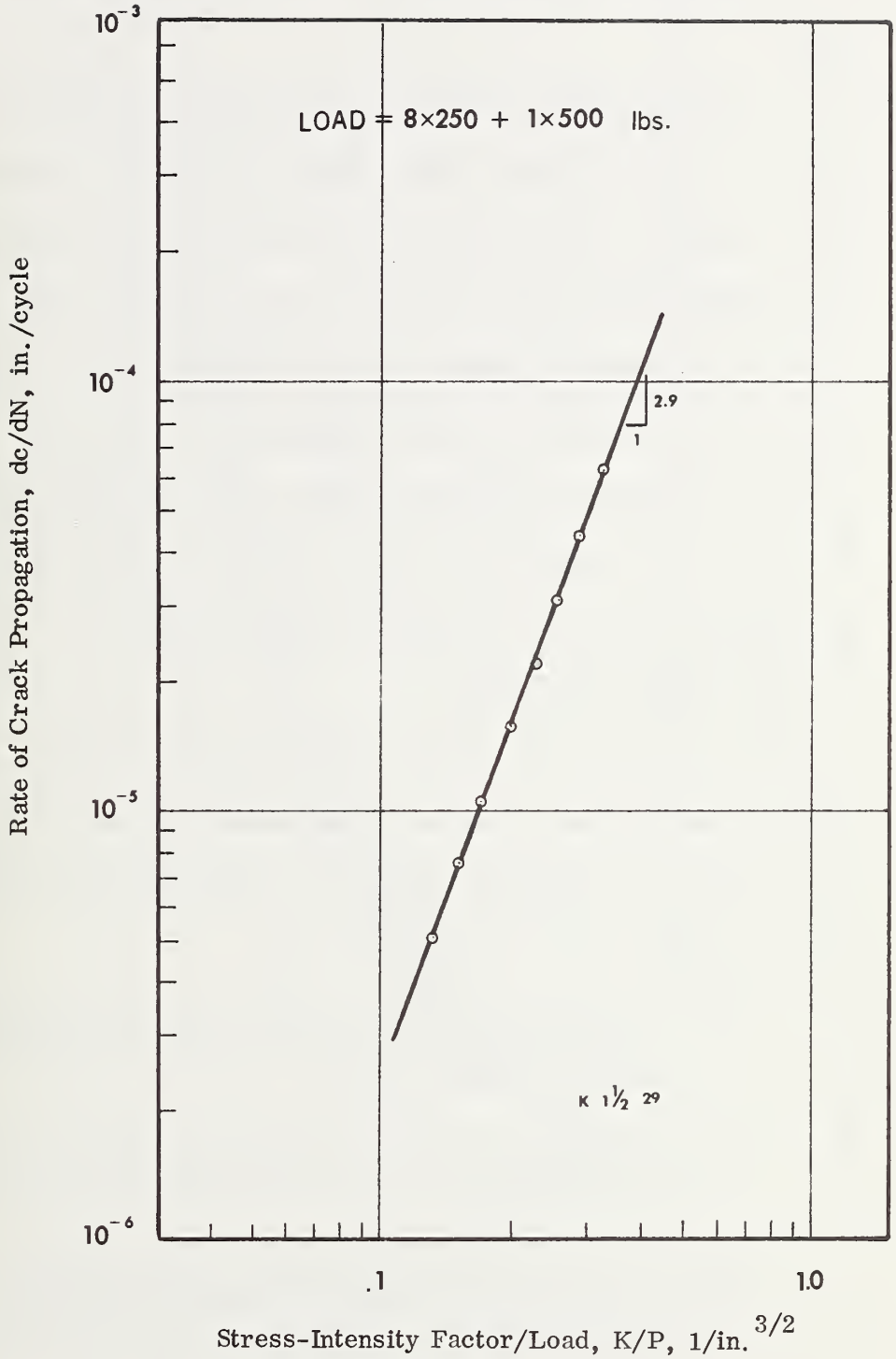

Figure 3.33. $\frac{dc}{dN} - \frac{K}{P}$ Relationship for 8 x 250 + 1 x 500 lbs. Sequence

of load sequence can be established by testing a beam on an elastic foundation.

The final loading sequence used consisted of 5 cycles of 300 pounds plus 4 cycles of 400 pounds. This loading sequence is the one that approaches more closely the case of loads of constant amplitude. In fact, the results presented in Figures 3.34 (c - N) curve, and 3.35 (dc/dN - K/P) relation, show that although the sequence also caused a delay in the rate at which the cracks grew, this delay was smaller than any of the other sequences used. That is to say that the smaller the variation in the load amplitudes, the closer the rate of crack propagation will follow Paris' law, with dc/dN being proportional to the fourth power of the stress-intensity factor.

(3) Significance of Results

In this chapter, the effect of variable loading functions on the crack propagation of asphaltic mixtures was presented. The experimental variables investigated included specimen geometry, load amplitude and load sequence. The conclusions reached from this study are:

(i) The effects of variable loading on the crack propagation is identical for beams on elastic foundation and slabs resting on elastic media.

(ii) The fatigue crack growth process in asphaltic mixtures is considered as a stress-independent, stress-interaction type phenomena.

(iii) It has been observed that for the range of variables investigated, the rest period does not significantly affect the fatigue life.

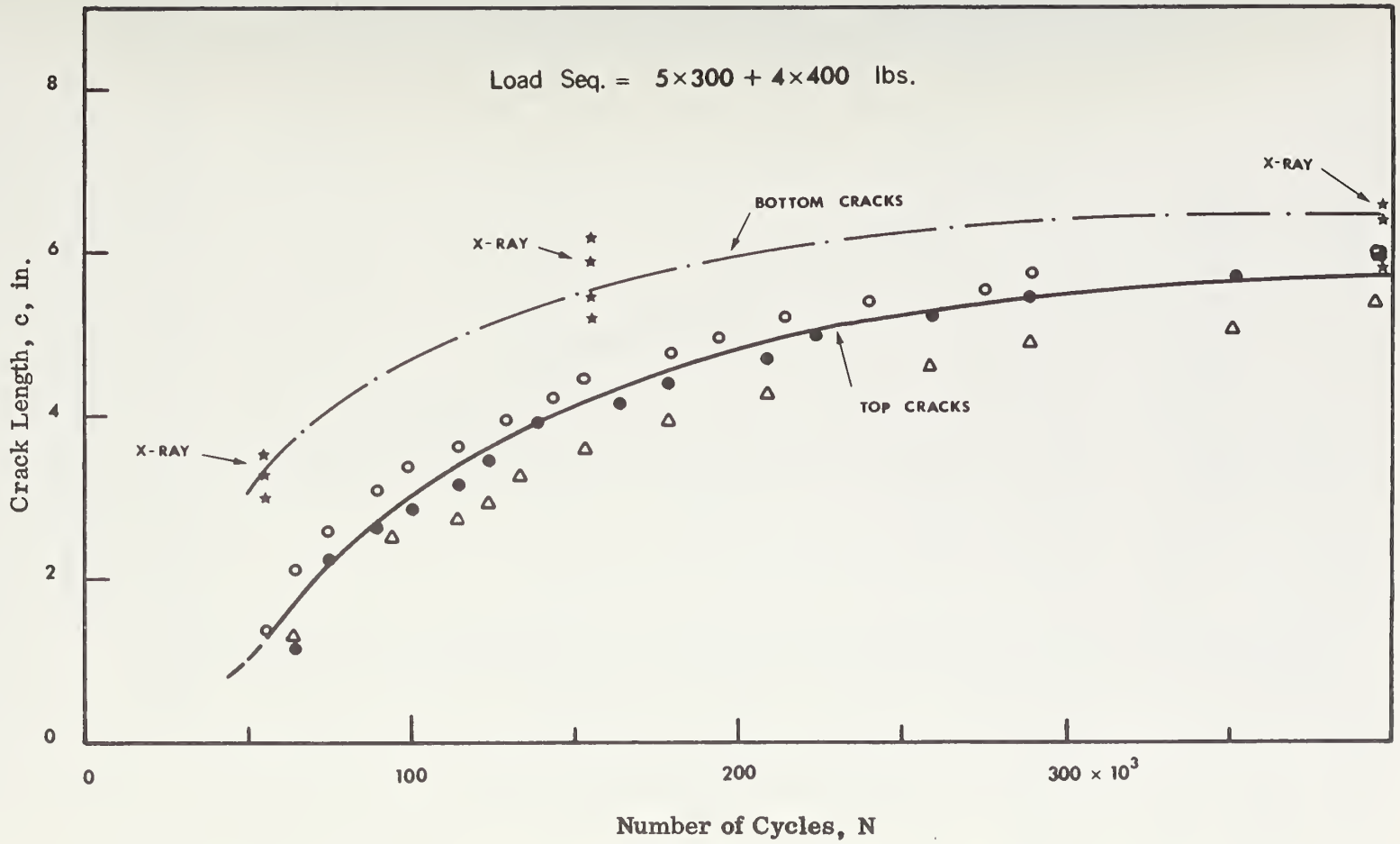

Figure 3.34. Crack Growth Versus Number of Cycles for 5 x 300 + 4 x 400 lbs. Sequence

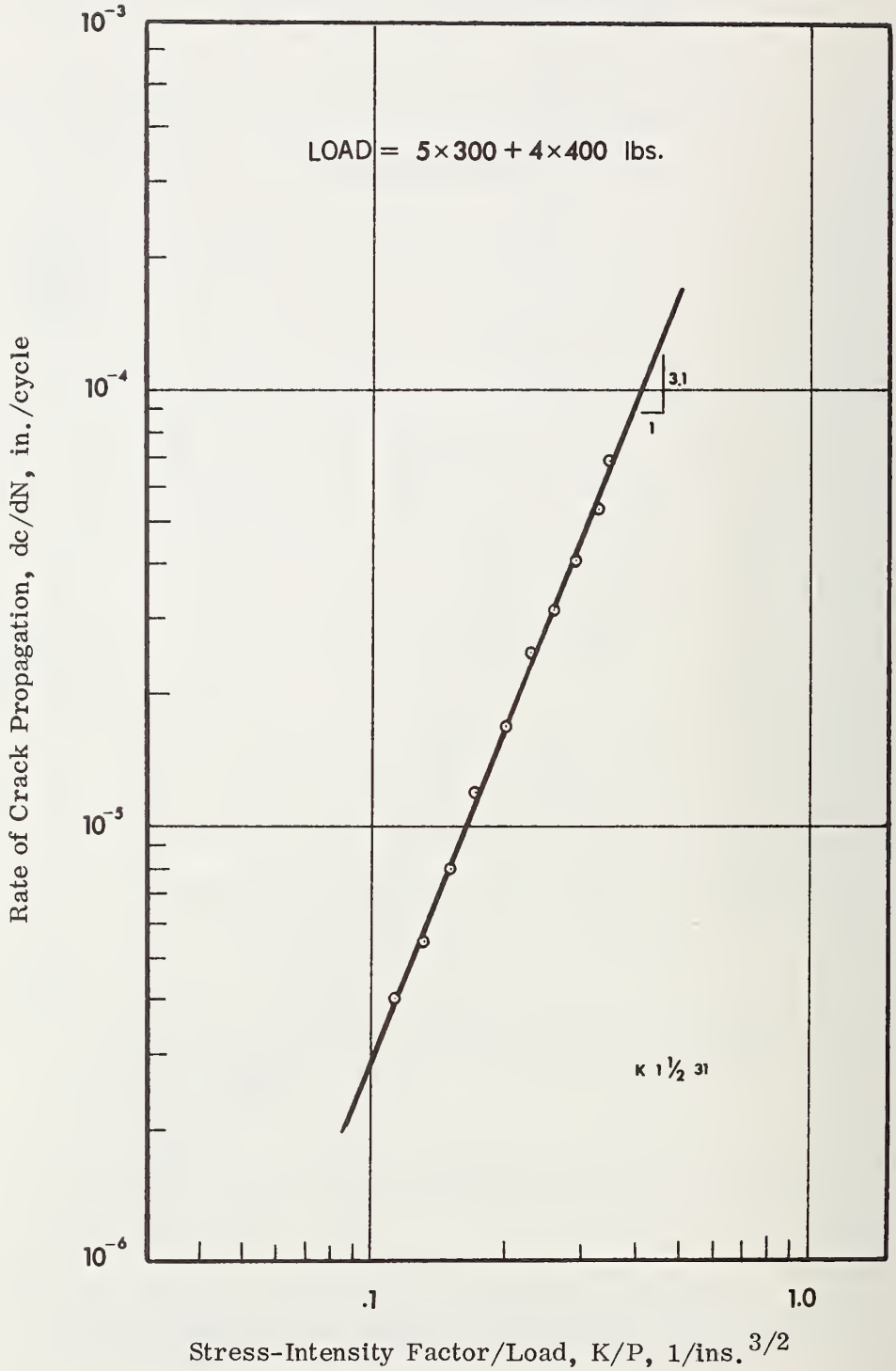

Figure 3.35. $\frac{dc}{dN} - \frac{K}{P}$ Relation for 5 x 300 + 4 x 400 Sequence Loading

(iv) It has been shown that load sequence has a significant affect on the fatigue life. The delay in the rate of crack propagation due to loads of variable amplitude in the loading sequence is attributed to the beneficial effects of residual stresses at the crack tip. Although the mathematical formulation of the delay phenomena has not yet been fully developed, the reduction in the crack growth rate can be evaluated experimentally.

(v) A comparison of the experimental data using dc/dN - K/P relation with the Paris crack growth law indicates that the use of Paris' equation for design purposes leads to a conservative estimate of the fatigue life.

These conclusions will be further elaborated in the final chapter of this report where a tentative outline of a method for flexible pavement design is presented.

CHAPTER IV

THE EFFECT OF TEMPERATURE ON FATIGUE CRACK PROPAGATION

A. Introduction

In the previous chapter, the effect of variable loading functions on the fatigue crack propagation of pavements was investigated. It is well-known that pavement systems during service life are subjected not only to variable loads but also to variable temperature conditions. In this section, the validity of mechanistic method of fatigue design at various temperature conditions is investigated and guidelines pertinent to environmental factors are developed.

In order to incorporate the effect of environmental parameters into a rational design concept the following prerequisites must be fulfilled: (i) determination of temperature distribution within pavement system, (ii) determination of the effect of temperature on material properties, and (iii) selection of a suitable distress model capable of predicting the pavement response under extreme environmental conditions.

The analysis of temperature distribution within pavement systems has been researched and fully documented in the literature. Most recently, Dempsey (44) has developed a heat transfer model for evaluation of the temperature related effects in multi-layered pavement systems using the finite difference method. Wilson and Nickel (45) have developed a finite element

program for heat conduction analysis. These analyses are based on the energy balance equation at the pavement surface which considers the effects of incident short wave radiation, long wave radiation emitted by the atmospher and pavement surface, convective heat flow, the heat flux due to condensation, evaporation, etc. and finally the head conduction in the soil.

It has been found that heat flux due to solar radiation received at the ground surface accounts for the largest portion of the flux. Although, theoretically this parameter can be calculated and can be expressed in terms of location and time variables, empirical equations have been developed for practical application.

Utilizing transient heat flow equation with appropriate boundary conditions and thermal properties of pavement materials, temperature distribution within pavement systems can be accurately predicted. Therefore, for rational pavement design purposes, the temperature field at a given point of a pavement structure can be easily calculated.

Secondly, with respect to the effect of temperature on the material properties, extensive laboratory and theoretical data are available to provide an accurate measure of the temperature dependency of paving mixtures. The final task, therefore, involves the incorporation of temperature depedent material variables into a suitable distress model capable of predicting pavement performance. Before this could be achieved, however, the validity of the distress model for the range of parameters involved must be verified. The distress

model selected for this investigation, as has been indicated previously, is a crack propagation law in which the rate of crack propagation is expressed in terms of stress-intensity factor. In this section, the validity of the proposed distress model at three temperatures (41°F, 77°F and 90°F) is discussed.

B. Verification of the Proposed Model at 77.5°F

The previous research conducted at the Ohio State University under contract FH-11-7281, RF 2873 and FH-11-7257, RF 2845 (11,15), have been primarily concerned with the verification of fracture mechanics at 77.5°F. The results of these studies, as shown in Figures (4.1,4.2 ,4.3), lead to the following conclusions:

(i) Tests on sand-asphalt beams, simply supported and loaded at mid-span, conducted at 77.5°F, showed that there was considerable interaction between creep and fatigue. To minimize the amount of creep and simulate more realistic conditions, the beams were supported on an elastic foundation.

(ii) The results of the tests on beams supported on an elastic foundation provided futher verification of the crack propagation law. The prediction of the fatigue life was independent of the method of loading (controlled stress or controlled strain).

(iii) Experiments on asphalt concrete beams supported on an elastic foundation and performed at 77.5°F, also showed excellent correlation with the crack growth law.

(iv) Sand-asphalt slabs (44 inches in diameter) were tested on an elastic foundation at 77.5°F, provided further verification of the validity of Paris' law. The value of the constant A was found to be approximately the same as the value for the sand asphalt beams of the same composition as the slabs, showing that A was indeed a property of the material.

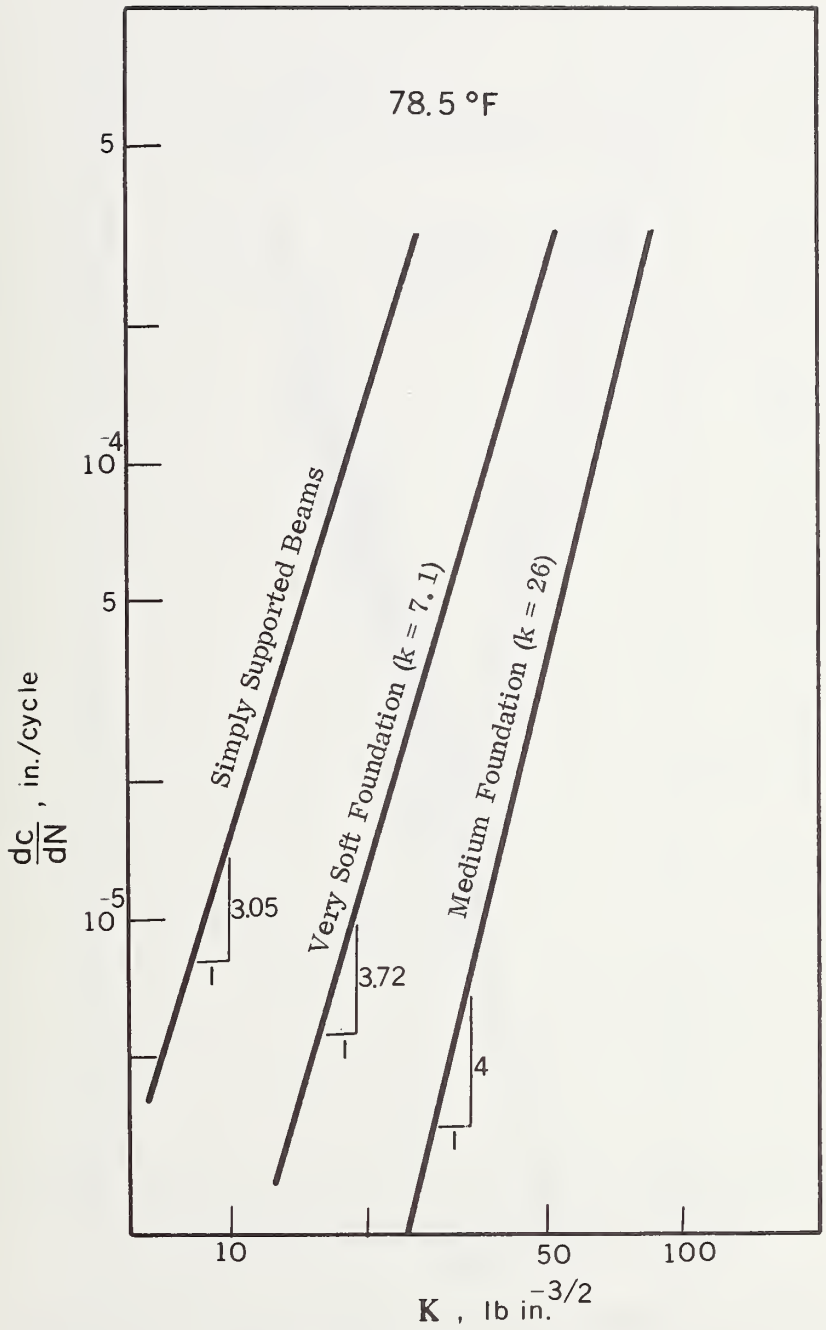

Figure 4.1. Comparison of Rates of Crack Propagation in Simply Supported Beams and Beams on Elastic Foundation

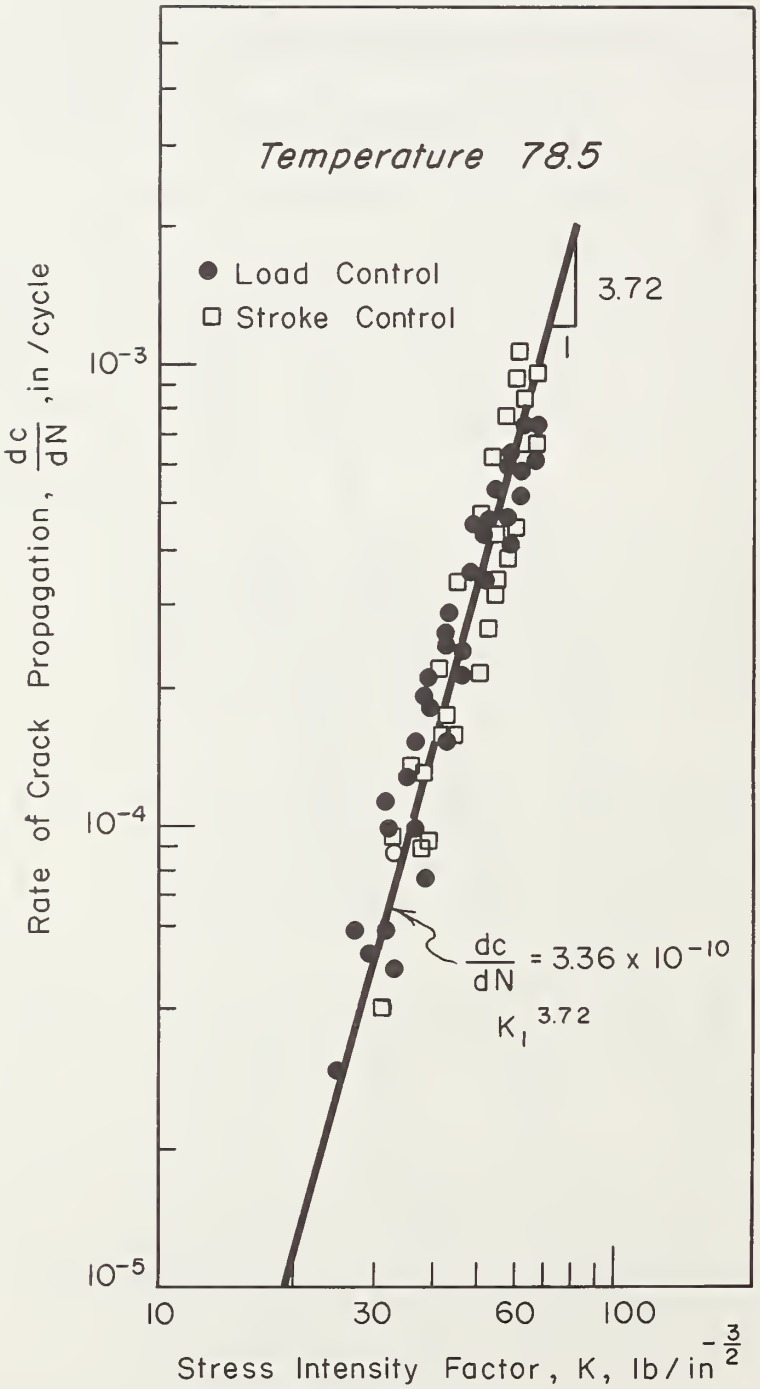

Figure 4.2. $\frac{dc}{dN}$ - K Relation for all Beams on Elastic Foundation Tests

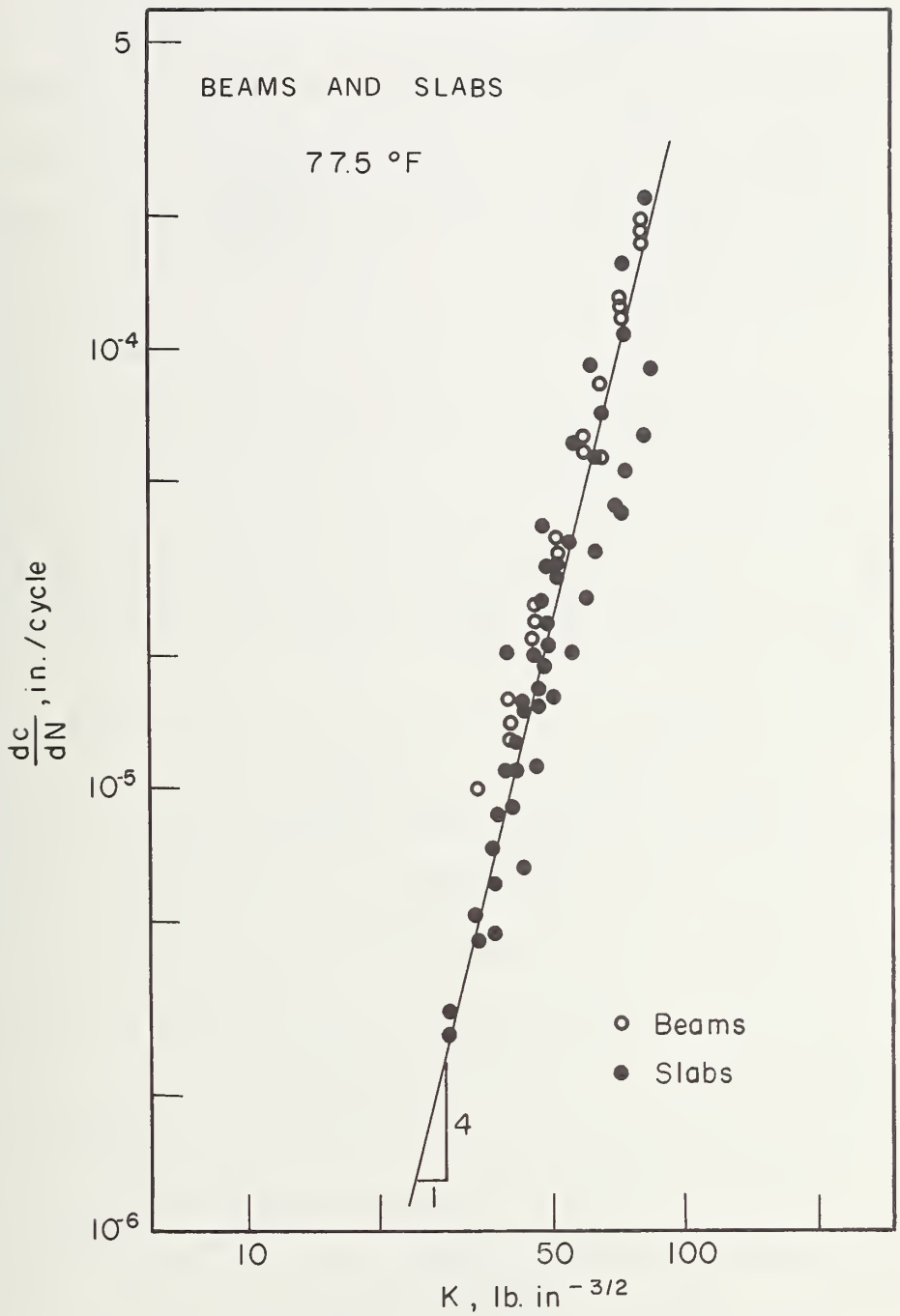

Figure 4.3. Comparison of the Crack Growth Rates for Beams on Elastic Solid and Slab Tests

(v) K_{1c} was found to be the failure criterion for both monotonic fracture and fatigue and is a material property.

As has been shown in Chapter II, an anaytical method was also developed to investigate the problem of crack propagation in the asphaltic slab. To further verify the validity of this anaytical method, measurements of radial and tangential strains were made and were correlated with the theoretical values.

Radial and tangential strains at radial distances of 3, 4, 5, 6 and 8 inches were measured by paperbacked SH4-5-S13 strain gages. The gages were cemented to the asphalt slab using epoxy cement. The terminal wires were connected to Wheatstone bridges and Sanborn or CEC recorders. Dummy gages were also cemented to a "dummy" slab similar to the test slab to provide for temperature compensation.

The results are presented in Figures 4.4 and 4.5. The theoretical values plotted in these figures were calculated using the computer program developed previously. The value of the modulus of subgrade reaction, k, used in this program to obtain the strains in the slab was corrected using Vesic's recommendations (15) since the measurements of k were done using the center deflection and not the stress, i.e. k was calculated from:

$$k = \frac{p}{w} \tag{4.1}$$

where p = intensity of the load (psi)

w = deflection under the load (inches)

This correction is explained graphically in Figure 4.6.

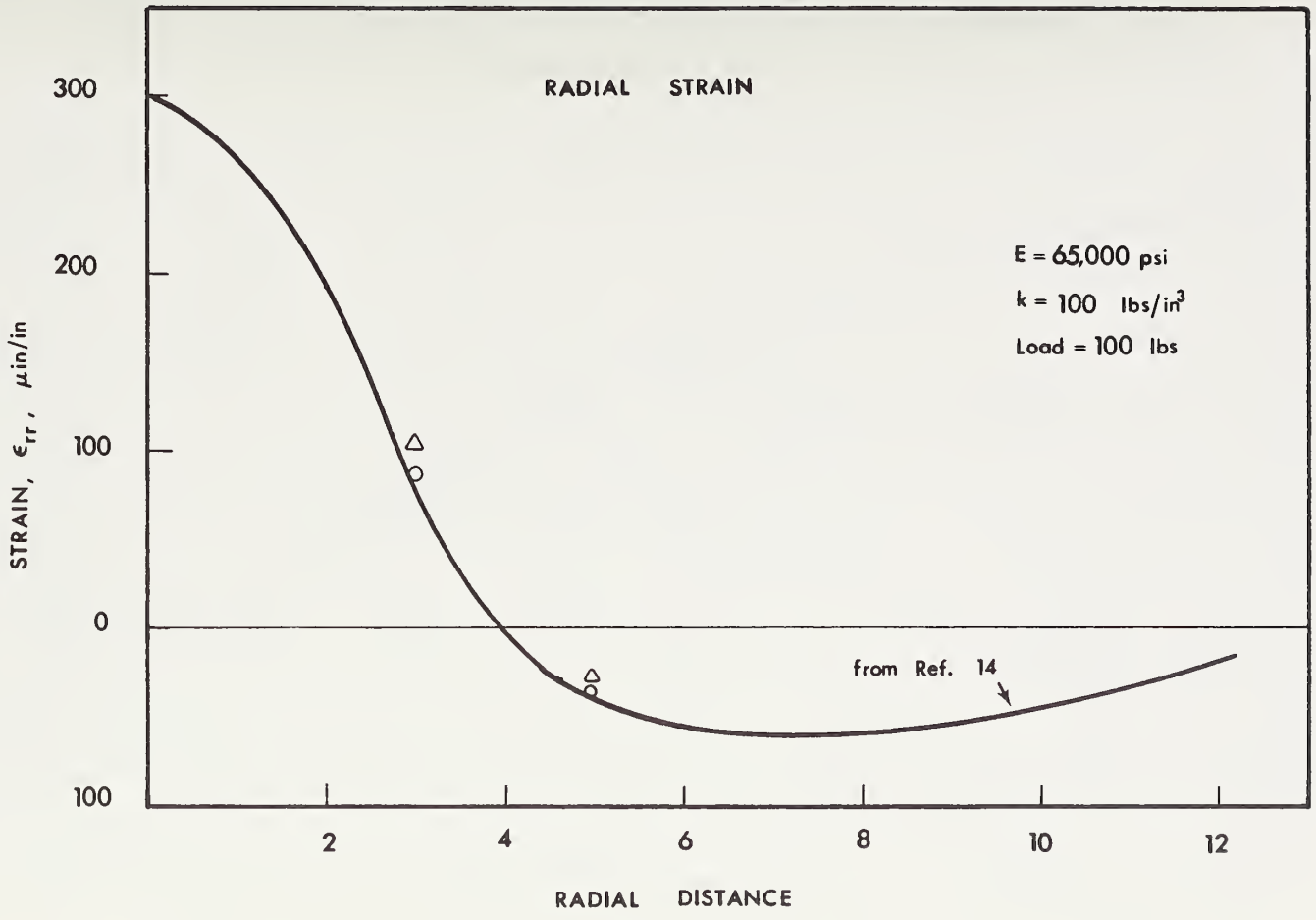

Figure 4.4. Comparison of Theoretical Radial Strains and Experimental Results

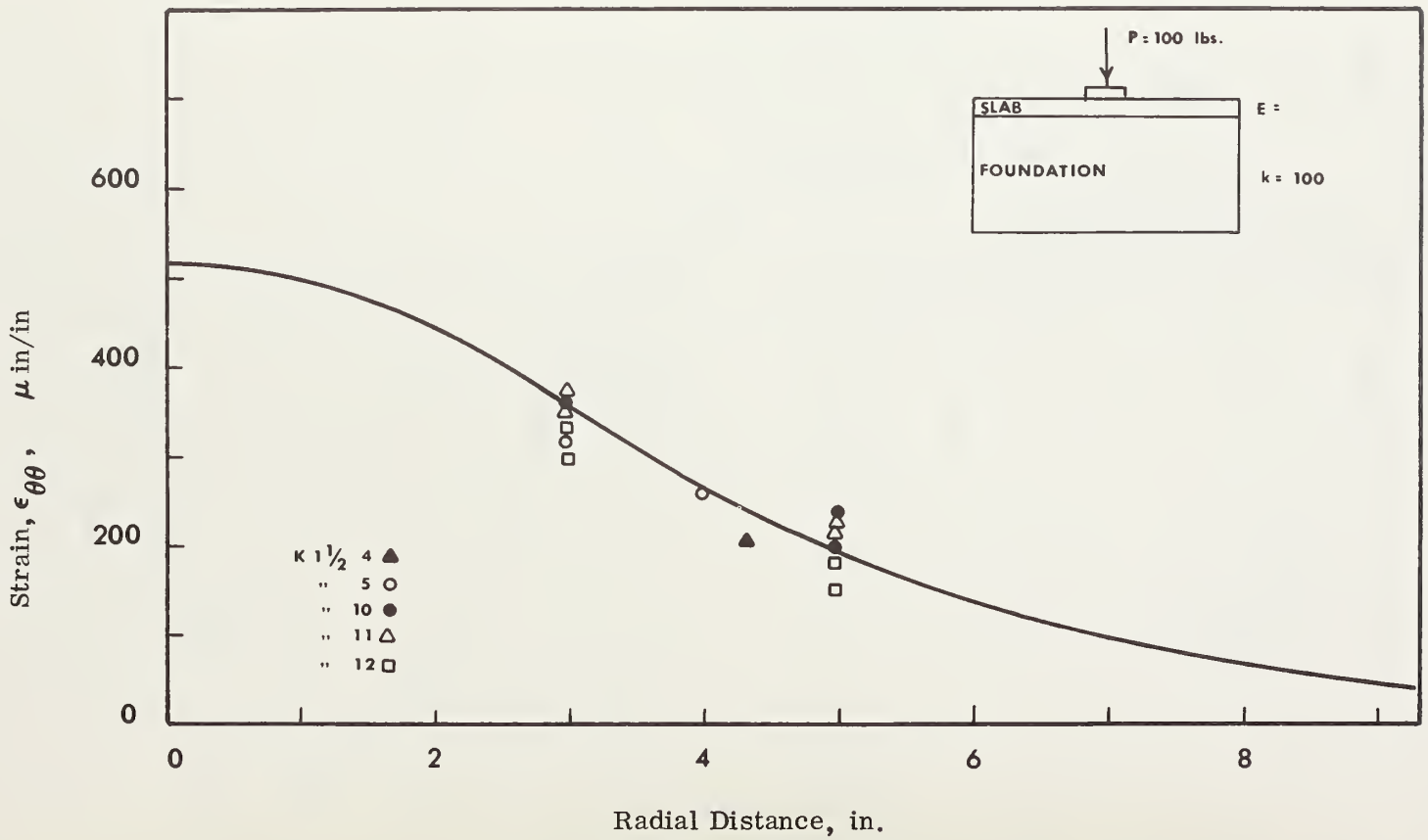

Figure 4.5. Comparison of Theoretical Tangential Strain and Experimental Results

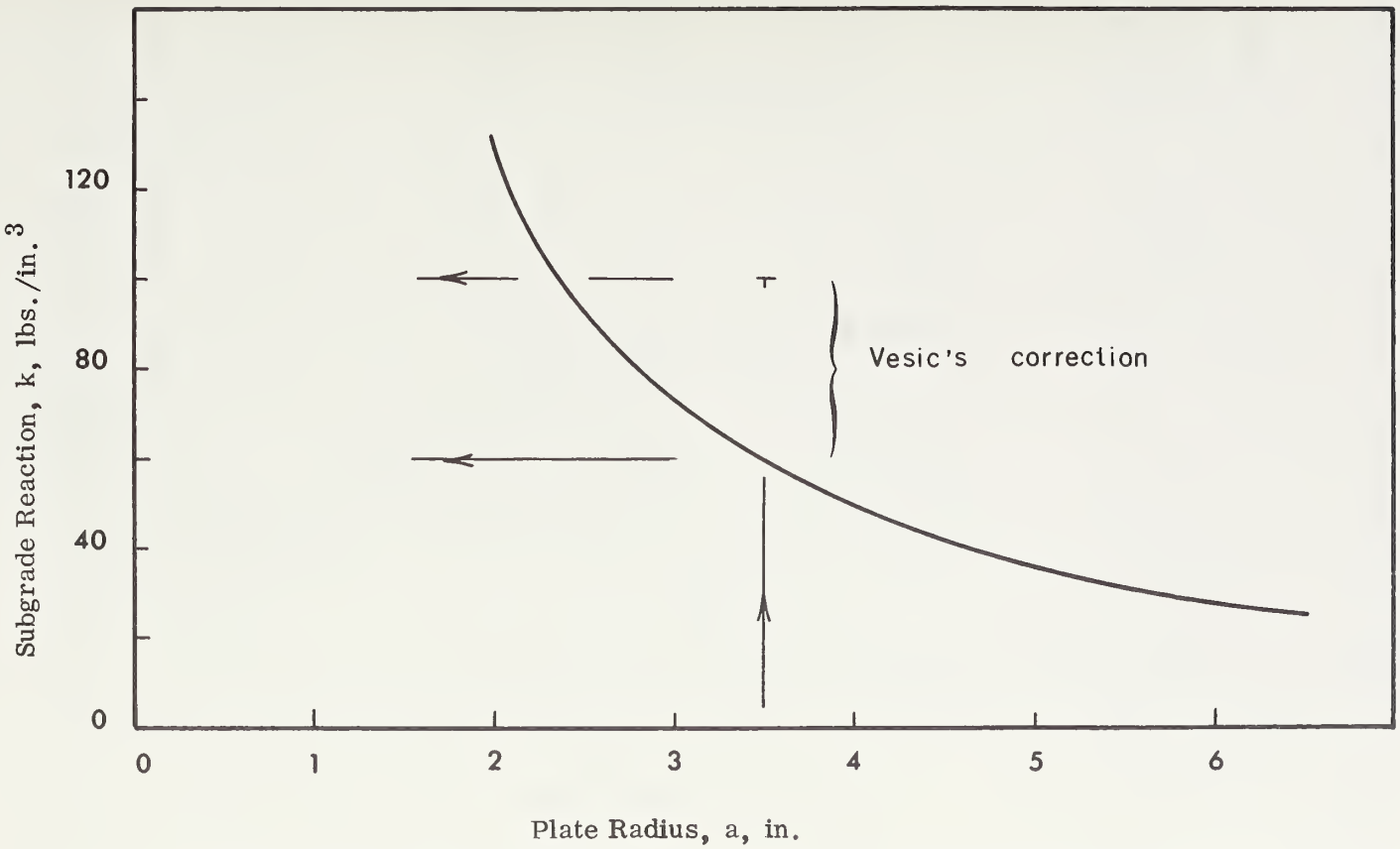

Figure 4.6. Subgrade Reaction as a Function of the Size of the Loaded Area

The agreement between the experimental and theoretical value of the radial and tangential strains, after the correction to the modulus of subgrade reaction was applied, was considered very satisfactory.

Furthermore, the analytical method of calculation of stress-intensity-factor was verified experimentally. For this purpose, the experimental stress-intensity-factor, K_1, for various crack lengths was obtained from Irwin's equation (2.23) given by:

$$K_1^2 = \frac{E}{2(1-\nu^2)} \quad P^2 \quad \frac{\partial L}{h\,\partial(2c)} \tag{4.2}$$

where L = compliance = inverse slope of the load/deflection diagram

$2c$ = crack length

h = slab thickness

The experimental procedure used consisted of sawing radial cuts and simulating cracks in the slab with a Saber saw using a thin blade. For each cut or crack length, the compliance L was determined by loading the slab for a few cycles of half-sine loading function and then plotting the load versus deflection diagram. Then, a plot of compliance versus crack length was made and it is presented in Figure 4.7. Once the rate of change in the compliance was known, the stress-intensity-factor K_1 was determined by using the above formula. A plot of K_1 versus crack length is presented in Figure 4.8. These analyses further substantiate the validity of the proposed distress model at 77.5 °F.

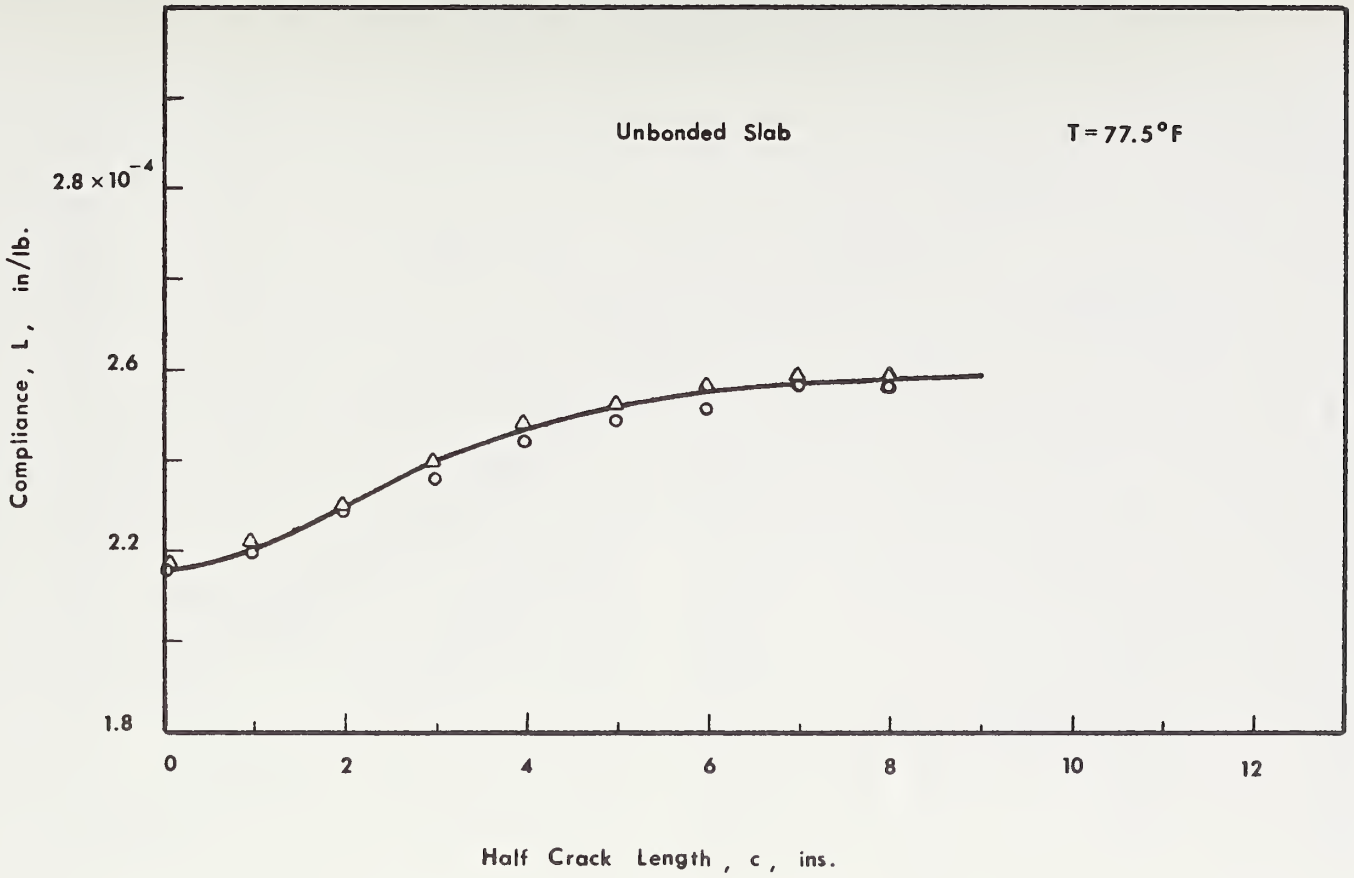

Figure 4.7. Compliance Versus Crack Length for Slabs on Elastic Foundation

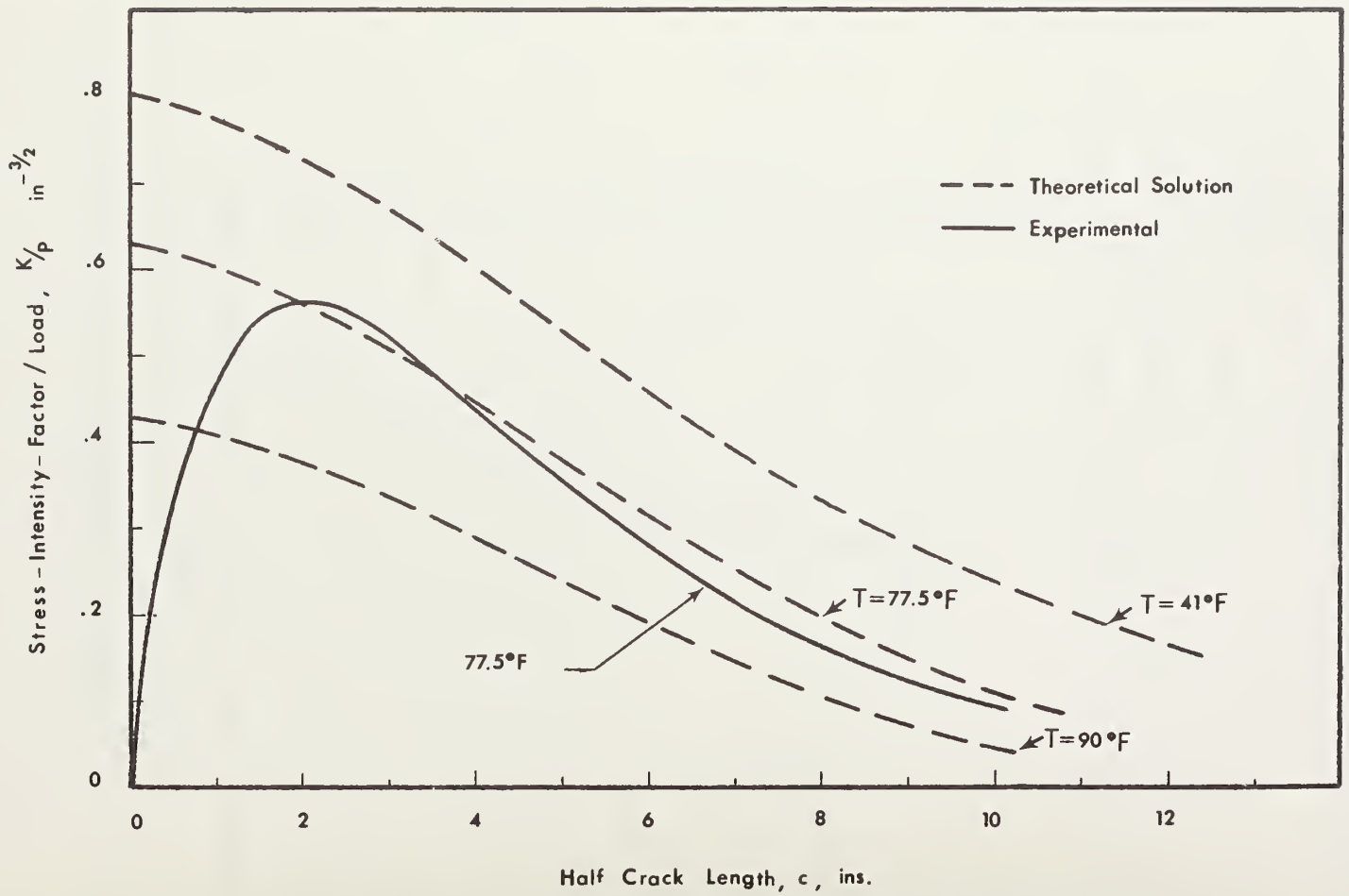

Figure 4.8. Stress-Intensity Factor/Load Versus Crack Length

C. Verification of Distress Model at 41° and 90°F

(1) Experimentation on Slabs Resting on an Elastic Foundation

To perform these experiments, an environmental cell was built around the test area with the inside dimensions of $6\frac{1}{2}$ feet by 6 feet. The walls of the cell were built out of plywood with 3 inches of styrofoam insulation. The compartment enclosed the elastic foundation, cooling unit and heater, as well as fans, used to ensure proper circulation of the air inside the box. Both the 3,000 watts heater with a capacity of 10,000 BTU/hour and the cooling unit with a BTU/hour rating of 4,500 (for 10° temperature differential) were controlled by a Thermac Twintrol unit. Plates 4.1 and 4.2 show the outside view of the compartment, and Plate 4.3 shows an inside view with the elastic foundation, cooling unit and heater.

The elastic foundation was protected on the outside with several layers of fiberglass wool. Before and after each test, plate load tests were performed on the elastic foundation to determine the variation of the modulus of subgrade reaction, k, with temperature. It was found that even after a period of ten days at 41°F or 90°F, the change in k was negligible, as shown in Figure 4.9

For this series of tests, the asphalt slabs were subjected to repetitive loads of constant amplitude using the MTS in load control. The loading function used consisted of a half-sine function with a duration of 0.1 second and a rest period between load pulses of 0.8 seconds. Before starting each test, the slab was placed on the foundation and left inside of the environmental cell for a

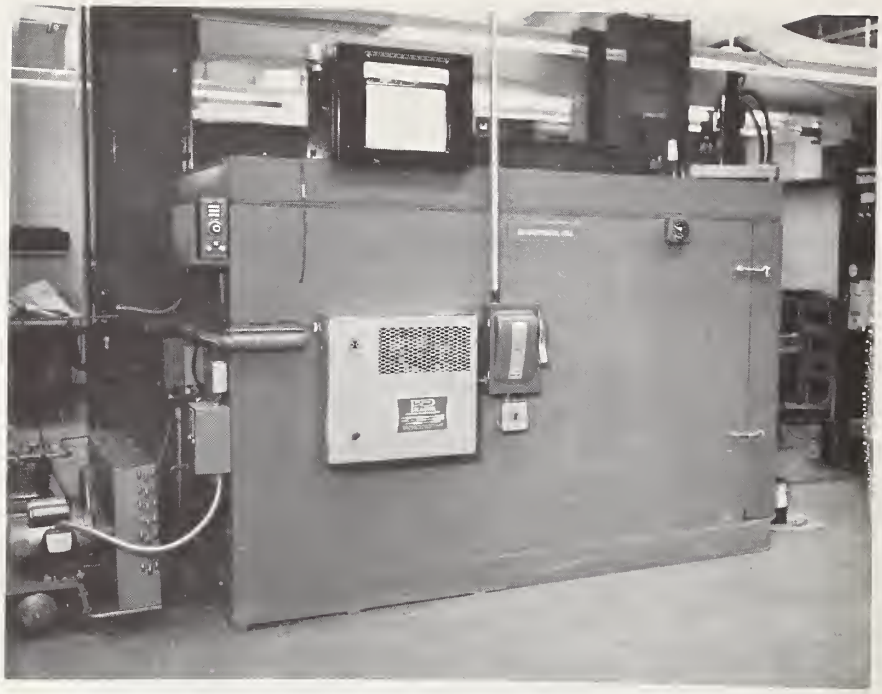

Plate 4.1
North Side of Environmental Cell Showing Temperature Controls

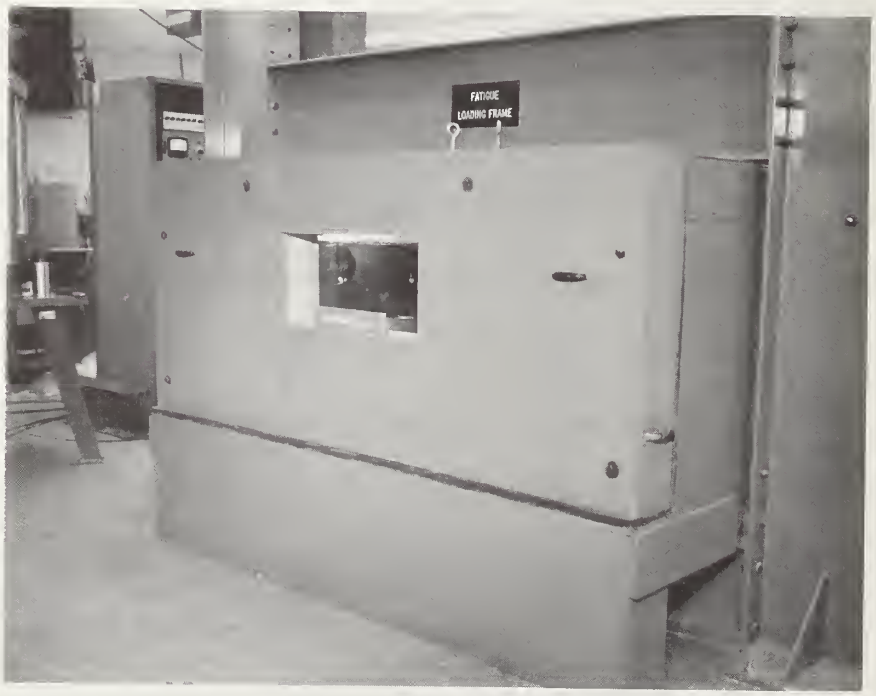

Plate 4.2
South Side of Environmental Cell Showing Removable Wall

Plate 4.3

South Wall of Cell Removed to Show Interior with Elastic Foundation

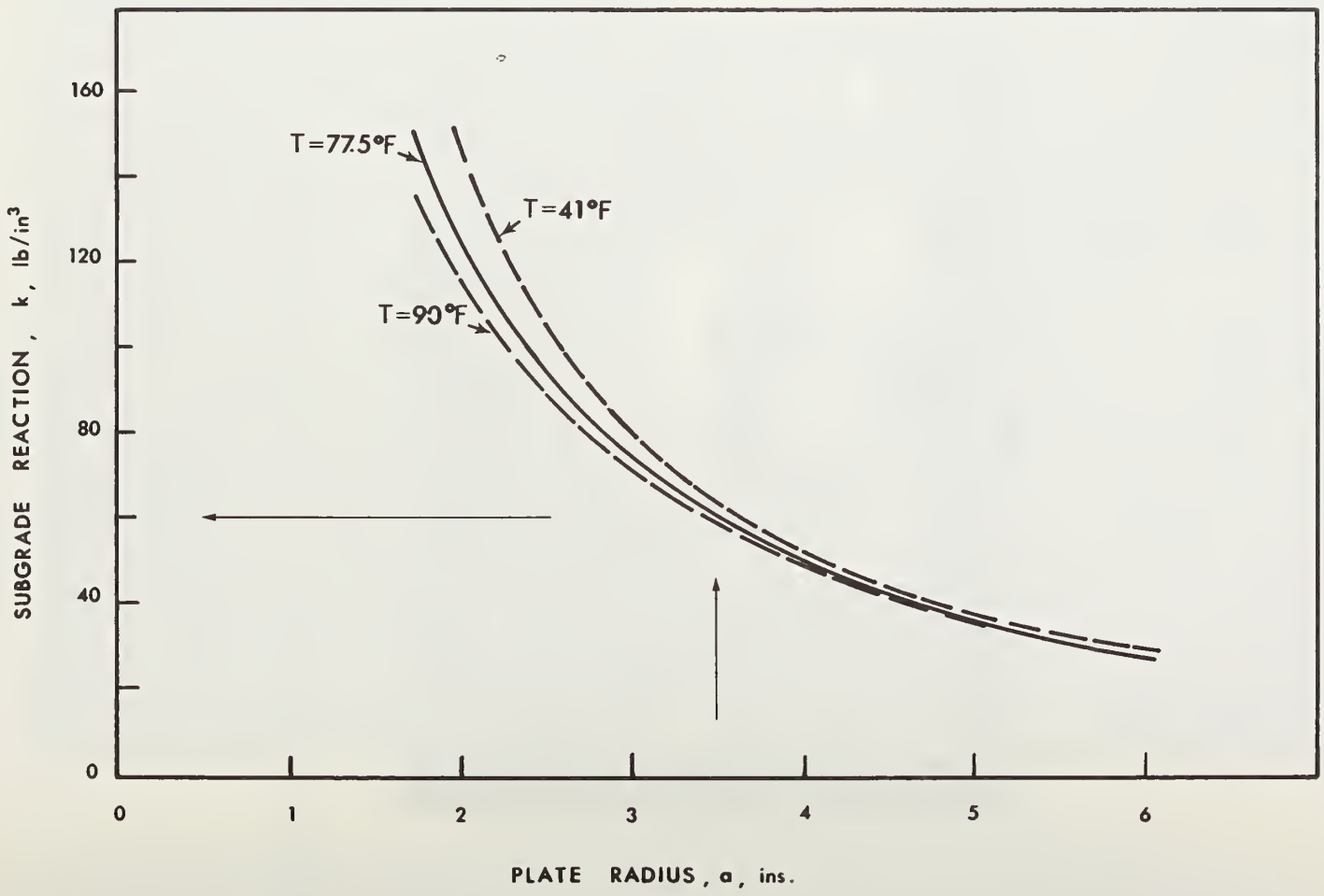

Figure 4.9. Variation of Subgrade Reaction with Temperature

period of at least two days, to ensure that the proper test temperature has been achieved. Copper-constant thermocouple wires were placed in different locations on the slab, foundation and at different points in the cell, and a constant record of the temperatures at those points was kept using a Barber-Coleman thermocouple recorder.

Figure 4.10 shows a schematic diagram of the temperature box with the location of the thermocouple wires. Figures 4.11 and 4.12 present a sample of the temperature recorder for tests at 41°F and 90°F. It is noted that the temperature differential in the slab was kept to a minimum, avoiding any nonuniform stress distributions.

(2) Analysis and Discussion of Results for Tests at 41°F

The first set of experiments at this temperature were conducted using a load of 800 pounds. The observed crack pattern from this test was noted to be very similar to those observed previously. On the contrary, however, the crack growth as presented in Figure 4.13 was rather different. It was noted that after the cracks had appeared in the top surface of the slab and were approximately 2 inches long, it propagated instantaneously to a length of about 6 inches. This fact is explained on the basis that for this test temperature, the stress-intensity-factor, for a crack of approximately 3 inches in length reaches the value of the critical stress-intensity-factor, K_{1c}, and catastrophic failure occurs. When the crack length reaches 6 inches, the value of the stress-intensity-factor dropped below the critical limit (see Figure 4.8) and the cracks then grew as those observed in previous tests.

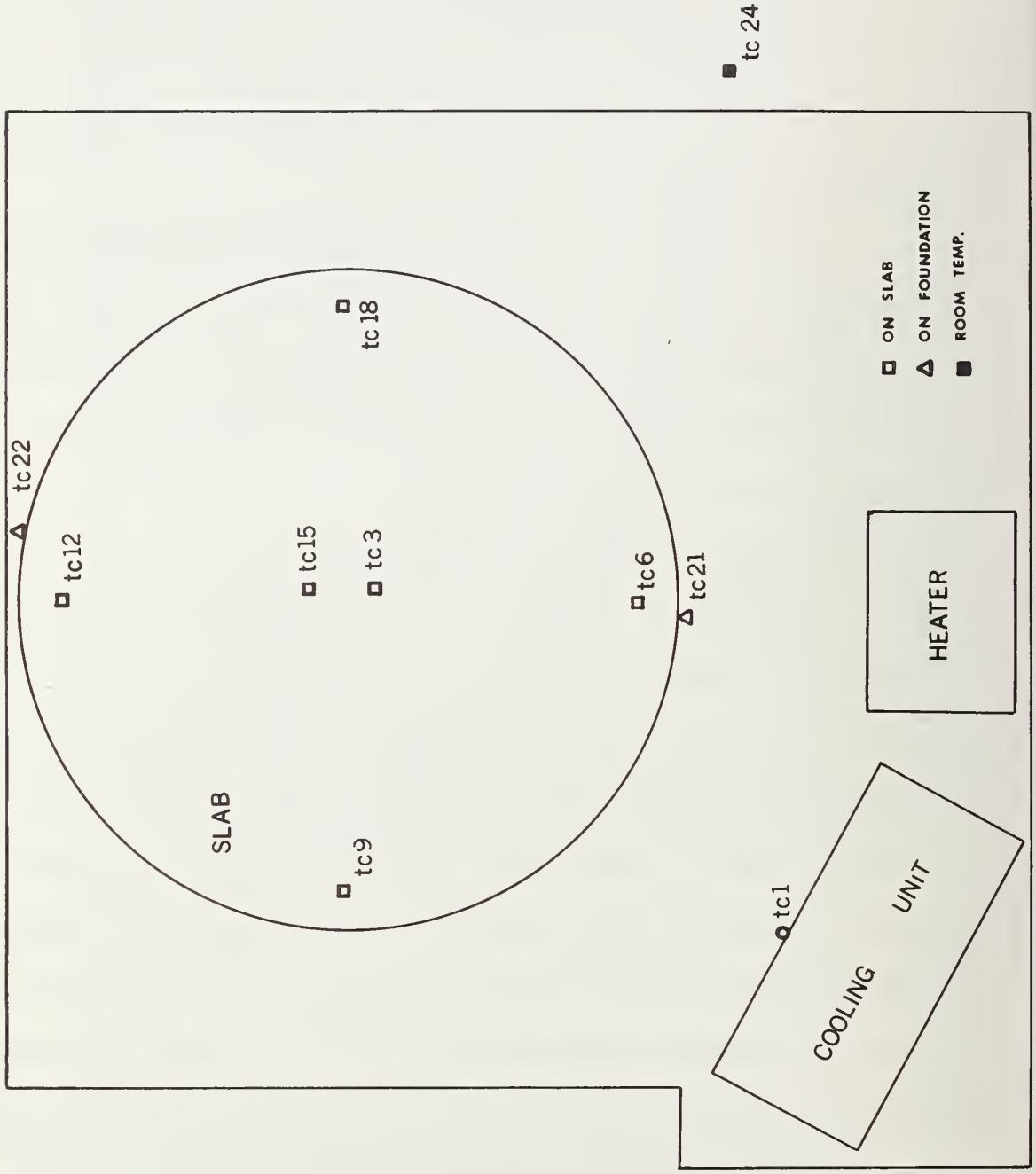

Figure 4.10. Schematic Diagram of the Environmental Cell

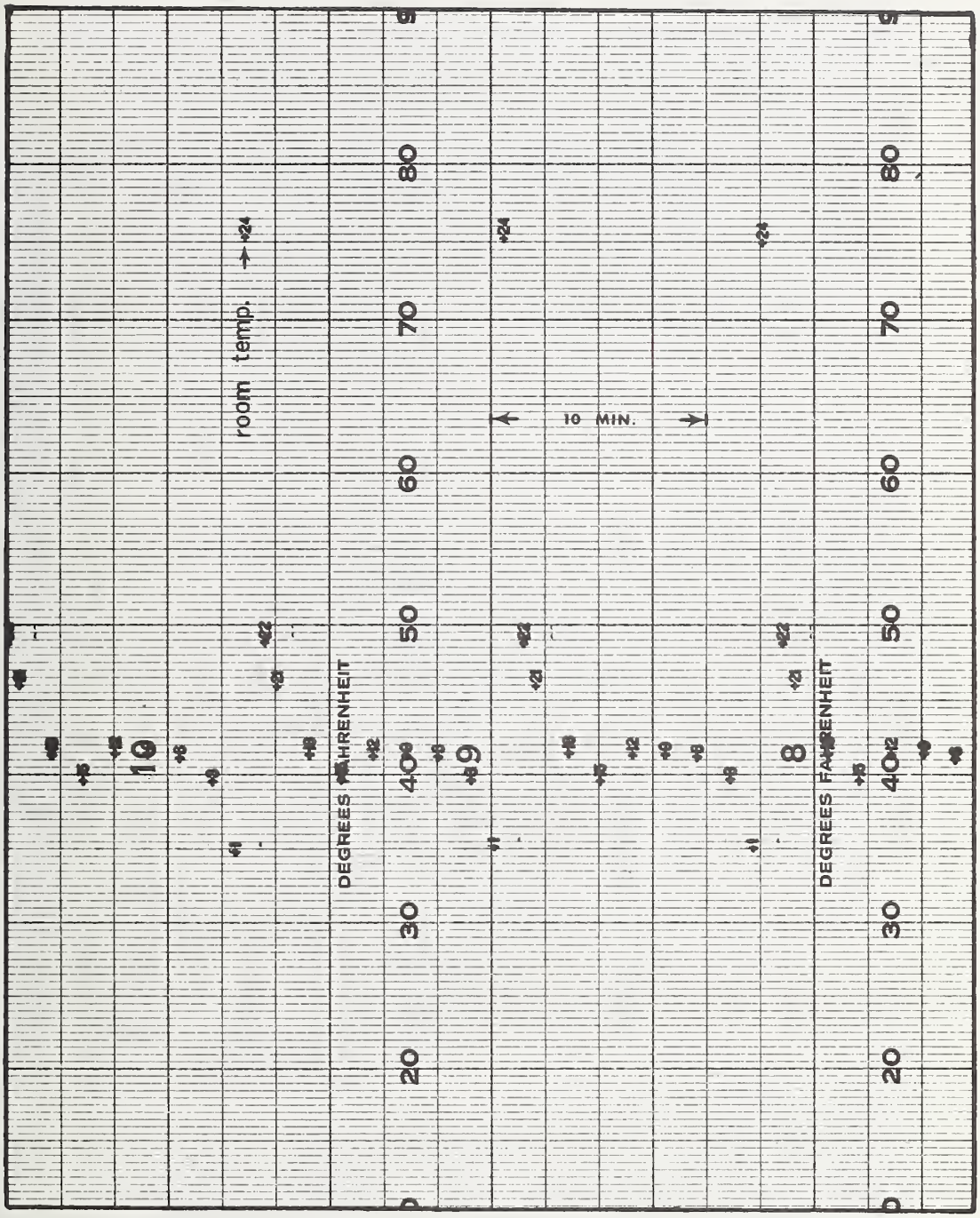

Figure 4.11. Temperature Control at 41°F

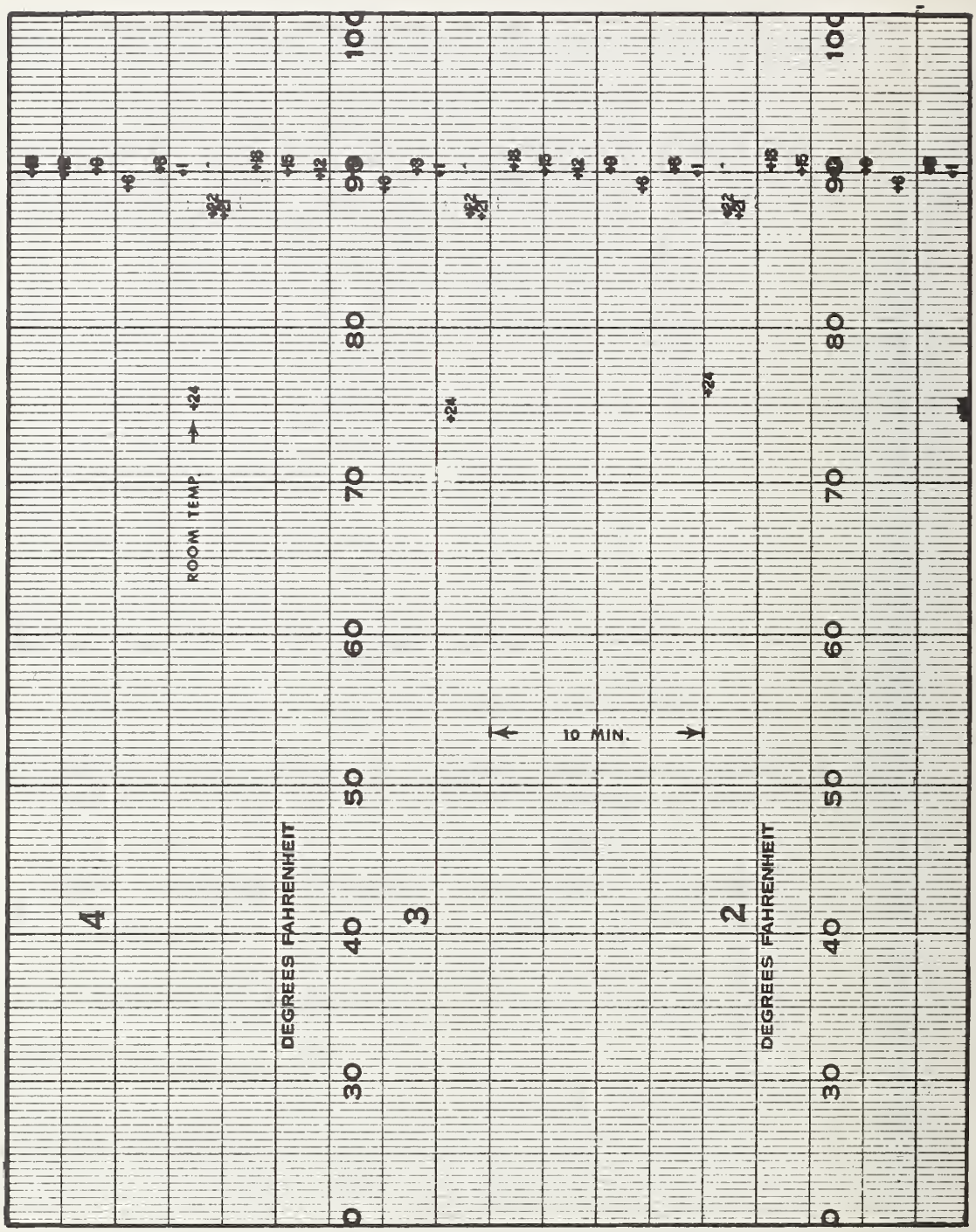

Figure 4.12. Temperature Control at 90°F

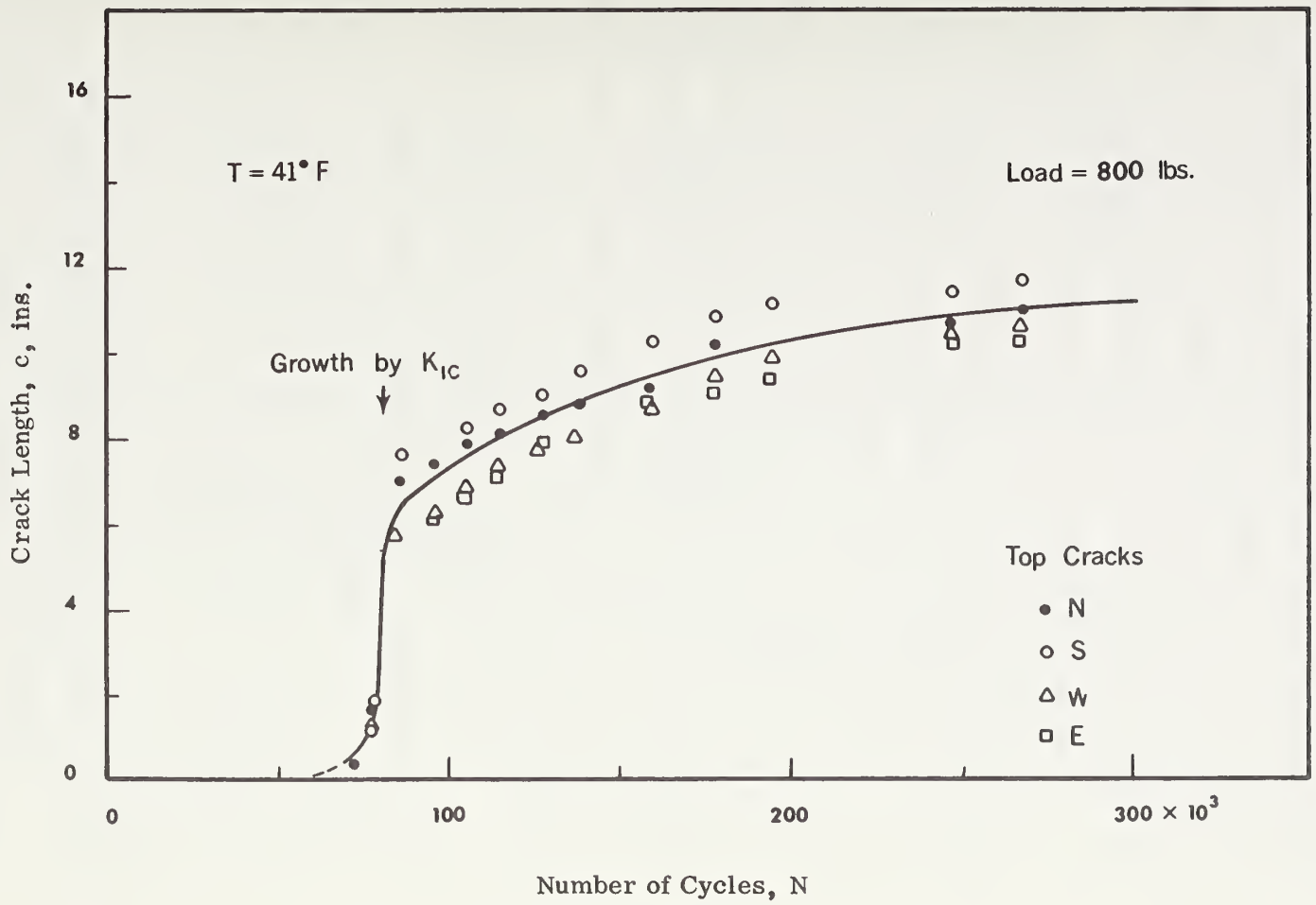

Figure 4.13. Crack Growth Curve at 41°F for 800 lbs.

The study of the rate of crack propagation was therefore carried out from the point in which the cracks were approximately 6 inches long, and this rate is plotted versus the stress-intensity factor (Figure 4.14). It is noted that once more the Paris law relating the rate of crack propagation to the stress intensity factor is applicable and the exponent is 4.

Another set of experiments were conducted at a smaller stress level corresponding to a load of 700 pounds. As was noted previously, once again the stress intensity factor exceeded its critical limit, K_{1c}, and cracks became unstable propagating instantaneously to a length of approximately $3\frac{1}{2}$ inches. At this crack length, however, due to reduction in the stress-intensity factor to a level below critical limit, the fatigue cracks resumed their normal growth pattern. The crack growth curve for this test is presented in Figure 4.15, and the plot of the rate of crack growth versus the stress-intensity factor is included in Figure 4.14.

Similar conclusions can be reached by noting that for a crack length of about 2 inches and a load of 700 pounds, the stress-intensity factor has a value of 504 lbs./in.$^{3/2}$ (Figure 4.8). For a 4-inch long crack, however, K = 420 lbs./in.$^{3/2}$ which corresponds to the critical stress-intensity-factor, K_{1c}, for the material tested. This result agrees very closely to results of K_{1c} previously reported (11).

(3) Analysis and Discussion of Results for Tests at 90°F

At this test temperature, experiments were carried out at two load levels of 250 and 300 pounds which were selected with consideration to the yield stress

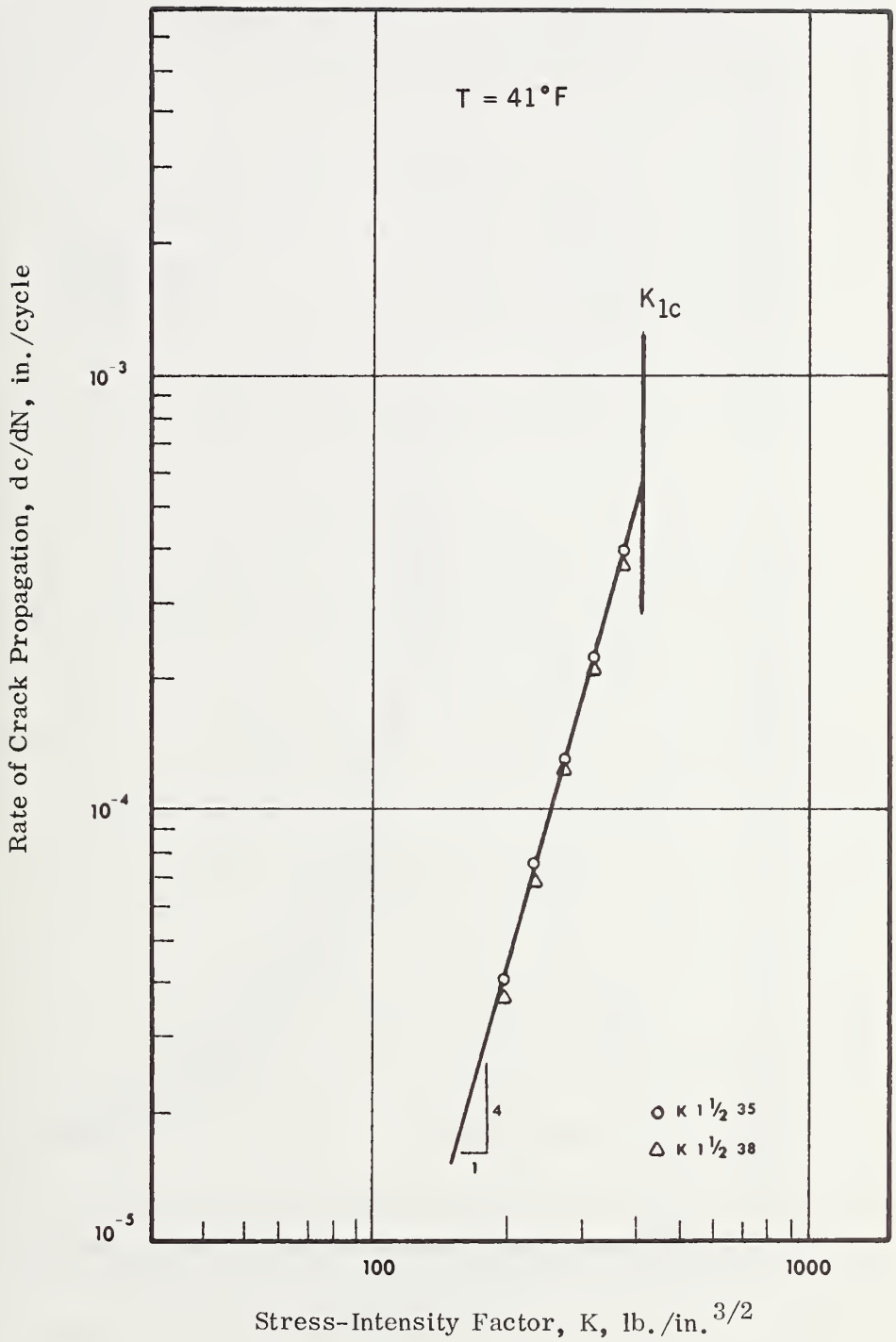

Figure 4.14. $\frac{dc}{dN}$ - K Relation for Tests at 41°F

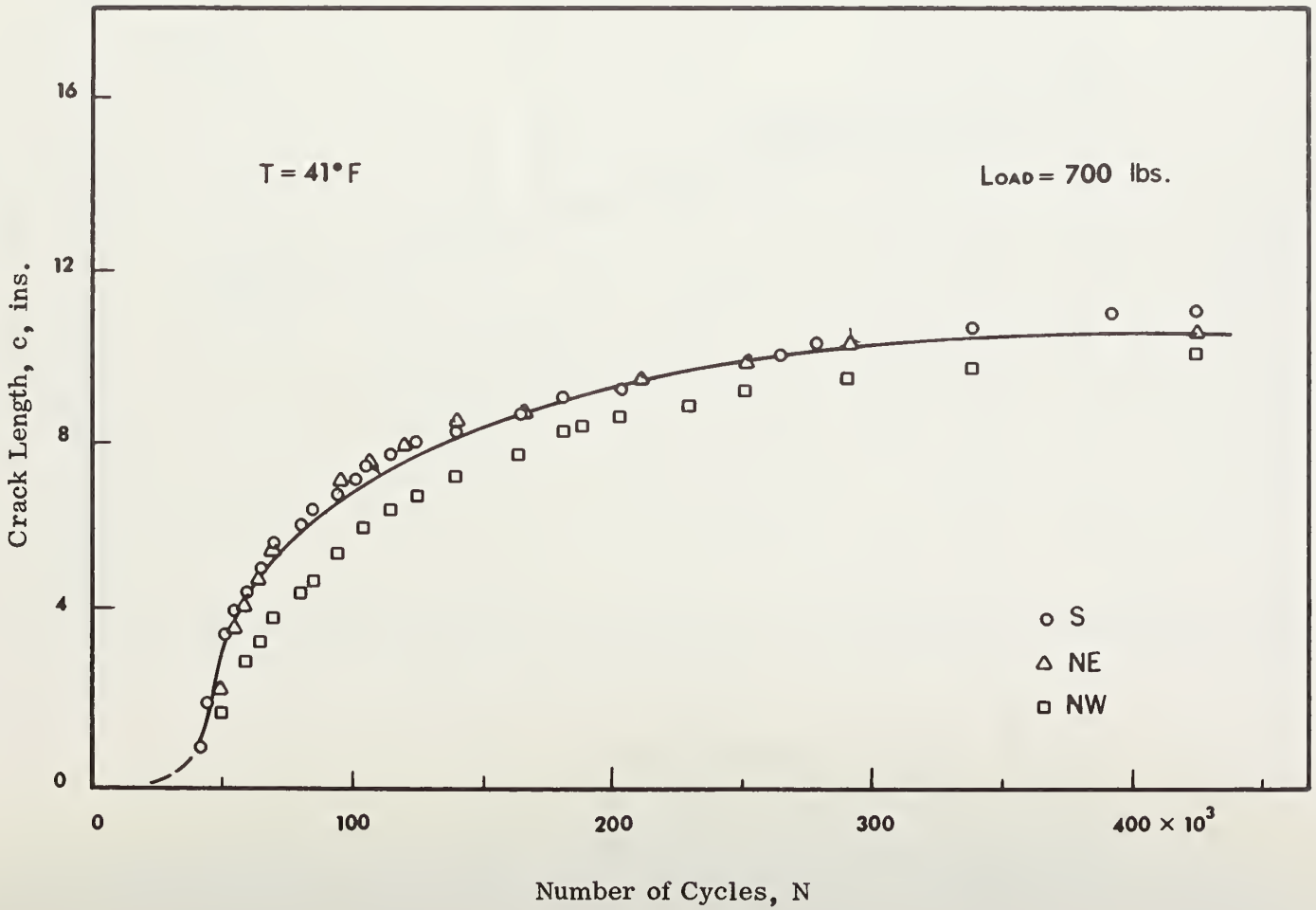

Figure 4.15. Crack Growth Curve at 41°F for 700 lbs.

of asphaltic mixture studied. The analysis of stress distribution within the pavement model indicated that at points near the center of the loaded area, the induced stresses exceed the yield stress of sand asphalt mixture. The analysis of stresses at points further away from the center of loaded area, however, indicated that induced stresses are sharply reduced with an increase in the radial distance. Therefore at points located outside of the loaded area, these stresses are found to be significantly smaller than the yield stress of sand asphalt, and the state of elastic stress distribution might be assumed as an approximation.

During these experiments a limited number of x-ray photographs were taken to establish the crack growth pattern of asphaltic slabs. The number of x-ray observations were, however, limited due to problems associated with the temperature control and the time required for bringing the test specimens to equilibrium temperature. Nevertheless, the results of these observations indicate that at this temperature the equilbrium shape of the top and bottom cracks are very similar to the results obtained for "high stress level" experiments (see discussion in Chapter V). The typical crack growth curves for experiments at 250 and 300 pounds load levels are presented in Figs. 4.16 and 4.17. It is noted that during crack growth process, the top and bottom cracks have approximately the same length and furthermore a substantial amount of permanent deformation occurs under the loaded area. It should be noted that the analysis of crack propagation for the pavement

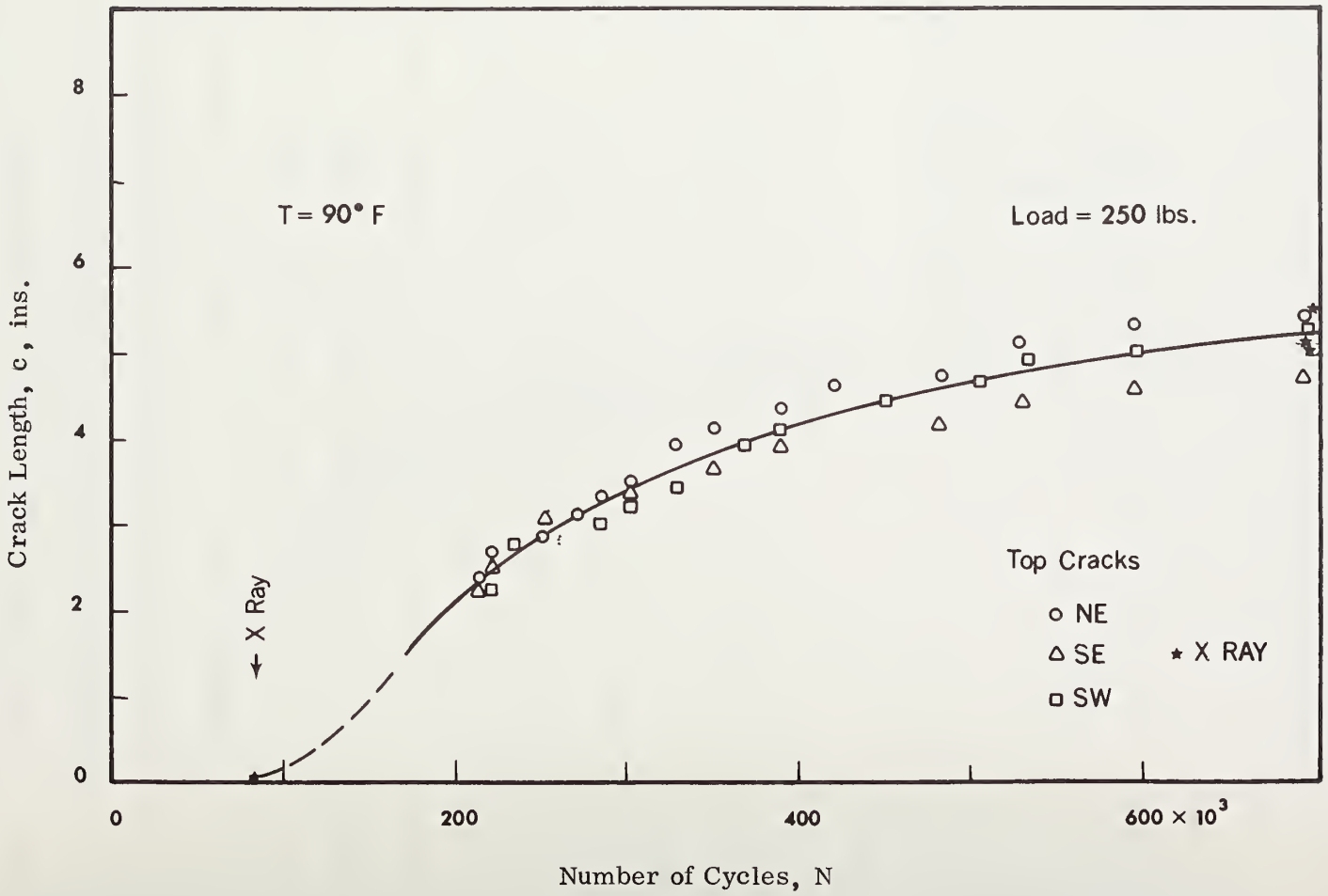

Figure 4.16. Crack Growth Curve at 90°F for 250 lbs.

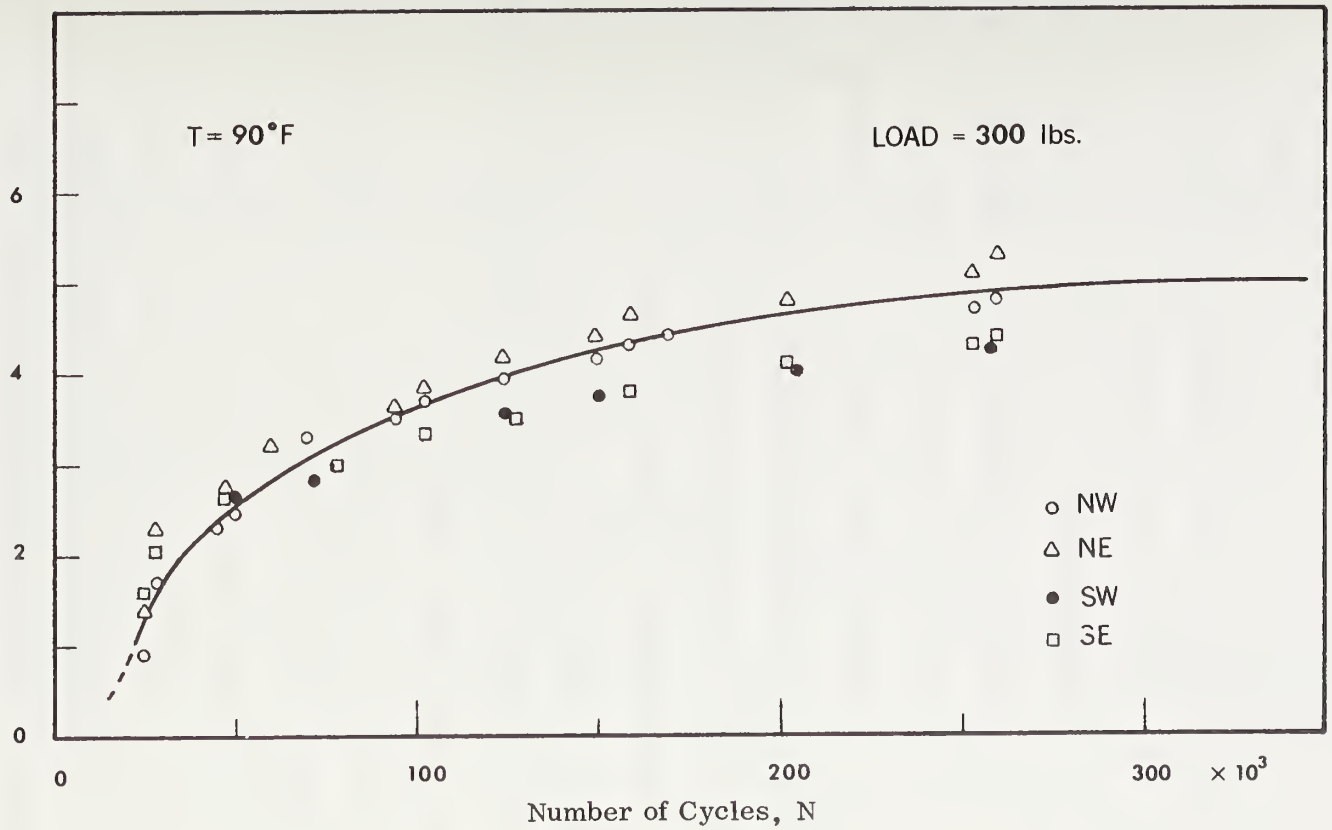

Figure 4.17. Crack Length Versus Number of Cycles for a Load of 300 lbs. at 90°F

sections located directly under the load is not sufficiently accurate to establish the validity of crack growth law.

This experimental inaccuracy in the crack growth rate evaluation is associated with the mode of crack propagation under the loaded area. It has been pointed out previously (15) that the first crack originates under the center of the load at the most critical flaw or near the pavement interface and grows radially. For simplicity, one might assume that the initial flaw is penny shaped and grows as a plane crack in both the depth and length as an elipse. Eventually this crack will reach to the top surface and with further growth, the crack length would become the dominating dimension (Fig. 3.26-ref.15). However during the period that this half penny of half elipse shaped flaw is propagating upward and appears partly at the top surface, an accurate crack length measurement is rather impossible. A check on the accuracy of x-ray techniques and compliance method has been carried out indicating extreme variability in the observed crack length measurements in this region.

The study of crack propagation in the regions outside of the loaded area indicates a similar crack pattern as shown previously. It is interesting to note that even though these experiments were carried out at a relatively high temperature, the crack propagation rate follows the proposed distress model. The analysis of results of the top cracks as shown in Figure 4.18 indicates that the proposed distress model is also applicable at this test temperature.

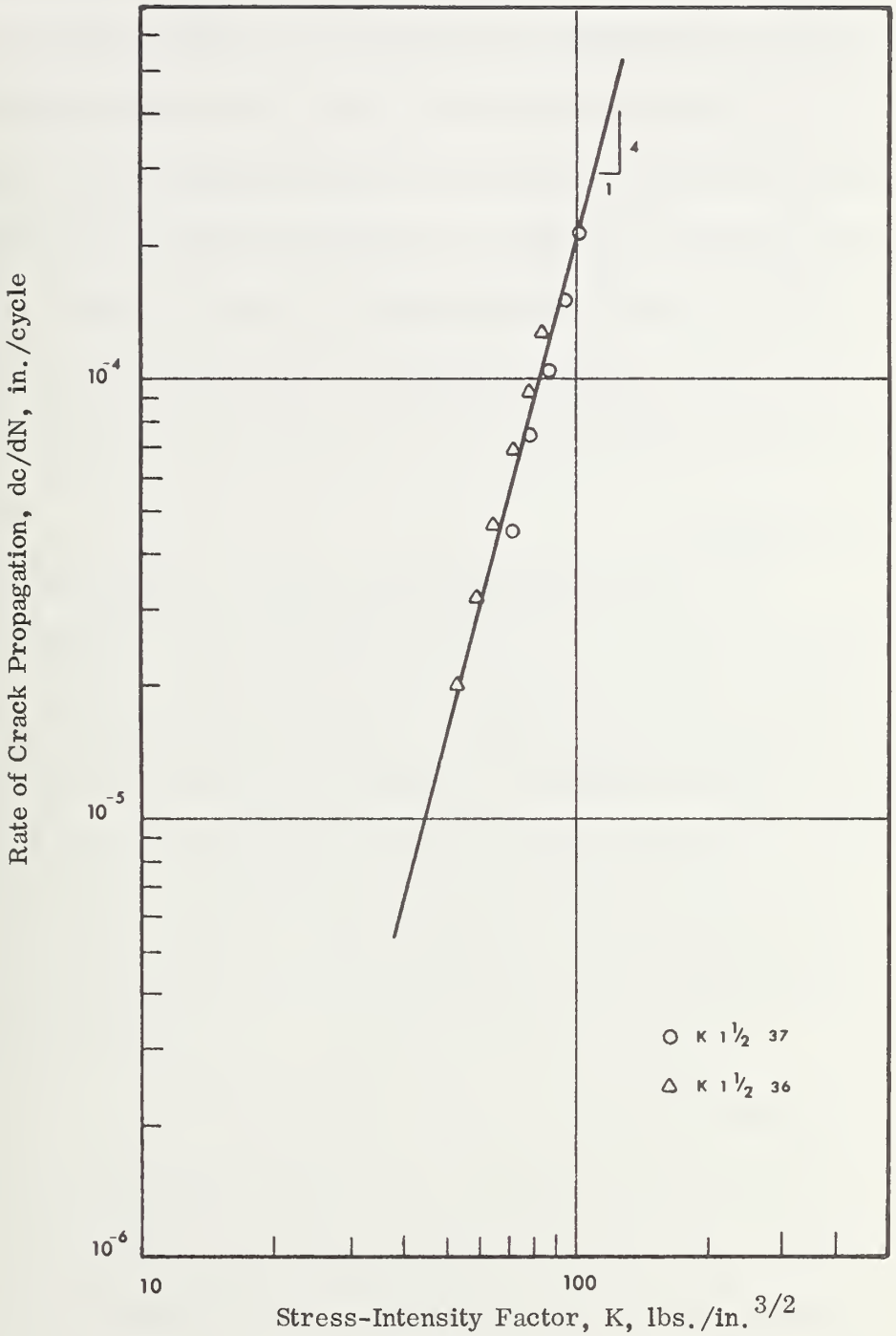

Figure 4.18. $\frac{dc}{dN}$ - K Relationship for Tests at 90°F

At this point it should be mentioned that the same conclusion cannot be extened to analysis of beam on elastic foundation. In the beams on the elastic foundation tested for Mode 1 fracture, the propagating crack is located directly under the load area and is greatly influenced by the state of elastic-plastic stress distribution. At high temperatures or for excessive loading condition, where large scale yielding occurs under the loaded area, a delay in the crack propagation is imminent. A further discussion of this subject is presented in Chapter V.

D. Conclusion

The experimental data and the analysis of results presented in this chapter indicates that for the range of temperatures investigated, the mechanistic approach to the fatigue life of pavement can be applied to predict the rate of crack propagation. It was also demonstrated that at low temperatures the critical stress-intensity factor is the failure criterion. Although excessive permanent deformation occurs under the loaded area at high temperatures, the crack propagation outside the region follows the proposed distress model.

It should be noted that in this study due to limitations of experimental set up and the boundary conditions of the pavement model, the evaluation of the effect of cyclic temperature on the crack propagation was not carried out. However, an analytical simulation of temperature variability in a real pavement has been conducted indicating the extent of temperature differential in a typical pavement constructed in Ohio. Considering the temperature dependency

of asphaltic mixtures, the problem can then be approximated with a layered system of varying moduli. For the analysis of the initial phase of crack propagation, which is nucleated directly under the load and propagates upward, the prismatic finite element model can easily be adapted to a layered system of varying moduli. For the analysis of crack propagation occurring outside of the loaded area, the proposed distress model is not directly applicable to a multi-layered pavement system. The analysis requires either an approximation of moment function generated independently for a multi-layered system and then inputed into the moving load program or selection as an average modulus for the pavement system with consideration to the temperature distribution. Then, an incremental crack growth analysis can be carried out using the distribution of average temperatures and the corresponding pavement modulus for the expected load duration. Considering that the distress model is related to the fourth power of the load and square root of the modulus (15), the error associated with such an approximation for the pavement modulus is rather insignificant when compared to the effect of loads of variable magnitude on the crack propagation.

CHAPTER V

EFFECT OF HIGH STRESS LEVELS ON FATIGUE CRACK PROPAGATION

A. Introduction

This part of the investigation is concerned with the analysis of crack propagation when fracture phenomena is accompanied by some permanent deformation. The permanent deformation and shear distortions are due to repeated application of stresses of high magnitude inducing localized or large scale yielding under the loaded area.

In this chapter, the influence of such a phenomena on the crack propagation of pavement systems and the method of material characterization using fracture mechanics principles is discussed.

As was pointed out previously, the input variables needed for verification of the proposed distress model are determined using two-dimensional systems of beam on elastic foundation. In such a system, the zone of stress singularity lies directly under the loaded area, and the crack propagation is greatly influenced by the state of yielding occurring at the regions ahead of the crack tip. In real pavement systems, similar yielding might be observed directly under the loaded area influencing the first stage of crack propagation. In the regions outside the loaded area, however, the state of elastic stress distribution predominates. The theoretical evaluation of the effect of localized yielding on the fatigue crack propagation requires understanding of

elastic-plastic behavior of pavement systems under induced loading and geometrical conditions. The theoretical formulation of the problem and the development of basic constitutive equations are discussed in the following sections.

B. A Review of Mathematical Formulations

Purely elastic fracture mechanics studies of crack tip stress and deformation are useful but limited as mentioned by Rice, Drucker and Rice (46, 47). The limitation is mainly due to the inherent assumption in elasticity, which disregards the geometrical singularity or material strength limit at the point where stresses are concentrated. As observed by many researchers, the in-plane stresses for plane stress and plane strain are the same for behavior under the assumption of pure elasticity, yet they are quite different in the plastic range where the triaxiality becomes predominant and cannot be neglected. This also indicates the limitation on elastic plane analyses and hints that the triaxiality would be taken care of automatically by a more general three-dimensional analysis. Another important point which cannot be overlooked is that the incremental nature of plasticity which gives the fracture instability. It has been a common belief that most ductile or brittle materials undergo some plastic deformation in regions of high stress concentration, and fracture precipitated by a crack is always preceded by an amount of plastic deformation at the crack tip.

In recent years, the plastic analyses have been successfully applied to certain simple cases contigious to fracture via continuum mechanics

approach. Most of these analyses were based upon the deformation theory of plasticity (46,47,48,49). The reason for using the deformation theory in lieu of the more reasonable flow theory is primarily to take the advantage of mathematical simplicity while at the expenses of some physical actuality. Since it has been commonly accepted and confirmed by very extensive experiments that the plastic behavior is of incremental type, it is more appropriate to employ the flow theory to develop the method of analysis, particularly when the mathematical complexity of such a theory is overcome by the availability of the numerical methods associated with computer utilization, such as the finite element technique.

It should be understood that the theory of plasticity, either in its physcial or mathematical sense, takes as its starting point some experimental observations. The theory in its physical sense interprets the material behavior in terms of general concepts concerning the microscopic structure, while the mathematical theory discusses the material behavior on a purely phenomenological basis.

Some basic assumptions are necessary for a tractable mathematical theory of plasticity to be developed. They are based on the experimental observation and mathematical expediency such that the constitutive equations can be formulated.

In the first place, the material is assumed to be inviscid; it is free from the effects of time such as creep, strain rate and viscosity. The pro-

cess is quasi-static and the deformation is infinitesimal as required in the conventional linear elasticity.

It is assumed that the material belongs to a class of isotropic, homogeneous continuum. The initial isotropy is preserved through the whole process. This assumption greatly simplifies our problem by neglecting the dim possibility of anisotropy after the yielding. Since it is also assumed that the elastic strain rate is on the same order of plastic strain, the assumption of isotropy would give us a good approximation in the engineering sense.

As seen from the mechanical properties of the material in which we are interested as well as from the experiments on other materials (50,51), the effect of hydrostatic pressure on yielding point and the plastic strain increment are neglected. It follows that the incompressibility holds in the plastic range.

The decrease in the yield point during a cyclic loading process is noted as Bauchinger effect, which is very important for certain materials in cyclic plasticity. But for our present interest, it is neglected. As a direct consequence, the yielding points become identical for tension and compression.

The absence of Bauchinger effect enables us to invoke the isotropic hardening rule, which simply states that the consecutive yield surfaces which are described by the load function during the hardening process are geometrically similar expansions in scale of the initial yield surface.

The last assumption of fundamental importance is convexity of yield surface. It states that any radius drawing from the center of the enclosure of a yield surface cannot intersect the surface twice (52).

With consideration to these assumptions and the mathematical theory of plasticity in recent years, numerical methods (particularly the finite element method) have been used to obtain solutions for plastic stress-strain fields of various material bodies. Many numerical elastic-plastic solutions for cracked or sharply notched bodies have been published, employing finite element and finite difference methods. In this study, a general purpose elastic-plastic finite element program developed at Ohio State University by Dr. R. Sandhu and Dr. R. Singh (53) has been employed. Utilizing this program, it is possible to predict the development of plastic zones, the displacements strains and stresses at various stages of loading and the residual strain distribution on load removal. The yield criterion used in the program is a modification of the model used by DiMaggio and Sandler (54). The difference is that the yield surface expands when the plastic volume increases, but upon unloading the yield surface will not contract. This is in line with the classical theory of plasticity of work-hardening materials.

The yield function combines ideal plasticity and strain-hardening. The ideal plastic yield condition is the Drucker and Prager line which is the same as extended VonMises yield criterion. The equation for this line is given as:

$$f_1 = \alpha J_1 + J_2^{\frac{1}{2}} = k \tag{5.1}$$

where J_1 , J_2 are the first and second stress invariant. The strain hardening of the yield surface consists of a family of ellipses each of which corresponds to a single value of plastic volumetric strain. The ellipses are assumed to be of constant eccentricity and having axes parallel to the $J_2^{\frac{1}{2}}$ and J_1 axes and their centers on the hydrostatic axis. The equation of the ellipse is:

$$f_2 = \frac{(J_1 - P_0)^2}{a^2} + \frac{J_2}{b^2} - 1 = 0 \qquad (5.2)$$

The movement of the cap is controlled by the increase in the plastic volumetric strain and work-hardening is not reversible in any stress path.

Upon selection of proper yield function and using incremental analysis, the elastic-plastic boundaries for various load increments are determined. For the material under investigation, i.e. sand asphalt, it is assumed that VonMises non-strain hardening failure criteria is applicable and the yield function corresponds to a $f_1(\sigma_{ij}) = 0$. The analysis was carried out for both conditions of $\phi = 0$ and $\phi = 30°$, and typical results are presented in Figures 5.1 5.2 , 5.3 , 5.4 , and 5.5 corresponding only to C = 70 psi and $\phi = 0$ condition (T = 90°F).

In these analyses, an asphaltic beam of 2" x 2" x 24" resting on an elastic foundation has been studied (Figure 5.6). The crack length was 0.2 inches and the modulus of sand asphalt was selected as 32,000 psi corresponding to the mechanical properties of sand asphalt at 90°F. A similar analysis was carried out using E = 65,000 psi, C = 180 and $\phi = 30$ corresponding to a sand asphalt mixture tested at 77°F.

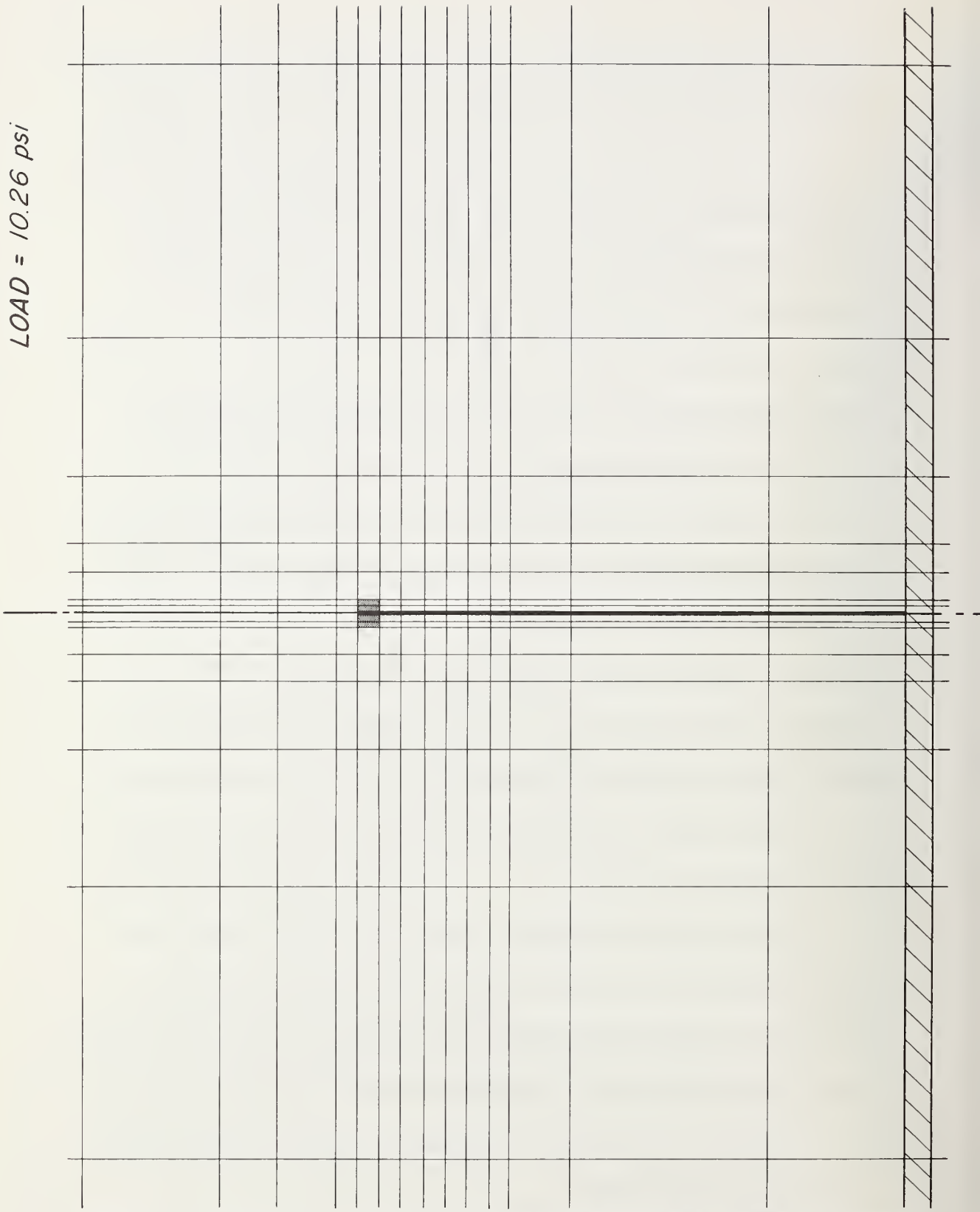

Figure 5.1. Plastic Zone Ahead of the Crack Tip at Stress Increment = 10.26 psi

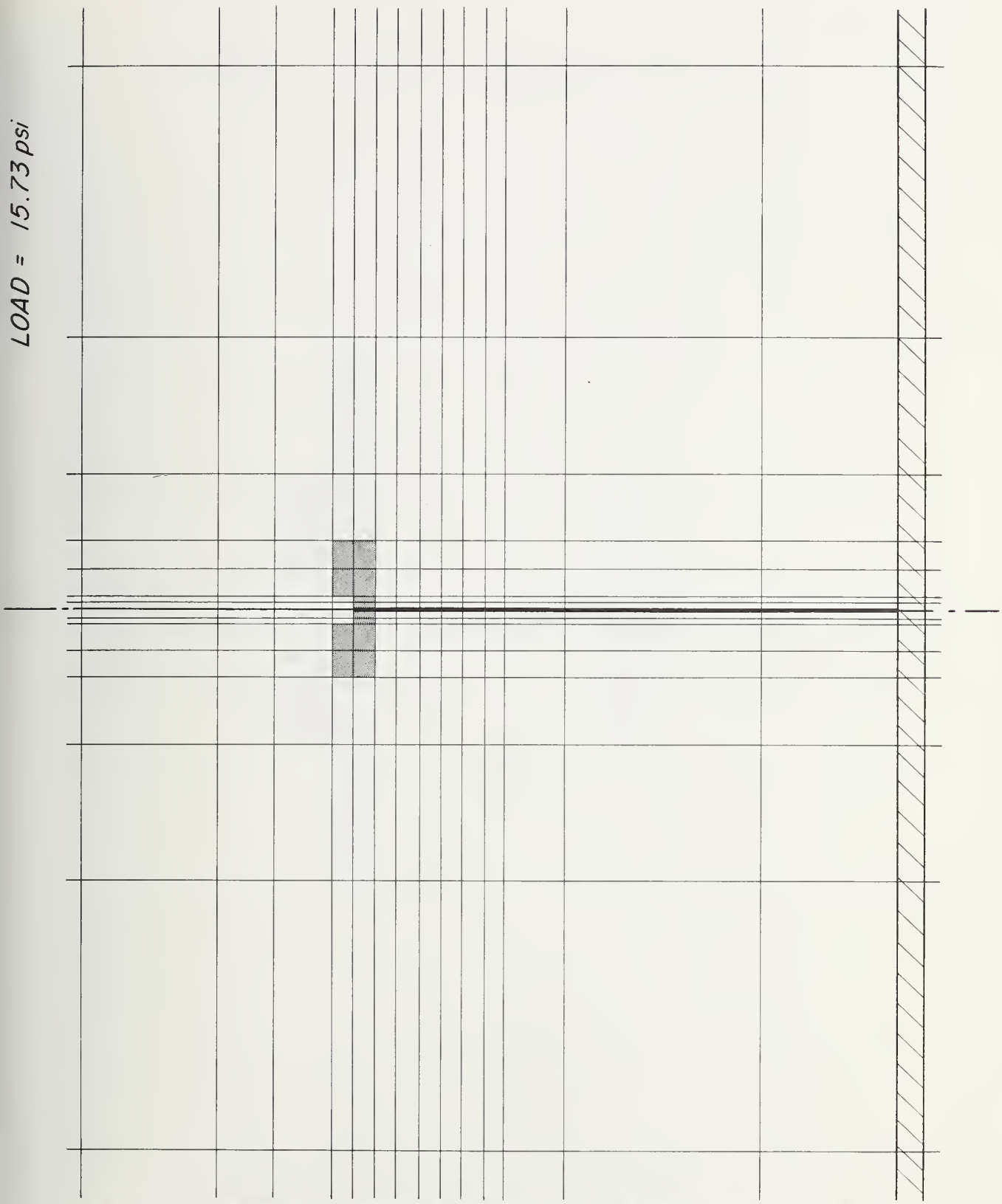

Figure 5.2. Plastic Zone Ahead of the Crack Tip at Stress Increment = 15.73 psi

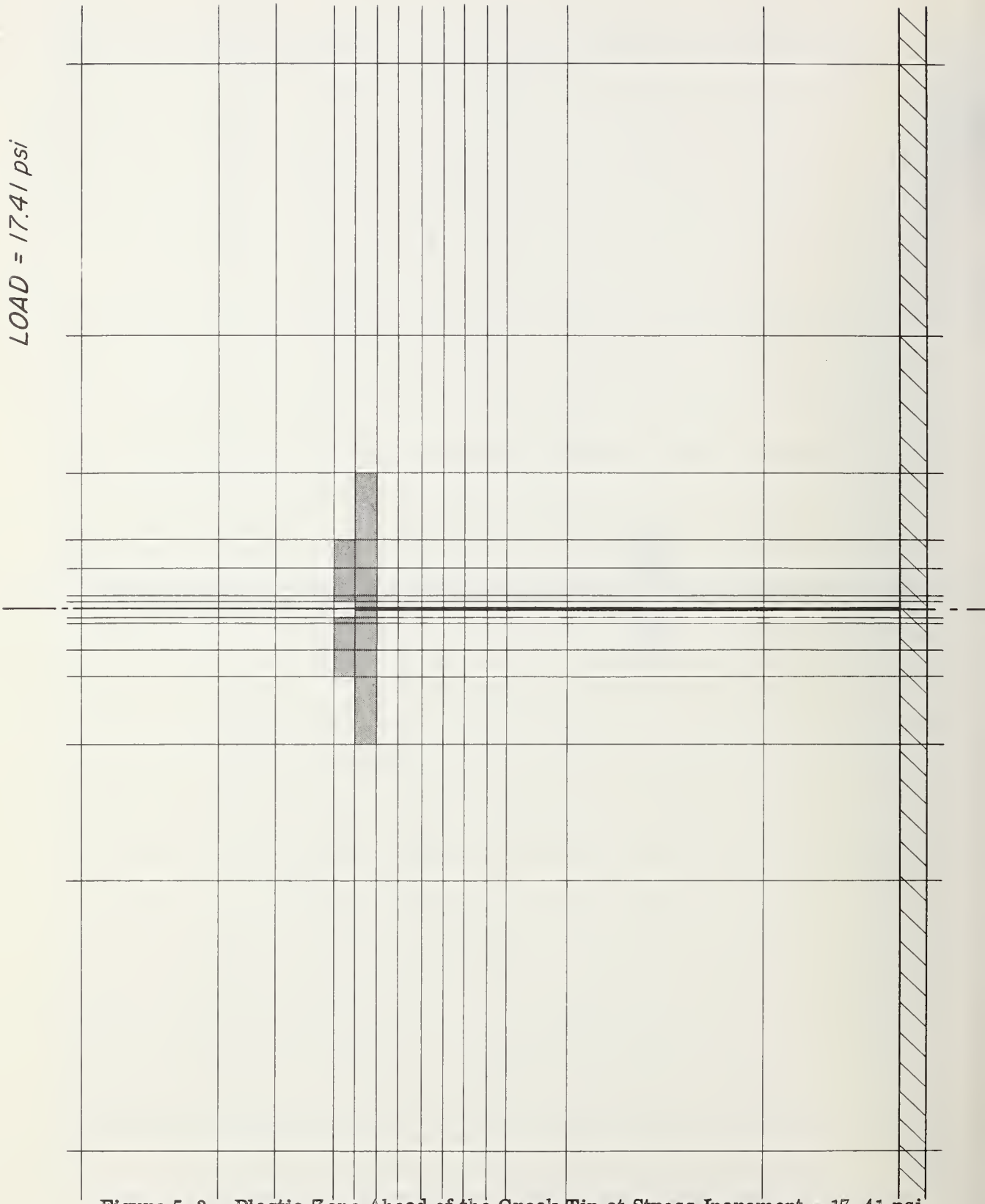

Figure 5.3. Plastic Zone Ahead of the Crack Tip at Stress Increment = 17.41 psi

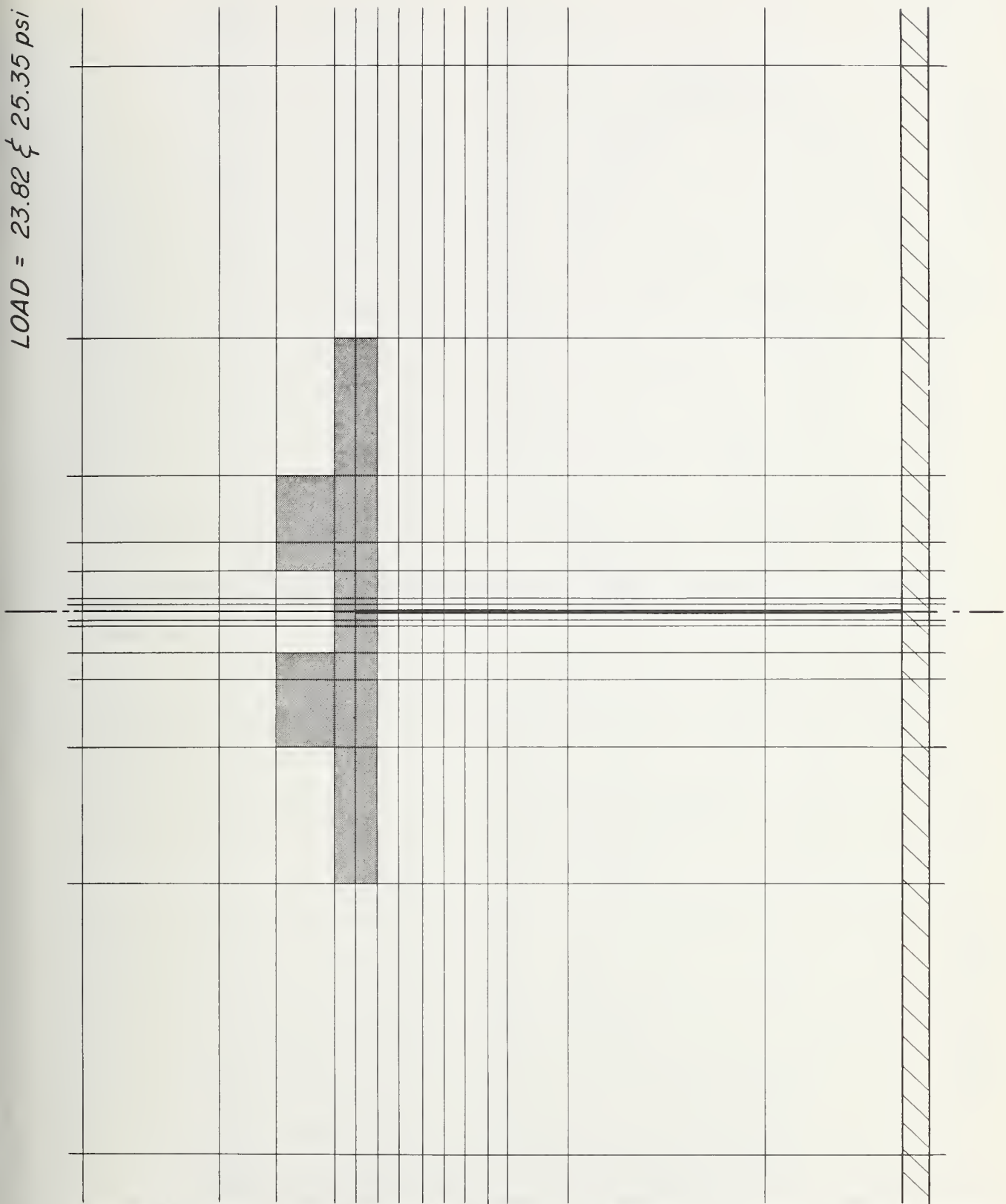

Figure 5.4. Plastic Zone Ahead of the Crack Tip at Stress Increments = 23.82 & 25.35 psi

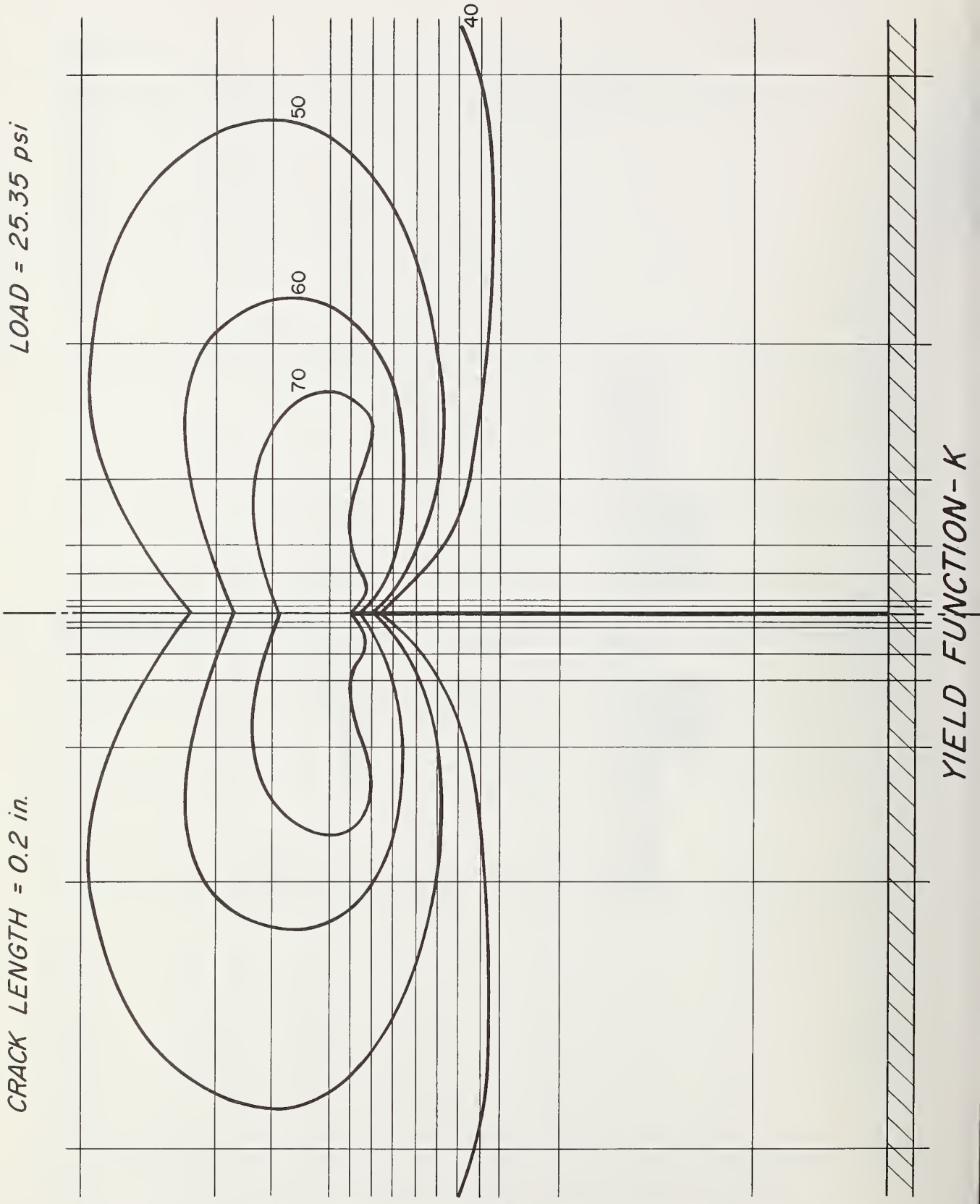

Figure 5.5. Elastic-Plastic Boundaries for C = 70 psi, $\Phi = 0$, and T = 90°F

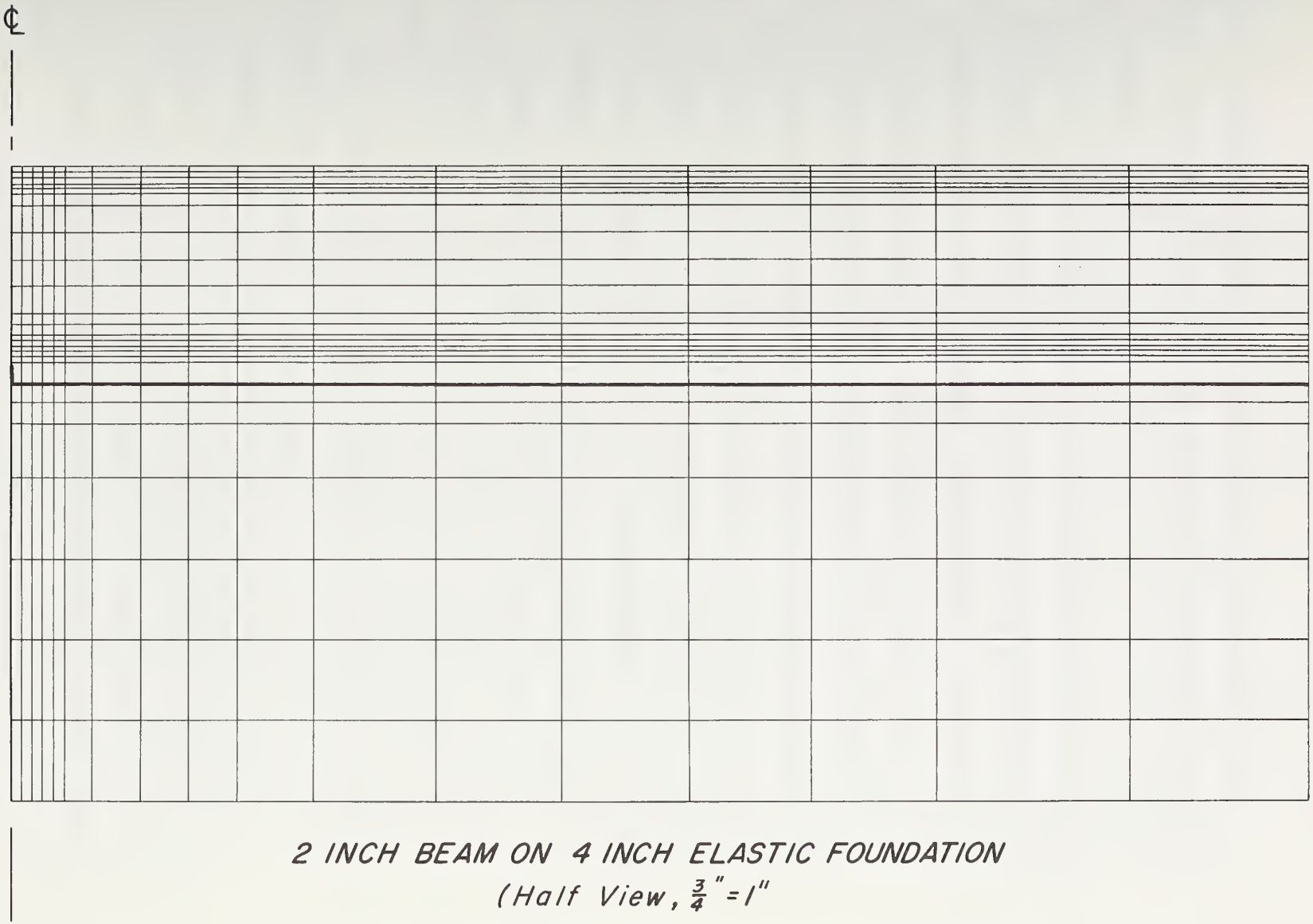

Figure 5.6. Finite Element Mesh of a Beam on Elastic Foundation

In accordance with the results reported by Hilton (55), Hutchinson (56), Marcal (57) and Rice (58), it is noted that elastic-plastic boundaries grow with an increase in the load increments. Furthermore, the maximum radius of plastic zone does not occur directly ahead of the crack tip, rather the line of maximum plastic radius makes an angle of approximately 80 degrees with the crack tip direction as shown by other investigators (57 ,58). Two interesting observations are relevant at this point. First, the comparison of plastic zone at two temperatures at 77°F and 90°F indicates that at higher temperatures a substantially large elastic-plastic boundary is formed at the crack tip. Secondly, at high temperatures such as 90°F, a plastic yielding is also observed directly under the loaded area which extends toward the interior. The existance of such yielding conditions at higher temperatures, therefore, it expected to influence the state of stress distribution and the rate of crack propagation.

As has been argued by Liu (59), it is probable that due to the size of the plastic zone ahead of the crack tip, the exponent n in the crack propagation model might deviate from 4 as has been predicted by the Paris model. In fact, unpublished results by Karamians indicates that at 90°F, the exponent n for an asphaltic concrete mixture is 3.5 as compared to value of 4 obtained at 77°F.

Recently, Hilton and Hutchinson (25) performed an elastic-plastic analysis involving the plastic intensity factor for cracked plates, and suggested that the initial fracture prediction from classical fracture mechanics are accurate for applied stresses up to approximately half of the yield stress.

Although at the half yield stress the elastic-plastic boundary is distorted from that associated with small scale yielding, it appears that the classical approach is still applicable.

Under the condition of $\sigma_{yy} < .5\ \sigma$ yield, the effect of plastic yielding can be incorporated in the stress intensity factor as given by equation 2.22 in Chapter II. From the material characterization viewpoint, it is appropriate that for tests to be conducted at high temperatures, such as 90°F or over, the specimen dimension, crack size and load magnitudes should be selected with consideration to the radius of plastic zone and the elastic-plastic boundary. The finite element program used in this study or similar available programs can provide an accurate estimate of elastic-plastic boundaries and their influence on the crack propagation. It should be pointed out, however, that at this time a general purpose three-dimensional elastic-plastic finite element program capable of analyzing cracked bodies is unavailable. Besides, the operational cost of such a program will prohibit its use for routine analysis purposes. Therefore, in this investigation, which is concerned with the response of a cracked slabs resting on elastic foundation, an experimental technique was utilized.

C. Experimental Procedures for Slabs Resting on an Elastic Foundation

To verify the effect of high stress levels applied to asphalt slabs resting on an elastic foundation, two series of tests were performed. All the tests were done using the MTS in load control and a loading function consisting of a

half-sine function with a duration of 1.0 second and a rest period of 0.8 seconds. These experiments were conducted at room temperature, and the elastic foundation used was the one referred to as the "old foundation" (see appendix). Consequently, the modulus of subgrade reaction, k, corresponding to the experiments described in this chapter was somewhat lower than the value used in all other experiments described previously (see Appendix A).

In the first series of test, a load of 500 pounds (corresponding to 25.5 psi under the loaded area) was applied to the asphalt slab. This load level was selected because it was found experimentally that stresses under the load in excess of 20 psi were sufficient to cause permanent deformation under the load. The second set of experiments was performed using a high load (600 pounds) for 3,000 cycles so as to develop some permanent deformation under the load, and then the load was changed to 300 pounds and continuing the test until failure occurred.

D. Analysis and Discussion of Results

The results from these tests where high loads were used show that the crack pattern in the slabs was very similar to that reported in Chapter IV. Crack measurements were made using the same technique, i.e., visual measurements to determine the length of the top cracks and x-ray photographs to determine the length of the bottom cracks. The change in the center deflection amplitude was also similar, as it can be seen in Figures 5.7 and 5.8, where the center deflection amplitude measured by the MTS LVDT is plotted versus the

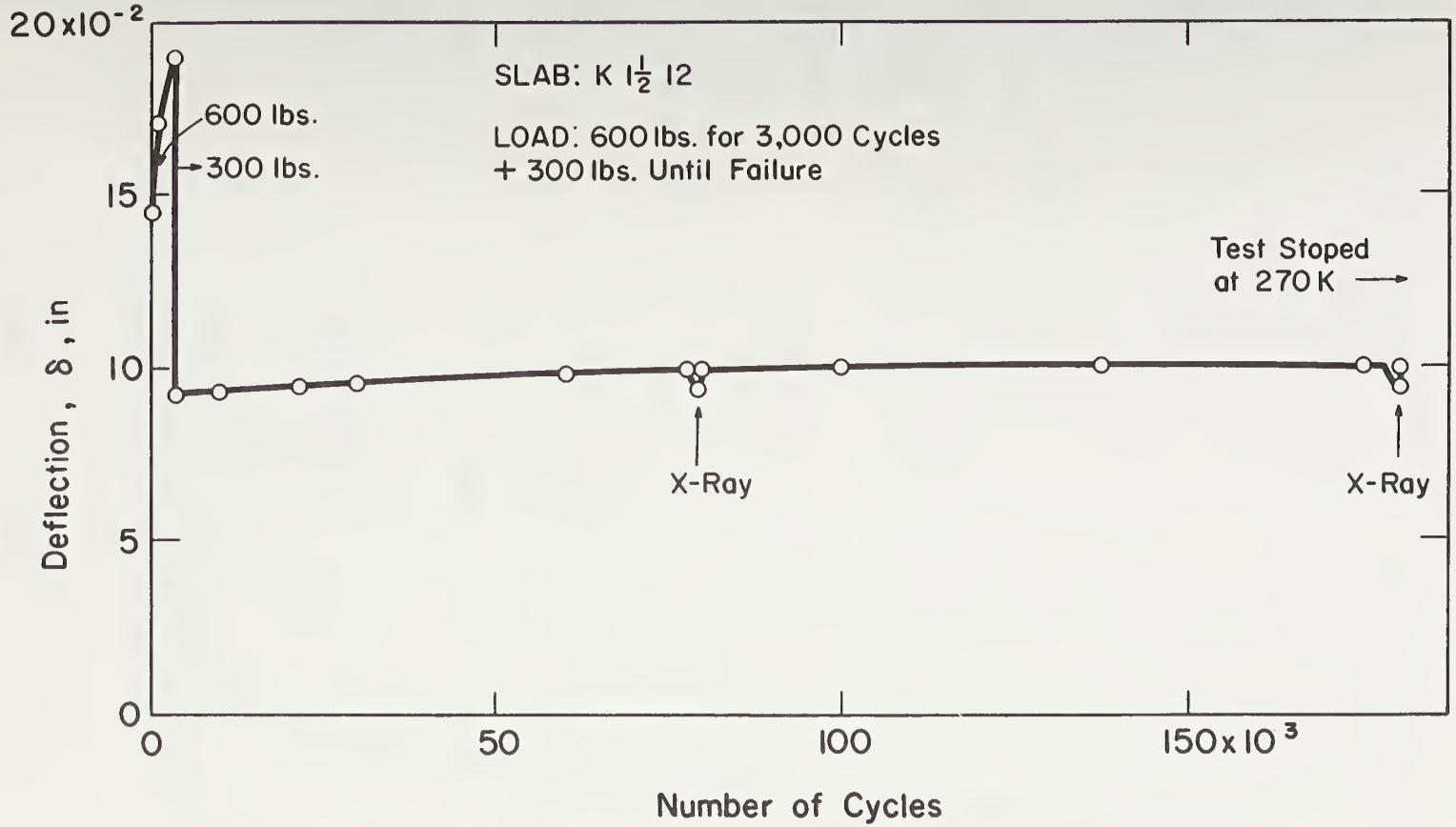

Figure 5.7. Variation of Deflection with Number of Load Cycles for 600 lbs.-300 lbs. Load Sequence

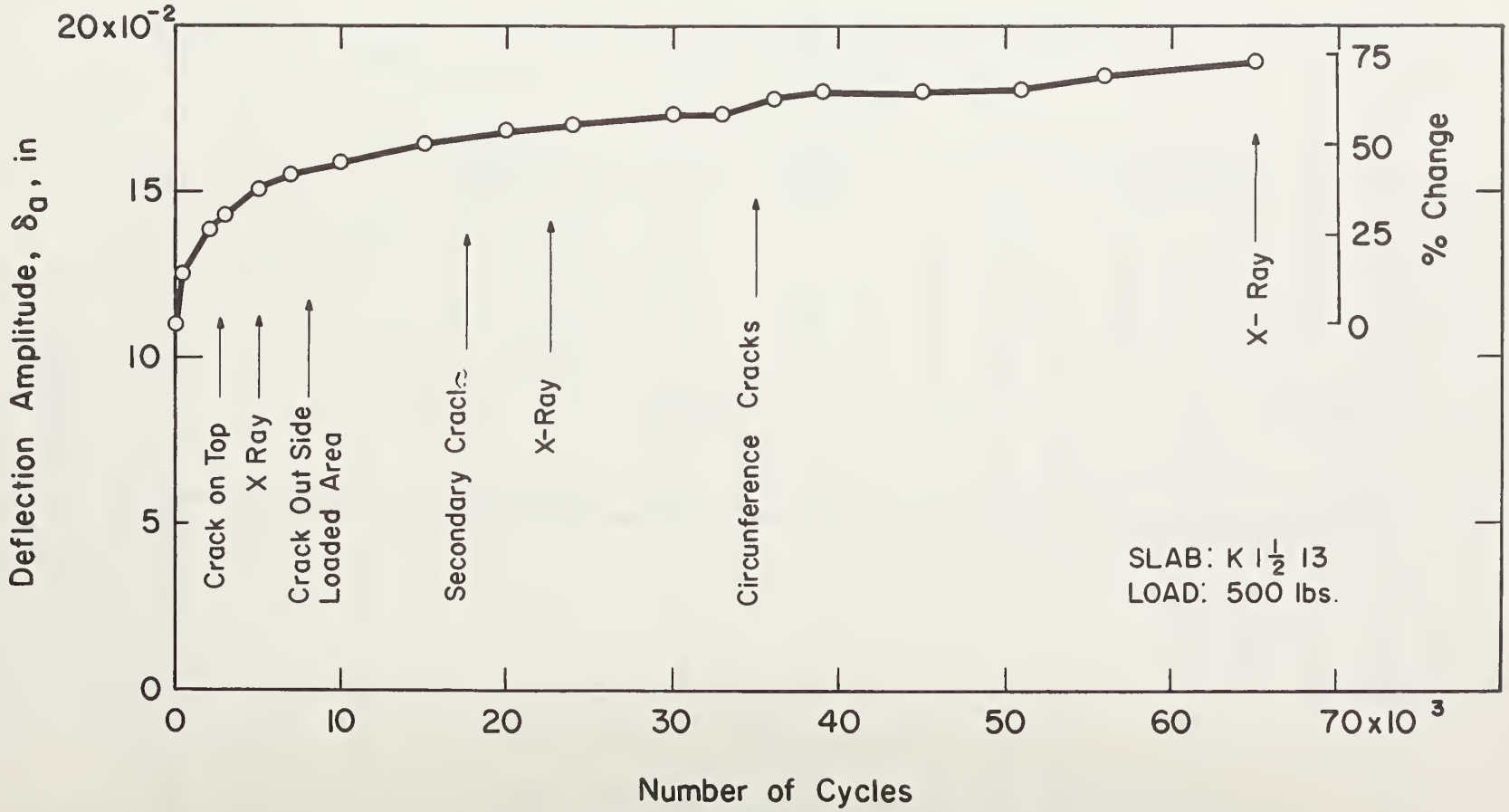

Figure 5.8. Variation of Deflection with Load Repetition for 500 lbs. Load Series

number of cycles. These figures also show that the time lapsed between x-rays was considerably smaller than 80,000 to 100,000 cycles, mainly due to the fact that the duration of these experiments was much shorter.

The main difference observed in these tests was the fact that there was a large amount of permanent deformation under the loaded area. Figure 5.9 shows the permanent deformation under the load, plotted versus the number of cycles. Except for the initial portion where the initial curvature is significant and probably due to some viscoelastic effect, it is noted that the rate of change in the permanent deformation was approximately constant with the change in the number of cycles, i.e. following a relationship of the form:

$$\frac{d\delta_p}{dN} = C \tag{5.3}$$

It is important to notice that this amount of permanent deformation was not caused by densification of the material under the load. This fact, can be substantiated by inspecting Plate 5.1, where two x-ray photographs for a test in which a load of 500 lbs. was used is presented. It is noted that the dark portion at the center of the picture, corresponding to the area of the slab under the load, gets darker as the test progresses. The dark area in the x-ray is an indication of less material and not of denser material. The conclusion, therefore, is that there was some flow of material from under the loaded area to adjacent areas, and this was the cause for the permanent deformation under the load.

1. X-Ray Photograph Showing the Center of the Slab after 25,000 Cycles of Load Application.

2. X-Ray Photograph Showing the Center of the Slab after 65,000 Cycles of Load Applications.

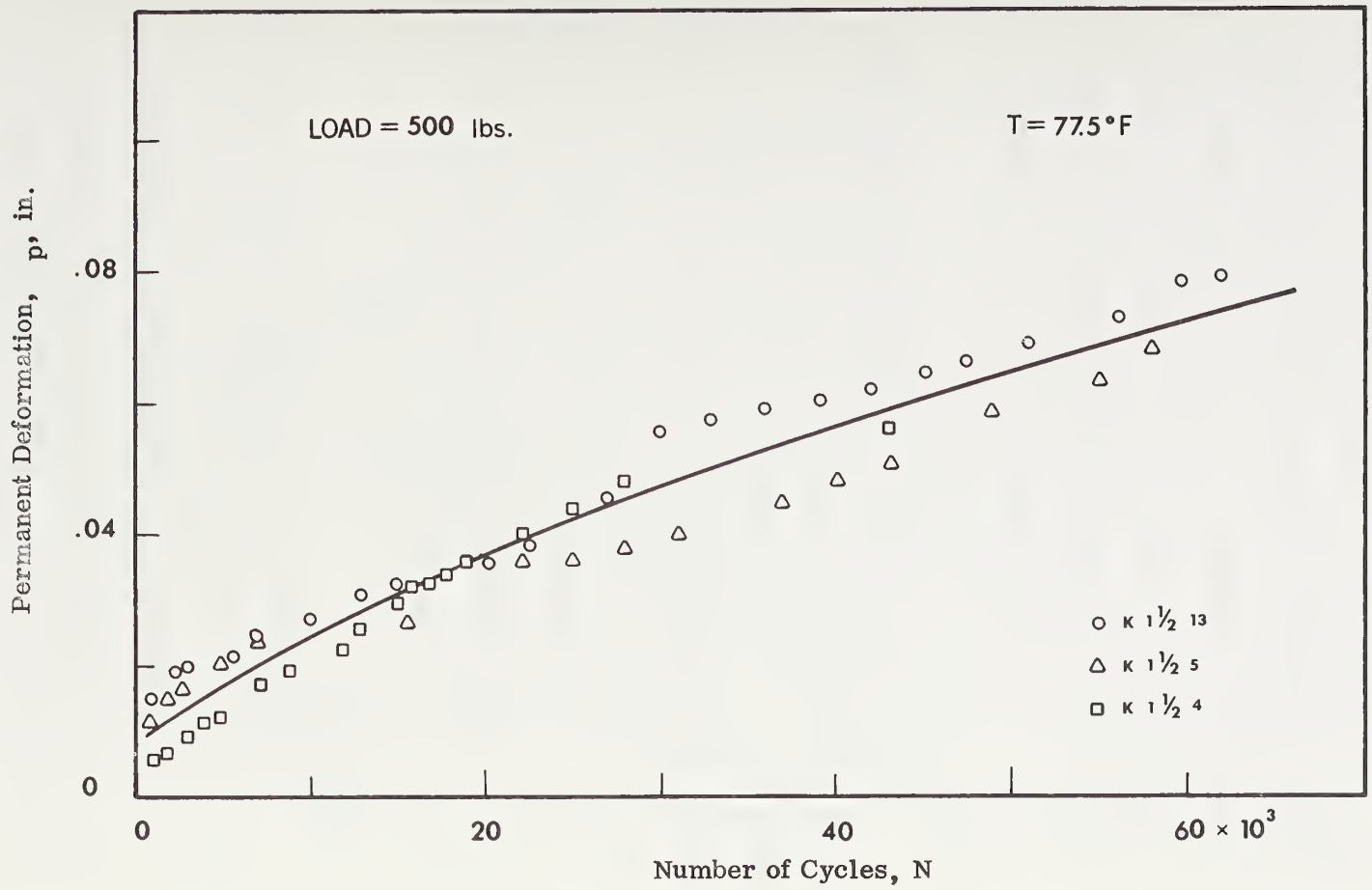

Figure 5.9. Variation of Permanent Deformation with Load Repetition for 500 lbs. Load Series

The x-ray photographs also showed that the equilibrium shape of the cracks was different in these tests than those previously reported. This fact is presented graphically in Figures 5.10 and 5.11 where the bottom and top cracks are plotted versus the number of cycles. It is noted that the difference in length between the top cracks and bottom cracks was smaller than before. In the tests where the load was changed to 300 pounds after the first 3,000 cycles, the bottom and top cracks had approximately the same length from the point where the load was changed until the end of the test.

Based on the assumption explained in item A of this chapter, that the elastic stress-intensity factor can be used whenever the stress does not exceed half of the yield strength, plots were made of the rate of crack propagation versus the stress-intensity factor. The results are presented in Figures 5.12 and 5.13, and it can be seen that indeed the rate of crack propagation followed Paris' law and was not affected by the amount of permanent deformation under the loaded area. The analysis of these cracks were made from the point where the cracks were outside of the load, to the point of failure.

E. Conclusions

The experimental work reported in this chapter involved tests on slabs supported on an elastic foundation and subjected to high stress levels. The results showed a substantial amount of permanent deformation under the loaded area which was attributed to some form of flow of the material from under the load to adjacent areas. The permanent deformation measured indicated that

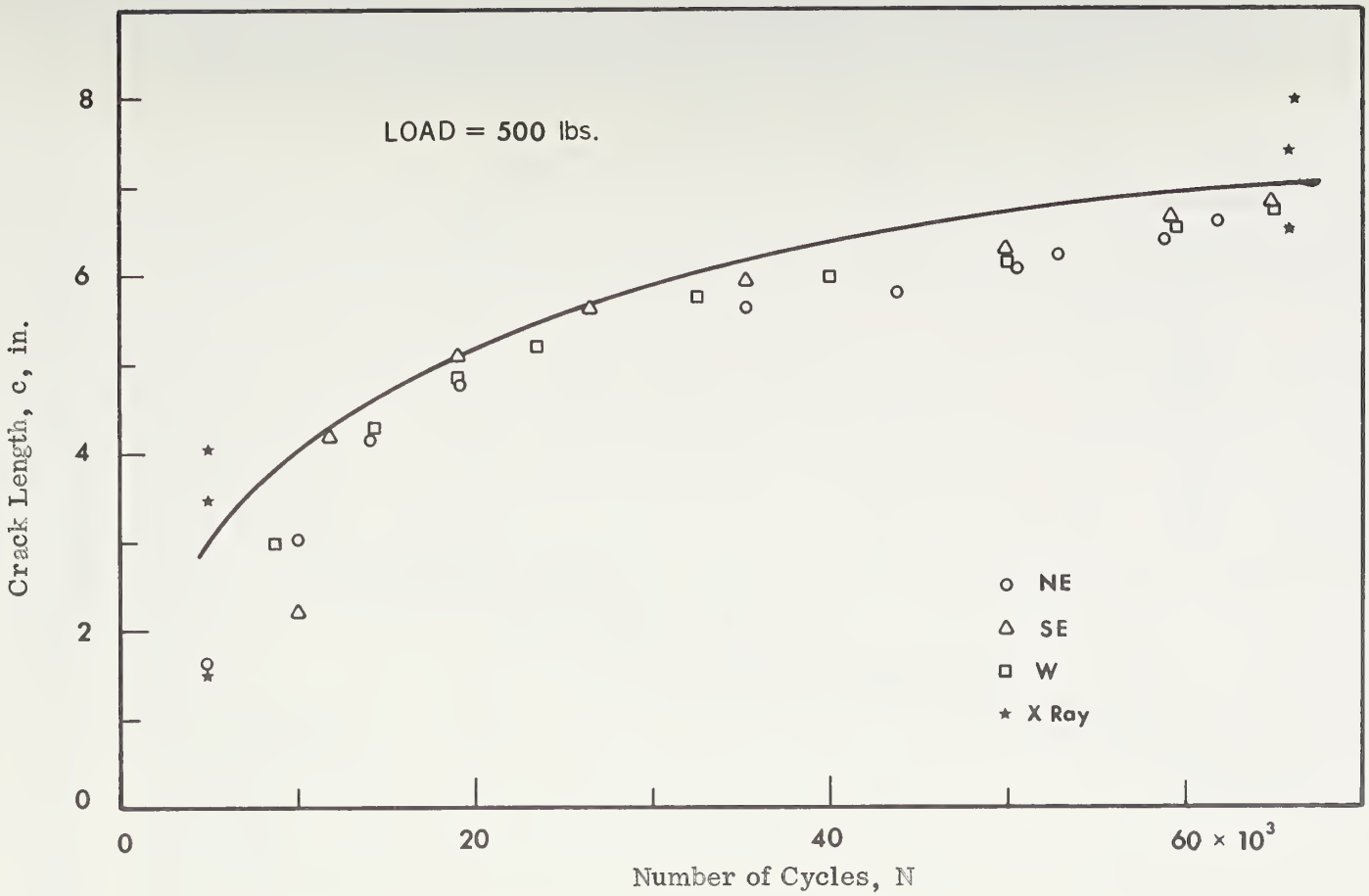

Figure 5.10. Variation of Crack Length with Number of Load Cyles for 500 lbs. Load Series

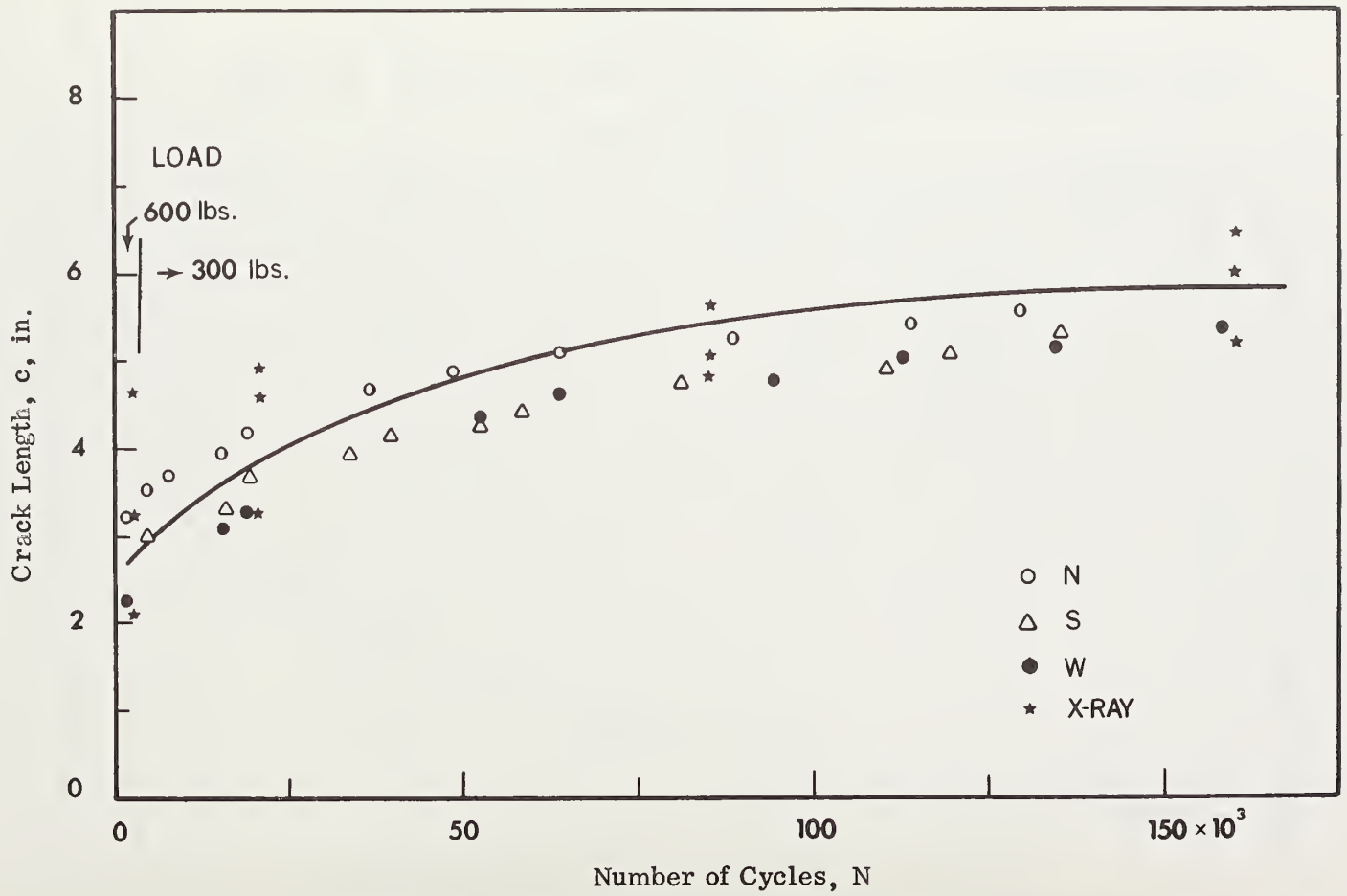

Figure 5.11. Variation of Crack Length with Number of Load Cycles for a 600 lbs.-300 lbs. Load Sequence

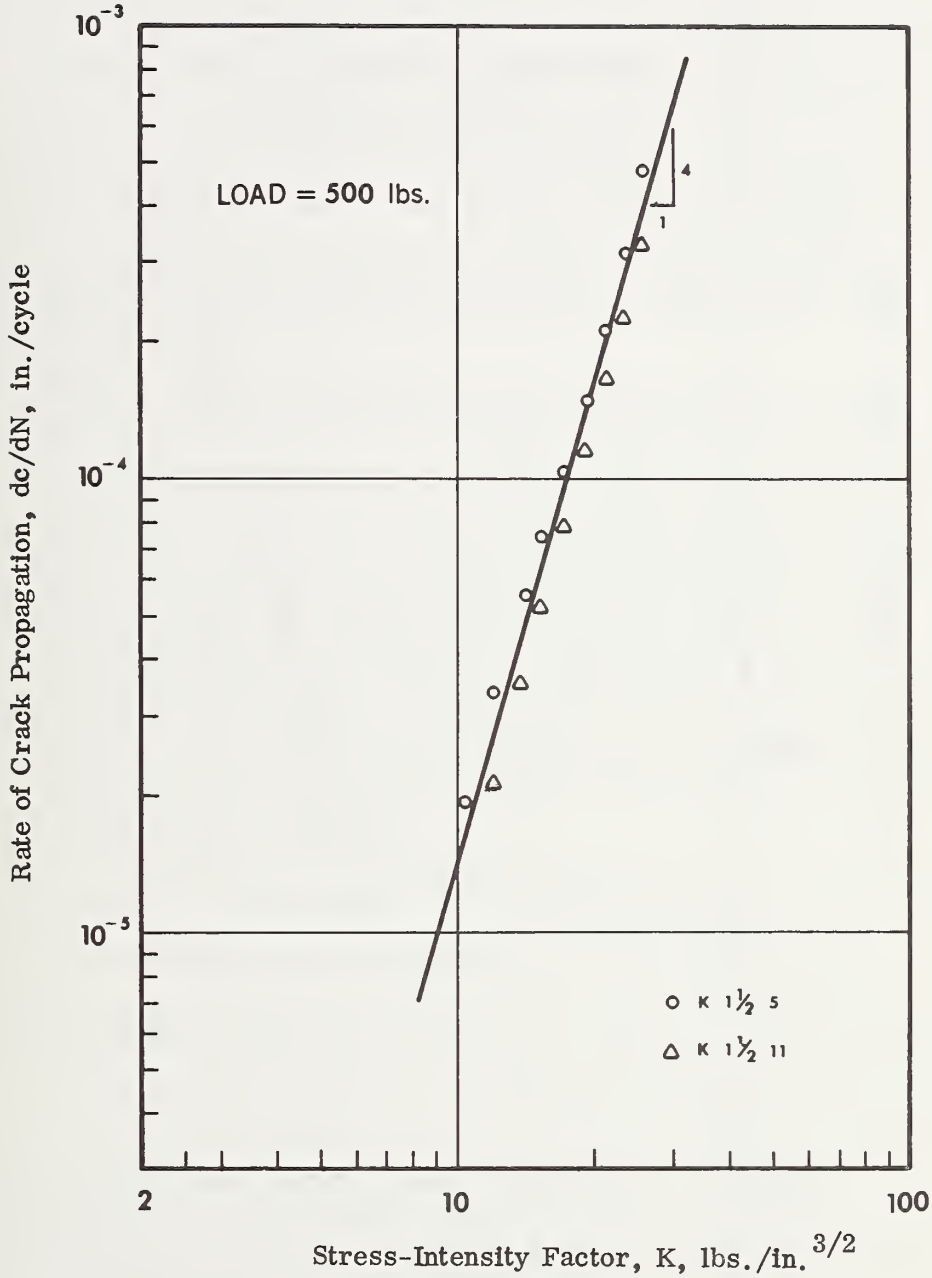

Figure 5.12. $\frac{dc}{dN}$ - K Relation for a 500 lbs. Load Series

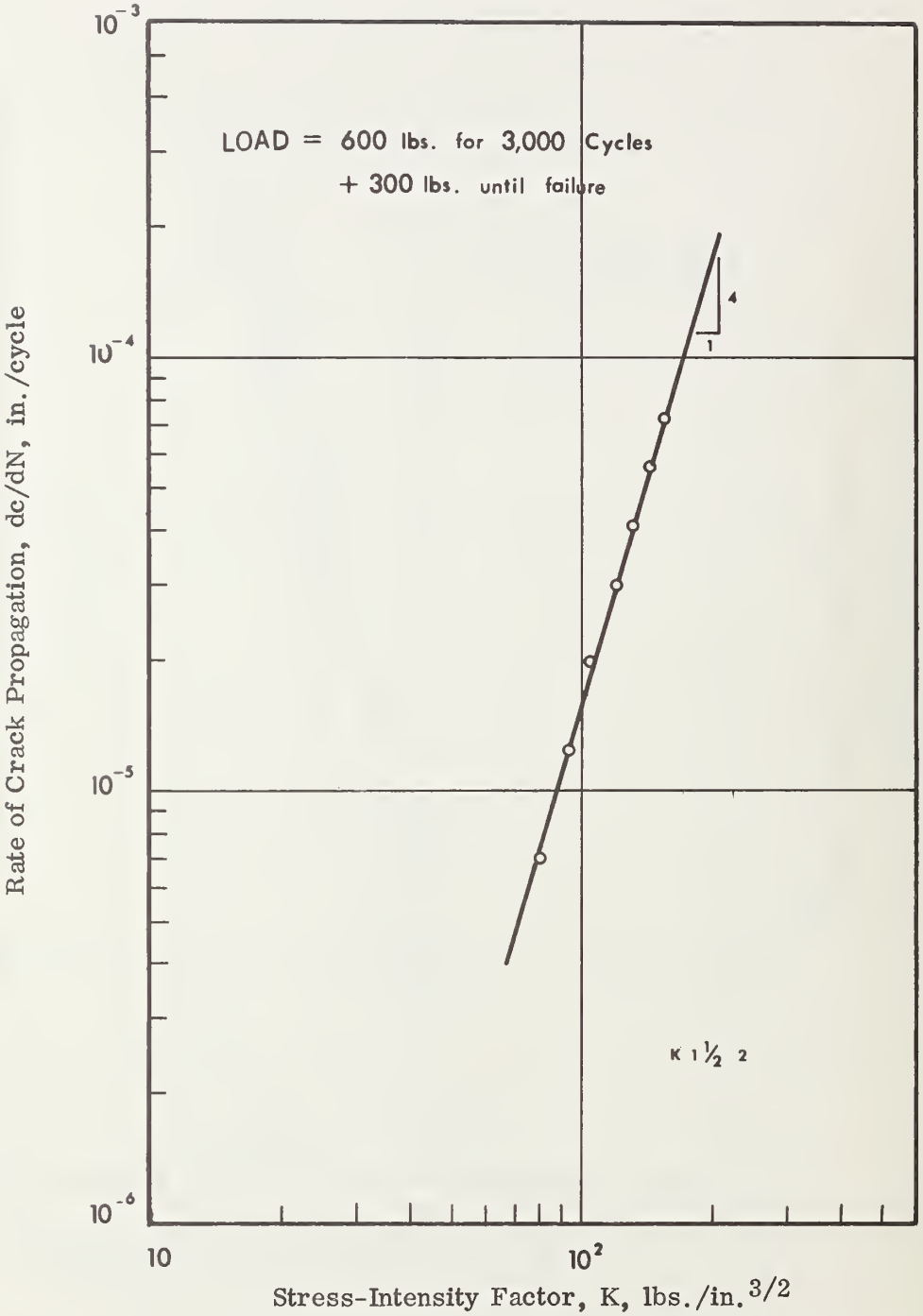

Figure 5.13. $\frac{dc}{dN}$ - K Relation for a 600 lbs.-300 lbs. Load Sequence

this phenomenon was of a cumulative nature and that the amount of irrecoverable deformation varied almost linearly with the number of load applications.

The rate of crack propagation was investigated for the top and bottom cracks from the point in which these cracks were outside of the area under the load. It was found that the Paris law relating the rate of crack propagation to the stress-intensity-factor was applicable and that the power n in that law was found experimentally to be 4.

It should be mentioned that the permanent deformation induced in these experiments by applying high loads to the asphalt slab, was of an entirely different nature than that occuring due to creep or viscoelastic flow which is so common in parking lots and areas of the highways where vehicles travel at slow speeds. The tests reported in this section involved very high rates of loading, rates at which the asphaltic material composing the slabs is expected to behave as an elastic and elastic-plastic material.

The analysis of elastic-plastic stress distribution carried out for a two-dimensional system indicates that depending on the load magnitude and the material characteristics, elastic-plastic boundaries are formed in the vicinity of the crack tip. For small scale yielding, the elastic stress-intensity-factor can be modified by the equation given in Chapter II. However for sufficiently large zones of plasticity, the power n in the Paris crack propagation model might deviate from its theoretically expected value of 4.

CHAPTER VI

APPLICATION OF THE PROPOSED MODEL TO ANALYSIS AND DESIGN OF FLEXIBLE PAVEMENTS

A. Introduction

In the previous chapters of this report, the effect of load and environmental variables on the crack propagation of a pavement model was presented. The experimental data and the theoretical formulations of the fracture mechanics method of analysis were documented and the applicability of the proposed distress concept to analysis of fatigue crack propagation of a pavement model was presented. As the ultimate objective of this study, it is necessary to demonstrate the validity of the proposed model to analysis and design of flexible pavements having realistic boundary and geometrical characteristics. Since the proposed method of analysis was developed using an asphalt slab resting on an artificial foundation, it would be necessary, as a first step, to investigate the validity of the concepts developed for pavement slabs resting on real subgrade soils. Having achieved this objective, the applicability of the proposed model to analysis and design of typical flexible pavements will then be discussed.

B. Verification of the Model for a Pavement Resting on Subgrade Soil

To investigate the applicability of the proposed distress model for the prediction of fatigue crack propagation in a flexible pavement resting on subgrade soil, two alternate methods of analysis were reviewed. Firstly, consideration was given

to the modification of the pavement model which was developed in this study and was subsequently used for the experimental verification of the mechanistic approach. However, considering the geometry of a typical flexible pavement and the boundary conditions of this facility, it can easily be deduced that this model cannot fulfill the stress distribution requirements. Besides the construction of a subgrade support with uniform properties, as might be required for this theoretical verification, cannot be easily achieved.

As a second alternate approach, consideration was given to the use of an experimental full-scale flexible pavement for which in-put variables and material characteristics can easily be obtained. The results of the studies by the late Bonner Coffman (59) on the analysis of fatigue of full-scale pavements, fulfill the above requirements. In this study, the data presented in the research report of project EES 296 (59), "The Fatigue of Flexible Pavements," conducted under joint sponsorship of the Ohio Department of Transportation and the U.S. Department of Transportation, was utilized.

In such a full-scale flexible pavement, depending on the constructional procedures, frictional resistance is expected to be fully or partially developed between various layers. Before the applicability of the proposed distress model to such a pavement model can be investigated, the effect of bonding conditions on the crack propagation needs to be verified. The mathematical model of pavement fatigue presented by Ramsamooj (14,15) incorporates a bonding parameter to be determined with consideration to the moment function and induced stresses and strains in the pavement system.

In this study an independent verification of the proposed model was carried out by evaluating the rate of crack propagation in a bonded slab resting on the elastic foundation. The results of observations on the growth of fatigue with the number of cycles of load repetition are presented in Figure 6.1. The stress-intensity factor - crack length relation calculated for the bonded slab resting on the elastic foundation is presented in Figure 6.2. The evaluation of the rate of crack propagation as presented in Figure 6.3, indicates that the proposed distress model is also applicable to bonded slabs resting on elastic foundation. However, in the full-scale flexible pavement used in the Coffman's study, the nature of bond between the flexible pavement and the subgrade soil is not exactly known. Apparently for the material sampling purposes, the bond between the pavement and the subgrade was partially destroyed using a layer of lime. Therefore in this study, it has been assumed that during the second stage of crack propagation where the lateral extension of cracks occur, the unbonded analysis will be applicable. This assumption leads to a more conservative analysis. However, for the analysis of the first stage of crack propagation, due to relatively large shear stresses developed under the loaded area and its vicinity, the assumption of friction interface is more appropriate.

With respect to the geometrical characteristics, it should be noted that this pavement was constructed as a full depth structure with uniform material properties. This experimental pavement was constructed in sections of varying thicknesses, ranging from 3.5" to 9.5". However, observing the crack growth pattern and the experimental data available, the pavement section with 6.5" thickness was found

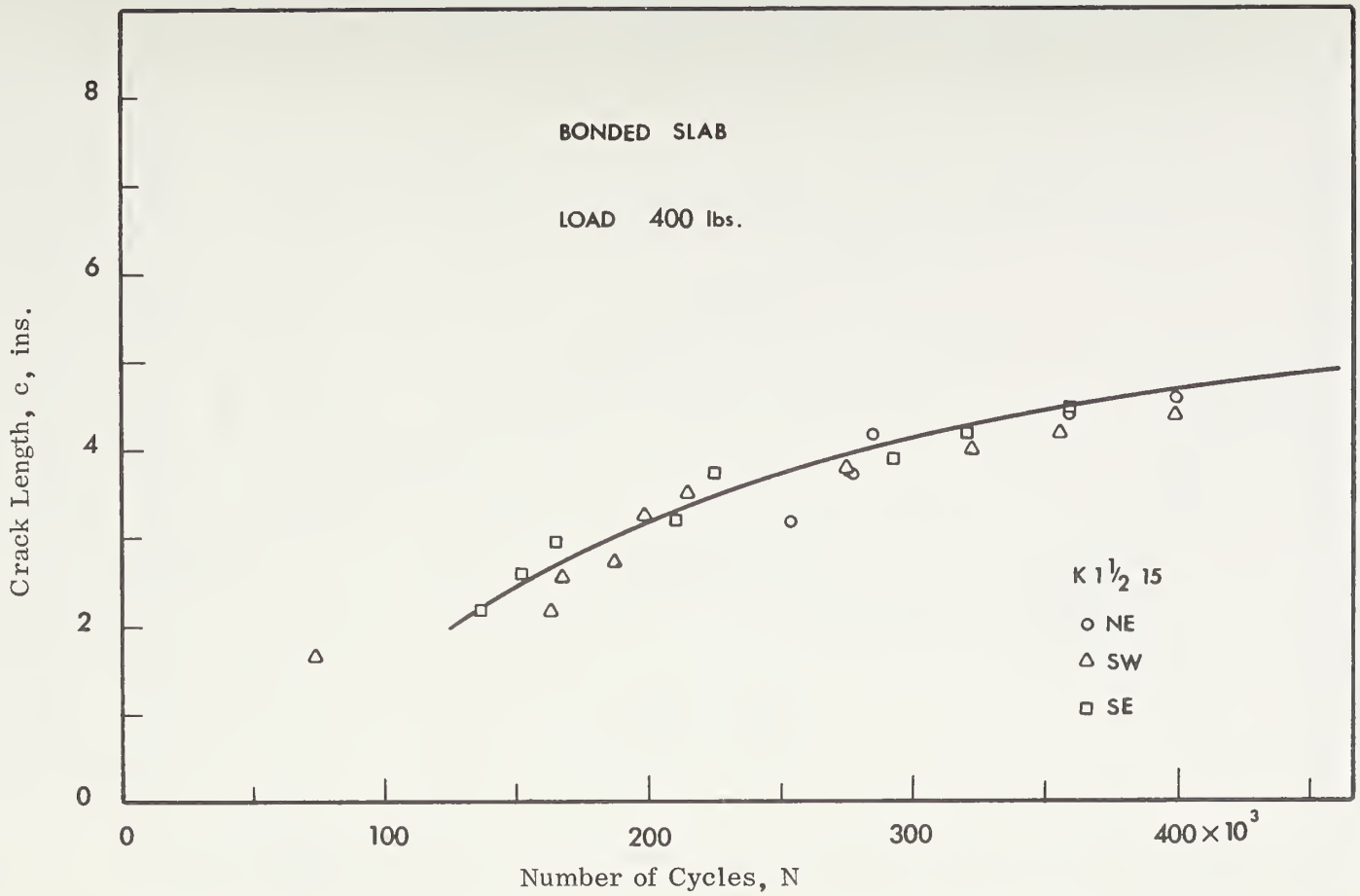

Figure 6.1. Variation of Crack Length with Load Cycles for a Bonded Slab at 77.5°F

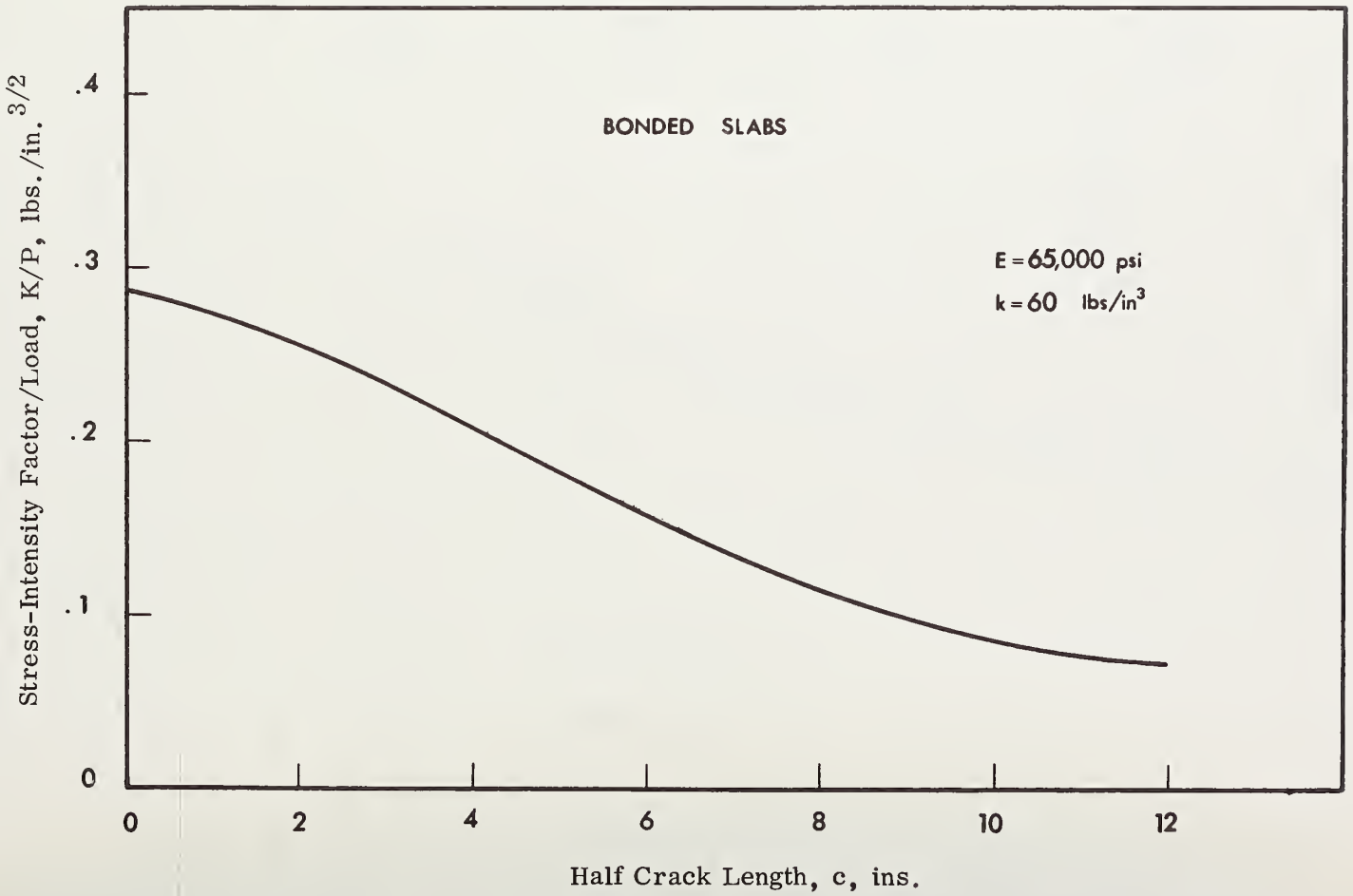

Figure 6.2. Variation of Stress-Intensity Factor, K, with Crack Length for a Bonded Slab

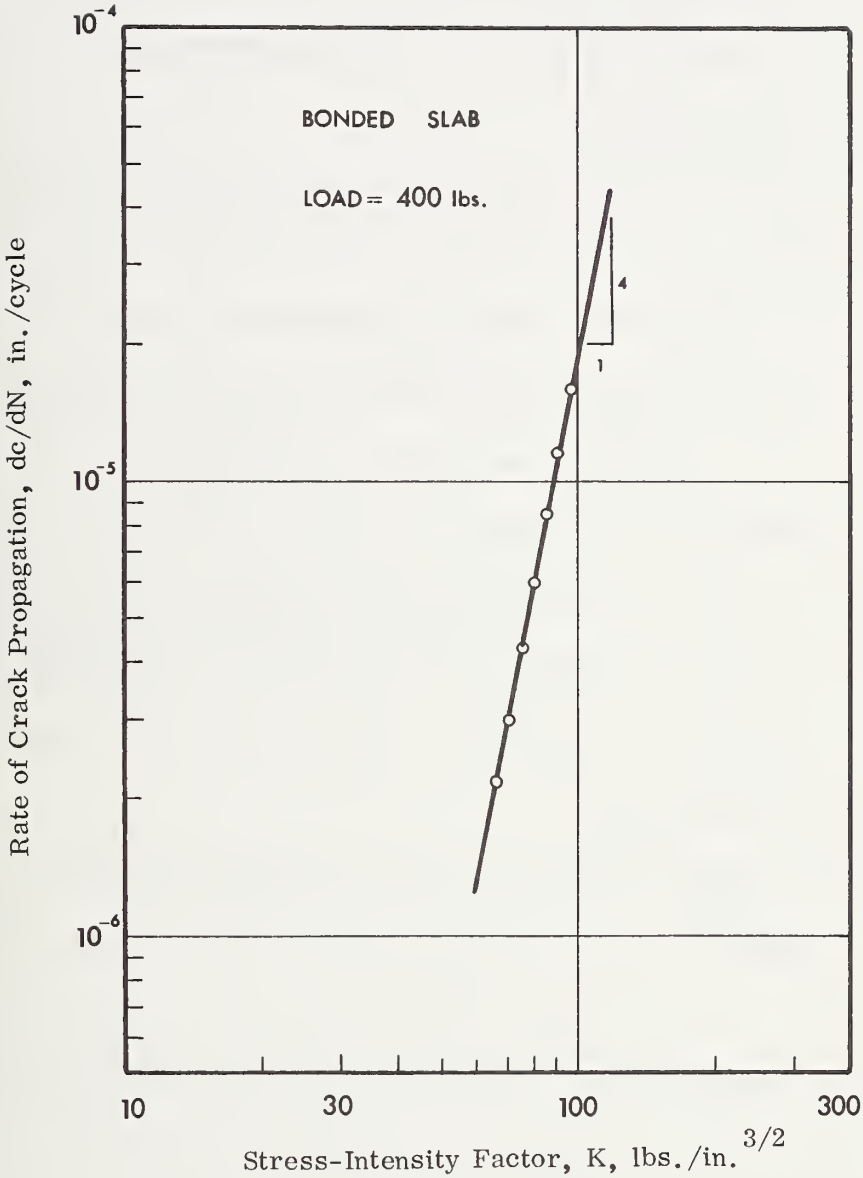

Figure 6.3. $\frac{dc}{dN}$ - K Relation for a Bonded Slab at 77.5°F

to be most suited for this study. This pavement was tested under a dynamic load of 18 kips distributed over a circular area of 13.2 inches in diameter. (The details of the experimental data in this test section is summarized in Figure A-7 of the appendix (ref. 59).

The first crack observed during this experiment was located on the northeastern section of the loaded area which was then followed by the other cracks appearing on the western and southeastern directions (Figure 6.4). The only crack that followed a normal growth pattern was that of the southeastern direction. The crack on the west side of the loaded area, however, grew at first in a normal pattern and then suddenly deviated from the norm and became unstable. The observation of the overall crack pattern in this experiment indicates that the pavement slab failed unsymmetrically. The unstable crack growth of the western crack was most probably due to the premature failure of the slab on the west side of the loaded area (Figure 6.4).

The analysis of crack growth of this test pavement indicates that the first crack was sighted outside of the loaded area after 277,000 cycles of load application. There is no data available for the first stage of crack propagation, during which the crack is initiated at the bottom of the slab and grows upward in an elliptical shape. However, considering the crack growth pattern of the pavement model reported in this study, it is logical to assumed that the first crack appeared on the surface within 100,000 - 150,000 cycles of load repetition.

To verify the applicability of the proposed crack growth model to the analysis of fatigue of this test pavement, the experimental results presented by Coffmann (59)

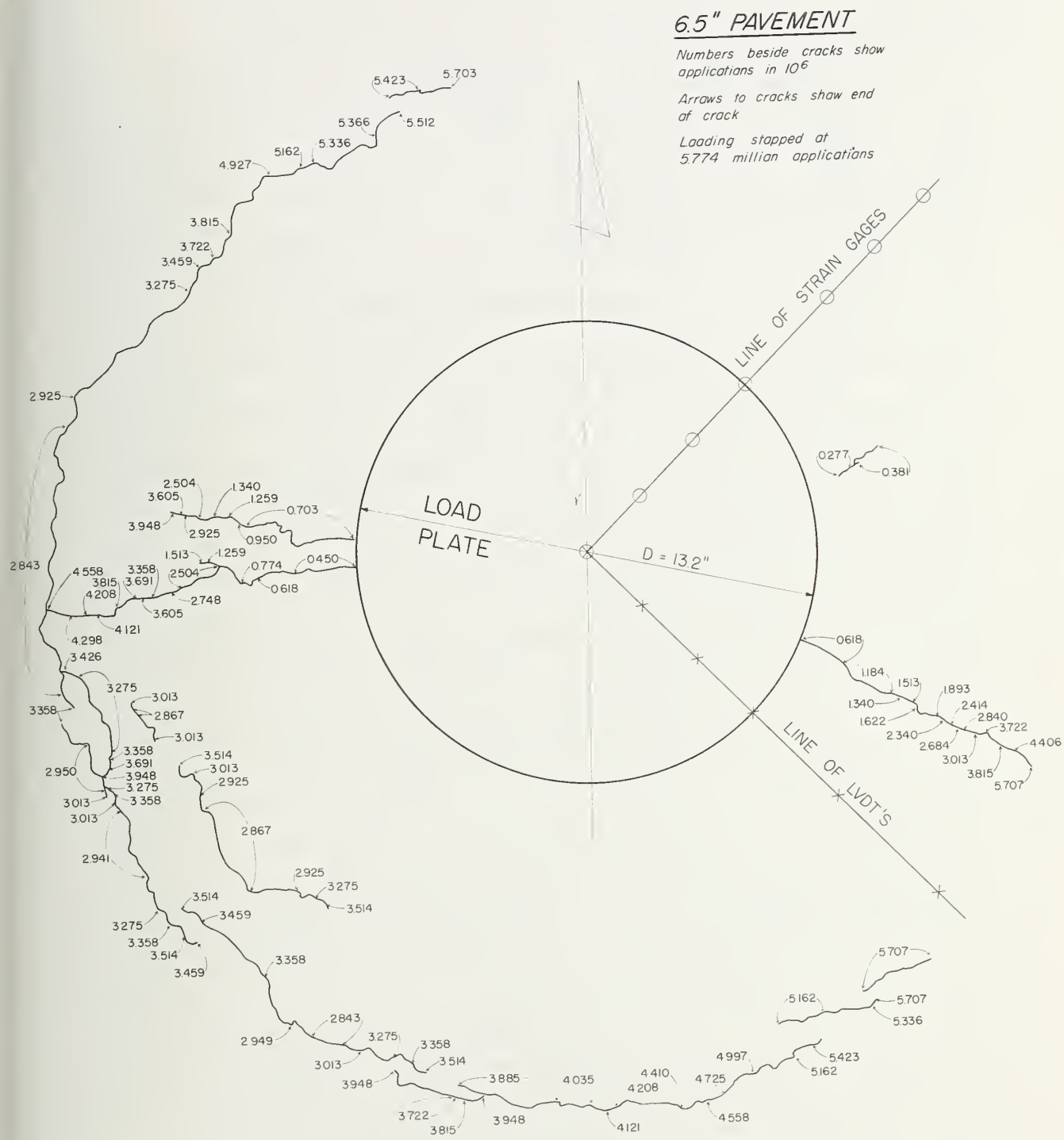

Figure 6.4. Cracking History on the 6.5" Pavement

were utilized. The observed data on dynamic deflection, strain, pavement temperature and the material properties are presented in reference 59.

The asphaltic concrete mixture used in the Coffman investigation corresponds to the Ohio Department of Transportation's mixture 404. The Marshall test results on this mixture is presented in Figure 6.5. The results of the dynamic modulus experiments conducted at various frequencies and temperatures are presented in Figure 6.6. The dynamic modulus of the asphaltic concrete was tested at a frequency of 30 radians/second and at a temperature of 70°F. The test temperature was estimated at 500,000 psi. This value corresponds very closely to the modulus of mixtures 404 and 402 used in the State of Ohio. From the experimental data presented for the variation of dynamic modulus with frequency, the modulus of subgrade soil was selected at 19,500 psi. Considering the support characteristics of subgrade soil in Ohio, this value corresponds to a relatively good subgrade soil with an equivalent CBR = 13 and K = 200.

Utilizing the available data, a crack length - number of cycles relation can be developed as shown in Figure 6.7. In this figure the data for a southeast and west crack are presented along with actual temperature measurements on the test pavement. By incorporating the moduli of the pavement layers, pavement thickness and load magnitude into the mathematical model previously described, the stress-intensity factor - crack length relation for this pavement is calculated. The results of K - C relation is presented in Figure 6.8. It is interesting to note that in this pavement, the rate of change in stress-intensity factor woth the crack length is rather small. That is, even at a crack length of over 24 inches, the

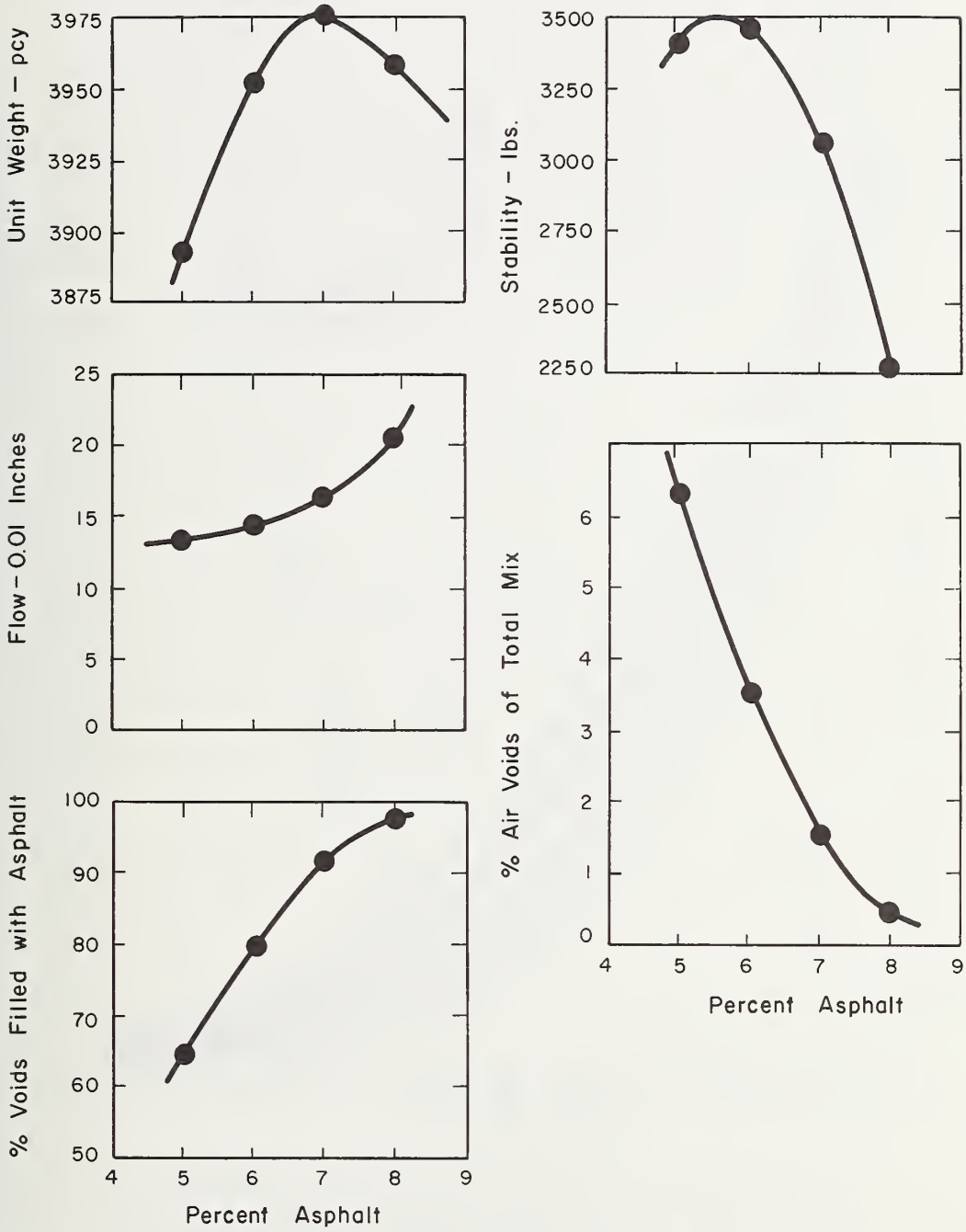

Figure 6.5. Marshall Test Results

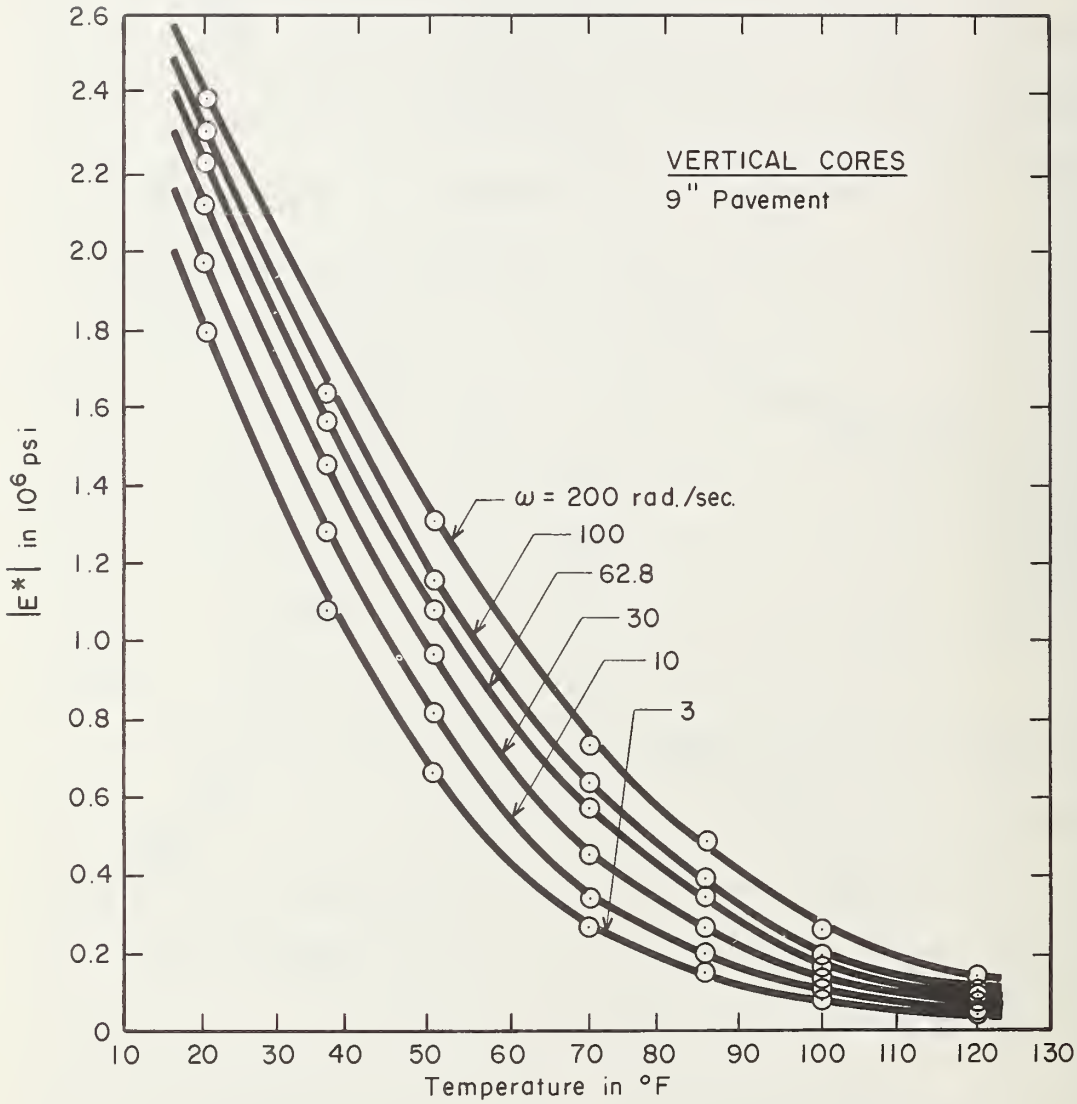

Figure 6.6. Complex Moduli of Asphaltic Concrete

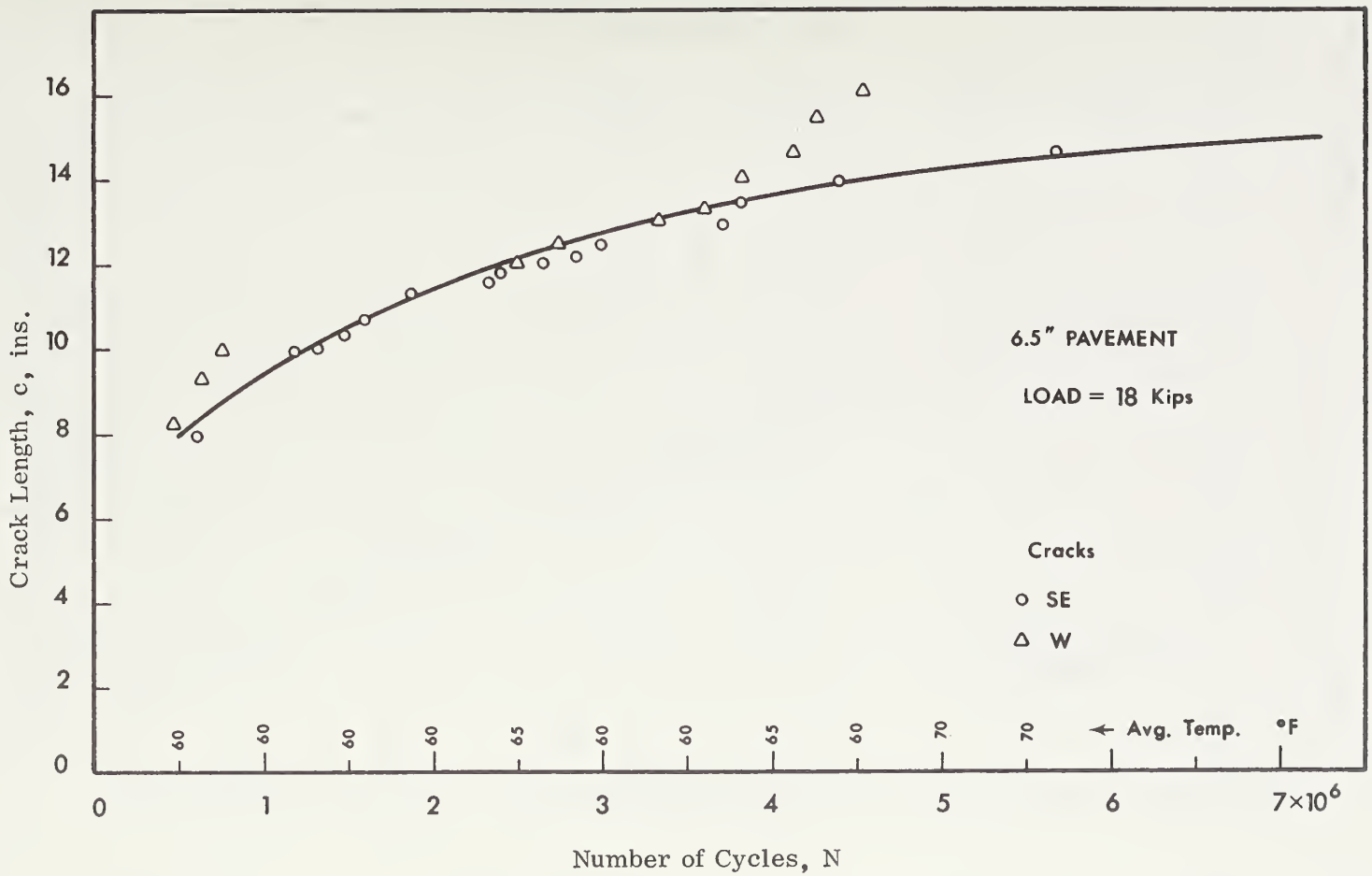

Figure 6.7. Variation of Crack Length with Load Cycles for a Typical Pavement (EES 296, ref. 59)

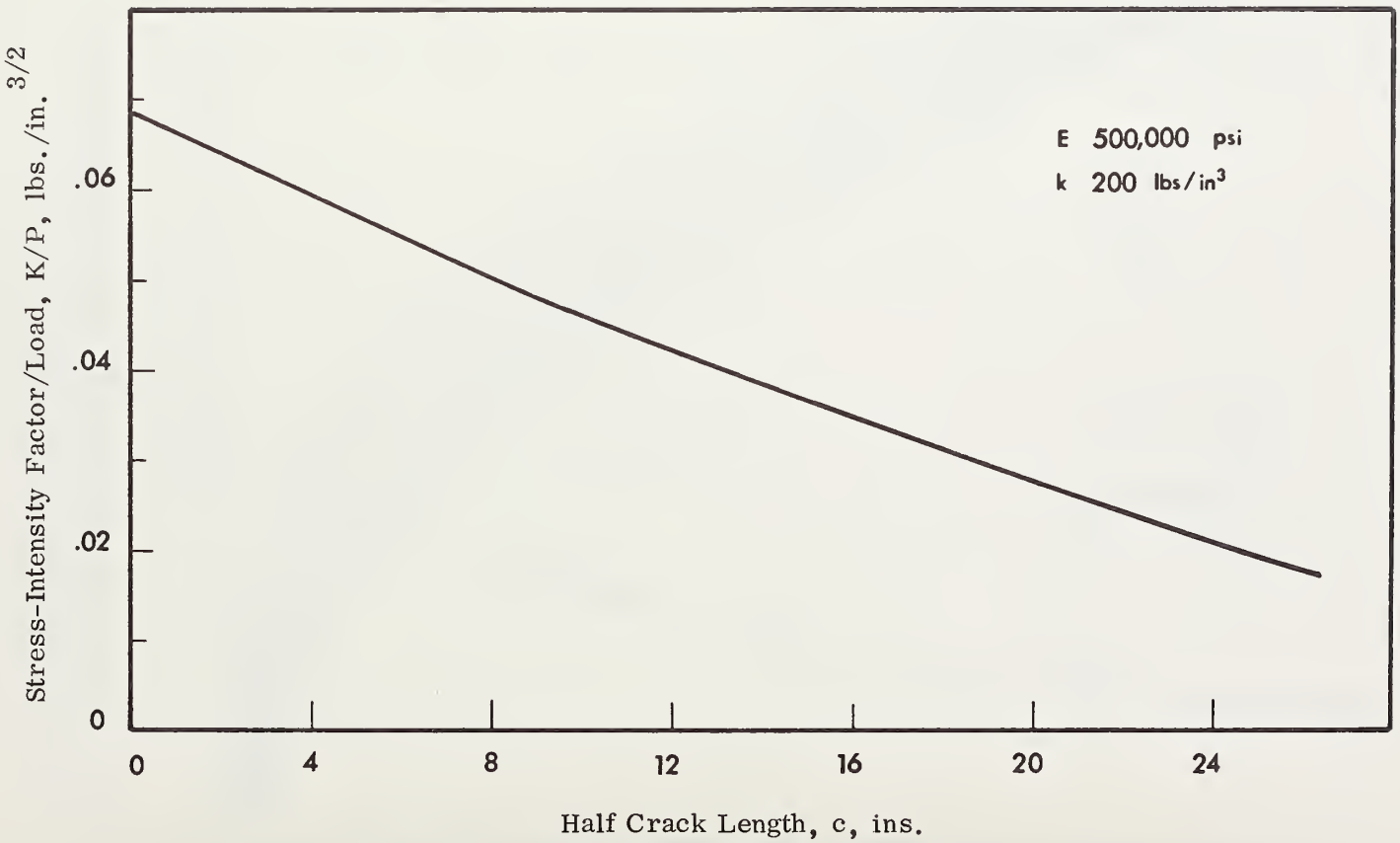

Figure 6.8. K - c Relation for a Typical Flexible Pavement, H = 6.5 Inches

stress-intensity factor can be considered large enough to influence the rate of crack propagation. However, examining the experimental data presented in Figure 6.4 (59), it is noted that the crack growth measurements are only available for cracks ranging between 8 to 15 inches. The reason for the crack growth retardation or test stoppage at a crack length of 15 inches as shown by Coffman (59) is not clear. However, it is believed that the premature failure observed on the west side of the loaded area might have resulted in the termination of this experiment.

The analysis of crack growth rate carried out on this full-scale pavement is shown in Figure 6.9. It is noted that the proposed distress model of fatigue crack propagation is also applicable for this pavement structure. The exponent of the crack growth law is found to be 4.0. It should be noted that recent works by other investigators (60)(61) has shown that for fine grained asphaltic concrete mixtures such as mixture 404 (Ohio Department of Transportation mix designation) the exponent n is equal to 4. However in mixtures with large size aggregates, such as binder and asphaltic base course (mix 301 and 402 of Ohio specifications), the crack growth rate is retarded leading to a lower value for this exponent.

As it has been pointed out previously, the crack propagation process is influenced by two material constants, c_o and A. The recent works by Saraf (60) and Karamians (61) have indicated that for fine-grained asphaltic concrete mixture as that used by Coffman (59), a reasonable value for c_o is between 0.20 and 0.25 inches. The constant A in the crack propagation model is influenced by the material type and temperature. For the asphaltic concrete mixture used in Coffman's

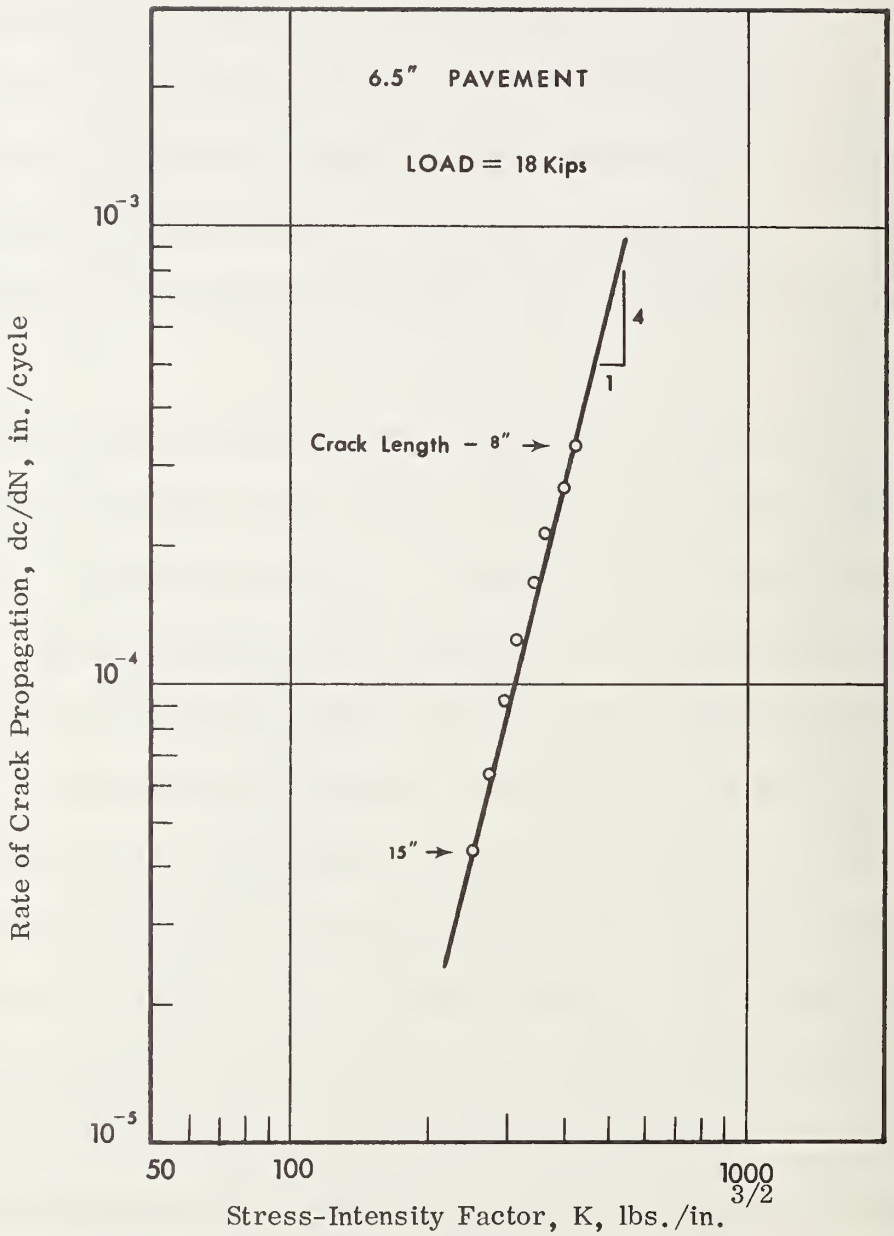

Figure 6.9. $\frac{dc}{dN}$ - K Relation for a Typical Flexible Pavement (EES 296, ref. 59)

experiment A is equal to 1×10^{-14}. Recently Saraf (60), investigating the crack propagation characteristics of asphaltic mixtures using the fracture mechanics concepts, has arrived at a correlation between the dynamic modulus E* and parameter A as given by

$$A = a\,(E^*)^{-m}$$

where a and m are constants, A is the crack growth parameter and E* is the dynamic modulus determined at 8 cycles/second frequency. The constant A calculated using the empirical equation is almost identical to the value determined from Figure 6.9.

As it was indicated previously, Coffman's data did not provide any information with respect to the initial stage of crack propagation. However, it was estimated that fatigue cracks appeared on the surface probably after 100,00 to 150,000 cycles of load application. To verify this estimate, fatigue life analysis can be carried out using the crack growth rate equation as given by:

$$N_f = \int_{c_o}^{c_f} \frac{1}{A\,K^4}\,dc$$

where $c_o = 0.2$, $A = 1 \times 10^{-14}$ and $c_f = h$ (pavement thickness). The input parameter K can be determined using either the 3-dimensional solution given by Ramsamooj (14) or a two-dimensional appoximation of the pavement system. In the two-dimensional approximation, the pavement is replaced by a beam subjected to a reference bending stress equivalent to that of the pavement system. The K - c relation for such a system can easily be calculated by the methods discussed in

Chapter II. Another alternate method of analysis for the first stage of crack propagation is provided by the prismatic finite element program as discussed in Chapter II. In this study for the sake of simplicity , the two-dimensional approximation was used. The results indicated that under the test conditions presented, 105,000 cycles of load repetition are required for the flow of c_o = 0.20 inches to propagate upward reaching to the top surface. The lateral growth of this crack or others reaching to the top surface, however, require a substantially greater number of load repetitions. This longer fatigue life or slower propagation of cracks in the lateral direction is attributed to the sharp reduction of stress-intensity factor with an increase in the radial distance as shown in Figure 6.8. The results of Coffman's investigation as well as the data presented in this report indicate that the number of cycles of load repetition required for the first cracks appear on the surface is only a fraction of the total number of load applications needed for the aeral extension of the cracks. The lateral growth of the fatigue cracks and the fatigue of the pavement model requires 10 to 40 times greater number of load repetitions than needed for the initial stage of crack propagation.

C. An Outline of Method of Design

The design of pavement systems against fatigue distress involves many complex and interrelated variables. The theoretical and experimental data presented in this report have established that the rate of crack propagation in a pavement system could be expressed in terms of material properties of component layers, geometrical and boundary conditions. Any changes in the material

characteristics due to environment or time would then influence the stress distribution within the pavement system and the crack growth process. Similarly, the fatigue crack propagation is affected by the loading variables such as magnitude, frequency and pattern. In the following sections, an outline of method of analysis using fracture mechanics is presented.

(1) Material Characteristics

The fatigue crack propagation of asphaltic pavements is influenced by the material properties of the component layers. In the mechanistic method of fatigue, the effect of these input variables on the pavement distress can be incorporated with consideration to the environmental and climatic and boundary conditions. The following are the descriptions of the influence of important input variables.

(a) Subgrade Support

The subgrade support, expressed either in terms of modulus E*, subgrade reaction K or CBR, contributes greatly to the stress distribution in the pavement system and the rate of crack propagation. In Figure 6.10, the influence of subgrade support on the K - c relation of flexible pavement is presented. As is noted, an increase in the support characteristics of the subgrade support can also be presented in terms of pavement moduli ratio E_1/E_2. As is expected, a larger moduli ratio contributes to a larger magnitude of stresses in the pavement layer and a higher stress intensity factor.

For design purposes, it is recommended that the support characteristics of the subgrade soil and its statistical distribution be determined.

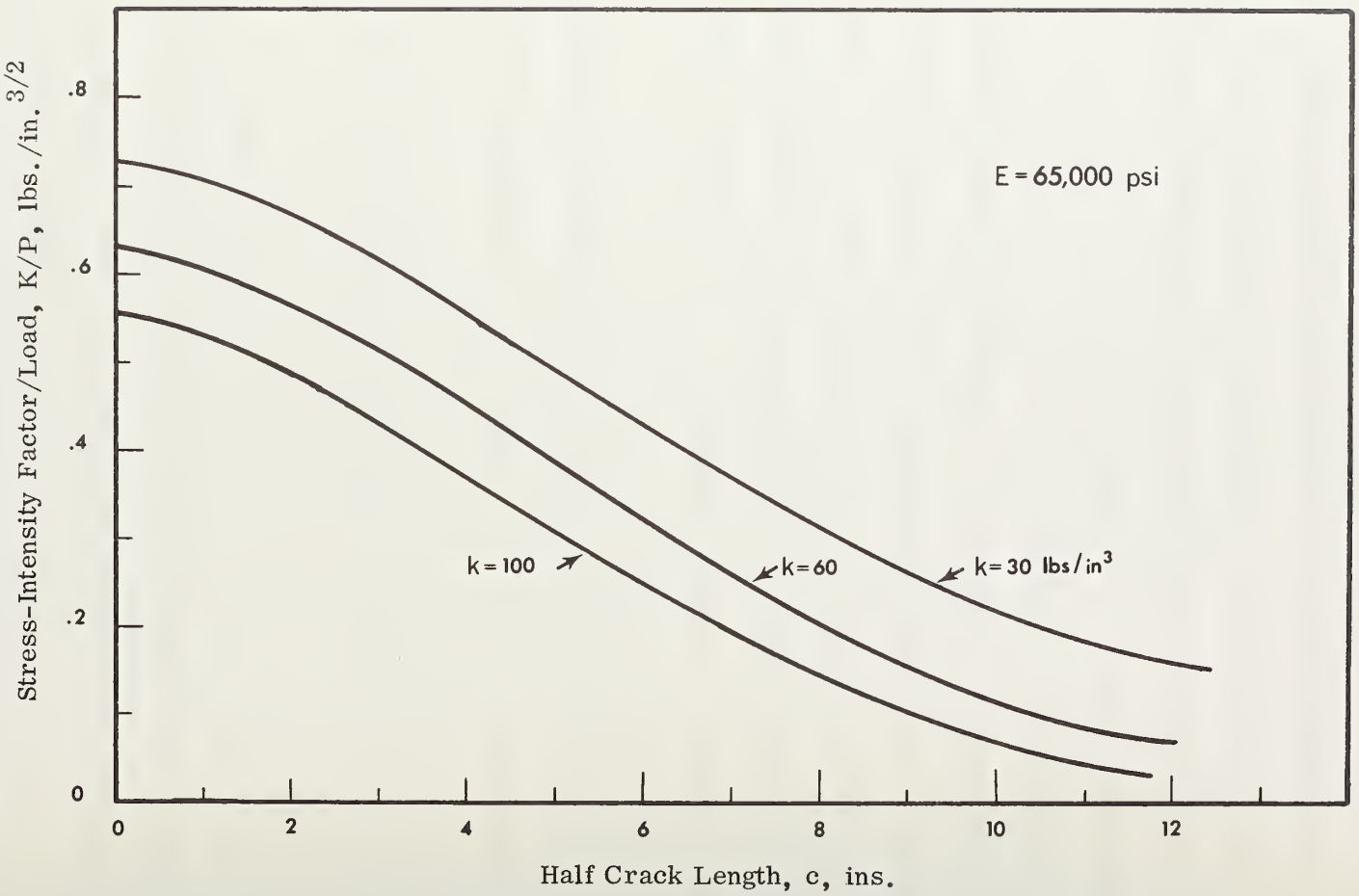

Figure 6.10. Stress-Intensity Factor Versus Crack Length for Different Subgrade Supports

Due to seasonal variations of the subgrade support characteristics, it would be desirable to construct a modulus-distribution curve for the anticipated design period. In the analysis of crack propagation, an appropriate subgrade modulus can then be selected for suitable time increments during which soil support characteristics remain relatively unchanged. Nevertheless, the final choice of this input variable rests on the required degree of confidence set forth in the design specifications.

(b) Pavement Moduli

The moduli of pavement component layers directly influences the extent of stress distribution in the pavement system and stress-intensity factor. As is noted from Figure 6.11, the stress-intensity factor for a given crack length and thickness is affected by the modulus of the pavement layer. A reduction in the pavement modulus or a lower E_1/E_2 ratio results in a lower stress-intensity factor and reduction in the zone of influence of the wheel load. Since the modulus of pavement layer is influenced by the environment and aging process of asphaltic mixtures, the fatigue design should incorporate the short term and long term variations of this input variable. With consideration to the temperature distribution in the pavement system and the seasonal variations of the pavement temperature, an average modulus distribution curve can be constructed for the anticipated design period. An incremental analysis of crack propagation can then be carried out using the average modulus of the pavement system for suitable time increments. During these selected time intervals, the subgrade modulus can be determined from the

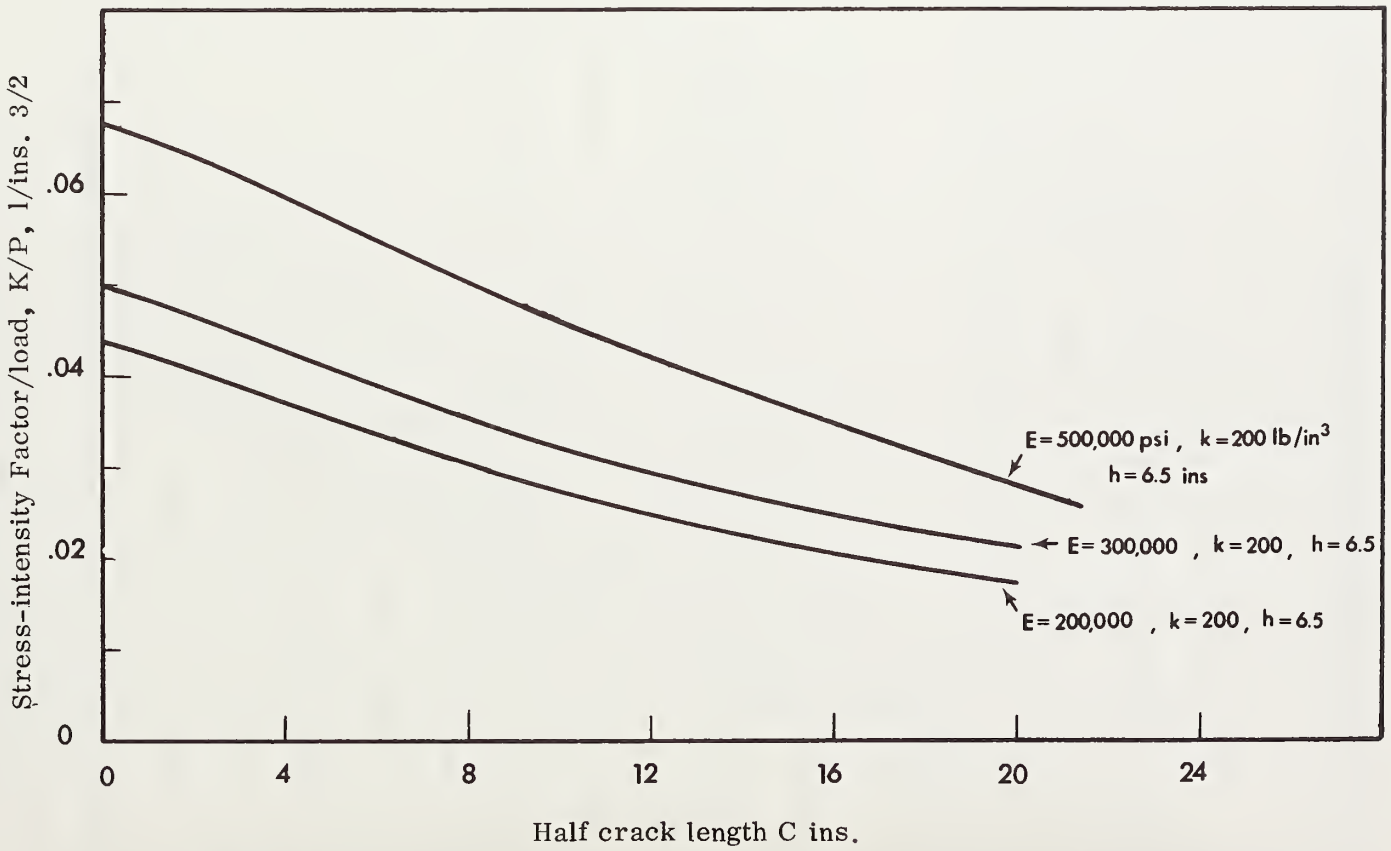

Figure 6.11. Stress Intensity Factor Versus Crack Length for Different Pavement Moduli

subgrade support distribution curve as discussed previously. Therefore, the crack growth increment Δc for a time interval of ΔT can be calculated using appropriate K/P - c curves and with consideration to the anticipated traffic volume for this time period.

(c) Fatigue and Fracture Constants

The input variables influencing the fatigue and fracture process of flexible pavements can be determined using laboratory characterization techniques discussed previously. Utilizing the fracture toughness experiments, the critical stress-intensity factors K_{1c} and K_{2c} of the paving mixture can be calculated. Fatigue experiments should also be conducted on beams supported on elastic foundation and the crack growth parameters A, c_o and n be determined.

Previously documented research results indicate that for fine-grained asphaltic concrete, the exponent n is equal to 4.0; whereas, the unpublished results on asphaltic concrete with large size aggregates such as mix 301 and 402 of Ohio specifications indicate that this exponent n is considerably smaller than 4.0. This reduction in the crack growth exponent is attributed to the effect of large aggregate particles retarding the crack propagation. This crack growth retardation, similar to the effect of sequential loadings, leads to a longer fatigue life. Considering typical flexible pavements constructed in Ohio, the layers of 301 and 402 materials comprise the greatest thickness of the pavement. The fine-grained asphaltic concrete mixture (mix 404) is only a fraction of the total thickness of the pavement ranging from 3/4 to 1-1/4 inches. As an example,

under the construction conditions prevailing in the State of Ohio, the average value of exponent n for 301 and 402 asphaltic concrete layers has been found to be 2.5, whereas for the fine-grained asphaltic concrete (404 mixture) $n = 4.0$. It is rather obvious then that the selection of $n = 4.0$ leads to a very conservative design. For a more realistic analysis, this exponent must be selected with consideration to its statistical variability and its influence on the life prediction.

It should be noted that the exponent n is also influenced by load and environmental factors. As has been discussed previously, sequential loadings result in crack growth retardation and reduction in this exponent. Similarly, experiments conducted at high temperatures and under high stress levels might result in large scale yielding which will subsequently influence the crack growth exponent.

The fatigue crack growth parameters c_o and A are two other material constants which can be determined from beam on elastic foundation experiments. The results of previous research has indicated an average value of c_o might be selected for fine-grained asphaltic concrete between 0.20 to 0.25 inches. For asphaltic concrete mixtures with large size aggregates, this parameter might vary between 0.20 to 0.5 inches. The fatigue parameter A has also been found to vary between 10^{-10} to 10^{-14} for bituminous mixtures of varying composition. For fine-grained asphaltic concrete mixtures, an average value of 1×10^{-14} might be selected for tentative design purposes.

(2) Traffic Loading

The experimental data presented in this report indicate that fatigue crack propagation is greatly influenced by the load sequence and pattern. It is evident from the findings of this study that the application of random loading results in a delay of the fatigue crack propagation rate as compared to the effect of monotonic loading. It is therefore recommended that when a conservative design is justified, the crack propagation model corresponding to a monotonic loading is to be used; whereas, for an exact analysis or for the purpose of determining safety factors, a crack propagation model for sequential loading would be appropriate.

In the design method using the monotonic loading, an equivalent daily traffic number for 18 kips axle load can be determined using procedures currently available. The Asphalt Institute method of determining design traffic number might be selected for this purpose. However, for an exact analysis of the fatigue crack propagation, it is recommended that traffic data be collected such that it can provide information with respect to load magnitude and pattern. From this data, a "load-train" simulating the actual load sequence and pattern of the anticipated traffic can be constructed (Figure 6.12).

Utilizing this "load-train," fatigue experiments should then be conducted on beams resting on elastic foundation from which the constants A, c_o and n are easily determined. It has been shown previously (Figure 4.2 and conclusions of Chapter III) that these material constants are the same for both beams on elastic foundation and the slabs resting of elastic support. Therefore, the results of a

two-dimensional distress model developed from beam on elastic foundation experiments would also be applicable to analysis of pavement systems.

The next step in the analysis of the traffic data is concerned with the determination of load equivalency factors. The load equivalency factor for tandem axles can be calculated with consideration to the axle spacing and the shape of the influence line for stress-intensity factor. The load equivalency factor is defined as the destructive ratio or crack ratio produced by one passage of the tandem axle load as compared to the effect of an 18,000 pound single axle load. Since the damage rate is proportional to the fourth power of the stress-intensity factor (or load), then the equivalency factor can be obtained by taking the ratio of the fourth power of the rises and falls in the influence lines for K.

Two typical influence lines for K for an 18 kip single axle and a 36 kip tandem axle load moving directly over a longitudinal crack of 2 feet long is shown in Figures 6.13 and 6.14.

Other similar influence lines can be developed for other pavement structures using the computer program presented in this report and in references (14) and (15). The load equivalency factor can then be expressed as:

$$\text{L.E. Factor} = \frac{(h_{k_1})^4 + (h_{k_2})^4}{(h_{k_s})^2}$$

where h_{k_s} is the rise and fall in the influence line of the 18 kip single axle load, and h_{k_1} and h_{k_2} are defined as shown in Figures 6.13 and 6.14.

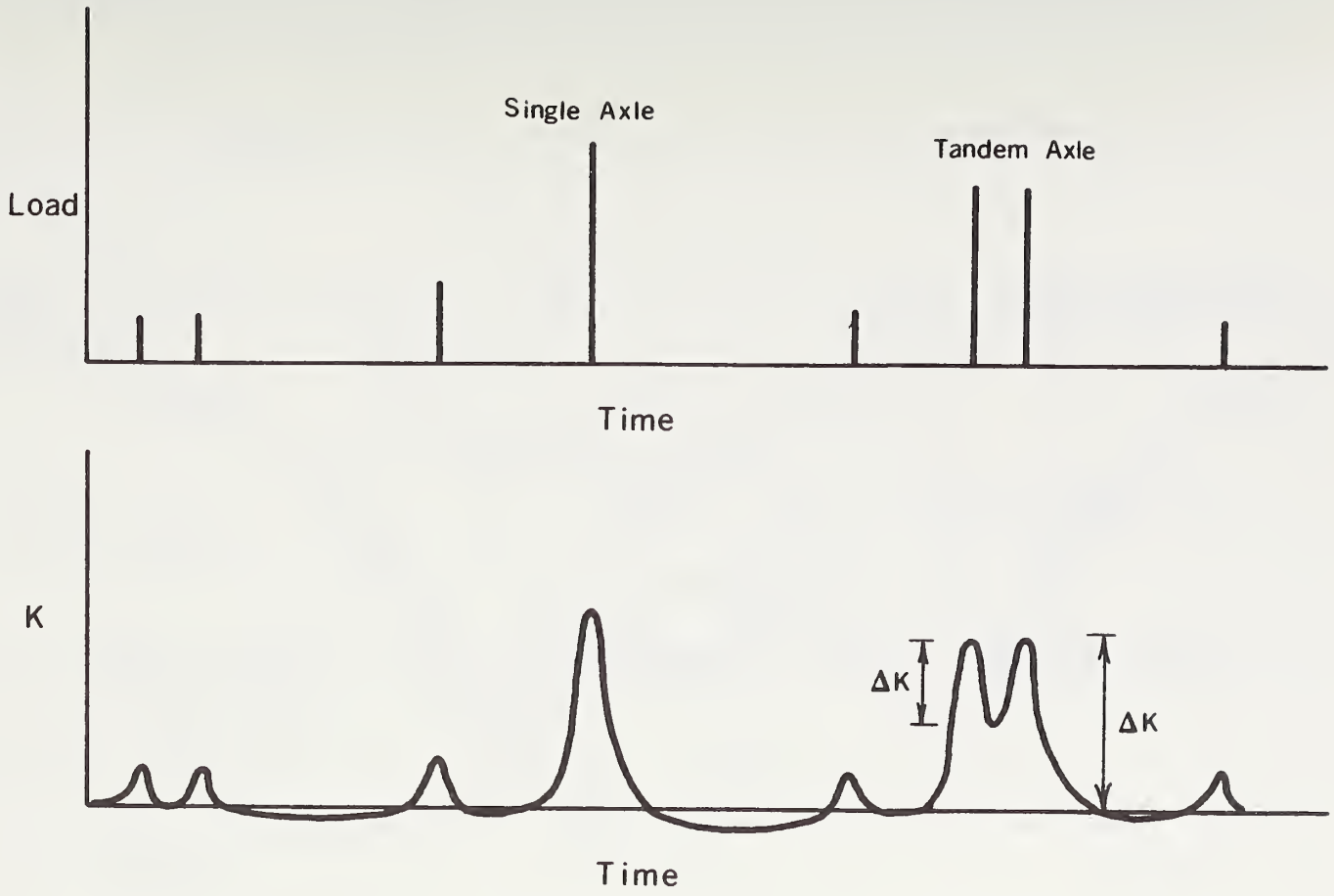

Figure 6.12. Load-Time and Stress-Intensity Factor-Time History of Random Loading

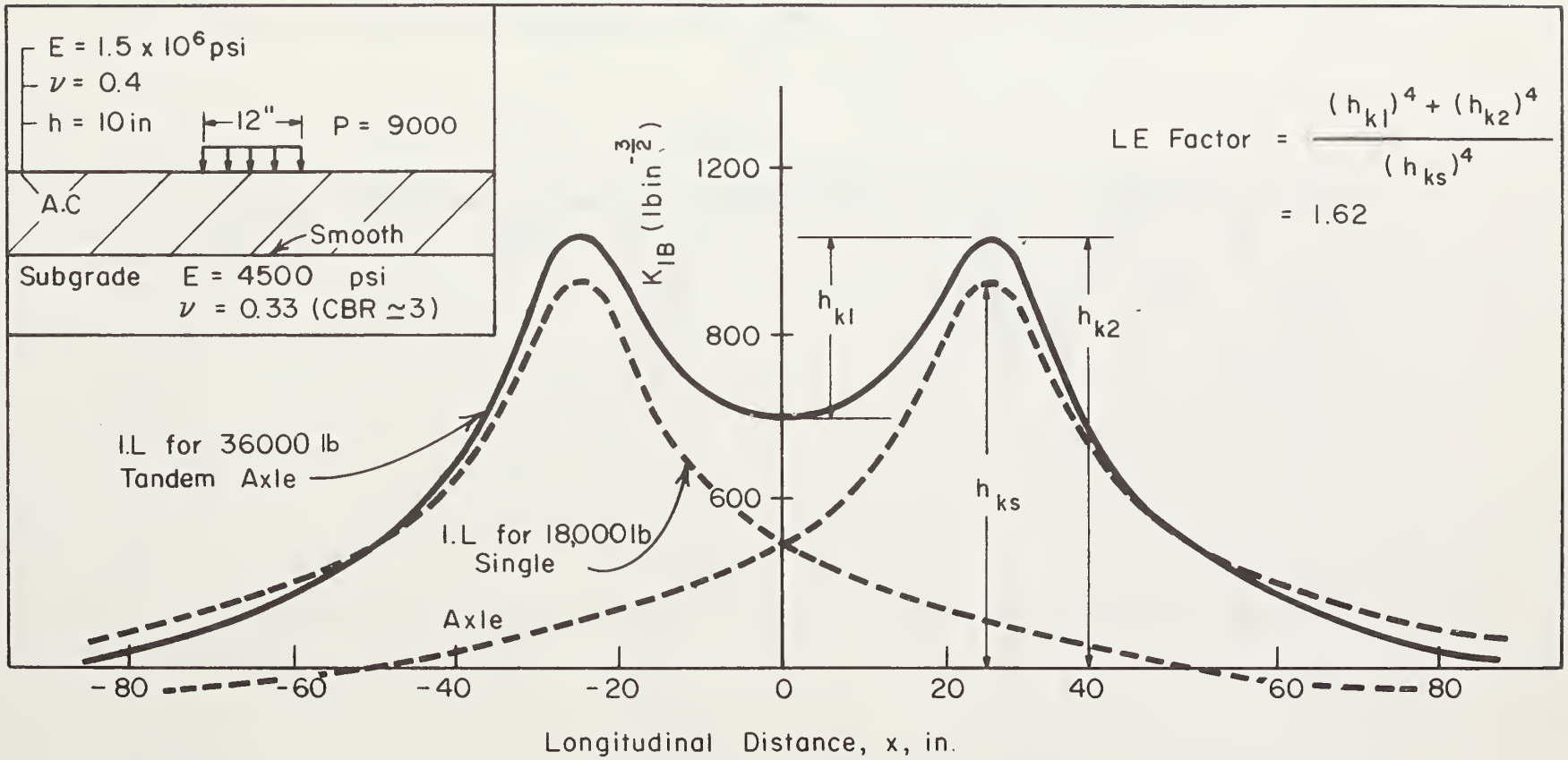

Figure 6.13. Load Equivalency Factor for High Relative Stiffness Pavement

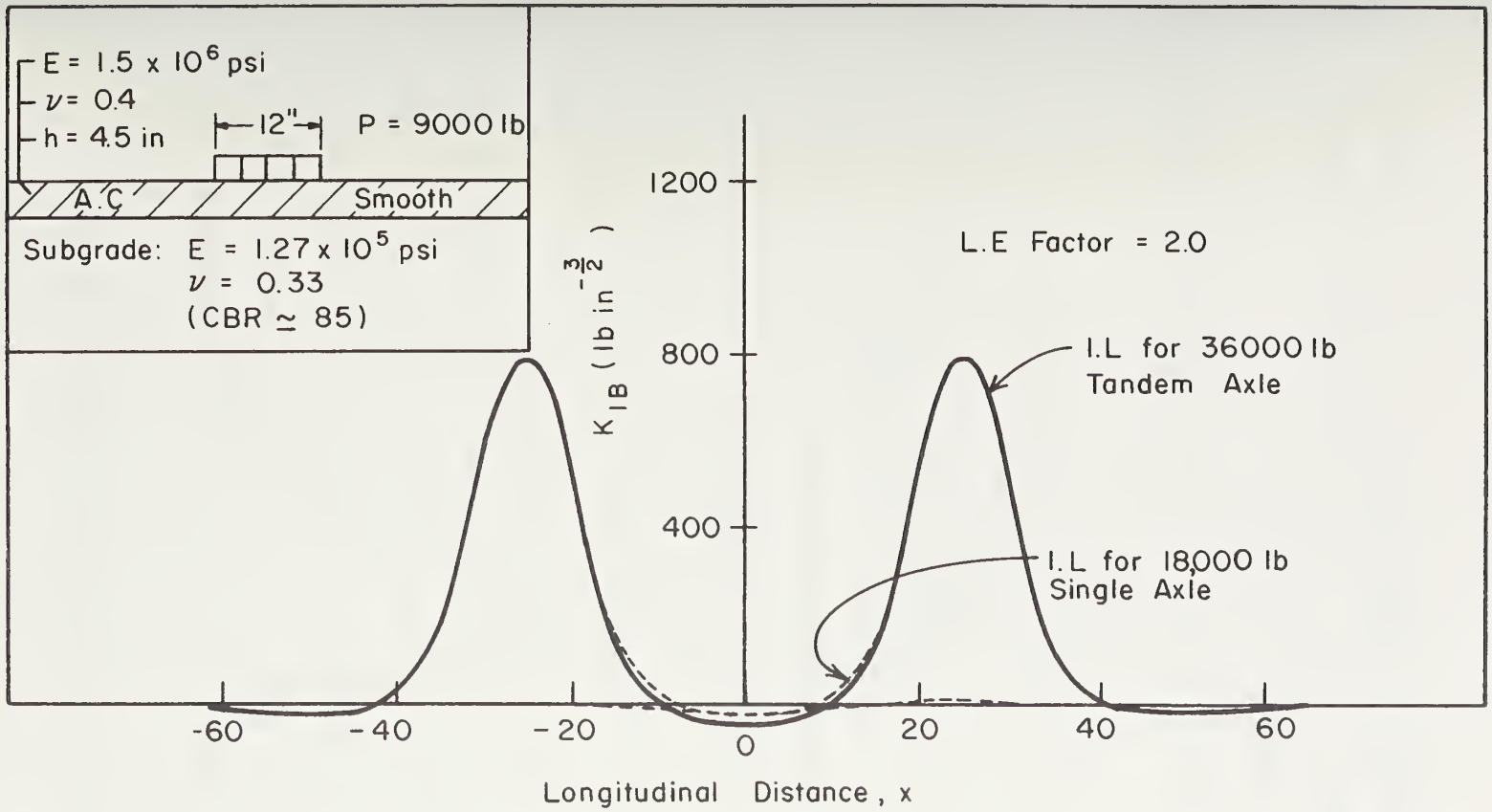

Figure 6.14. Load Equivalency Factor for Low Relative Stiffness Pavement

(3) Analysis and Evaluation

The basic principle of the fatigue analysis as presented in this report is that damage will be proportional to rises and falls in the load-time history of random loading as illustrated in Figure 6.12.

The exace damage per passage of axle load, dc/dN, might be expressed by

$$\frac{dc}{dN} = A_1 K_1^{n_1} + A_2 K_2^{n_2}$$

where K_1 and K_2 = average of the rises and falls of the stress-intensity factors corresponding to the peak-to-trough rises and falls in the K-time histories.

The components of the stress-intensity factors, K_1 and K_2, for a pavement slab for any configuration of wheel loads, for any size and location of crack, and for any combination of the thicknesses and material properties of the component layers, can be calculated by the procedures described previously. Typical influence lines for K_1 and K_2 for a semi-infinite crack for a full-scale pavement are shown in Figure 6.15 (see reference 14,15).

To determine the fatigue crack propagation in the pavement, it is necessary to determine the size and distribution of starter flaws, c_o, in the pavement. For a typical pavement, the lateral distribution of wheel loads may be assumed to be as shown in Figure 6.16. Evidently the fastest crack growth will take place under the greatest concentration of loading since the stress-intensity factor is highest there. Thus, the cracking will be assumed to be primarily along the wheel track and perpendicular to it as shown in Figure 6.16.

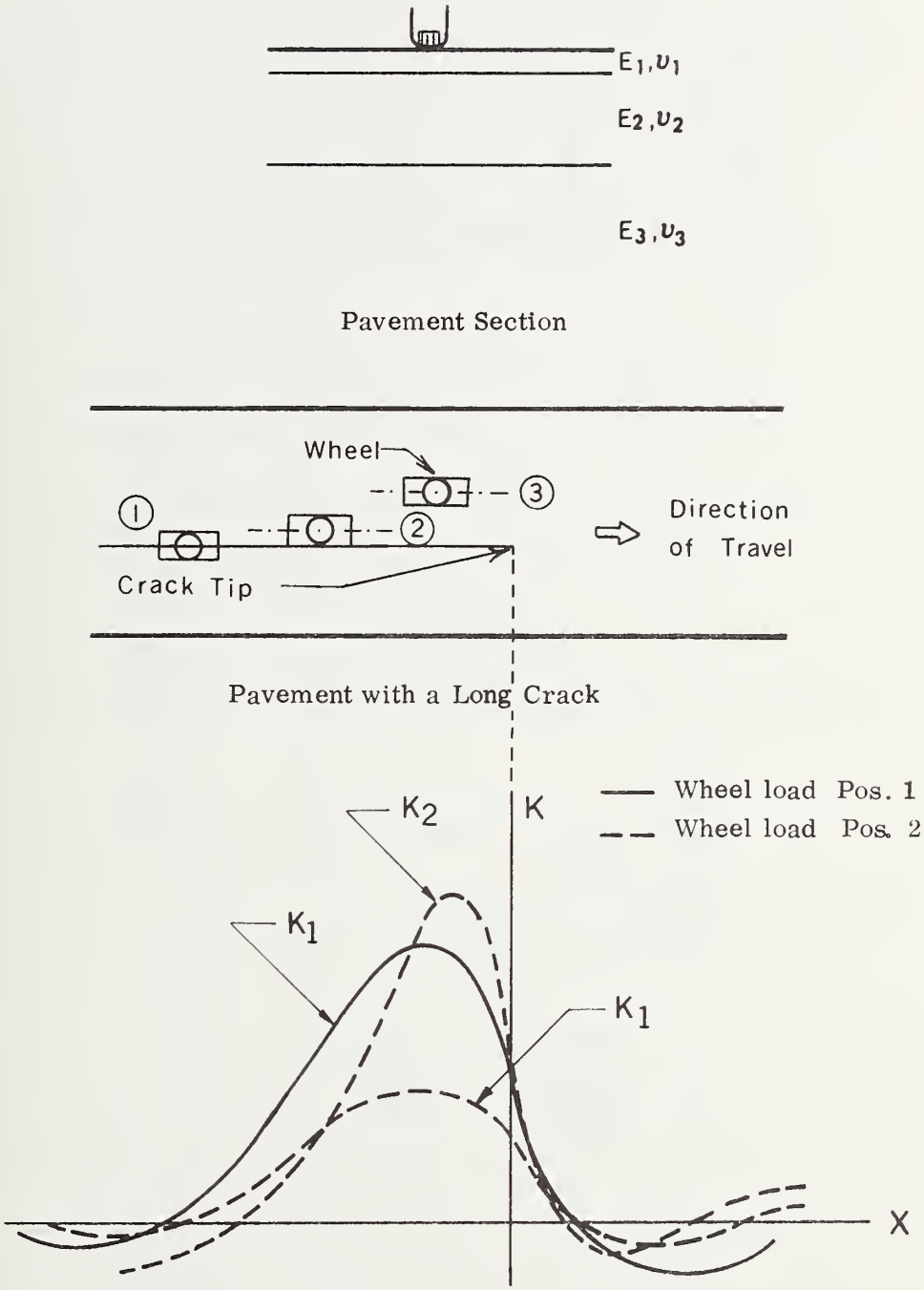

Figure 6.15. Typical Influence Lines for K_1 and K_2 for a Semi-Infinite Crack

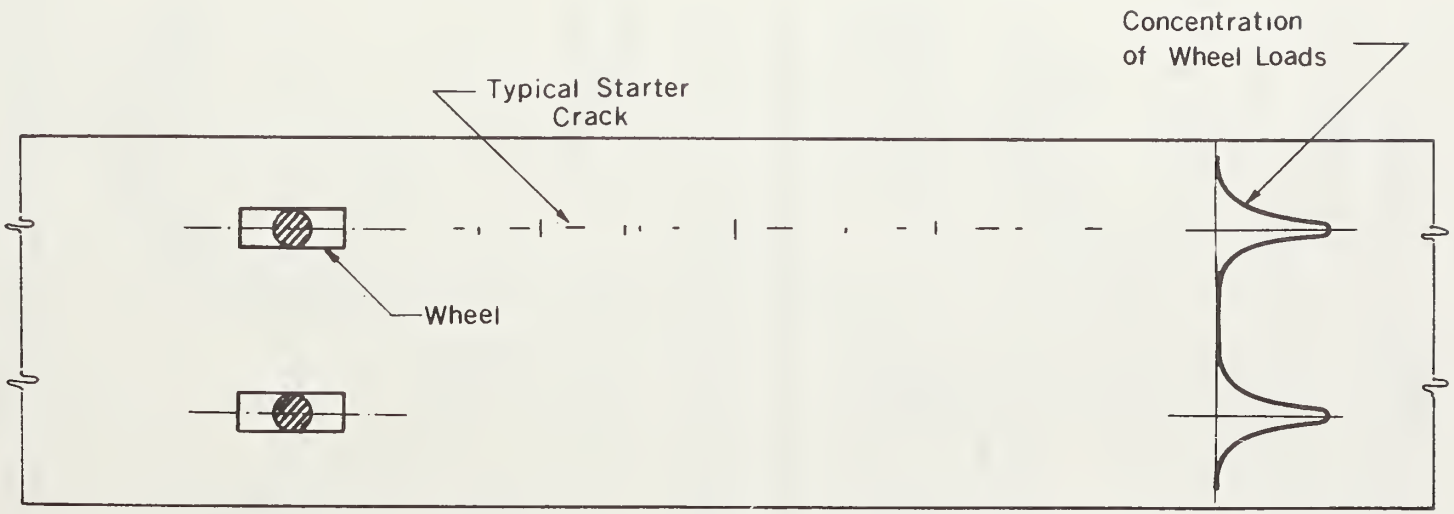

Figure 6.16. Typical Lateral Distribution of Wheel Loads in a Pavement and Assumed Idealized Random Distribution of Cracks

The size of the starter cracks along the line of cracking may be determined by applying statistical analysis to laboratory tests on specimens prepared in the laboratory or on specimens cut from the pavement at regular intervals. Only the upper range of c_o values will be of practical interest since for exceedingly small values the crack will not propagate to the surface in the design period of the pavement.

As it was pointed out previously, in flexible pavements the crack propagation is observed in two distinct stages. First, the inherent flaws located at the bottom of pavement layers propagate upward reaching to the top surface. Secondly, the lateral extension of cracks occur under induced K_1 and K_2 stress-intensity factors. An analysis of a typical flexible pavement constructed in Ohio indicates that the fatigue life for the first stage of crack propagation is only a fraction of the total life.

The number of load applications required for the first stage of crack propagation can be determined from a two-dimensional approximation of pavement systems. In this analysis, a hypothetical simply-supported beam or beams resting on elastic founcation is substituted for the pavement slab and is subjected to a reference bending stress, σ^*, equivalent to that of real pavement. The reference bending stress, σ^*, can be calculated using a mulit-layer elastic program and load, geometrical and material variables of real pavement structure. Thus, the load on the two-dimensional specimen would be selected such that to provide an equivalent reference bending stress. Since according to Figure 6.17 the rela-

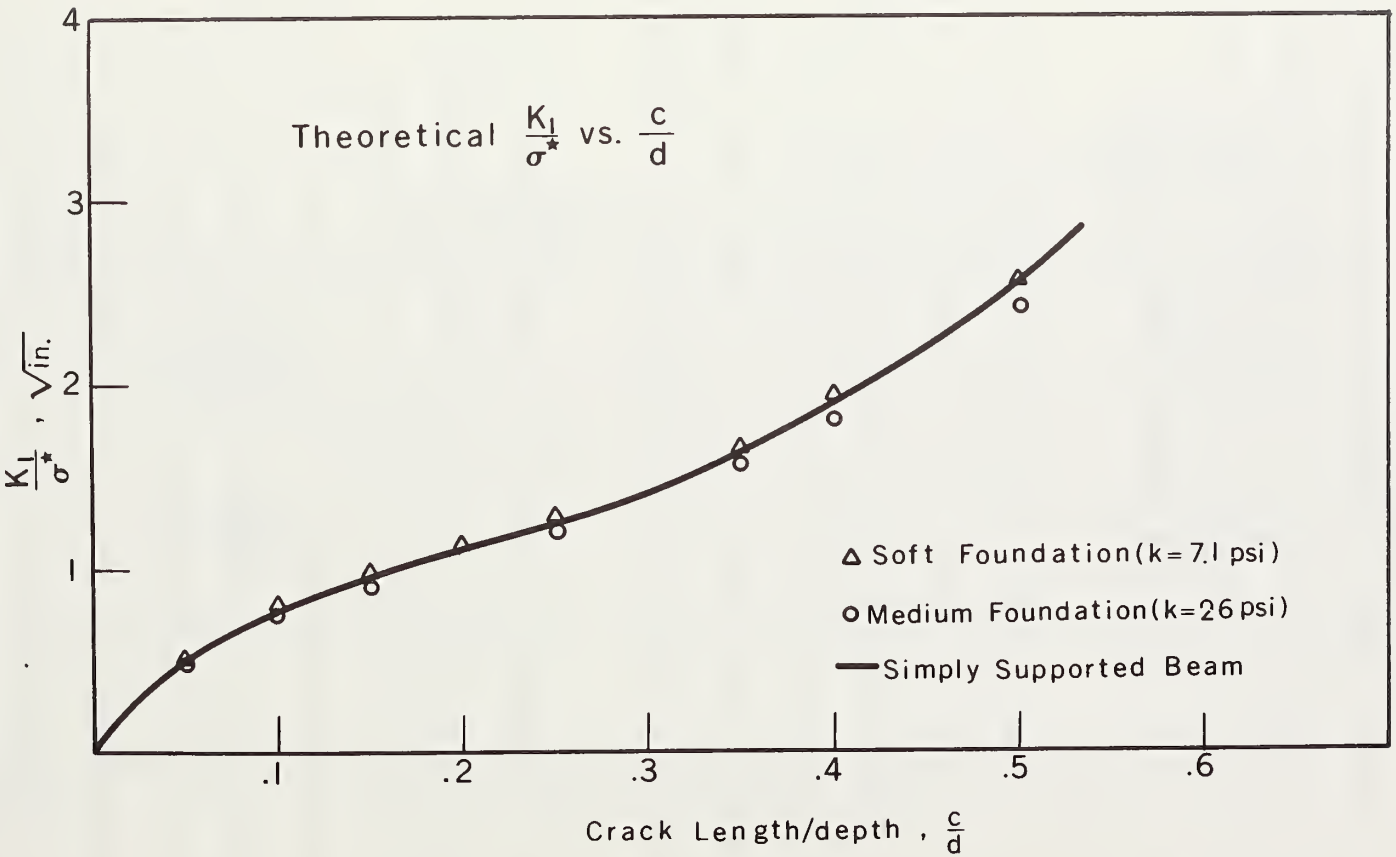

Figure 6.17. Theoretical Relation of $\frac{K_I}{\sigma^*}$ Versus $\frac{c}{d}$

tion between K/σ^* and c/d is independent of boundary conditions, the choice of two-dimensional system merely depends on the availability of the method of analysis for K - c relation. For a beam on elastic foundation test conditions, finite element program or boundary collocation method can be used to calculate K - c relation. For simply-supported beams, the non-dimensionalized relation shown in Figure 2.2 is applicable. The fatigue life for the first stage of crack propagation can then be estimated using equation 2.15 and parameters c_o, n and A determined from beam on elastic foundation experiments and K - c relation. As was pointed out, the use of simply-supported beams for determination of fatigue life of a hypothetical beam with a thickness, reference bending stress σ^* and material properties equal to that of real pavement is justified due to uniqueness of K/σ^* - c/d relation. However, the fatigue constants (parameters c_o, n and A) must be determined experimentally using a beam on elastic foundation and under a monotonic random loading or load-train simulation pavement condition. The use of beam on elastic foundation testing conditions is needed to eliminate the effect of creepon these material constants.

As a result of these fatigue life analyses and from a known statistical distribution of initial starter flaws at the bottom of asphalt layer, the distribution of top surface cracks as a function of time (load repetition) and space are easily determined.

Confining attention to the growth of these surface cracks in a small representative section of the pavement, it can be assumed for simplicity that

the distribution of these cracks are such that there is no interaction. For each crack, the stress-intensity factors K_1 and K_2 will be calculated. Then, integrate the rate of crack propagation numerically for one passage of the load train and obtain the increment of damage. Damage is defined as the length of crack inclusive of the plastic zone formed at the crack tip or for simplicity as the length of the crack. Thus, the increment of damage, Δc, is

$$\Delta c = \sum_{p=1}^{n} \left[A_1 (\Delta K_{1p})^n + A_2 (\Delta K_{2p})^n \right]$$

where K_{1p} and K_{2p} = averages of the rises and falls of the influence lines for K_1 and K_2 respectively, of the stress-intensity factor for each crack for the pth axle load.

Increase the length of the cracks and compute K_1 and K_2 again. If the maximum values of K_1 and K_2 exceed K_{1c} and K_{2c}, the critical values of K_I for any axle loads in the load train, the cracks will propagate rapidly and the pavement will be considered to have failed. If not, then increase each crack length by the increment of damage, Δc, and repeat the procedure.

Compute at reasonable intervals the length of longitudinal and transverse crack for each location of the assumed starter flaws, and determine the total cracking area as the product of the sum of the longitudinal cracks and the average length of the transverse cracks.

Thus at regular intervals, the maximum values of K_1 and K_2 and the total area of the cracking will be known. If K_1 and K_2 exceed the critical values of K_{1c}

and K_{2c}, then the pavement will fail by rapid crack expansion. On the other hand, K_1 or K_2 may never exceed K_{1c} or K_{2c} even if the length of cracks becomes exceedingly long. In such cases it is convenient to adopt the suggestion of Zube and Skog that when the "alligator" type cracking exceeds ten per cent of the total area, the pavement should be considered to have failed.

In this discusssion, longitudinal and transverse cracks have been considered as the primary mode of crack propagation. In reality, of course, cracks in other directions and parallel to the main cracks will also develop rapidly into the well-known alligator pattern (hexagonal shaped cracks). The alligator pattern may be deduced directly from the Griffith theory of fracture which requires that that total surface energy expended to form new surfaces must be a minimum. Mathematically it seems that this condition is best satisfied for hexagonal shape cracks in preference to triangular, quadrilateral or pentagonal shaped cracks.

Once the primary mode of crack propagation has reached an advanced stage, the secondary and tertiary modes of cracking leading to the completion of the alligator pattern will follow in rapid succession. Thus, the definition of the failure criteria based on the primary mode of crack propagation is sufficiently accurate to obtain an estimate of the service life. Should the pavement design prove to be unsatisfactory, a new design must be made and the analysis for the service life repeated.

(4) Design Example

To illustrate the applicability of the fracture mechanics principles as a fatigue design subsystem, consider as an example a full-depth flexible pavement constructed in Franklin County, Ohio, S.R. 317. The proposed asphaltic pavement structure is composed of $1\frac{1}{2}$" of asphaltic surface course (mixture 404), $1\frac{1}{2}$" of asphaltic leveling course (mixture 402) and 6" of asphaltic base course (mixture 301). This flexible pavement structure is constructed over a 4" granular subbase of 404 and a silty clay subgrade.

The activities involved in the design verification process of this pavement structure, as shown in Figure 6.18, are as follows:

(a) Material Properties

(i) Support Characteristics: The soil support characteristics of pavement structure has been determined using both undistrubed soil specimens as well as an in place - nondestructive method (dynaflect deflection). The deflection measurements at various stations and at various time intervals provide desired information with respect to the time and space variation of pavement support condition. In this analysis, the modulus of soil subgrade and granular base combined are assumed to be 20,000 psi.

(ii) Pavement Moduli: The moduli of pavement layers (mixtures 404, 402 and 301) have been determined from field cores as well as nondestructive measurements. The laboratory measurements have been conducted on cylindrical and beam specimens of mixture 301 (asphalt base course). The modulus

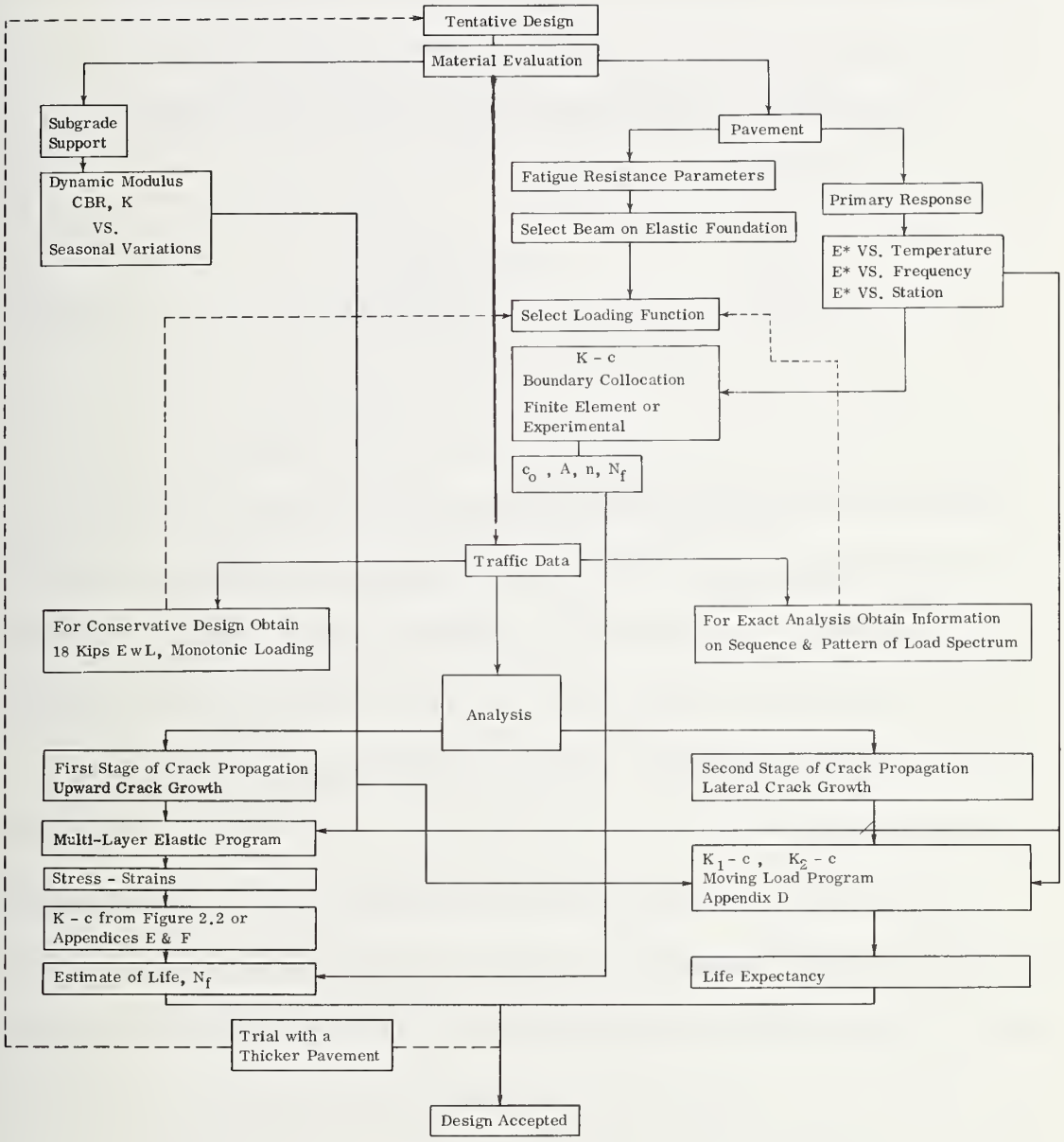

Figure 6.18. Mechanistic-Fatigue Subsystem

determination for mixtures 404 and 402 were carried out on beam specimens of individual mixtures as well as on composite beams. The in-situ nondestructive testing using dynaflect also has provided desired information.

Assuming that this trail design is based on the average temperature of 77°F, the moduli of pavement layers are:

Mix 404	E = 300,000 psi
Mix 402	E = 300,000 psi
Mix 301	E = 200,000 psi

(iii) Fatigue Resistance Parameters: Since in this trail design a conservative estimate of the fatigue life is sought, the sequential and random loading conditions experienced in the field is approximted by a monotonic loading. The beam specimen obtained from the field were then subjected to beam on elastic foundation experiments under monotonic loading condition. However, if a more exact analysis of fatigue life is required, the beam specimens should have been subjected to a random loading or sequential loading simulating the real traffic loading.

The fatigue parameters c_o, A and n for asphaltic mixtures are determined using beam on elastic foundation experiments. These parameters can be obtained using a minimum of three notched specimens, $c_o = 0.25''$ and three unnotched specimens. The K - c relation can be determined using finite element program, boundary collocation method or experimental method (Appendix E and F). From the results of notched specimens where c_o, c_f, K - c, and N_f are known, the parameters n and A can be determined. Similarly, from the results of unnotched

specimens using c - N and K - c relations, the parameters n and A can easily be obtained. Using the program given in Appendix G and known variables K - c, c_f, n, A, and N_f, the parameter c_o is determined.

The average fatigue parameters for mixtures 404 and 402 are as follows:

$$A = 1.68 \times 10^{-10}$$
$$n = 2.75$$
$$c_o = 0.19$$

For mixture 301, asphaltic base course, the average fatigue parameters are:

$$A = 1.5 \times 10^{-10}$$
$$n = 2.5$$
$$c_o = 0.22$$

It should be noted that for a rational analysis of fatigue life expectancy, the statistical distribution of these fatiuge parameters should be determined. However, for the purpose of simplicity in this analysis, only the average values of these parameters are used.

During the first stage of crack propagation, the crack grows very rapidly whenever the crack length exceeds half the pavement thickness. Therefore, the characteristics of a thin layer of surface course (mixes 404 and 402) does not significantly influence the first stage of crack propagation and the fatigue life depends mostly on the characteristics of asphaltic base course such as c_o, n and A.

(b) Traffic

A detailed traffic composition data on this roadway is not available at this time. The present design is based on an expected design traffic number (daily equivalent 18 kips axle) of 40 to 50. Without consideration to the wheel

path distribution of the loads, it can therefore be assumed that this pavement must tolerate 3×10^5 to 4×10^5 cycles of load repetition in 20 years of service.

It should be noted that in this trial example, a conservative estimate of fatigue life is determined using monotonic loading conditions. However, if an exact estimate of fatigue life is required, a detailed traffic survey should be conducted to determine the traffic load sequence and pattern.

(c) Analysis

Using a multi-layer elastic program for a wheel load of 9,000 lbs. and tire pressure of 75 psi, the reference bending stress of $\sigma^* = 74.9$ and a strain of 2.35×10^{-4} in./in. is obtained. This corresponds to a fatigue life of approximately 1×10^5 cycles of 9,000 lbs. load application when calculated using allowable tensile strain criteria.

To calculate the expected life for the upward crack propagation (first stage), a hypothetical beam of unit width and height of h = 8.5 and 36" span was envisioned. The load, P, required to result in a reference bending strain of $\sigma^* = 74.9$ was therefore calculated. From Figure (2.2), the K - c relation was then determined using the non-dimensionalized parameters. The expected fatigue life for the average values of fatigue parameters is found to be 80,000 cycles of 9,000 lbs. wheel load.

At this point, it can then be stated that after 80,000 cycles of load application, all starter flaws of $c_o > 0.22$ inches have propagated to the surface. All starter flaws of smaller than this value require a greater number of load applications before appearing on the top surface. Therefore at any time, the distribution of the top

surface cracks can be determined using the distribution of the initial starter flaws and the number of load applications that pavement has experienced during this period. Then lateral extension of cracks (second stage of crack propagation) can be determined using computer programs presented in Appendix D. In Figure 6.19 the effect of thickness on the $K_1/P-c$ relation is shown. The effect of K_2 on the pavement fatigue can also be calculated using the moving load program (Appendix D).

Depending on the degree of reliability sought by the designer, the pavement might be considered failed either after the first stage of crack propagation, or whenever the lateral extension of cracks occupies a known percentage such as 10% of the total pavement surface area. The first case, however, appears to be more critical and the pavement thickness should be selected to maximize the time required for the initial flaws to propagate upward. Since an 8.5 inch pavement thickness appears to be unsatisfactory, the next design trial is carried out using $h = 10$ inches. The reference bending stress σ^*, is calculated to be 60.8 psi, and the strain at the bottom of the asphalt layer is found to be 190.5 micro in./in. Considering the allowable tensile strain criteria, the fatigue life is estimated at 250,000 cycles. However using the fracture mechanics subsystem, as outlined previously and for the average $c_o = 0.22$ inch, the fatigue life is found to be $N_f = 154,300$.

As was indicated previously, in the pavement section having $c_o > 0.22$ inches, the fatigue life is smaller than the average value. As an example, when

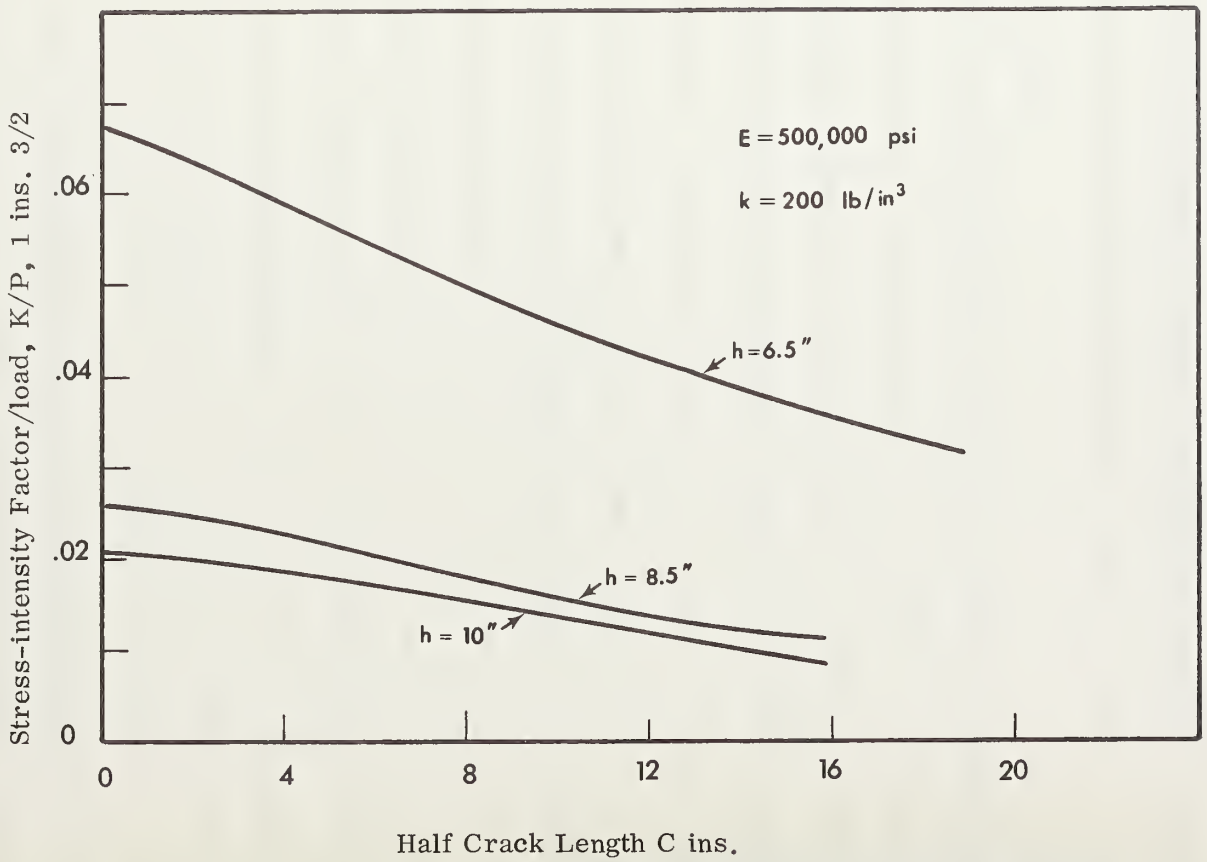

Figure 6.19 Stress-intensity Factor Versus Crack Length for Different Pavement Thicknesses

c_o is equal to 0.3, N_f is equal to 135,000 and when c_o is equal to 0.5, N_f is equal 105,000. Therefore, after an approximate 100,000 cycles of equivalent 18 kips load application, cracks start appearing on the surface. The frequency of occurrence of these cracks depends on the statistical distribution of all input variables discussed.

CHAPTER VII

SUMMARY AND CONCLUSIONS

The design of pavement systems against fatigue distress involves many complex and interrelated variables. In this report the principles and concepts of linear fracture mechanics were used to study the fatigue behavior of flexible pavements. The foregoing experimental work, done in a laboratory sand-asphalt pavement model, established that fatigue in bituminous paving material is a gradual progressive process beginning with the initiation of small cracks which propagate until the remaining section of the structure becomes too weak or fails catastrophically. The experimental work also indicated a strong correlation between the rate of crack growth and the stress-intensity factor, which measures the load transmission capability of the material to the vicinity of the crack tips. Therefore, the rate of crack propagation can be expressed in terms of the properties of the component layers of the system, the geometrical and boundary conditions.

The concept of the stress-intensity factor, K, is an important tool in the fatigue analysis since it not only measures the crack extension force, but also its critical value, K_{1c}, is a material property and the failure criterion for the material. Expecially during the winter months, when the pavement experiences very low temperatures, the critical value of the stress-intensity factor can by itself explain rapid crack propagation which so often occurs.

The crack propagation law, $dc/dN - A K^n$, which is the basis of the mechanistic approach, was shown to be applicable for bituminous paving mixtures subjected to loads of constant amplitude and tested at room temperature. In this report it has also been shown that the approach is certainly applicable for temperatures other than 77.5°F, or in a range from 41°F to 90°F. Therefore, it can be stated that the method is applicable over the entire range of practical interest for highway engineers, 0-100°F.

It was also shown that the process of fatigue crack propagation can be explained in terms of Paris' law when cracking is accompanied by some permanent deformation, whenever the rate of loading, i.e., the vehicular speeds, are sufficiently high as to ensure the elastic response of the pavement material. The application of the method for other situations where the rate of loading is small, such as those encountered in parking lots and near stop signs, cannot be done without some modifications in the analytical method to take into account the creep and viscoelastic effects. An elastic-plastic model developed at the Ohio State University was utilized to study the effect of plastic zones on the problem of crack propagation. It was pointed out that in two-dimensional analysis such as localized yielding might result in crack growth retardation.

The work was conducted to study crack propagation in sand-asphalt pavements subjected to blocks of load or variable amplitude. The findings shown that Paris' fourth power law of crack propagation is a conservative estimate of the rate of crack propagation since the introduction of loads of different magnitudes causes a

delay in crack growth and the exponent n in Paris' relationship was found to be less than four. Then if the fourth power is used in the prediction of the fatigue life on the basis of a maximum equivalent load, one would arrive at a conservative estimate of the fatigue life for the pavement system. Although no quantitative analytical solution is yet available to this problem, the use of Paris' law is justifiable on the basis that most engineering structures are designed with safety factors. Therefore, the use of the fourth power relationship is analagous to the introduction of a safety factor.

The following are the main conclusions applicably given by the conditions expressed in this study:

1. The fatigue crack propagation process in bituminous materials is considered as a stress independent, stress interaction type phenomena.

2. For the range investigated, it was found that the rest period has little or no effect on the fatigue life of pavements.

3. The sequence of load application has a significant effect on the fatigue life of asphaltic materials, causing a delay in the rate of crack propagation.

4. The fatigue life of pavement slabs subjected to loads of variable amplitude can be predicted from tests on beams resting on an elastic solid.

5. Paris' law is applicable when the fatigue phenomenon is accompanied by some permanent deformation, provided that the rate of loading is sufficiently high.

6. The mechanistic approach to predict cracking of flexible pavements is applicable in the range of temperatures from 41° to 90°F.

7. The critical stress-intensity factor, K_{1c}, is the failure criterion for low temperatures.

8. The concepts of linear fracture mechanics can be used to predict the fatigue life of pavements by means of the analysis encompassed by the mechanistic approach. The application of this method to a typical flexible pavement has also been demonstrated in this study.

BIBLIOGRAPHY

1. Finn, F.N., "Observation of Distress in Full-Scale Pavements," Highway Research Board, Special Report 126., 1970.

2. McEvily, A.J., Boettner, R.C. and Johnston, T.L., "On the Foundation and Growth of Fracture Cracks in Polymers," Fatigue An Interdisciplinary Approach, Syracuse University Press, 1964.

3. HRB-SR 126- "Structural Design of Asphalt Concrete Pavement Systems," Proceedings of a Workshop held Dec. 7-10, 1970, Austin, Texas.

4. Monismith, C.L., Secor, K.E., and Blackmer, E.W., "Asphalt Mixture Behavior in Repeated Flexure," Proceedings, AAPT, Vol. 30, 1961, pp. 188-222.

5. Monismith, C.L., and Deacon, J.A. "Fatigue of Asphalt Paving Mixtures," Transportation Engineering Journal, ASCE, Vol. 95 No. TE2, May 1969, pp. 317-346.

6. Monismith, C.L., "Asphalt Mixture Behavior in Repeated Flexure," Report No. TE-66-6, University of California, Berkeley, Dec. 1966.

7. Pell, P.S., and Taylor, I.F., "Asphaltic Road Materials in Fatigue," Proceedings, AAPT, Feb. 1969.

8. Pell, P.S., "Fatigue of Asphalt Pavement Mixes," Proceedings, Second International Conference on the Structural Design of Asphalt Pavements, 1968, pp. 577-599.

9. Kasianchuk, D.A., "Fatigue Considerations in the Design of Asphalt Concrete Pavements," Ph.D. Dissertation, University of California, Berkeley, 1968.

10. Deacon, J.A., "Fatigue of Asphalt Concrete," Graduate Report, 1965, ITTE, University of California, Berkeley.

11. Majidzadeh, K., and Kauffmann, E.M., "Analysis of Fatigue and Fracture of Bituminous Paving Mixtures," Final Report, Phase I and II, Project RF 2845, Ohio State University Research Foundation. Sept. 1971.

12. Majidzadeh, K., Ramsamooj, D.V., and Chan, A.T., "Fatigue and Fracture of a Bituminous Paving Mixture," AAPT, 1969.

13. Majidzadeh, K., Kauffmann, E.M., and Ramsamooj, D.V., "Application of Fracture Mechanics in the Analysis of Pavement Fatigue," AAPT, Vol. 40, 1971.

14. Ramsamooj, D.V., "The Design and Analysis of the Flexibility of Pavements," Ph.D. Dissertation, The Ohio State University, 1970.

15. Majidzadeh, K., Ramsamooj, D.V., "Development of Testing Procedures and A Method to Predict Fatigue Failures of Asphaltic Concrete Pavement Systems," Final Report, Project RF 2873, The Ohio State University Research Foundation, March 1971.

16. Ramsamooj, D.V., Majidzadeh, K., and Kauffmann, E.M., "The Design and Analysis of the Flexibility of Pavements." The Third International Conference on the Structural Design of Asphalt Pavements, Sept. 1972.

17. Paris, C.P., Gomes, M.P., and Anderson, W.E., "A Rational Analytic Theory of Fatigue," Trend in Engineering, (University of Washington), Seattle, Washington, Vol. 13, No. 1, 1961.

18. Paris, C.P., "The Growth of Cracks Due to Variation in Load," Ph.D. Dissertation, Lehigh University, Sept. 1962.

19. Paris, C.P., and Erdogan, F.J., "A Critical Analysis of Crack Propagation Laws," Journal of Basic Engineering, Transactions ASME, Series D, Vol. 85, 1963, pp. 528-553.

20. Paris, C.P., "The Fracture Mechanics Approach to Fatigue," Fatigue An Interdisciplinary Approach, Syracuse University Press, 1964.

21. McEvily, A.J., Boettner, R.C. and Johnson, T.L., "On Foundation and Growth of Fracture Cracks in Polymers," Fatigue An Interdisciplinary Approach, Syracuse University Press, 1964.

22. Irwin, G.R. and Kies, J.A., Welding Journal, 1952, 31-955.

23. Irwin, G.R., "Fracture Mechanics," Proceedings, First Symposium on Naval Structures Mechanics, MacMillan Press, 1958.

24. Strawley, J.E., "Plane Strain Fracture Toughness," Fracture An Advance Treatise, edited by Liebowitz, H., Vol. IV, Chapter II, pp. 45-68, 1969.

25. Hilton, P.D., and Hutchinson, J.W., "Plastic Intensity Factors for Cracked Plates," Engineering Fracture Mechanics, Vol. 3, pp. 435-451, 1971.

26. Winne, D.H., and Wundt, B.M., "Application of the Griffith-Irwin Theory of Crack Propagation to the Bursting Behavior of Disce, Including Analytical and Experimental Studies," Transactions ASME, Vol. 80, pp. 1643-1655, 1968.

27. Gross, B. and Strawley, J.E., "Stress-Intensity-Factors for Three Point Bend Specimens by Boundary Collocation," NASA TN D-3092, Lewis Research Center, Cleveland, Ohio.

28. Ang, D.D., Folias, E.S. and Williams, M.L., "The Bending Stress in a Cracked Plate on an Elastic Foundation, "Journal of Applied Mechanics, June 1963.

29. Bokowski, G.A., Private Communications, The Ohio State University, 1973.

30. Kauffmann, E.M. "The Application of Fracture Mechanics Concepts to Predict Cracking of Flexible Pavements," Ph.D. Dissertation, Ohio State University, 1973.

31. Westmann, R.A., "Pressurized Star Crack," Journal of Mathematics and Physics Vol. XLIII, No. 3, Sept. 1964.

32. Chang, Che-Wei, "Private Communication on Prismatic Finite Element Program," Ohio State University, Sept. 1972.

33. Luther, Michael, "Stress-intensity Factors for Pavement Overlays, " Private Communication, Ohio State University, March 1973.

34. Irwin, G. R., "Plastic Zone Near a Crack Tip and Fracture Toughness," Seventh Sagamore Ordnance Materials Research Conference, Aug. 1960.

35. Hartman, A., and Schijve, J., "The effects of Environment and Load Frequency on the Crack Propagation Law for Mono Fatigue Crack Growth in Alluminum Alloys," Engineering Fracture Mechanics, Vol. 1, p. 45, 1970.

36. Smith, S.H., "Fatigue Crack Growth Under Axial Narrow and Broad Band Random Loading," Accoustical Fatigue in Aerospace Structures, Proceedings of the Seventh International Conference, p.331, 1964.

37. Porter, T. R., "Method of Analysis and Prediction for Variable Amplitude Fatigue Crack Growth," Engineering Fracture Mechanics, Vol. 4, No. 4, 1972.

38. Wheeler, O.E., "Spectrum Loading and Crack Growth," Journal of Basic Engineering, ASME, Vol. 94, Series D, No. 1.

39. Mukherejee, B., and Burns, D.J., "Growth of Part Through Thickness Fatigue Cracks in Sheet Polymethylmethacrylate," Engineering Fracture Mechanics, Vol. 4, No. 4, Dec. 1972.

40. Kuzmanovic, B.O., and Willems, N., "Influence of Rest Periods on the Fatigue Strength of Structural Steel." Engineering Fracture Mechanics, Vol. 4, No. 4, 1972.

41. Pearson, S. "The Effect of Mean Stress on Fatigue Crack Propagation in Half Inch Thick Specimens of Aluminum Alloys of High and Low Fracture Toughness," Engineering Fracture Mechanics, Vol. 4, p. 9, 1972.

42. Forman, R.G., Kearney, V.E., and Engle, R. M., "Numerical Analysis of Crack Propagation in Cyclic Loaded Structures," American Society of Mechanical Engineering, Paper No. 66, Met-4, 1966.

43. Cherepanov, G.P., and Halmanov, H., "On the Theory of Fatigue Crack Growth," Engineering Fracture Mechanics, Vol. 4, p. 219, 1972.

44. Dempsey, B. J., and Marek, C. R., "A Model Utilizing Climatic Factors for Determining Stresses and Deflections in Flexible Permanent Systems," The Third International Conference on the Pavement Design, Vol. 1, 1972.

45. Wilson, E.L., and Nickell, R.E., "Application of the Finite Element Method to Heat Conduction," Nuclear Engineering and Design, Vol. 4, 1966.

46. J.R. Rice, "Mechanics of Crack Tip Deformation and Extension by Fatigue," Fatigue Crack Propagation, ASTM, 1967, p. 247.

47. D.C. Drucker, and J. R. Rice, "Plastic Deformations in Brittle and Ductile Fracture," Engr. Fract. Mech., Vol. 1, 1970 P.577-602.

48. J.R. Rice, "Stress due to Sharp Notch in a Work-Hardening Elastic-Plastic Material Loaded by Longitudinal Shear," J. Applied Mechanics, June 1967, p. 287.

49. J.R. Rice, "A Path Independent Integral and the Approximate Analysis of Strain Concentration by Notches and Cracks," J. Applied Mechanics, June 1968, p. 379.

50. P.M. Naghdi, "Stress-Strain Relations in Plasticity and Thermoplasticity," in Plasticity, Proc. 2nd Sym. Naval Structural Mechanics, Pergamon Press, 1960, p. 121-169.

51. P.W. Bridgman, "The Effect of Hydrostatic Pressure on the Fracture of Brittle Substances, " J. Applied Phys., Vol. 18, p. 246, 1947.

52. P.W. Bridgman, Studies in Large Plastic Flow and Fracture with Special Emphasis on the Effects of Hydrostatic Pressure, McGraw-Hill, New York, 1952.

53. Sandhu, R.S. "Elastic-Plastic Finite Element Analysis," Ohio State University, June 1972.

54. Singh, R.D. "Mechanical Characterization and Finite Element Analysis of Elastic-Plastic Work Hardening Soils," Ph.D. Dissertation, Ohio State University, 1972.

55. Hutchinson, J.W. "Plastic Stress and Strain Fields at a Crack Tip," Journal of Mech. Phys. of Solids, Vol. 8, p. 337, 1968.

56. Marcal, P.V. and King, I. P. "Elastic-Plastic Analysis of Two Dimensional Stress Systems by the Finite Element Method," International Journal of Mech. Science, Vol. 9, P. 143, 1967.

57. Levy, N. and Marcal, P.V. and Rice, J.R. "Small Scale Yielding Near a Crack in Plane Strain," International Journal of Fracture Mechanics, Vol. 7, No. @, 1971.

58. Liu, H.W. "Fatigue Crack Propagation and Applied Stress Range-An Energy Approach," Journal of Basic Engineering, Transaction, American Society of Mechanical Engineering, Series D, 1963.

59. Coffman, B.S., Ilves, G.J. and Edwards, W.F. "The Fatigue of Flexible Pavements," Ohio State University Engineering Experiment Station, Final Report Project EES 296, 1971.

60. Saraf, C. L. "Effect of Mix Variables on the Fatigue Reponse of Asphaltic Mixes," Ph.D. Dissertation, Ohio State University, June 1973.

61. Karamians, V. "Effect of Temperature on Fatigue Life Of Asphaltic Mixtures," M.S. Thesis, Ohio State University, June 1973.

APPENDIX A

EXPERIMENTAL PROCEDURES

EXPERIMENTATION ON SLABS SUPPORTED ON AN ELASTIC FOUNDATION

A. Specimen Preparation

The experimental work on circular slabs resting on an elastic foundation was carried out in three distinct phases. First, tests on slabs subjected to fatigue loads of variable amplitude and frequency were done at room temperature (77.5°F). The second set of tests, also done at room temperature, consisted of testing the asphalt slabs under loads of high intensity, of constant amplitude, so as to produce permanent deformation under the load, and to check the effects of rutting in the process of crack propagation. Finally, tests on slabs subjected to fatigue loads of constant amplitude were performed at temperatures of 41° and 90° F to study the applicability of fracture mechanics concepts at these temperatures.

The preparation of the test specimens as well as the procedures used in these experiments was the same as and will be described in this section. Also, the determination of some material properties needed to perform the analysis of the results is presented in this chapter. In Figure A-1 a view of the test set up showing the sand-asphalt slab resting on the elastic foundation is presented.

The sand-asphalt mixtures used to fabricate the circular slabs was the same

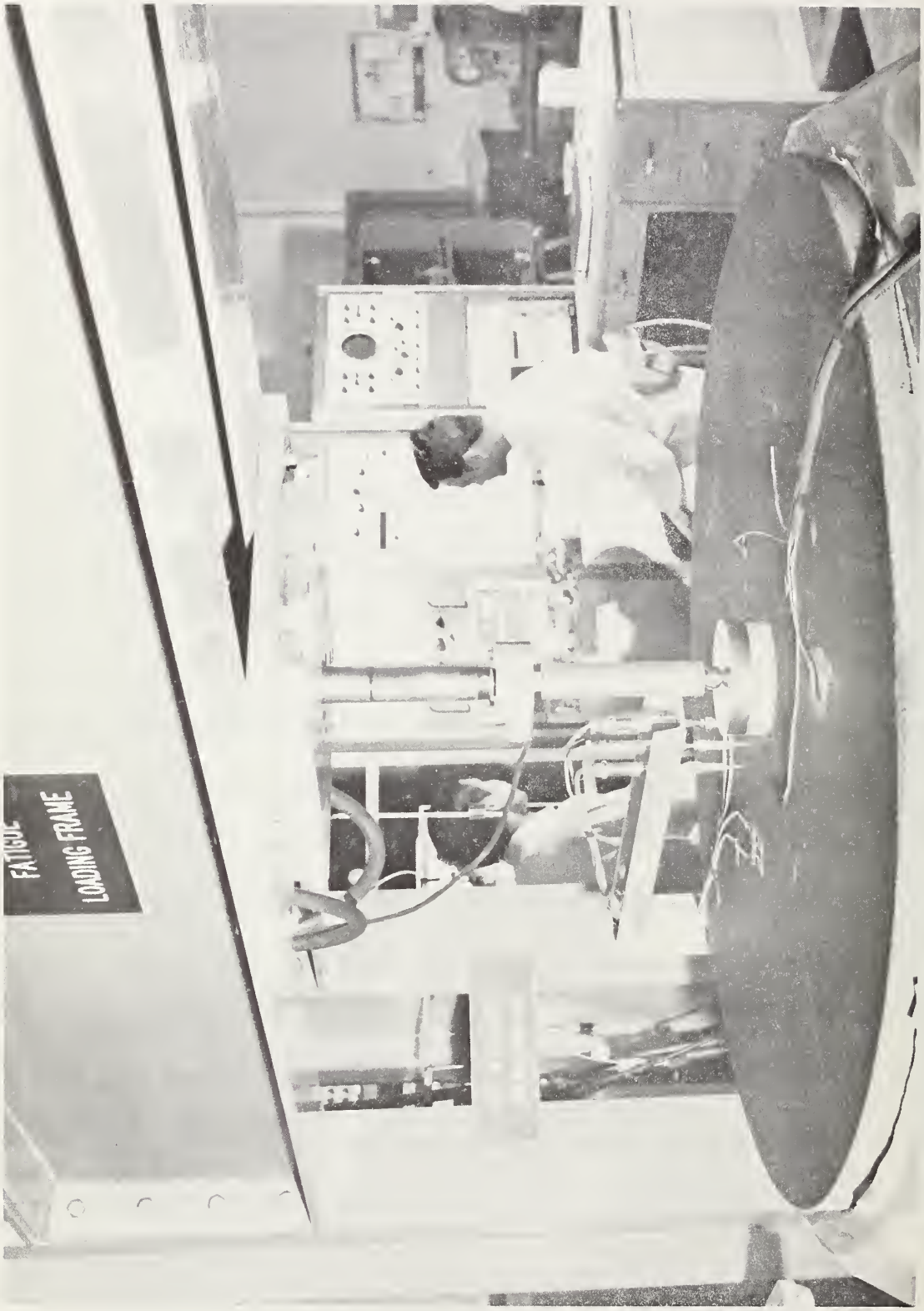
FATIGUE
LOADING FRAME

as the one used to prepare the beams (see Table A-1)and also used in previous Research Projects at OSU. The manufacturing procedures used were the same as those described in reference (14) (15) and basically consisted in pouring the pre-mixed sand-asphalt mixture into a circular steel mold which was coated with a film of mild soap to prevent sticking of the asphalt slab to the mold. After spading and carefully leveling the mix in the mold, a reinforced steel compaction head was placed over the mix and the compaction was accomplished by using a 12 H.P. mechanical vibrator. The compaction operation was stopped whenever thickness adjustment screws, attached to the rigid compaction head, made contact with the rim of the mold.

The compacted slab weighed approximately 168 pounds and was 44 inches in diameter and 1 1/2 inches thick, corresponding to a density of about 128 pcf. The slabs were stored from one to four weeks before being tested, and, after the tests, cores of 1 1/2 inches in diameter were extracted to make density measurements and control the quality and uniformity of the manufacturing process.

All the handling and transportation of the samples was done in such a manner as to prevent bending or damage. While being transported the slab was placed in between two rigid plates and to place it on the elastic foundation the slab was enclosed along with the upper rigid plate by a sheet of 6 mil plastic and a vacuum was applied through the upper plate to hold the slab weight when lifted. Then the slab was run on rails while being held by a vacuum from above and lowered by gently lowering the rails onto the foundation for testing.

TABLE A-1

Test Characteristics of Sand-Asphalt Mixtures

A. Asphalt Cement

Test	60/64
Specific Gravity	1.010
Softening Point, Ring and Ball	123°F
Ductility 77°F	150 + cm
Penetration, 100 gm., 5 sec., 77°F	63
200 gm., 60 sec., 39.4°F	23.5
Flash Point, Cleveland Open Cup	455°F
Viscosity, 140°F = 2970 Poises	
275°F = 4.68 Poises	

B. Aggregate

Sieve Number	% Passing (Samples)	ASTM Specification D1663-59T
16	100.0	85-100
30	88.0	70-95
50	64.2	45-75
100	30.1	20-40
200	15.7	9-20

C. Mixture

% Asphalt Cement (by weight of aggregate)	6%
Average Density	2.052 ± 0.011 gm/cm^3
Average Air Voids	17.0 ± 0.5%

The majority of those tests were performed with the asphalt slab unbonded from the foundation. For this purpose, the slab was placed on a sheet of plastic over the foundation to ensure a bondless surface between the slabs and the foundation. For bonded slab experiments, the plastic sheet was replaced with an asphaltic tack coat.

The elastic foundation consisted of two four-feet diameter layers bonded together by a rubber cement, the upper layer being a one-inch thick slab of armorite rubber and the lower layer being a slab of commercial art-gum rubber twelve inches thick. Tests performed in both layers separately showed a perfectly linear stress-strain curve, ensuring the elastic behavior of the system. During the course of the experiment work, the bottom layer was damaged and a detailed examination revealed the presence of several shrinkage cracks. It is believed that these cracks were caused by some process of aging in the art-gum rubber involving evaporation of the solvents used in its manufacturing process (see Figure A-2). At this point, a new foundation was built to replace the damaged bottom layer, and the new foundation used the same top layer of armorite rubber one-inch thick. The properties of the new system were again measured, and the results are shown in the following sections.

B. Testing Equipment

An MTS Electro-Hydraulic System was used in this investigation to apply a repeated load to the pavement system. The wave form consisted of a half sine function with a pulse duration of 0.1 second, and was programmed by the MTS

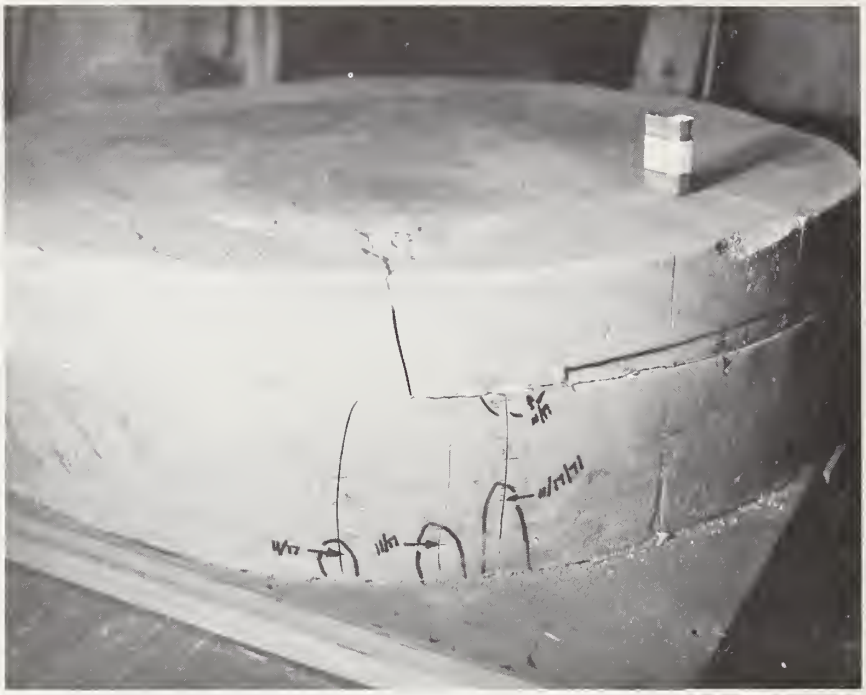

Function Generator. All tests were conducted in the load control mode and had in addition to the dynamic load, a static load with amplitude equal to about 5% of the total dynamic load.

The load was transfered to the asphalt slab from the hydraulic actuator through a steel ball to a steel plate to which a one inch thick rubber pad of 2 1/2 " radius was cemented. A thin sheet of teflon was placed between the rubber pad and the slab to minimize friction and the resulting shearing forces.

The center deflection of the slab was measured by the MTS actuator's LVDT. To obtain the actual value of the deflection, it was necessary to deduct the deflection of the rubber pad from the total measured deflection. A continuous recording of load and deflection was made using a Mark 280 Brush recorder, which also served as a monitor of the load function being applied to the slab.

With the exception made to those tests done at a temperature different than room temperature, all other tests were performed at 77.5°F. Care was taken to maintain the temperature at 77.5 $\pm$ 1° F by by blowing hot or cold air across the pavement model. The temperatures at various points on the slab were measured by copper-constantan thermocouple wires and recorded on a Barber Coleman thermocouple recorder.

C. Determination of the Material Constants

The theoretical analyses requires knowledge of the modulus of elasticity, E, and the Poisson's ratio, μ , of the sand-asphalt slab, and the modulus of subgrade reaction, k, of the elastic foundation, to find the stresses, displacements and stress-intensity factor of the cracked slab.

The modulus of elasticity was determined from Figure A-3 where the

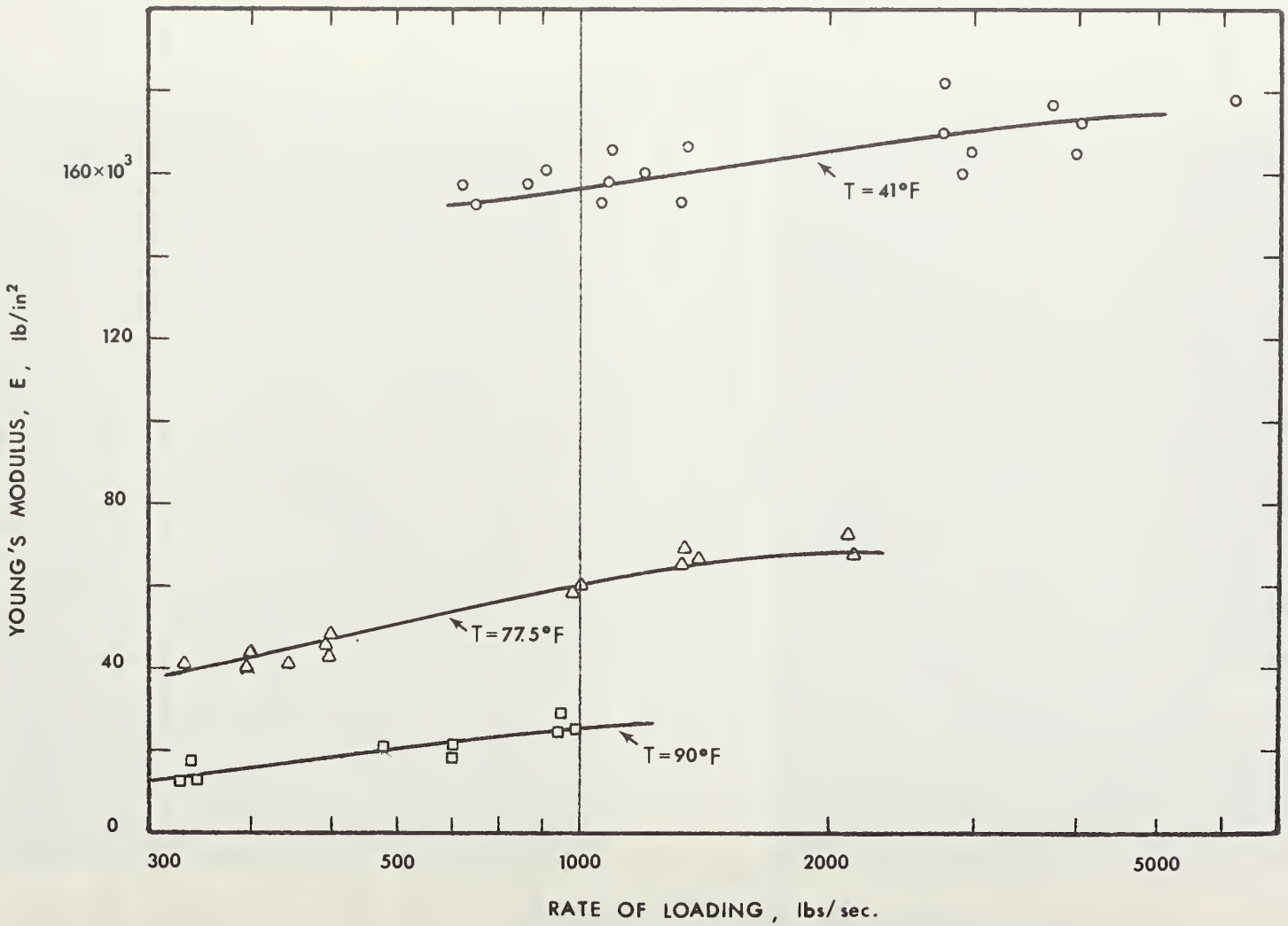

Figure A-3. Variations of Subgrade Modulus with Plate Radius

dynamic modulus, E*, determined from tests on simply-supported beams loaded at mid-span, is plotted versus the rate of loading. This plot shows that the assumption of elastic response for the pavement model, provided that the rate of loading is sufficiently large, ia a reasonable one. The determination of Poison's ratio, μ , for sand asphalt is very difficult and it was assumed to be 0.40, an average value of those reported in previous research.

To determine the modulus of subgrade reaction, k, of the elastic foundation, plate load tests using rigid plates of various sizes were performed to examine the variation of k with the size of the loaded area. The results for the subgrade reaction as a function of the radius of the loaded area, a, are presented in Figure A-4, showing an approximate inverse proportionality between k and a. This figure also shows the difference between the new and the old foundations used in this investigation, expressed in terms of k.

The value of the subgrade reaction modulus used in the analysis of the test results was selected as that for a plate size of radius 3", allowing for some distribution through the 1 1/2" asphalt slab.

The material constants used in the experiments were then as follows:

Sand-Asphalt Slab

Modulus of Elasticity, E= 25,000 psi (T=90°F)
E= 60,000 psi (T=77.5°F)
E= 175,000 psi (T=41°F)

Poisson's Ratio, = 0.40

Elastic Foundation

K=50 lbs/in^3(Old foundation)

K= 60 lbs/in^3(New foundation)

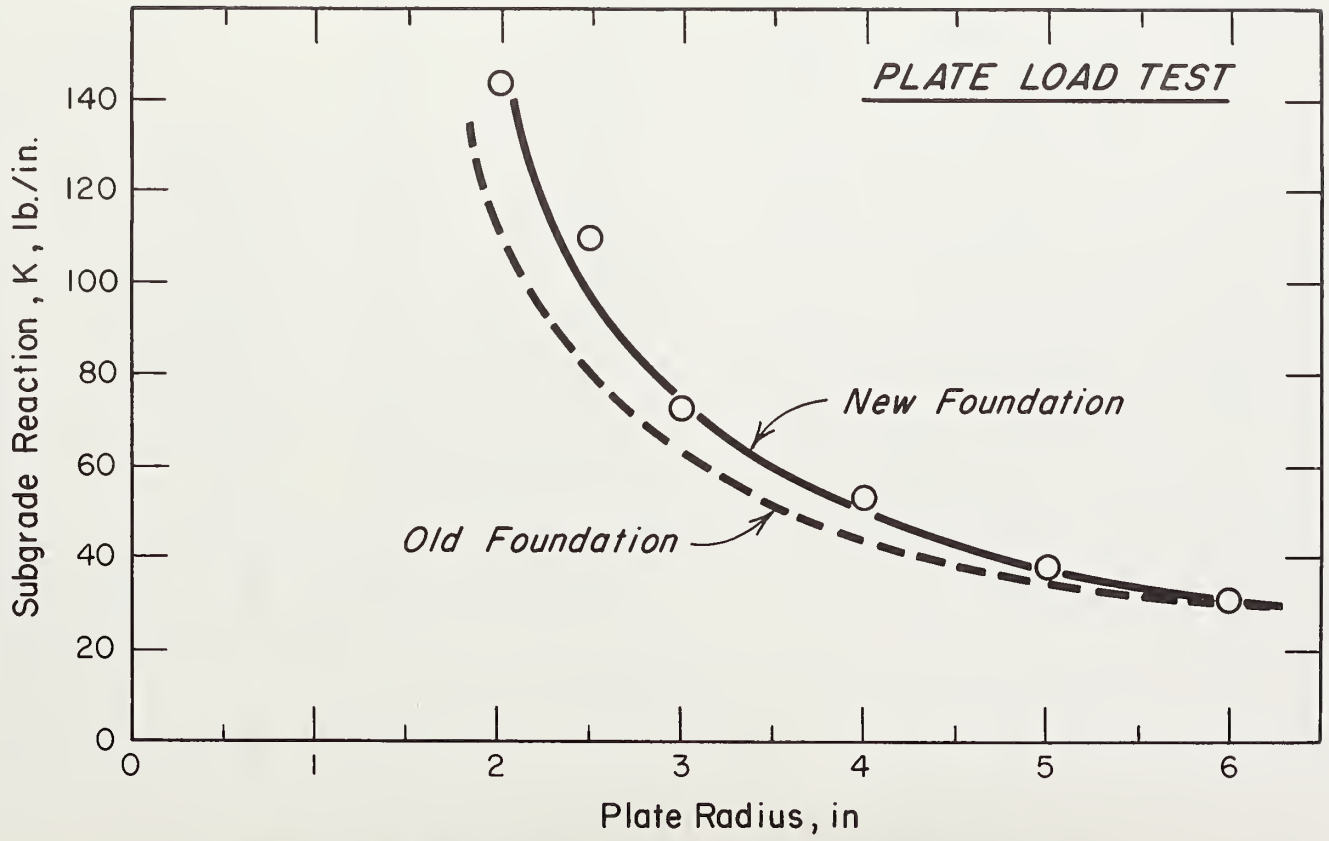

Figure A-4. Variations of Subgrade Modulus with Plate Radius

APPENDIX B

Prismatic Finite Element Program

OPERATING MANUAL t_2

ANALYSIS OF PRISMATIC SOLIDS PROGRAM

The first step is to select a finite element representation of the two-dimensional cross-section of the body. Elements and nodal points are then numbered in two numerical sequences, each starting with one. The following group of punched cards numerically defines the two-dimensional structure to be analyzed. A reference list has been included attaching the development of this procedure.

1. START

The first card has "START" in columns 1-5. This indicates the beginning of a new problem.

2. JOB TITLE (72 H)

This card will give the description identification for the job.

3. CONTROL INFORMATION (5I5, F 10, 2)

Information	Columns
Total number of nodal points	1-5
Total number of elements	6-10
Number of different materials	11-15
Number of pressure boundary cards	16-20
Number of harmonics	21-25
Half of the period length	26-35

4. CRACK INFORMATION (4 F 10, 2)

Information	Columns
X-ordinate of crack tip	1-10
Y-ordinate of crack tip	11-20
Radius of crack tip	21-30
Total load	31-40

5. MATERIAL PROPERTY INFORMATION

One set of cards must be provided for each material. In each set:

a. First card (2I 5) will give the following information:

Information	Columns
Material identification number	1-5
Number of different Y- ordinates for which properties are given (8 maximum)	6-10

b. Subsequent cards, one for each Y-ordinates, the number being defined in columns 6-10 of the first card, will carry the following information (3F 10.0)

Information	Columns
Y-ordinate of material for which property is given	1-10
Young's Modulus	11-20
Poisson's Ratio	21-30

6. NODAL POINT CARDS (I5, F5.0, 5F 10.0)

One card for each nodal point with the following information.

Information	Columns
Nodal point numbers	1-5
Type of nodal point	6-10
X-ordinate	11-20
Y-ordinate	21-30
UX	31-40
UY	41-50
Loaded length in z-direction	51-60

If the number in columns 6-10 is

0 UX is the specified X-load
UY is the specified Y-load

1 UX is the specified X-displacement
UY is the specified Y-load

2 U_X is the specified X-load
U_Y is the specified Y-displacement

3 U_X is the specified X-displacement
U_Y is the specified Y-displacement

All loads are considered to be total forces acting on the nodal point. Loaded length is half the total loaded length in the Z-direction. Nodal point cards must be in numerical sequence. If cards are omitted, the omitted nodal points are generated at equal intervals along a straight line between the defined nodal points. The boundary code (columns 6-10), UX, UY and loaded length, are set equal to zero.

7. ELEMENT CARDS (6I5)

One card for each element will provide the following data.

Information	Columns
Number of element	1-5
Nodal point I	6-10
Nodal point J	11-15
Nodal point K	16-20
Nodal point L	21-25
Material Type	26-30

Nodal points I, J, K, L are corners of each individual element in a counter-clockwise order for a right handed system of coordinates. For triangular elements set nodal point L same as nodal point K. The element cards must be in the numerical sequence. Any cards that are omitted will be automatically generated in the program by incrementing each of the I, J, K and L nodal points by one. The material type will be taken same as for the last element defined.

8. PRESSURE BOUNDARY CARDS (2I5, 2 F 10, 0)

One card for each boundary element which is subjected to a normal pressure will carry the following information:

Information	Columns
Nodal point I	1-5
Nodal point J	6-10
Normal pressure at I	11-20
Normal pressure at J	21-30

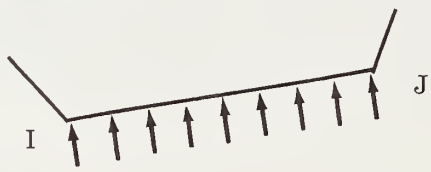

As shown in the sketch, the boundary element must be on the left as one progresses from I to J. Surface tensile force is input as a negative pressure.

9. LONGITUDINAL DISTANCE (F 10, 0)

This distance defines the cross-sections in the longitudinal (z) directions where stresses and strains are to be printed.

Information	Columns
ZZ - length	1-10

10. STOP

This card carries "STOP" in columns 1-4 and indicates the end of the problem.

OUTPUT INFORMATION

The following information is developed and printed at each desired cross-section in the Z-direction by the program.

1. Reprint of input data
2. Nodal point displacements for each harmonic
3. Nodal point displacements
4. Stresses at the center of each element
5. Stress intensitive factors K_1, K_2 at the vicinity of the crack

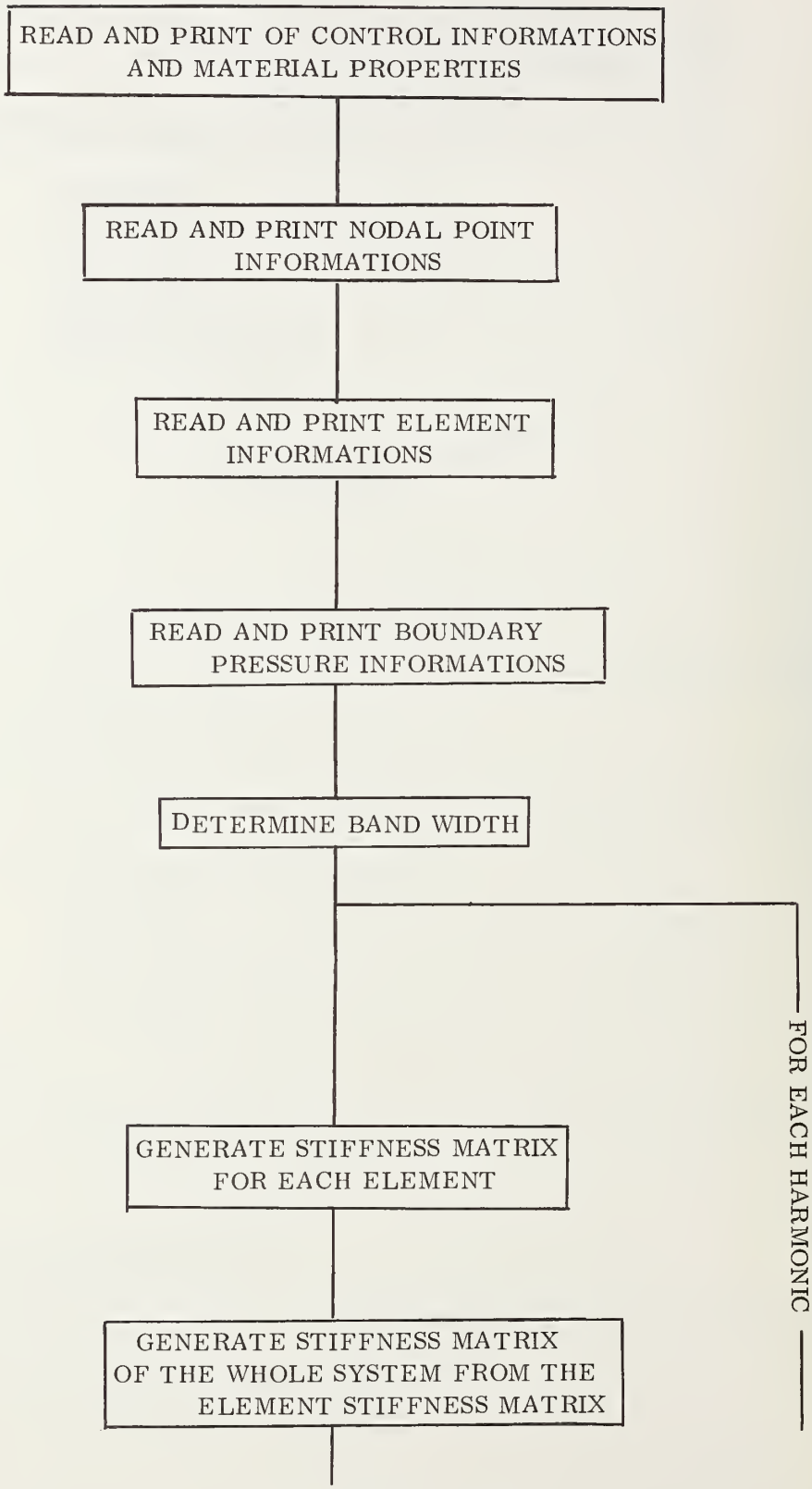
READ AND PRINT OF CONTROL INFORMATIONS AND MATERIAL PROPERTIES
READ AND PRINT NODAL POINT INFORMATIONS
READ AND PRINT ELEMENT INFORMATIONS
READ AND PRINT BOUNDARY PRESSURE INFORMATIONS
DETERMINE BAND WIDTH
GENERATE STIFFNESS MATRIX FOR EACH ELEMENT
GENERATE STIFFNESS MATRIX OF THE WHOLE SYSTEM FROM THE ELEMENT STIFFNESS MATRIX
FOR EACH HARMONIC

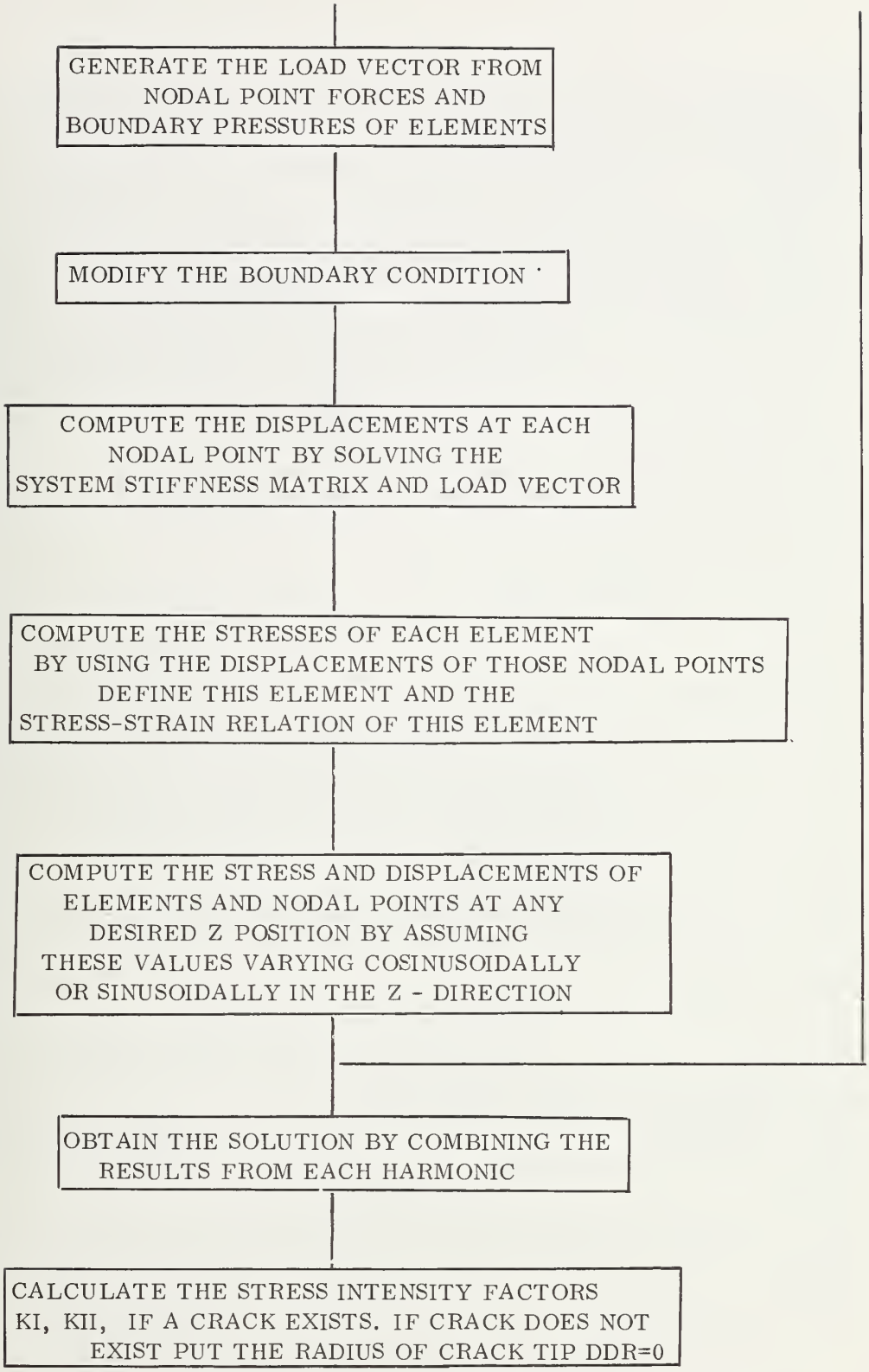
GENERATE THE LOAD VECTOR FROM NODAL POINT FORCES AND BOUNDARY PRESSURES OF ELEMENTS
MODIFY THE BOUNDARY CONDITION
COMPUTE THE DISPLACEMENTS AT EACH NODAL POINT BY SOLVING THE SYSTEM STIFFNESS MATRIX AND LOAD VECTOR
COMPUTE THE STRESSES OF EACH ELEMENT BY USING THE DISPLACEMENTS OF THOSE NODAL POINTS DEFINE THIS ELEMENT AND THE STRESS-STRAIN RELATION OF THIS ELEMENT
COMPUTE THE STRESS AND DISPLACEMENTS OF ELEMENTS AND NODAL POINTS AT ANY DESIRED Z POSITION BY ASSUMING THESE VALUES VARYING COSINUSOIDALLY OR SINUSOIDALLY IN THE Z - DIRECTION
OBTAIN THE SOLUTION BY COMBINING THE RESULTS FROM EACH HARMONIC
CALCULATE THE STRESS INTENSITY FACTORS KI, KII, IF A CRACK EXISTS. IF CRACK DOES NOT EXIST PUT THE RADIUS OF CRACK TIP DDR=0

```
C*********************************************************************
C     PROGRAMMED BY K.MAJIDZADEH AND C.W.CHANG, THE OHIO STATE UNI.
C     ARBITRARY PRISMATIC SOLIDS
C     USING CST-4 ELEMENTS AND STRESS INTENSITIVE FACTORS K1, K2 ARE
C     INCLUDED
C*********************************************************************
      IMPLICIT REAL*8(A-H,O-Z),INTEGER*4(I-N)
      COMMON/SYSTEM/NUMNP,NUMEL,NUMMAT,NUMHAR,NUMPC,NHAR,NTC(12),IBC(20)
     1,JBC(20),PR(20,2),XHAR,HED(18),E(8,3,12),DDX,DDY,DDR,DDP,PI,ZL
      COMMON/NODPNT/X(600),Y(600),UX(600),UY(600),CODE(600),T(600),
     1UZ(600)
      COMMON/ELEMNT/C(6,6),S(15,15),ST(6,15),XX(6),YY(6),EE(2),XC,YC,VOL
     1,SIG(560,6),IX(560,5),N,MTYPE,LM(4)
      COMMON/BANARG/B(156),A(156,78),MBAND,NUMBLK,JA
      DIMENSION WORD(2)
      DATA WORD/ 6HSTART ,6HSTOP  /
      DEFINE FILE 1(300,1500,U,NBK)
      CALL ERRSET (208,256,-1,1)
   10 READ(5,1000) WORD1
      IF(WORD1.EQ.WORD(1)) GO TO 30
      IF(WORD1.EQ.WORD(2)) STOP
      GO TO 10
   30 REWIND 4
      STOP=0.0
      PI=3.1415927
C*********************************************************************
C     READ AND PRINT OF CONTROL INFORMATION AND MATERIAL PROPERTIES
C*********************************************************************
      READ  (5,1010) HED,NUMNP,NUMEL,NUMMAT,NUMPC,NUMHAR,ZL
      WRITE (6,2010) HED,NUMNP,NUMEL,NUMMAT,NUMPC,NUMHAR,ZL
      READ(5,1020) DDX,DDY,DDR,DDP
      WRITE(6,2020) DDX,DDY,DDR,DDP
   40 DO 50 M=1,NUMMAT
      READ(5,1030) MTYPE,NTC(MTYPE)
      WRITE (6,2030) MTYPE,NTC(MTYPE)
      NUMTC=NTC(MTYPE)
      READ (5,1040) ((E(I,J,MTYPE),J=1,3),I=1,NUMTC)
      WRITE (6,2040) ((E(I,J,MTYPE),J=1,3),I=1,NUMTC)
   50 CONTINUE
C*********************************************************************
C     READ AND PRINT OF NODAL POINT DATA
C*********************************************************************
      WRITE (6,2050)
      L=0
      X(L)=0.
      Y(L)=0.
   60 READ  (5,1060) N,CODE(N),X(N),Y(N),UX(N),UY(N),T(N)
      NL=L+1
      ZX=N-L
      DX=(X(N)-X(L))/ZX
```

```
      DY=(Y(N)-Y(L))/ZX
   70 L=L+1
      IF(N-L) 100,90,80
   80 CODE(L)=0.0
      X(L)=X(L-1)+DX
      Y(L)=Y(L-1)+DY
      UX(L)=0.0
      UY(L)=0.0
      T(L)=0.0
      GO TO 70
   90 WRITE (6,2060) (K,CODE(K),X(K),Y(K),UX(K),UY(K),T(K),K=NL,N)
      IF(NUMNP-N) 100,110,60
  100 WRITE (6,2070) N
      CALL EXIT
  110 CONTINUE
C*********************************************************************
C     READ AND PRINT OF ELEMENT PROPERTIES
C*********************************************************************
      WRITE (6,2080)
      N=0
  130 READ (5,1090) M,(IX(M,I),I=1,5)
  140 N=N+1
      IF (M-N) 170,170,150
  150 IX(N,1)=IX(N-1,1)+1
      IX(N,2)=IX(N-1,2)+1
      IX(N,3)=IX(N-1,3)+1
      IX(N,4)=IX(N-1,4)+1
      IX(N,5)=IX(N-1,5)
  170 WRITE (6,2090) N,(IX(N,I),I=1,5)
      IF (M-N) 180,180,140
  180 IF (NUMEL-N) 190,190,130
  190 CONTINUE
C*********************************************************************
C     READ AND PRINT BOUNDARY PRESSURE DATA
C*********************************************************************
      IF(NUMPC) 200,300,200
  200 WRITE (6,2100)
      DO 250 L=1,NUMPC
      READ(5,1110) IBC(L),JBC(L),PR(L,1),PR(L,2)
  250 WRITE(6,2110) IBC(L),JBC(L),PR(L,1),PR(L,2)
  300 CONTINUE
C*********************************************************************
C     DETERMINE BAND WIDTH
C*********************************************************************
      J=0
      DO 340 N=1,NUMEL
      DO 340 I=1,4
      DO 325 L=1,4
      KK=IABS(IX(N,I)-IX(N,L))
      IF(26-KK) 310,315,315
```

```
  310 WRITE (6,2120) N
      STOP=1.0
  315 IF (KK-J) 325,325,320
  320 J=KK
  325 CONTINUE
  340 CONTINUE
      MBAND=3*J+3
C*********************************************************************
C     DETERMINE DISPLACEMENTS AND STRESSES FOR EACH HARMONIC
C*********************************************************************
      IF (STOP) 350,345,350
  350 CALL EXIT
  345 NUMUK=3*NUMNP
      DO 500 NHAR=1,NUMHAR
      XHAR=NHAR-1
C
C     FORM STIFFNESS MATRIX
C
      CALL STIFF
C
C     SOLVE FOR HARMONIC DISPLACEMENTS
C
      CALL BANSOL
C
      WRITE (4) (B(N),N=1,NUMUK)
      WRITE (6,2130) (N,B(3*N-2),B(3*N-1),B(3*N),N=1,NUMNP)
C
      CALL STRESS
C
  500 CONTINUE
C*********************************************************************
      CALL OUTPUT
C*********************************************************************
      GO TO 10
 1000 FORMAT(A6)
 1010 FORMAT (18A4/5I5,1F10.2)
 1020 FORMAT(4F10.2)
 1030 FORMAT (2I5)
 1040 FORMAT (3F10.0)
 1060 FORMAT (I5,F5.0,4F10.5,F10.5)
 1090 FORMAT (6I5)
 1110 FORMAT(2I5,2F10.3)
 2010 FORMAT (1H1 18A4/
     1 30H0 NUMBER OF NODAL POINTS------ I4 /
     2 30H0 NUMBER OF ELEMENTS---------- I4 /
     3 30H0 NUMBER OF DIFF. MATERIALS--- I3 /
     4 30H0 NUMBER OF PRESSURE CARDS---- I3 /
     5 30H0 NUMBER OF HARMONICS--------- I3 /
     6 30H0 Z-LENGTH------------------- F10.3)
```

```
2020 FORMAT(//' CRACK TIP X                = ',F10.5/
    1          ' CRACK TIP Y                = ',F10.5/
    2          ' RADIUS OF THE CRACK TIP = ',F10.5/
    3          ' CONCENTRATED LOAD          = ',F10.5/)
2030 FORMAT (17HOMATERIAL NUMBER= I3, 20H, NUMBER OF Y CARDS=  I3)
2040 FORMAT ( 14X 1HY 14X 1HE 13X 2HNU / (F15.3,E15.7,F15.3))
2050 FORMAT  (48H1NODAL POINT        TYPE  X-ORDINATE  Y-ORDINATE
    118X 6HX-LOAD 18X 6HY-LOAD 2X 12HLOAD LENGTH )
2060 FORMAT (I12,F12.2,2F12.4,2E24.7,F12.5)
2070 FORMAT (26HONODAL POINT CARD ERROR N= I5)
2080 FORMAT (49H1ELNMENT NO.      I     J     K     L    MATERIAL  )
2090 FORMAT (1I13,4I6,1I12)
2100 FORMAT(29HOPRESSURE BOUNDARY CONDITIONS/40H     I     J    PRESSUR
    1E I     PRESSURE J)
2110 FORMAT(2I6,2F14.3)
2120 FORMAT (30HON.P. DIFF. TOO LARGE EL.NO.= I4)
2130 FORMAT (12H1N.P. NUMBER 18X 2HUX 18X 2HUY 18X 2HUZ /(1I12,3E20.7))
C
     END
```

```
      SUBROUTINE STIFF
C
      IMPLICIT REAL*8(A-H,O-Z),INTEGER*4(I-N)
      COMMON/SYSTEM/NUMNP,NUMEL,NUMMAT,NUMHAR,NUMPC,NHAR,NTC(12),IBC(20)
     1,JBC(20),PR(20,2),XHAR,HED(18),E(8,3,12),DDX,DDY,DDR,DDP,PI,ZL
      COMMON/NODPNT/X(600),Y(600),UX(600),UY(600),CODE(600),T(600),
     1UZ(600)
      COMMON/ELEMNT/C(6,6),S(15,15),ST(6,15),XX(6),YY(6),EE(2),XC,YC,VOL
     1,SIG(560,6),IX(560,5),N,MTYPE,LM(4)
      COMMON/BANARG/B(156),A(156,78),MBAND,NUMBLK,JA
C
C*********************************************************************
C     INITIALIZATION
C*********************************************************************
      NB=26
      ND=3*NB
      ND2=2*ND
      STOP=0.0
      NUMBLK=0
      NBK=1
      JA=ND2*(MBAND+1)/1500+1
      DO 50 N=1,ND2
      B(N)=0.0
      DO 50 M=1,ND
   50 A(N,M)=0.0
C*********************************************************************
C     FORM STIFFNESS MATRIX IN BLOCKS
C*********************************************************************
   60 NUMBLK=NUMBLK+1
      NH=NB*(NUMBLK+1)
      NM=NH-NB
      NL=NM-NB+1
      KSHIFT=3*NL-3
      DO 210 N=1,NUMEL
      IF (IX(N,5)) 210,210,65
   65 DO 80 I=1,4
      IF (IX(N,I)-NL) 80,70,70
   70 IF (IX(N,I)-NM) 90,90,80
   80 CONTINUE
      GO TO 210
   90 CALL QUAD
      IX(N,5)=-IX(N,5)
      IF(VOL) 100,100,110
  100 WRITE(6,2000) N
      STOP=1.0
C*********************************************************************
C     ADD ELEMENT STIFFNESS TO TOTAL STIFNESS
C*********************************************************************
  110 MM=4
      IF(IX(N,3)-IX(N,4)) 130,120,130
```

```
  120 MM=3
  130 DO 140 I=1,MM
  140 LM(I)=3*IX(N,I)-3
      DO 200 I=1,MM
      DO 200 K=1,3
      II=LM(I)+K-KSHIFT
      KK=3*I-3+K
      DO 200 J=1,MM
      DO 200 L=1,3
      JJ=LM(J)+L-II+1-KSHIFT
      LL=3*J-3+L
      IF(JJ) 200,200,175
  175 IF(ND-JJ) 180,195,195
  180 WRITE (6,2001) N
      STOP=1.0
      GO TO 210
  195 A(II,JJ)=A(II,JJ)+S(KK,LL)
  200 CONTINUE
  210 CONTINUE
      IF(STOP) 215,220,215
  215 CALL EXIT
C*********************************************************************
C     ADD EXTERNAL FORCES WITHIN BLOCK
C*********************************************************************
  220 IF (NUMPC) 225,270,225
  225 DO 260 L=1,NUMPC
      I=IBC(L)
      J=JBC(L)
      DX=Y(I)-Y(J)
      DY=X(J)-X(I)
      PP2=(PR(L,2)+PR(L,1))/6.
      PP1=PP2+PR(L,1)/6.
      PP2=PP2+PR(L,2)/6.
      II=3*I-KSHIFT
      JJ=3*J-KSHIFT
      IF(II) 240,240,230
  230 IF(II-ND) 235,235,240
  235 B(II-1)=B(II-1)+PP1*DX
      B(II)=B(II)+PP1*DY
  240 IF(JJ) 260,260,245
  245 IF(JJ-ND) 250,250,260
  250 B(JJ-1)=B(JJ-1)+PP2*DX
      B(JJ)=B(JJ)+PP2*DY
  260 CONTINUE
  270 DO 300 N=NL,NM
      IF (N-NUMNP) 280,280,310
  280 K=3*N-KSHIFT-1
      IF (XHAR.EQ.0.0) TM=T(N)/2.0
      IF (T(N).EQ.0.0) TM=1.0/NUMHAR
      IF (T(N)*XHAR.NE.0.0) TM=ZL*DSIN(XHAR*PI*T(N)/ZL)/(XHAR*PI)
```

```
  290 B(K)=(B(K)+UY(N))*TM
  300 B(K-1)=(B(K-1)+UX(N))*TM
C*********************************************************************
C     BOUNDARY CONDITIONS
C*********************************************************************
  310 DO 400 M=NL,NH
      IF (M-NUMNP) 315,315,400
  315 U=UX(M)
      N=3*M-1-KSHIFT-1
      IF (CODE(M)) 390,400,316
  316 IF (CODE(M)-1.) 317,370,317
  317 IF (CODE(M)-2.) 318,390,318
  318 IF (CODE(M)-3.) 390,380,390
  370 CALL MODIFY(A,B,ND2,MBAND,N,U)
      GO TO 400
  380 CALL MODIFY(A,B,ND2,MBAND,N,U)
  390 U=UY(M)
      N=N+1
      CALL MODIFY(A,B,ND2,MBAND,N,U)
  400 CONTINUE
C*********************************************************************
C     WRITE BLOCK OF EQUATIONS ON FILE AND SHIFT UP LOWER BLOCK
C*********************************************************************
      WRITE(1'NBK)(B(N),(A(N,M),M=1,MBAND),N=1,ND)
      NBK=NBK+JA
      DO 420 N=1,ND
      K=N+ND
      B(N)=B(K)
      B(K)=0.0
      DO 420 M=1,ND
      A(N,M)=A(K,M)
  420 A(K,M)=0.0
C*********************************************************************
C     CHECK FOR LAST BLOCK
C*********************************************************************
      IF (NM-NUMNP) 60,480,480
  480 CONTINUE
  500 RETURN
 2000 FORMAT (26HONEGATIVE AREA ELEMENT NO. I4)
 2001 FORMAT (29HOBAND WIDTH EXCEEDS ALLOWABLE I4)
      END
```

```
      SUBROUTINE QUAD
C
      IMPLICIT REAL*8(A-H,O-Z),INTEGER*4(I-N)
      COMMON/SYSTEM/NUMNP,NUMEL,NUMMAT,NUMHAR,NUMPC,NHAR,NTC(12),IBC(20)
     1,JBC(20),PR(20,2),XHAR,HED(18),E(8,3,12),DDX,DDY,DDR,DDP,PI,ZL
      COMMON/NODPNT/X(600),Y(600),UX(600),UY(600),CODE(600),T(600),
     1UZ(600)
      COMMON/ELEMNT/C(6,6),S(15,15),ST(6,15),XX(6),YY(6),EE(2),XC,YC,VOL
     1,SIG(560,6),IX(560,5),N,MTYPE,LM(4)
      COMMON/BANARG/B(156),A(156,78),MBAND,NUMBLK,JA
      DIMENSION U(3),V(3)
      I=IX(N,1)
      J=IX(N,2)
      K=IX(N,3)
      L=IX(N,4)
      MTYPE=IX(N,5)
      VOL=0.
      XHAR2=XHAR**2
      PI2=PI**2
      ZL2=ZL**2
  100 DO 105 KK=1,2
  105 EE(KK)=E(1,KK+1,MTYPE)
C*********************************************************************
C     FORM STRESS STRAIN RELATION OF ELEMENT
C*********************************************************************
      COMM=EE(1)*(1.0-EE(2))/((1.0+EE(2))*(1.0-2.0*EE(2)))
      C(1,1)=COMM
      C(1,2)=COMM*EE(2)/(1.0-EE(2))
      C(1,3)=0.
      C(1,4)=C(1,2)
      C(1,5)=0.0
      C(1,6)=0.0
      C(2,1)=C(1,2)
      C(2,2)=C(1,1)
      C(2,3)=0.
      C(2,4)=C(1,2)
      C(2,5)=0.0
      C(2,6)=0.0
      C(3,1)=0.
      C(3,2)=0.
      C(3,3)=COMM*(1.0-2.0*EE(2))/(2.0*(1.0-EE(2)))
      C(3,4)=0.0
      C(3,5)=0.0
      C(3,6)=0.0
      C(4,1)=C(1,4)
      C(4,2)=C(2,4)
      C(4,3)=C(3,4)
      C(4,4)=C(1,1)
      C(4,5)=0.0
      C(4,6)=0.0
```

```
      C(5,1)=C(1,5)
      C(5,2)=C(2,5)
      C(5,3)=C(3,5)
      C(5,4)=C(4,5)
      C(5,5)=C(3,3)
      C(5,6)=0.0
      C(6,1)=C(1,6)
      C(6,2)=C(2,6)
      C(6,3)=C(3,6)
      C(6,4)=C(4,6)
      C(6,5)=C(5,6)
      C(6,6)=C(3,3)
C*****************************************************************************
C     INITIALIZATION
C*****************************************************************************
      DO 130 J=1,15
      DO 120 I=1,6
  120 ST(I,J)=0.
      DO 130 I=1,15
  130 S(I,J)=0.
      DO 140 I=1,4
      NPP=IX(N,I)
      XX(I)=X(NPP)
  140 YY(I)=Y(NPP)
      IF(IX(N,3)-IX(N,4)) 145,150,145
  145 XC=(XX(1)+XX(2)+XX(3)+XX(4))/4.
      YC=(YY(1)+YY(2)+YY(3)+YY(4))/4.
      XX(5)=XC
      YY(5)=YC
      K=5
      J=1
      I=4
      LM(3)=13
      NT=4
      GO TO 160
  150 NT=1
      LM(3)=7
      I=1
      K=3
      J=2
C*****************************************************************************
C     FORM STIFFNESS OF ELEMENT
C*****************************************************************************
  160 DO 200 NN=1,NT
      LM(1)=3*I-2
      LM(2)=3*J-2
      U(1)=YY(J)-YY(K)
      U(2)=YY(K)-YY(I)
      U(3)=YY(I)-YY(J)
      V(1)=XX(K)-XX(J)
```

```
      V(2)=XX(I)-XX(K)
      V(3)=XX(J)-XX(I)
      AREA=(XX(J)*U(2)+XX(I)*U(1)+XX(K)*U(3))/2.
      VOL=VOL+AREA
      AREA2=AREA**2
      COMM=.25/AREA
      XNT=NT
      COM=2./XNT
      COM=COM*COMM
      COM11=ZL/(8.0*AREA)
      COM12=XHAR*PI/12.0
      DO 180 L=1,3
      II=LM(L)
      ST(1,II)=ST(1,II)+U(L)*COM
      ST(2,II+1)=ST(2,II+1)+V(L)*COM
      ST(3,II)=ST(3,II)+V(L)*COM
      ST(3,II+1)=ST(3,II+1)+U(L)*COM
      ST(4,II+2)=ST(4,II+2)+2.0*AREA*XHAR*PI*COM/(3.0*ZL)
      ST(5,II+1)=ST(5,II+1)-AREA*XHAR*PI*COM*(1.0+(-1.0)**NHAR)/(3.0*ZL)
      ST(5,II+2)=ST(5,II+2)+V(L)*COM*(1.0+(-1.0)**NHAR)/2.0
      ST(6,II)=ST(6,II)-AREA*XHAR*PI*COM*(1.0+(-1.0)**NHAR)/(3.0*ZL)
      ST(6,II+2)=ST(6,II+2)+U(L)*COM*(1.0+(-1.0)**NHAR)/2.0
      DO 180 M=1,3
      JJ=LM(M)
      MULT=1.0
      IF(L.EQ.M) MULT=2.0
      S(II,JJ)=S(II,JJ)+(U(L)*C(1,1)*U(M)+V(L)*C(3,3)*V(M)+AREA2*XHAR2*P
     1I2*C(5,5)*MULT/(3.0*ZL2))*COM11
      S(II,JJ+1)=S(II,JJ+1)+(U(L)*C(1,2)*V(M)+V(L)*C(3,3)*U(M))*COM11
      S(II,JJ+2)=S(II,JJ+2)+U(L)*C(1,4)*COM12-(2.0*AREA*XHAR*PI*U(M)*C(5
     1,5)/(3.0*ZL))*COM11
      S(II+1,JJ+1)=S(II+1,JJ+1)+(V(L)*C(1,1)*V(M)+U(L)*C(3,3)*U(M)+AREA2
     1*XHAR2*PI2*C(5,5)*MULT/(3.0*ZL2))*COM11
      S(II+1,JJ+2)=S(II+1,JJ+2)+V(L)*C(1,4)*COM12-(2.0*AREA*XHAR*PI*V(M)
     1*C(5,5)/(3.0*ZL))*COM11
      S(II+2,JJ+2)=S(II+2,JJ+2)+(AREA2*XHAR2*PI2*C(4,4)*MULT/(3.0*ZL2)+U
     1(L)*C(5,5)*U(M)+V(L)*C(5,5)*V(M))*COM11
      S(JJ+1,II)=S(II,JJ+1)
      S(JJ+2,II)=S(II,JJ+2)
      S(JJ+2,II+1)=S(II+1,JJ+2)
  180 CONTINUE
      I=J
      J=J+1
  200 CONTINUE
C*********************************************************************
C     CONDENSATION
C*********************************************************************
      IF(IX(N,3)-IX(N,4)) 220,250,220
  220 DO 240 I=1,3
      KK=15-I
```

```
      DO 240 K=1,KK
      CC=S(KK+1,K)/S(KK+1,KK+1)
      DO 230 J=1,6
  230 ST(J,K)=ST(J,K)-CC*ST(J,KK+1)
      DO 240 J=1,KK
  240 S(J,K)=S(J,K)-CC*S(J,KK+1)
  250 CONTINUE
      RETURN
      END
```

```
      SUBROUTINE MODIFY(A,B,NEQ,MBAND,N,U)
C
      IMPLICIT REAL*8(A-H,O-Z),INTEGER*4(I-N)
      DIMENSION B(156),A(156,78)
      DO 250 M=2,MBAND                                                  MODI00 3
      K=N-M+1                                                           MODI00 4
      IF(K) 235,235,230                                                 MODI00 5
  230 B(K)=B(K)-A(K,M)*U                                                MODI00 6
      A(K,M)=0.0                                                        MODI00 7
  235 K=N+M-1                                                           MODI00 8
      IF(NEQ-K) 250,240,240                                             MODI00 9
  240 B(K)=B(K)-A(N,M)*U                                                MODI00 0
      A(N,M)=0.0                                                        MODI00 1
  250 CONTINUE                                                          MODI00 2
      A(N,1)=1.0                                                        MODI00 3
      B(N)=U                                                            MODI00 4
      RETURN                                                            MODI00 5
      END                                                               MODI00 6
```

```
      SUBROUTINE BANSOL
C
      IMPLICIT REAL*8(A-H,O-Z),INTEGER*4(I-N)
      COMMON/BANARG/B(156),A(156,78),MBAND,NUMBLK,JA
C                                                                       BANS0004
      MM=MBAND
      NN=96
      NL=NN+1
      NH=NN+NN                                                          BANS0007
      NB=0                                                              BANS00 8
      NBK=1
      FIND(1'1)
      GO TO 150                                                         BANS00 9
C*********************************************************************BANS0012
C     REDUCE EQUATIONS BY BLOCKS                                        BANS0013
C*********************************************************************BANS0014
C                                                                       BANS0015
C     1. SHIFT BLOCK OF EQUATIONS                                       BANS001
C                                                                       BANS0017
  100 NB=NB+1                                                           BANS0018
      DO 125 N=1,NN                                                     BANS0019
      NM=NN+N                                                           BANS0020
      B(N)=B(NM)                                                        BANS0021
      B(NM)=0.0                                                         BANS0022
      DO 125 M=1,MM                                                     BANS0023
      A(N,M)=A(NM,M)                                                    BANS0024
  125 A(NM,M)=0.0                                                       BANS0025
C                                                                       BANS0026
C     2. READ NEXT BLOCK OF EQUATIONS INTO CORE                         BANS0027
C                                                                       BANS0028
      IF (NUMBLK-NB) 150,200,150                                        BANS0029
  150 READ (1'NBK) (B(N),(A(N,M),M=1,MM),N=NL,NH)
      NNK=NBK
      NBK=NBK+JA
      IF (NB) 200,100,200                                               BANS0031
C                                                                       BANS0032
C     3. REDUCE BLOCK OF EQUATIONS                                      BANS0033
C                                                                       BANS0034
  200 DO 300 N=1,NN                                                     BANS0035
      IF (A(N,1)) 225,300,225                                           BANS0036
  225 B(N)=B(N)/A(N,1)                                                  BANS0037
      DO 275 L=2,MM                                                     BANS0038
      IF (A(N,L)) 230,275,230                                           BANS0039
  230 C=A(N,L)/A(N,1)                                                   BANS0040
      I=N+L-1                                                           BANS0041
      J=0                                                               BANS0042
      DO 250 K=L,MM                                                     BANS0043
      J=J+1                                                             BANS0044
  250 A(I,J)=A(I,J)-C*A(N,K)                                            BANS0045
      B(I)=B(I)-A(N,L)*B(N)                                             BANS0046
```

```
      A(N,L)=C
  275 CONTINUE
  300 CONTINUE
      NBK=NNK-JA
      IF(NUMBLK.EQ.NB) GO TO 410
      WRITE (1'NBK) (B(N),(A(N,M),M=2,MM),N=1,NN)
      NBK=NNK+JA
      GO TO 100
C*********************************************************************
C     BACK-SUBSTITUTION
C*********************************************************************
  410 DO 450 M=1,NN
      N=NN+1-M
      DO 425 K=2,MM
      L=N+K-1
  425 B(N)=B(N)-A(N,K)*B(L)
      NM=N+NN
      B(NM)=B(N)
  450 A(NM,NB)=B(N)
      NB=NB-1
      IF(NB.EQ.0) GO TO 500
      READ  (1'NBK) (B(N),(A(N,M),M=2,MM),N=1,NN)
      NBK=NBK-JA
      GO TO 410
  500 K=0
      DO 600 NB=1,NUMBLK
      DO 600 N=1,NN
      NM=N+NN
      K=K+1
  600 B(K)=A(NM,NB)
      RETURN
      END
```

```
      SUBROUTINE STRESS
C
      IMPLICIT REAL*8(A-H,O-Z),INTEGER*4(I-N)
      COMMON/SYSTEM/NUMNP,NUMEL,NUMMAT,NUMHAR,NUMPC,NHAR,NTC(12),IBC(20)
     1,JBC(20),PR(20,2),XHAR,HED(18),E(8,3,12),DDX,DDY,DDR,DDP,PI,ZL
      COMMON/NODPNT/X(600),Y(600),UX(600),UY(600),CODE(600),T(600),
     1UZ(600)
      COMMON/ELEMNT/C(6,6),S(15,15),ST(6,15),XX(6),YY(6),EE(2),XC,YC,VOL
     1,SIG(560,6),IX(560,5),N,MTYPE,LM(4)
      COMMON/BANARG/B(156),A(156,78),MBAND,NUMBLK,JA
      NUMUK=3*NUMNP
C*********************************************************************
C     COMPUTE STRESSES OF ELEMENTS FOR EACH HARMONIC AND STORE ON TAPE 4
C*********************************************************************
      DO 300 M=1,NUMEL
      N=M
      IX(N,5)=IABS(IX(N,5))
      MTYPE=IX(N,5)
      DO 50 I=1,6
   50 SIG(N,I)=0.0
   90 CALL QUAD
      MM=4
      IF(IX(N,3)-IX(N,4)) 170,160,170
  160 MM=3
  170 DO 180 I=1,6
      XX(I)=0.
      DO 180 J=1,MM
      II=3*J
      JJ=3*IX(N,J)
  180 XX(I)=XX(I)+ST(I,II)*B(JJ)+ST(I,II-1)*B(JJ-1)+ST(I,II-2)*B(JJ-2)
      DO 190 I=1,6
      DO 190 J=1,6
  190 SIG(N,I)=SIG(N,I)+C(I,J)*XX(J)
  300 CONTINUE
      WRITE (4) ((SIG(N,I),I=1,6),N=1,NUMEL)
C
      RETURN
      END
```

```
      SUBROUTINE OUTPUT
C
      IMPLICIT REAL*8(A-H,O-Z),INTEGER*4(I-N)
      COMMON/SYSTEM/NUMNP,NUMEL,NUMMAT,NUMHAR,NUMPC,NHAR,NTC(12),IBC(20)
     1,JBC(20),PR(20,2),XHAR,HED(18),E(8,3,12),DDX,DDY,DDR,DDP,PI,ZL
      COMMON/NODPNT/X(600),Y(600),UX(600),UY(600),CODE(600),T(600),
     1UZ(600)
      COMMON/ELEMNT/C(6,6),S(15,15),ST(6,15),XX(6),YY(6),EE(2),XC,YC,VOL
     1,SIG(560,6),IX(560,5),N,MTYPE,LM(4)
      COMMON/BANARG/B(156),A(156,78),MBAND,NUMBLK,JA
      NUMUK=3*NUMNP
      NUMST=6*NUMEL
C*********************************************************************
C     COMPUTE THE CENTER OF ELEMENT
C*********************************************************************
      DO 400 N=1,NUMEL
      CODE(N)=0.0
      T(N)=0.0
      IF(IX(N,3)-IX(N,4)) 300,100,300
  100 DO 200 I=1,3
      II=IX(N,I)
      T(N)=T(N)+X(II)/3.0
  200 CODE(N)=CODE(N)+Y(II)/3.0
      GO TO 400
  300 DO 350 I=1,4
      II=IX(N,I)
      T(N)=T(N)+X(II)/4.
  350 CODE(N)=CODE(N)+Y(II)/4.
  400 CONTINUE
C
      REWIND 4
C
  450 READ (5,1000,END=900) ZZ
C
      DO 550 N=1,NUMNP
      UX(N)=0.0
      UY(N)=0.0
  550 UZ(N)=0.0
C
      DO 675 N=1,NUMEL
      DO 675 I=1,6
  675 SIG(N,I)=0.0
C
C*********************************************************************
C     ADD TOGETHER THE STRESSES FOR EACH HARMONIC
C*********************************************************************
      DO 800 NHAR=1,NUMHAR
      XHAR=NHAR-1
      ZX=PI*XHAR*ZZ/ZL
      SINZ=DSIN(ZX)
```

```
      COSZ=DCOS(ZX)
C
      READ  (4) (B(N),N=1,NUMUK)
C
      DO 600 N=1,NUMNP
      UX(N)=UX(N)+B(3*N-2)*COSZ
      UY(N)=UY(N)+B(3*N-1)*COSZ
  600 UZ(N)=UZ(N)+B(3*N)*SINZ
C
      READ (4) (B(N),N=1,NUMST)
C
      DO 700 N=1,NUMEL
      SIG(N,1)=SIG(N,1)+B(6*N-5)*COSZ
      SIG(N,2)=SIG(N,2)+B(6*N-4)*COSZ
      SIG(N,3)=SIG(N,3)+B(6*N-3)*COSZ
      SIG(N,4)=SIG(N,4)+B(6*N-2)*COSZ
      SIG(N,5)=SIG(N,5)+B(6*N-1)*SINZ
  700 SIG(N,6)=SIG(N,6)+B(6*N)*SINZ
C
  800 CONTINUE
C
      WRITE (6,2001) (N,X(N),Y(N),ZZ,UX(N),UY(N),UZ(N),N=1,NUMNP)
C
      WRITE (6,2002) (N,T(N),CODE(N),ZZ,(SIG(N,I),I=1,6),N=1,NUMEL)
C
C*********************************************************************
C     COMPUTE STRESS INTENSITIVE FACTORS OF ELEMENTS NEAR CRACK
C*********************************************************************
      WRITE(6,2003)
      DO 850 N=1,NUMEL
      IF((T(N).LT.DDX).OR.(CODE(N).LT.DDY)) GO TO 850
      DXC=T(N)-DDX
      DYC=CODE(N)-DDY
      DRC=DSQRT(DXC**2+DYC**2)
      IF(DRC.GT.DDR) GO TO 850
      SPI=DSQRT(2.0*PI)
      SDRC=DSQRT(DRC)
      ANG=DATAN2(DXC,DYC)
      SINX=DSIN(ANG*0.5)
      SINY=DSIN(ANG*1.5)
      COSX=DCOS(ANG*0.5)
      COSY=DCOS(ANG*1.5)
      COM=SDRC*SPI
      DENO=2.0*(1.0+SINX*SINY+COSX*COSY)
      SI=COM*(SIG(N,1)*(2.0+COSX*COSY)+SIG(N,2)*COSX*COSY)/(COSX*DENO)
      SII=COM*(SIG(N,1)*(1.-SINX*SINY)-SIG(N,2)*(1.+SINX*SINY))/(SINX*DE
     1NO)
      SSI=SI/DDP
      SSII=SII/DDP
      THETA=ANG*57.296
```

```
      WRITE(6,2004)N,THETA,DRC,SI,SSI,SII,SSII
  850 CONTINUE
      GO TO 450
  900 RETURN
C
 1000 FORMAT (1F10.2)
 2001 FORMAT (10H1 N.P. NO. 9X 1HX 9X 1HY 9X 1HZ 13X 2HUX 13X 2HUY 13X
     1 2HUZ /(I10,3F10.2,3E15.7))
 2002 FORMAT (10H1  EL. NO. 9X 1HX 9X 1HY 9X 1HZ 12X 3HSXX 12X 3HSYY 12X
     1 3HSXY  2X 3HSZZ 12X 3HSYZ 12X 3HSZX /(I10,3F10.3,6E15.7))
 2003 FORMAT(1H1,5X,' EL. NO. ',8X,' ANGLE ',10X,' RADIUS ',14X,' KI ',8
     1X,' NORM. KI ',13X,' KII ',7X,' NORM. KII '//)
 2004 FORMAT(I10,6G18.4/)
C
      END
```

APPENDIX C

Results of Three-dimensional and Prismatic Finite Element Programs

Description of Figures

In Figure C-1, a finite element mesh for 3-D finite element program is shown. This mesh was developed for the pavement model used in this investigation.

In Figure C-2, the variation of σ_y stresses with depth at various distances away from the loaded area is presented. The results are compared with the analysis of stresses using a Chevron program and an original version of axi-symmetric program.

In Figures C-3, C-4, and C-5, the results of analysis of pavement systems using prismatic finite element program is shown. The data is compared with the results obtained from a multilayer elastic program. (Chevron).

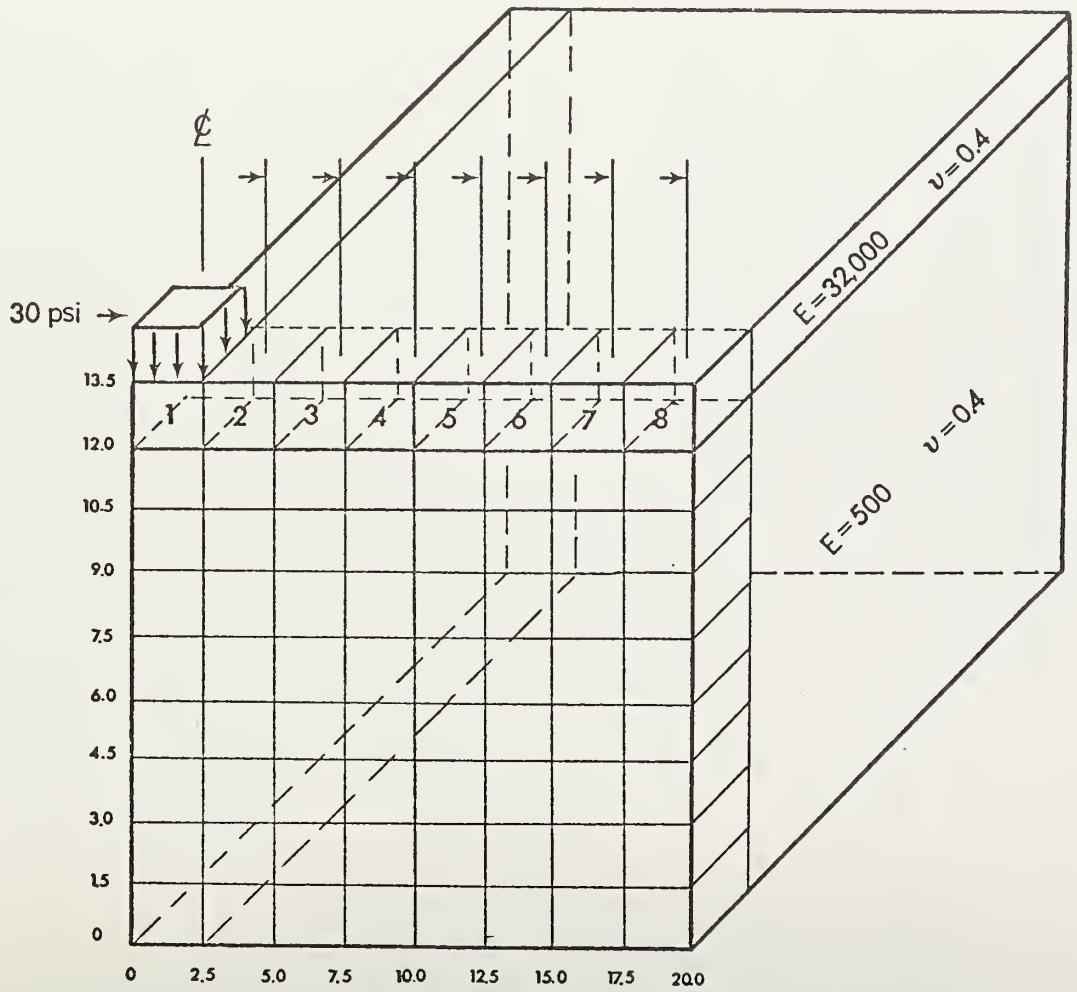

Figure C-1 Finite Element Mesh for a 3-D Program

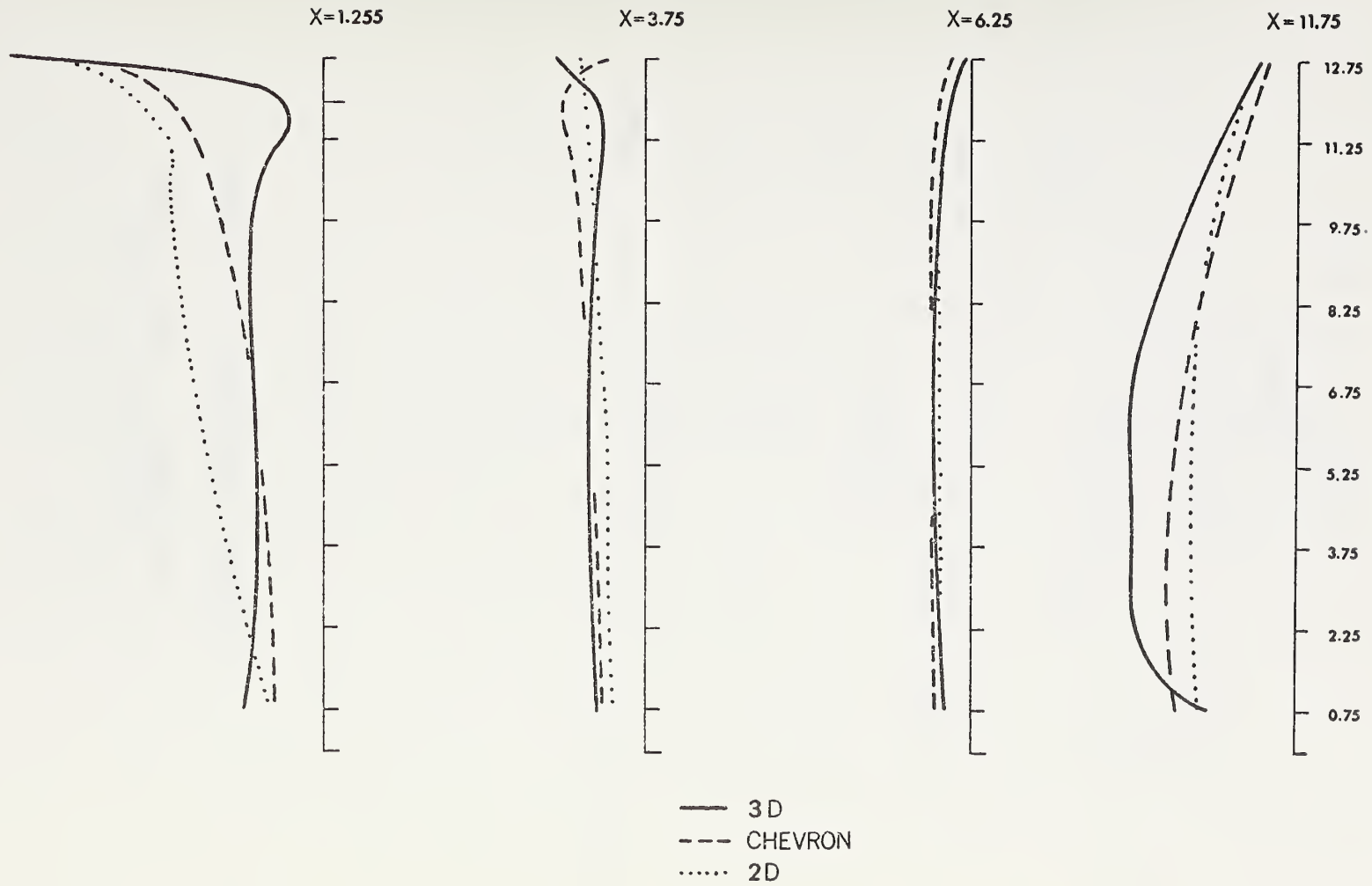

Figure C-2 The Comparison of σ_y at Different Radial Distance and Depths for 3-D and Chevron program

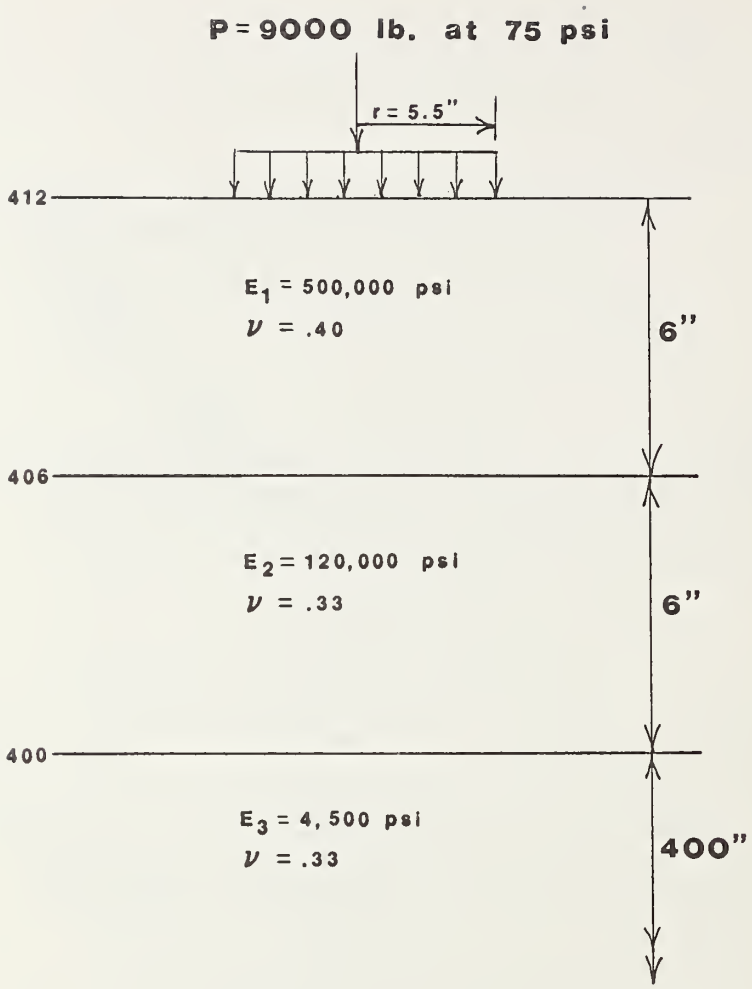

FIG. C-3

finite element 3 layer pavement and load

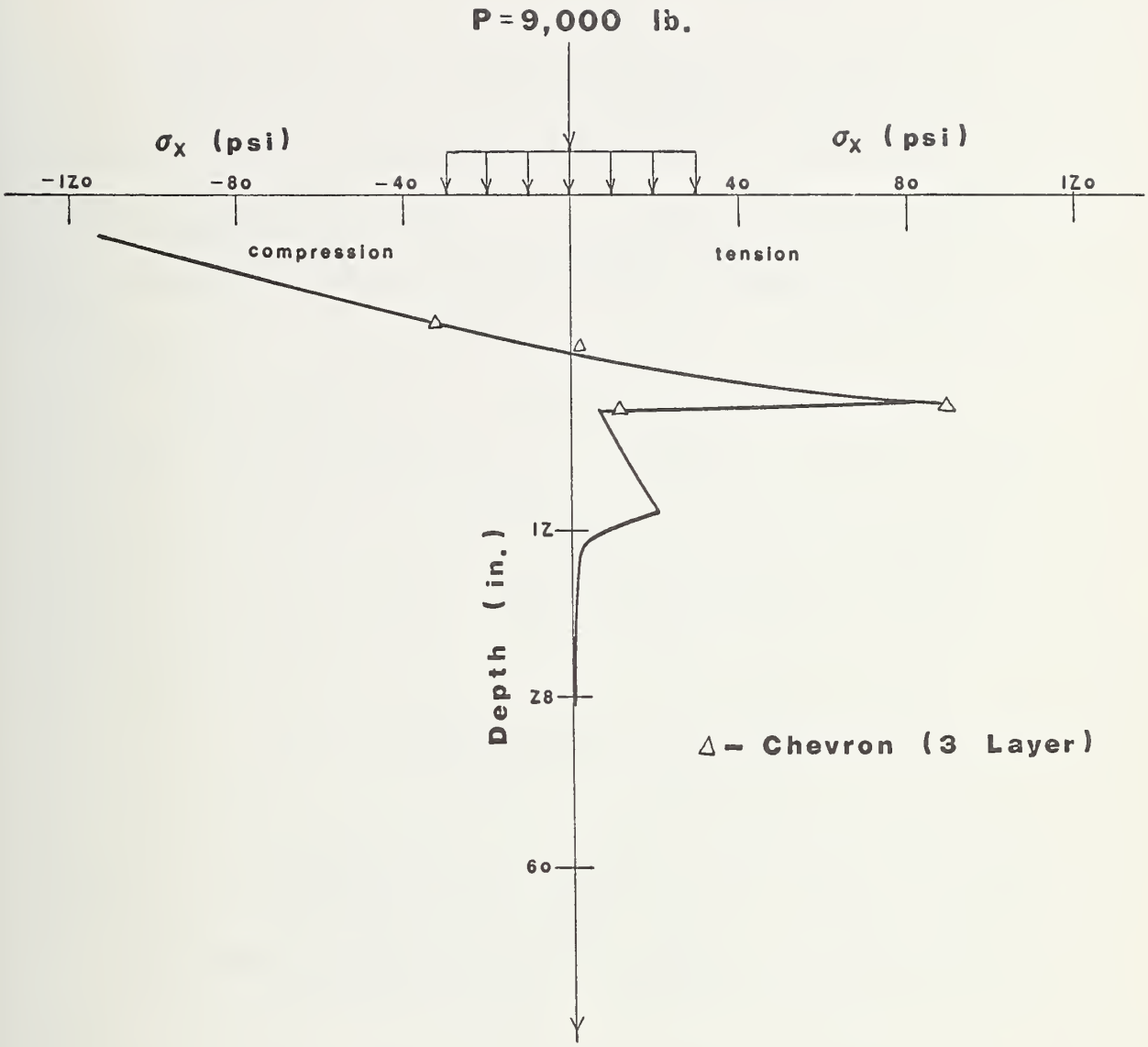

FIG. C-4

FINITE ELEMENT

σ_x VS. DEPTH (r = 0)

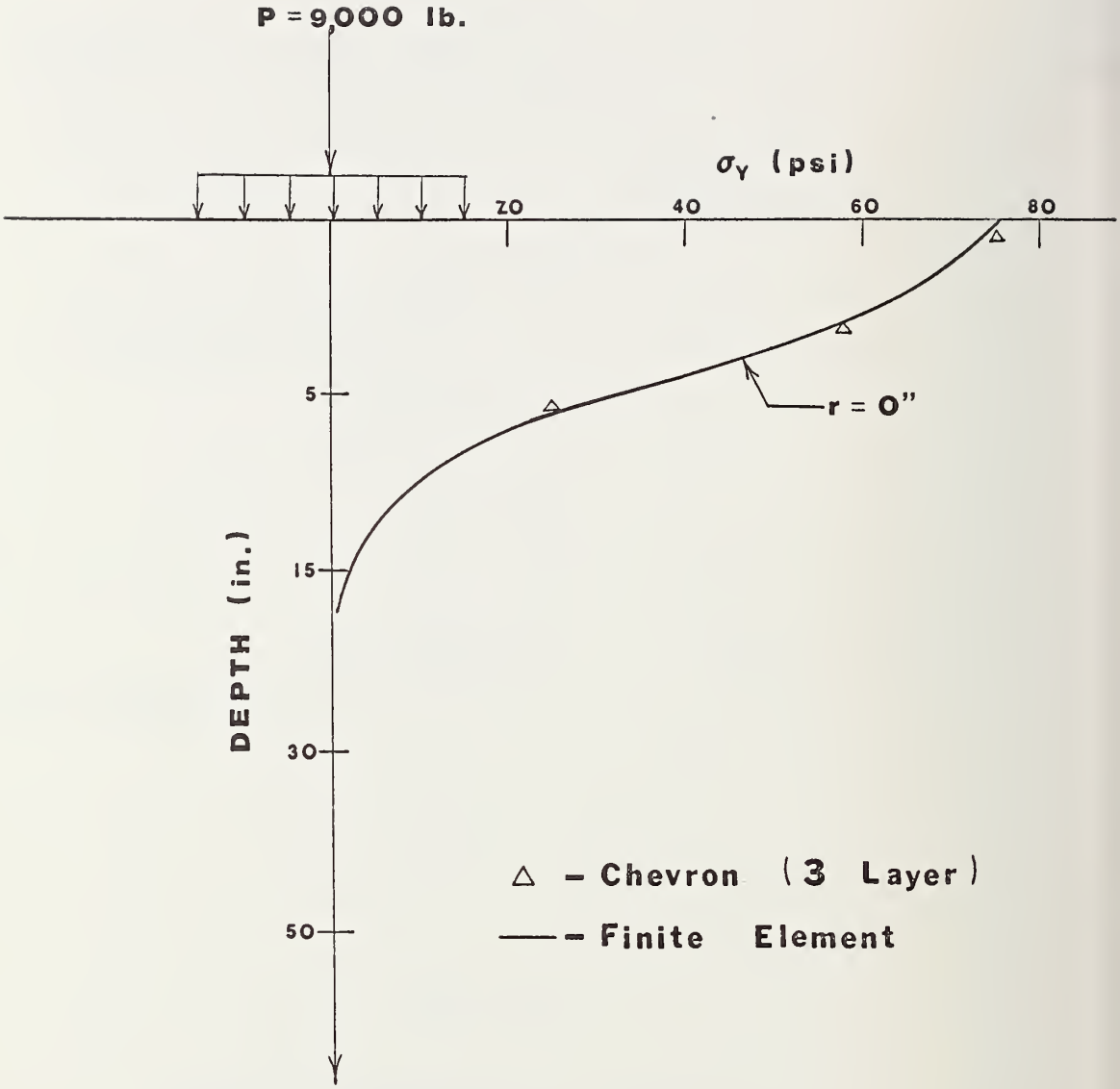

FIG. C-5

FINITE ELEMENT
σ_Y VS. DEPTH

APPENDIX D

Description and Use of Program for Calculation of Stress Intensity Factors K_1 and K_2 Under Moving Load

A group of programs, MAINSEFK, PUNCH, and FUNCTION, were written to solve for stress intensity factors for the case of a "moving load" on a cracked pavement. Refer to figure 1 for a schematic of the loading system. Three programs are required because of the length and complicated nature of the mathematics and the need for programmer response to certain phases of the computations. The layered-system used in the programs is defined in figure 2. Notice that only one foundation layer appears in the system. Therefore, to solve the stress intensity factors for other than a two-layered system, a equivalent two-layered system must be found. In general, the procedure for solving the stress intensity factor K1 is:

1) Find the moment function for the system in question. This may be found through some N-layered elastic program.

2) Use the program, FUNCTION, to solve an equivalent two layered system. In the program, use identical values for the parameters--pavement Young's modulus, pavement Poisson Ratio, pavement thickness, load, and load radius. Solve for the foundation's modulus K which will match the resulting moment function with the moment function obtained in the N-layer elastic program.

3) Run the program, PUNCH, with the same parameters as above. The output will be a "punched" deck of the moment function for the particular modulus K obtained in the above step.

4) Run the program, MAINSEFK, to solve the stress intensity factor K1.

To solve the stress intensity factor K2, repeat the above procedure matching the shear functions. Note, for the case of two layer system, steps 1 and 2

can be by passed.

These programs were written to solve the moving effects on a system with unbonded layers. After their completion, an investigation began and still is being carried out to study the same effects on a system with bonded layers. A variable, BONDFT, is introduced into the calculation of the rigidity parameter λ , which is given by

$$\lambda = \sqrt[4]{k/D} \quad .$$

Since the investigation is not yet completed, we recommend that the user restrict himself for the present to the "unbonded" case. This can be assomplished by entering "1." for variable BONDFT.

The program, MAINSEFK, solves the K1 and K2 stress intensity factors for the case of a pavement with a semi-infinite crack. The problem is so structured that for a given position of the load (which is described entirely by moment and shear functions), K1 and/or K2 will be calculated. Since it is of particular interest to study the effects of a "moving load", the program allows the load to be incremented in a direction parallel to the X axis.

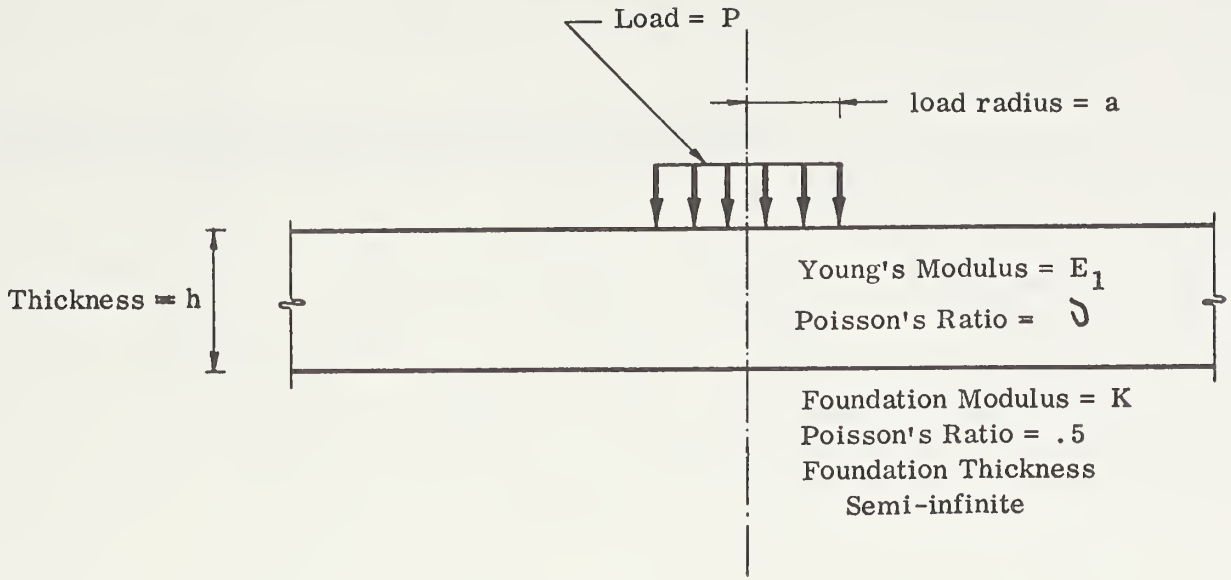

"Moving Load" Two-Layered Loading System
Figure 1

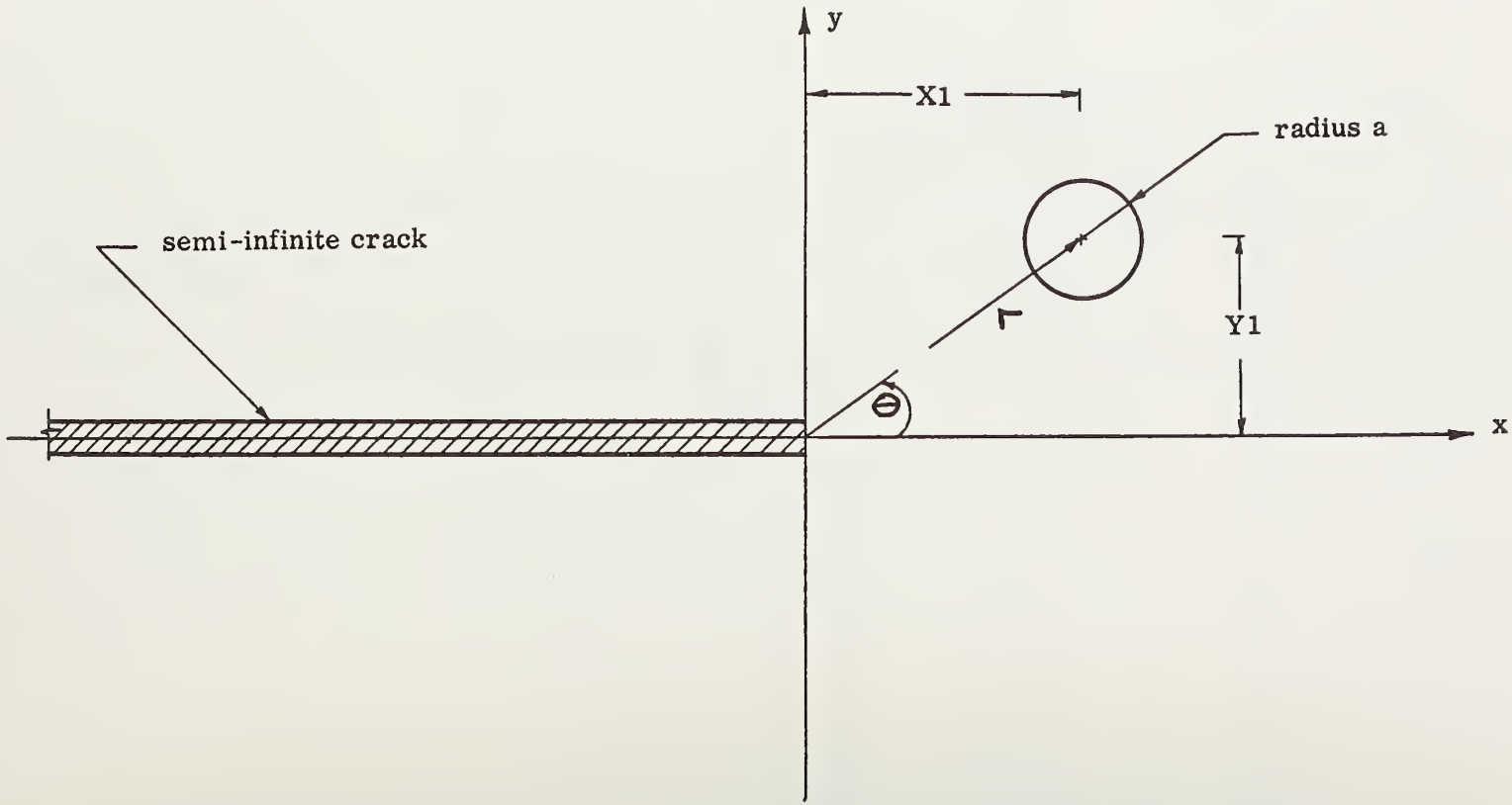

Layered System for programs MAINSEFK, PUNCH, AND FUNCTION
Figure 2

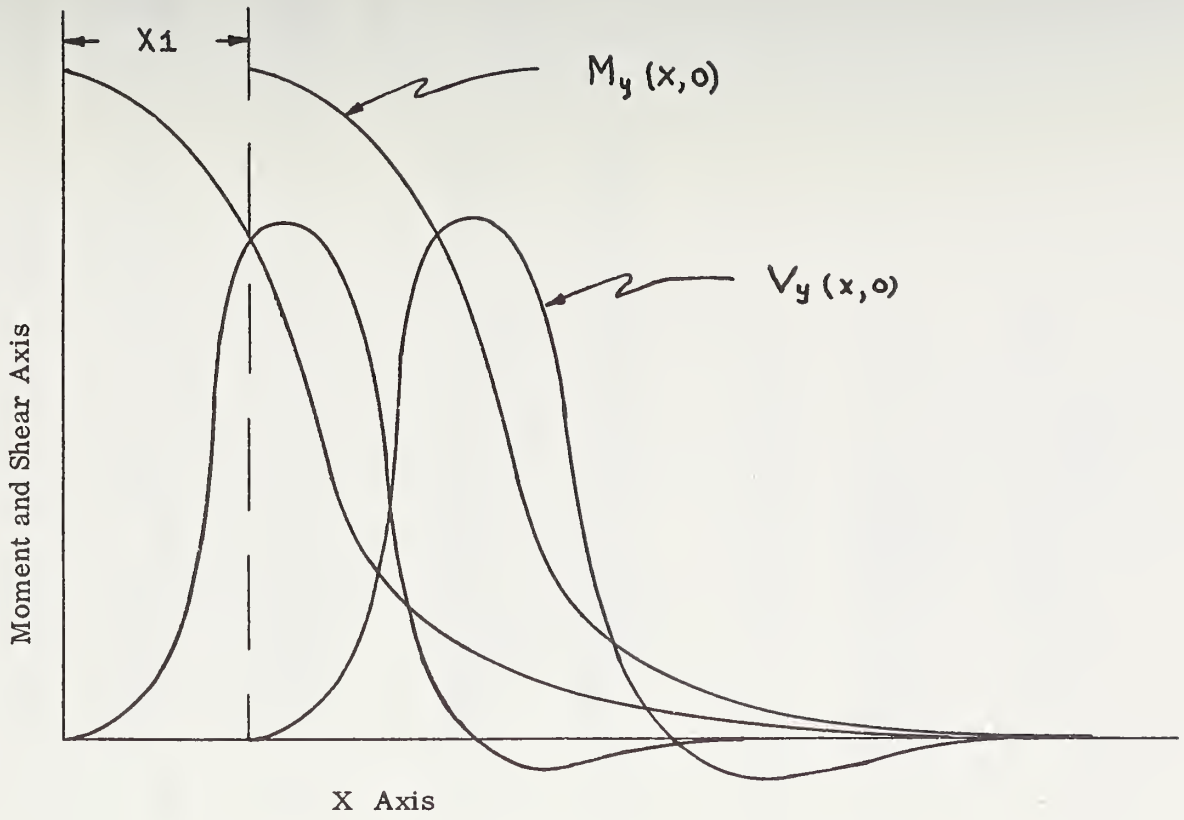

Figure 3.

MATHEMATICAL CONSIDERATIONS

The theory involved in this program can be summarized by the general expressions for the two stress intensity factors given as:

$$K_1 = \pi \frac{(3+\nu)}{(1+\nu)} (1-i)\, E\, h\, \lambda^{3/2} P_0 \qquad 1.$$

$$K_2 = \pi \frac{(3+\nu)}{(1+\nu)} (1+i)\, E\, h\, \lambda^{3/2} Q_0 \qquad 2.$$

The terms P_0 and Q_0 are complex and defined as:

for $a > \lambda$,

$$^1P_0 = \frac{-m_0\sqrt{a\lambda}}{2\pi(4-\nu_0)\nu_0\lambda^2 a} \left\{1 + \frac{s_1+s_2+c_0+\beta/2}{a}\lambda + O\left(\frac{\lambda^2}{a^2}\right)\right\} \qquad 3a.$$

$$^1Q_0 = \frac{-u_0\sqrt{\lambda}}{2\pi(4-\nu_0)\nu_0\lambda^2 a^{3/2}} \left\{1 + \frac{s_1+s_2+c_0+\alpha/2}{a}\lambda + O\left(\frac{\lambda^2}{a^2}\right)\right\} \qquad 3b.$$

for $a < \lambda$,

$$^2P_0 = \frac{-i m_0 e^{-i\pi/4}}{2\pi(4-\nu_0)\nu_0\lambda^2} \left\{\frac{(4-\nu_0)\nu_0}{2}\right\}^{1/2} \left\{1 + \left(\frac{1}{2\beta} + \frac{1}{s_1} + \frac{1}{s_2} - \bar{c}_0\right)\frac{a}{\lambda} + O\left(\frac{a^2}{\lambda^2}\right)\right\} \qquad 3c.$$

$$^2Q_0 = \frac{-i u_0 e^{-i\pi/4}}{2\pi(4-\nu_0)\nu_0\lambda^3} \left\{\frac{(4-\nu_0)\nu_0}{\sqrt{2}}\right\}^{1/2} \left\{1 + \left(\frac{1}{2\alpha} + \frac{1}{s_1} + \frac{1}{s_2} - \bar{c}_0\right)\frac{a}{\lambda} + O\left(\frac{a^2}{\lambda^2}\right)\right\} \qquad 3d.$$

where:

$\lambda = \sqrt[4]{k/D}$

$D = Eh^3/(12(1-\nu^2))$

$a = n\pi/p$, a variable of the Fourier representation

$i = \sqrt{-1}$

$\alpha^2 = i$

$\beta^2 = -i$

$N = \left[\!\left[\frac{n\pi}{p\lambda} \right]\!\right]$, where $[\![\ ]\!]$ is the greatest integer function

$\nu_0 = 1 - \nu$

$m_0 =$ a complex constant used in representing the moment function

$u_0 =$ a complex constant used in representing the shear function

The terms s_1, s_2, and c_0 are complex constants and are small - in fact, these terms can be disregarded as it will be shown later.

As it is necessary to calculate the stress intensity factor for different load positions and since the moment (or shear) function has the same shape at different locations of the load - an important property from Plate Theory, (see figure 3) the most efficient approach is to calculate the moment function once with the load at the origin of the coordinate system. Then, different moment functions, for the same load, can be expressed by means of different sets of Fourier coefficients. That is, a set of coefficients for the moment corresponding to a different position of the load can easily be calculated from the original moment values obtained with the load at the origin by merely translating a "moving coordinate system" along with the load. Mathematically, this is expressed by:

$$m_n = \frac{1}{2p} \sum_{j=-p}^{+p} \frac{M_j}{D} \cos\left(\frac{n\pi}{p}\right)(X_j - X_1) \quad \Delta X = 2m_o \qquad 4.$$

where M_n is the nth modified Fourier coefficient, M_j is a tabulated value of the moment function, and x_1 is the distance the moving coordinate system, or the load, is displaced from the fixed origin. The parameter p needs special mention as it will have an influence in severl ways. In the calculation of the M_n values, which represent the moment function, p defines the half-period of the moment function. That is, the value chosen for p must be such as to not have the moment repeat itself too close to the area of interest since it is treated as a periodic function in the Fourier expansion.

Likewise, the shear function is expanded into a set of modified Fourier coefficients for different positions of the load relative to the fixed coordinate system:

$$v_n = \frac{1}{2p} \sum_{j=-p}^{+p} \frac{v_j}{D} \cos \left(\frac{n\pi}{p} (x_j - x_1) \right) \Delta x = 2u_0, \qquad (5)$$

where v_j is a tabulated value of the shear function.

Now, if we substitute the coefficients m_n into the expressions for P_0 in place of m_o and sum over n from -p to tp, we will find the following, First, since $a = \frac{n\pi}{p}$ and P_o is represented by different expressions over different ranges of a, we must sum the expression ${}^2P_0$ in the range $-N < n < +N$ and then add to it the sums of ${}^1P_o$ for the ranges $n < -N$ and $n > N$. The second result of the substitution to be noted is that for ${}^2P_0$ and ${}^2Q_o$, the second terms in the square brackets will cancel as they contain a factor a/λ (or $n\pi/p$ and the sum is symmetrical around zero. The terms of second order in a/λ and λ/a will always be disregarded as contributing too little to be of importance. In the case of ${}^1P_0$ and ${}^1Q_o$, the second terms in the square brackets will be small becoming very small as n approaches $\pm$ p. It must also be noted that the transition values for n, i.e. $n = \pm N$, which determine the particular forms of p_o and Q_0 to use, are deleted from the sum on the additional assumption that these two terms in the overall sum will be small.

We are now left with the following:

$$P_o = \left\{ \sum_{n=-p}^{N-1} + \sum_{n=N+1}^{+p} \right\} \left\{ \frac{-m_n \sqrt{p}}{4\pi (4-\nu_0)\, \nu_0 \sqrt{\lambda^3 n \pi}} \right\}$$

$$+ \sum_{n=-N+1}^{N-1} \frac{-i\, m_n\, e^{-i\pi/4}}{4\pi (4-\nu_0)\nu_0\, \lambda^2} \left[\frac{(4-\nu_0)\nu_0}{\sqrt{2}} \right]^{1/2} \qquad 6.$$

$$Q_0 = \left\{ \sum_{n=-p}^{-N-1} + \sum_{n=N+1}^{+P} \right\} \left\{ \frac{-V_n P^{3/2}}{4(4-\nu_0)\nu_0 \sqrt{\lambda^3 n^3 \pi^5}} \right\}$$

$$+ \sum_{n=-N+1}^{N-1} \frac{-i V_n e^{-i\pi/4}}{4\pi(4-\upsilon_0)\upsilon_0 \lambda^3} \left[\frac{(4-\upsilon_0)\upsilon_0}{\sqrt{2}} \right]^{1/2} \qquad 7.$$

The input parameter p, which was shown to be mathematically the half period of the moment function in the Fourier expansion, can now be seen to have a second influence that of controlling the relative amounts of the two expressions for either P_0 or Q_0. In other words, if E or K is such as to make λ quite small, P_0 would be determined almost exclusively by $^2P_0$ unless the parameter p is made large enough to compensate this.

PROGRAMMING CONSIDERATIONS

All of the equations for this program were broken into real and imaginary parts, primarily for possible minor component analyses of K1 and K2 at some future date.

The program begins with reading in the system data, those pavement and foundation parameters which describe the loading system. Next, the tabulated moment and/or shear functions, which were calculated by the program PUNCH, are read from punched cards.

A word of caution is in order here concerning the moment and shear functions. Because of limitations in the approximating function for the JBessel function in the program PUNCH (and in FUNCTION) the calculated moment and shear tend to become inaccurate outside of the range of 0 to -45 inches. In order to correct for this inaccuracy, the program MAINSEFK has two input variables, ZEROM and ZEROS, which allow the user to zero the number of moment and shear values he deems necessary, from an inspection of the output of PUNCH, in order to insure that the input functions will behave nicely and decay to zero with distance from the load as the actual moment and shear do.

Also, it is to be noted that in order to minimize execution time, each set of moment (or shear) values corresponds to a set of X values and a particular Y value. Because of the procedure involved here, however, the X values must be spaced in intervals equal to, or in integral multiples of, DELTAX. This requirement also holds for the parameters X1BEG, X1END, and X1INT.

After the reading in of the program constants and options. the MAIN pro-

gram enters a loop where the load position X1 is made equal to X1beg. The control is then transfered to the subroutine SOLVE where a set of modified Fourier coefficients is calculated according to the expressions 4.) and 5.) for the load at position X1 and using the set of moment (or shear) values that were input to the program. Control then is transfered to the subroutine, STREFT, where K1 and/or K2 are calculated similar to expressions 6.) and 7.). After these calculations control returns to MAIN where the K1 and/or K2 values are printed and the load position X1 is incremented by X1INT. The cycle then repeats through SOLVE and STREFT until X1 equals X1END.

There exists an option in the subroutine SOLVE where the moment (or shear) function can be reconstructed from the calculated set of Fourier coefficients for the load at the origin. This is accomplished by inputing, TRUE, for the logical variable PRISK and specifying where the moment (or shear) should be calculated. If the fit of this calculated moment (or shear) is not too close to the original, it will be necessary to increase the value of NOOFN explicity in the MAIN program.

It should also be noted that sometimes while attempting to have the load move, the calculations are aborted and a message is printed to the effect that the X translated value is too positive or too negative. This results from the method used to translate the load position or in the handling of the set of x values that correspond to the set of moment (or shear) values supplied as input. What is needed to correct this problem is a larger value for ZEROM (or ZEROS); thus, it is necessary that the program PUNCH calculate values for a sufficient distance to give the user enough latitude to move the load position as needed in MAINSEFK.

The program, FUNCTION, solves for the moment, shear, strain and deflection functions for the case of a pavement with a semi-infinite crack. See figure 1 for interpretation of the system. The problem is structured so that a load can be located anywhere on the pavement surface and the program will calculate the above functions for any point along the crack.

The theory behind the program is basically "Plate Theory." The deflection function, $\omega(r)$, is defined as

$$\omega(r) = \frac{P}{K\pi a} \int_0^\infty \frac{J_1(ma)\, J_0(ma)\, dm}{1 + m^4 l^4}$$

where K represents the foundation's equivalent Young's modulus, P represents the load, a represents the load radius, E represents the pavement's Young's modulus, ν represents the pavement's Poisson ratio, h represents the pavements thickness, J_n represents the J Bessel function of degree n, X1 represents the distance along the X axis from the origin to the load, Y1 represents the distance along the Y axis from the origin to the load, and l, D, r , and θ are given as

$$l = \sqrt[4]{D/K}$$

$$D = E h^3 / (12(1-\nu^2))$$

$$r = \sqrt{[X - X1]^2 + [Y - Y1]^2}$$

$$\theta = \tan^{-1}\left(\frac{Y - Y1}{X - X1}\right)$$

To numerically solve the "$\omega(r)$" integral, we transpose the function into "sum" calculus, which is given by

$$\omega(r) = \frac{P}{K\pi a} \sum_{m=0}^{M} \frac{J_1(ma)\, J_0(mr)\, \Delta m}{1 + m^4 l^4}$$

It was found that the sum converges for M equal to 6 and Δ m equal to .01. The moment and shear functions, $M_{y(X,0)}$ and $V_{y(K,0)}$ respectively, are derivative functions of ω (r) and are given as

$$M_y(X,0) = -D\left(\frac{\partial^2 \omega(r)}{\partial y^2} + \nu \frac{\partial^2 \omega(r)}{\partial x^2}\right)$$

$$V_y(x,0) = -D\left(\frac{\partial^3 w(r)}{\partial y^3} + (2-\nu)\frac{\partial^3 w(r)}{\partial x^2 \partial y}\right)$$

where

$$\frac{\partial^2 w(r)}{\partial x^2} = \frac{\partial^2 w(r)}{\partial r^2}\cos^2\theta + \frac{\partial w(r)}{\partial r}\frac{\sin^2\theta}{r}$$

$$\frac{\partial^2 w(r)}{\partial y^2} = \frac{\partial^2 w(r)}{\partial r^2}\sin^2\theta + \frac{\partial w(r)}{\partial r}\frac{\cos^2\theta}{r}$$

$$\frac{\partial^3 w(r)}{\partial y^3} = \frac{\partial^3 w(r)}{\partial r^3}\sin^3\theta + 3\frac{\partial^2 w(r)}{\partial r^2}\frac{\sin\theta\cos^2\theta}{r}$$

$$- 3\frac{\partial w(r)}{\partial r}\frac{\sin\theta\cos^2\theta}{r}$$

$$\frac{\partial^3 w(r)}{\partial x^2 \partial y} = \frac{\partial^3 w(r)}{\partial r^3}\sin\theta\cos^2\theta + \frac{\partial^2 w(r)}{\partial r^2}\left(1-3\cos^2\theta\right)\frac{\sin\theta}{r}$$

$$- \frac{\partial w(r)}{\partial r}\frac{\sin\theta}{r^2}\left(1-3\cos^2\theta\right)$$

The partial derivatives, $\frac{\partial w(r)}{\partial r}$, $\frac{\partial^2 w(r)}{\partial r^2}$ and $\frac{\partial^3 w(r)}{\partial r^3}$ are solved numerically, and are given by

$$\frac{\partial w(r)}{\partial r} = \frac{P}{K\pi a} \sum_{m=0}^{M} \frac{J_1(ma)\, J_0'(mr)\, m}{1 + m^4 l^4} \Delta m$$

$$\frac{\partial^2 w(r)}{\partial r^2} = \frac{P}{K\pi a} \sum_{m=0}^{M} \frac{J_1(ma)\, J_0''(mr)\, m^2}{1 + m^4 l^4} \Delta m$$

$$\frac{\partial^3 w(r)}{\partial r^3} = \frac{P}{K\pi a} \sum_{m=0}^{M} \frac{J_1(ma)\, J_0'''(mr)\, m^3}{1 + m^4 l^4} \Delta m$$

Again, it was found that each sum converges for M equal to 6 and Δ M equal to .01. The strain components, ε_{xx} (x,y) and ε_{yy} (x,y), are also derivative terms of the deflection function and are given by

$$\varepsilon_{xx}(x,y) = -\frac{Ph}{2K\pi a} \sum_{m=0}^{M} \left[\frac{m^2 J_1(ma)\, J_0''(mr)}{1 + m^4 l^4} \cos^2\theta + \frac{m\, J_1(ma)\, J_0'(mr)}{1 + m^4 l^4} \frac{\sin^2\theta}{r} \right] \Delta m$$

$$\varepsilon_{yy}(x,y) = -\frac{Ph}{2K\pi a} \sum_{m=0}^{M} \left[\frac{m^2 J_1(ma)\, J''(mr)}{1 + m^4 l^4} \sin^2\theta + \frac{m\, J_1(ma)\, J_0'(mr)}{1 + m^4 l^4} \frac{\cos^2\theta}{r} \right] \Delta m$$

For convergence of these two sums, again M equals 6 and Δ M equals .01.

The program calculates each of the above mentioned functions in a simple, straight forward manner. First, the system data is read in. Then, for each desired value of X, the program iteratively solves for all numerical "sums." Each result is combined algebraically in the required form to find the moment, shear, strain and deflection for the particular value of X. The printed output then follows.

For this program, the execution time is roughly two seconds for each value of X. One should closely follow the calculated functions for the BESJ subroutine becomes slightly inaccurate beginning around a X value of-45. Aside from this small problem, no other difficulties exist.

The program, PUNCH, solves the moment and shear functions for the case of a pavement with a semi-infinite crack. See figure #1 for interpretation of the particular system. In addition, the program punches out the functions on data cards as they are needed as inputs to the program MAINSEFK. The problem is structured so that the load can be located anywhere on the Y axis and the program will calculate a moment and a shear for points along the crack. Since the programs FUNCTION and PUNCH have the same theoretical base, I will dispense with a theoretical discussion here. If need be, refer to the program FUNCTION for any questions.

This program calculates the moment and shear functions in a more "streamlined" manner compared to the program FUNCTION. This characteristic is needed for several hundred moments and shears are necessary as input to the program MAINSEFK. Briefly, the structure of the program is:

1) Read in system data
2) Calculate the moment and shear for each desired K value
3) Print and punch output.

For this program, the execution time is roughly one second for each value of X. One should closely follow the calculated functions for the BESJ subroutine becomes slightly inaccurate beginning around an x value of -45. I would, therefore, recommend that initially the beginning X value be equal to -45. To accomplish this, the variable CLCHEK should be set to "TRUE", and the variables SMSTAT and SMEND be set to -45 and 0 respectively. If one finds that the functions are still present, he need only to insert new upper and lower bounds.

Listing of Program FUNCTION

```
C****
C****     THIS PROGRAM CALCULATES POLAR COORDINATES, MOMENT, SHEAR
C****          DEFLECTION, STRAIN XX, AND STRAIN YY FUNCTIONS FOR A
C****          GIVEN SET OF X'S & Y'S.
C****
C
C****     ARRAY NAME CONTAINS TEST DATA DESCRIPTION
C****     NOOFX IS TOTAL NUMBER 'X' VALUES
C****     CONLPF IS MULTIPLING CONSTANT FOR FOURIER VARIBLE 'P'
C              'P' = CONLP = CONLPF * 3.1415962
C****     BCNOFT IS FACTER USED TO CONVERT THE UNBONDED CASE TO A BONDED
C              CASE   ---   USE '1.0D0' FOR THE UNBONDED CASE
C****     CONV IS PAVEMENT'S POSSION'S RATIO
C****     E1 IS PAVEMENT'S YOUNG'S MODULUS
C****     HLENGT IS PAVEMENT'S THICKNESS
C****     LOAD IS PAVEMENT'S LOAD
C****     ALENGT IS LOADED AREA'S RADIUS
C****     CONK IS FOUNDATION'S MODULUS K
C****     X1 IS AXIS X TRANSLATION
C****     Y1 IS AXIS Y TRANSLATION
C
      IMPLICIT REAL*8(A-H,O-Z)
      REAL*8 LOAD,MOMENT
      REAL*4      ACCUR,BJN,BJNN,BJNNN,CONMA,BJN,BJNNNN,RADM,STAR,NAME
      DIMENSION    W(01000),STRNXX(01000),STRNYY(01000),MOMENT(01000),
     *SHEAR(01000),X(01000),R(01000),THETAN(01000),STAR(30),NAME(18)
      DATA  STAR/30*'****'/,PIED00/3.1415962/,ACCUR/1.0E-03/,
     *PRIS/1.0D-16/,N/0/,NN/1/,NNN/2/,NNNN/3/,MSTOP/70/,Y/0./
 9997 READ(5,510,END=9998)    (NAME(I),I=1,18)
  510 FORMAT(18A4)
      DO 7913 MEME=1,1000
      W(MEME) = 0.
      STRNXX(MEME) = 0.
      STRNYY(MEME) = 0.
      MOMENT(MEME) = 0.
      SHEAR(MEME) = 0.
```

```
      X(MEME) = 0.
      R(MEME) = 0.
 7913 THETAN(MEME) = 0.
C
C        GENERATE VALUES OF X
C
      READ(5,506) NOOFTX, CONLP, DELTAX
  506 FORMAT(I10,2D24.16)
      XMAX = -CONLP
      DELTAX = -XMAX/NOOFX
      X(1) = -DELTAX/2.D0
      DO 1 I=2,NOOFX
    1 X(I) = X(I-1) - DELTAX
      NOOF2X = 2*NOOFX
      NOOFXC = NOOFX/2
      DO 2 I=1,NOOFXC
      K = NOOFX + 1 -I
      TEMP9 = X(I)
      X(I) = X(K)
    2 X(K) = TEMP9
C
C        READ IN CONSTANTS
C
      READ(5,501)BONDFT,CONV,E1,HLENGT,LOAD,ALENGT,CONK,X1,Y1
  501 FORMAT(3D24.16)
      D=  E1*HLENGT**3/(12.D0*(1.D0-CONV**2))
      CONLA = DSQRT(DSQRT(D/CONK))
      CONL4 = CONLA*BONDFT
      CONL44 = CONL4**4
      CONLA = DSQRT(DSQRT(CONK/D))
      CONLB = CONLA/BONDFT
      CONPKP = LOAD/(CONK*PIEDOO*ALENGT)
C
C        CALCUALTION LOOP
C
      DO 2000 J=1,NOOFX
```

```
      DWDR=0.
      D2WDR2=0.
      D3WDR3=0.
      WSUBR=0.
      SRNXX=0.
      SRNYY=0.
      VARM=.005D0
      VINK=.01D0
      R(J)  =  DSQRT((X(J) - X1)**2  +  (Y - Y1)**2)
      RADS=R(J)
      THETAN(J)=    DATAN2( (Y-Y1),(X(J) - X1))
      THETA=THETAN(J)
       ESIN=  DSIN(THETA)
       ECOS=  DCOS(THETA)
          IF(DABS(ESIN).LT.PRIS) ESIN=0.
      IF(DABS(ECOS).LT.PRIS) ECOS=0.
      DO 1000 M=1,MSTOP
      TEMP9=   1.D0 + VARM**4*CONL44
       RADM= RADS*VARM
      CONMA= VARM*ALENGT
       CALL BESJ(CONMA,NN,BJNA,ACCUR,IER)
   20 CALL BESJ( RADM,NN,BJNN,ACCUR,IER)
   30 CALL BESJ( RADM,N,BJN,ACCUR,IER)
   40 CALL BESJ( RADM,NNN,BJNNN,ACCUR,IER)
   50 CALL BESJ( RADM,NNNN,BJNNNN,ACCUR,IER)
   60 DWDR=  DWDR  + (BJNA*(-BJNN)*VARM*VINK)/ TEMP9*CONPKP
      D2WDR2= D2WDR2+ (BJNA *((BJNNN-BJN)/2.D0)*VARM**2*VINK)/ TEMP9*
     * CONPKP
      D3WDR3=  D3WDR3 +  (BJNA*((-BJNNNN+3.D0*BJNN)/4.D0 ))*VARM**3*VINK
     */ TEMP9*CONPKP
      WSUBR=WSUBR   + (BJNA*BJN*VINK)/TEMP9
      SRNYY=  SRNYY  - CONPKP*(VARM*VINK*BJNA*( VARM*ESIN**2*((BJNNN -
     *BJN)/2.D0)  +  ECOS**2*(-BJNN)/RADS)/TEMP9)
      SRNXX=  SRNXX  - CONPKP*(VARM*VINK*BJNA*( VARM*ECOS**2*((BJNNN -
     *BJN)/2.D0)  +  ESIN**2*(-BJNN)/RADS)/TEMP9)
      VINK=.C1D0
```

```
      IF(M.GE.10) VINK=.1D0
      IF(M.EQ.10) VARM=.05D0
 1000 VARM= VARM+VINK
      W(J) =WSUBR*CONPKP
      STRNXX(J)=    SRNXX*HLENGT/2.D0
      STRNYY(J)=    SRNYY*HLENGT/2.D0
      D2WDX2 = D2WDR2*ECOS**2  + DWDR*ESIN**2/RADS
      D2WDY2 = D2WDR2*ESIN**2  + DWDR*ECOS**2/RADS
      D3WDY3  =  D3WDR3*ESIN**3  +  3.D0*D2WDR2*ESIN*ECOS**2/RADS
     *      - 3.D0*DWDR*ESIN*ECOS**2/RADS**2
      D3WDXY  =  D3WDR3*ESIN*ECOS**2  + D2WDR2*ESIN*(1.D0-3.D0*ECOS**2)
     */RADS    -DWDR*ESIN*(1.D0-3.D0*ECOS**2)/RADS**2
      MCMENT(J)=    -   D*( D2WDY2  +CONV*D2WDX2)
 2000 SHEAR(J)   =  -   D*(D3WDY3  + (2.D0-CONV)*D3WDXY)
C
C        WRITE OUT DATA
C
      WRITE(6,511) (STAR(I),I=1,30)
  511 FORMAT(1H1/1H1 //  30A4)
      WRITE(6,800)    (NAME(I),I=1,18)
      WRITE(6,801)    E1,CONV,HLENGT,CONLP,CCNK,BONDFT,CONLB,LOAD,ALENGT
  800 FORMAT(   //16X,' M O M E N T ,  S H E A R ,  S T R A I N , A N D
     * D I S P L A C E M E N T  A N A L Y S I S'  //  20X,'CASE :',18A4)
  801 FORMAT(  //56X,'PARAMETERS'  //25X,'PAVEMENT :'  //30X,'YOUNG MODU
     *LUS',F10.1,20X,'POISSON|S RATIO',F10.4 / 30X,'THICKNESS',4X,F10.1,
     *20X,'PAVEMENT LENGTH',F10.2 // 25X,'FOUNDATION :'// 30X,'MODULUS K
     *',4X,F10.1,20X,'PCISSON|S RATIO    0.5000' / 30X,'THICKNESS',6X,'S
     *EMI-INFINITE',15X,'BONDING FACTER',1X,F10.5   / 30X,'CONSTANT LAMB
     *DA',F8.5   //  25X,'OTHERS :'//30X,'LOAD',09X,F10.1,20X,'LOAD RADI
     *US' ,4X,F10.2  )
      WRITE(6,830) X1,Y1,(I,X(I),Y,I=1,NOOFX)
  830 FORMAT(////20X,'AXIS X TRANSLATION =',F10.4,10X,'AXIS Y TRANSLATIO
     *N',F10.4//36X,'I',17X,'VALUES OF X',13X,'VALUES OF Y'//(35X,I3,2D3
     *0.10))
      WRITE(6,5)            (JI,R(JI),THETAN(JI),MOMENT(JI),SHEAR(JI),
     *STRNXX(JI),STRNYY(JI),W(JI),JI=1,NOOFX)
```

```
      WRITE(6,16)     (STAR(I),I=1,30)
   16 FORMAT(  /// 30A4)
      GO TO 9997
    5 FORMAT(  1H1  // 2X,'I',08X,'RADIUS',11X,'THETA',08X,'MOMENT(X,0)'
     *,06X,'SHEAR(X,0)',06X,'STRAIN XX(X,0)',03X,'STRAIN YY(X,0)',06X,
     *'W(X,0)'//   (1X,I3,2D16.6,5D17.7))
 9998 STOP
      END
```

```
      SUBROUTINE BESJ(X,N,BJ,D,IER)
      BJ=.0                                                     BESJ 440
   31 IF(X-15.)32,32,34                                         BESJ 510
   32 NTEST=20.+10.*X-X** 2/3                                   BESJ 520
      GO TO 36                                                  BESJ 530
   34 NTEST=90.+X/2.                                            BESJ 540
   36 IF(N-NTEST)40,38,38                                       BESJ 550
   38 IER=4                                                     BESJ 560
      RETURN                                                    BESJ 570
   40 IER=0                                                     BESJ 580
      N1=N+1                                                    BESJ 590
      BPREV=.0                                                  BESJ 600
      IF(X-5.)50,60,60                                          BESJ 640
   50 MA=X+6.                                                   BESJ 650
      GO TO 70                                                  BESJ 660
   60 MA=1.4*X+60./X                                            BESJ 670
   70 MB=N+IFIX(X)/4+2                                          BESJ 680
      MZERO=MAX0(MA,MB)                                         BESJ 690
      MMAX=NTEST                                                BESJ 730
  100 DO 190 M=MZERO,MMAX,3                                     BESJ 740
      FM1=1.0E-28                                               BESJ 780
      FM=.0                                                     BESJ 790
      ALPHA=.0                                                  BESJ 800
      IF(M-(M/2)*2)120,110,120                                  BESJ 810
  110 JT=-1                                                     BESJ 820
      GO TO 130                                                 BESJ 830
  120 JT=1                                                      BESJ 840
  130 M2=M-2                                                    BESJ 850
      DO 160 K=1,M2                                             BESJ 860
      MK=M-K                                                    BESJ 870
      BMK=2.*FLOAT(MK)*FM1/X-FM                                 BESJ 880
      FM=FM1                                                    BESJ 890
      FM1=BMK                                                   BESJ 900
      IF(MK-N-1)150,140,150                                     BESJ 910
  140 BJ=BMK                                                    BESJ 920
  150 JT=-JT                                                    BESJ 930
```

```
      S=1+JT                                                            BESJ 940
  160 ALPHA=ALPHA+BMK*S                                                 BESJ 950
      BMK=2.*FM1/X-FM                                                   BESJ 960
      IF(N)180,170,180                                                  BESJ 970
  170 BJ=BMK                                                            BESJ 980
  180 ALPHA=ALPHA+BMK                                                   BESJ 990
      BJ=BJ/ALPHA                                                       BESJ1000
      IF(ABS(BJ-BPREV)-ABS(D*BJ))200,200,190                            BESJ1010
  190 BPREV=BJ                                                          BESJ1020
      IER=3                                                             BESJ1030
  200 RETURN                                                            BESJ1040
      END
```

```
      TEST CASE FOR PROGRAM FUNCTION
      120 60.0D0                    0.5D0
1.0D0                   0.4D0                   200000.0D0
6.5D0                   100.0D0                 6.6D0
200.0D0                 0.0D0                   0.0D0
```

Listing of Program PUNCH

```
C****
C****     THIS PROGRAM CALCULATES THE MOMENT AND SHEAR FUNCTION
C****          INPUTS FOR THE MAIN PROGRAM. IT IS IMPORTANT TO NOTE
C****          THAT BECAUSE COMPUTATIONS ARE SLOW, A FEATURE HAS
C****          BEEN ADDED SO THAT CALCULATIONS CAN BEGIN AND END
C****          ANYWHERE IN THE DOMAIN OF X.
C****
C
C****     ARRAY NAME CONTAINS TEST DATA DESCRIPTION
C****     BONDFT IS FACTER USED TO CONVERT THE UNBONDED CASE TO A BONDED
C              CASE   ---   USE '1.0D0' FOR THE UNBONDED CASE
C****     CONV IS PAVEMENT'S POSSION'S RATIO
C****     E1 IS PAVEMENT'S YOUNG'S MODULUS
C****     HLENGT IS PAVEMENT'S THICKNESS
C****     LOAD IS PAVEMENT'S LCAD
C****     ALENGT IS LOADED AREA'S RADIUS
C****     CONK IS FOUNDATION'S MODULUS K
C****     Y1 IS AXIS Y TRANSLATICN
C****     NOOFX IS TOTAL NUMBER 'X' VALUES
C****     CONLP IS THE FOURIER VARIABLE "P" USED IN MAINSEFK
C****     CLCHEK IS LOGIAL CONSTANT DETERMINING WHETHER CALCULATIONS
C              AND PUNCHING WILL BEGIN AND END AT X'S LIMITS ----
C              '.TRUE.' INDICATES CALCULATIONS WILL BEGIN AND/OR END
C              AT OTHER THAN 'X' MAX AND 'X' MIN
C****     SMSTAT IS BEGINNING X VALUE
C****     SMEND IS ENDING X VALUE
C
      IMPLICIT REAL*8(A-H,O-Z)
      REAL*8 LOAD,MOMENT
      LOGICAL CLCHEK
      REAL*4     ACCUR,BJN,BJNN,BJNNN,CONMA,BJN,BJNNNN,RADM,STAR,NAME
     *,RCOFX1
      DIMENSICN MOMENT(1000),SHEAR(1000),X(1000),R(1000),THETAN(1000)
     *,STAR(30),NAME(18)
      DATA              STAR/30*'****'/,PIEDOO/3.1415962/,ACCUR/1.E-3/,
     *PRIS/1.D-16/,N/0/,NN/1/,NNN/2/,NNNN/3/,MSTOP/70/,Y/0./
```

```
 9997 READ(5,510,END=9998)     (NAME(I),I=1,18)
  510 FORMAT(18A4)
C
C        READ IN CONSTANTS
C
      READ(5,501)BONDFT,CONV,E1,HLENGT,LOAD,ALENGT,CONK,Y1
  501 FORMAT(3D24.16)
      D=  E1*HLENGT**3/(12.D0*(1.D0-CONV**2))
      CONLA = DSQRT(DSQRT(D/CONK))
      CONL4 = CONLA*BONDFT
      CONL44 = CONL4**4
      CONLA = DSQRT(DSQRT(CONK/D))
      CONLB = CONLA/BONDFT
      CONPKP=  LOAD/(CONK  *PIECOO*ALENGT)
C
C        GENERATE VALUES OF X
C
      READ(5,506) NOOFX, CONLP, DELTAX
  506 FORMAT(I10,2D24.16)
      XMIN = C.
      XMAX = -CONLP
      DELTAX = -(XMAX-XMIN)/NOOFX
      NOOF2X = 2*NOOFX
      NOOFXC = NOOFX/2
      X(1) = XMIN - DELTAX/2.D0
      DO 1 I=2,NOOFX
    1 X(I) = X(I-1) - DELTAX
      DO 2 I=1,NOOFXC
      K = NOOFX + 1 -I
      TEMP9 = X(I)
      X(I) = X(K)
    2 X(K) = TEMP9
      DO 190 J=1,NOOFX
      R(J)  =  DSQRT( X(J)**2     + (Y   -Y1)**2)
  190 THETAN(J)=    DATAN2((Y   -Y1), X(J))
C
```

```
C         CALCULATIONS
C
C
C         READ IN VALUE OF X WHERE MOMENT AND SHEAR FUNCTIONS BEGIN
C
      READ(5,280)    CLCHEK,SMSTAT ,SMEND
  280 FORMAT(L10,2D24.16)
      IF(CLCHEK) GO TO 250
      JBEG = 1
      JEND = NOOFX
      GO TO 260
  250 ROOFX1 = SMSTAT/DELTAX
      JBEG = NOOFX + IFIX(ROOFX1)
      JBEH = JBEG - 1
      DO 3000 I=1,JBEH
      MOMENT(I) = 0.
 3000 SHEAR(I) = 0.
      ROOFX1 = SMEND/DELTAX
      JEND = NOOFX + IFIX(ROOFX1)
      JENH = JEND + 1
      IF(JENH.GT.NOOFX) GO TO 260
      DO 3100 I=JENH,NOOFX
      MOMENT(I) = 0.
 3100 SHEAR(I) = 0.
C
C         CALCULATION LOOP
C
  260 DO 2000 J=JBEG,JEND
      DWDR=0.
      D2WDR2=0.
      D3WDR3=0.
      VARM=.005D0
      VINK=.01D0
      RADS=R(J)
      THETA=THETAN(J)
       ESIN=  DSIN(THETA)
```

```
      ECOS=  DCOS(THETA)
         IF(DABS(ESIN).LT.PRIS) ESIN=0.
      IF(DABS(ECOS).LT.PRIS) ECOS=0.
      DO 1000 M=1,MSTOP
      TEMP9=   1.D0 + VARM**4*CONL44
       RADM= RADS*VARM
      CONMA= VARM*ALENGT
       CALL BESJ(CONMA,NN,BJNA,ACCUR,IER)
   20 CALL BESJ( RADM,NN,BJNN,ACCUR,IER)
   30 CALL BESJ( RADM,N,BJN,ACCUR,IER)
   40 CALL BESJ( RADM,NNN,BJNNN,ACCUR,IER)
   50 CALL BESJ(RADM,NNNN,BJNNNN,ACCUR,IER)
   60 DWDR=  DWDR  + (BJNA*(-BJNN)*VARM*VINK)/ TEMP9
      D2WDR2= D2WDR2+ (BJNA *((BJNNN-BJN)/2.D0)*VARM**2*VINK)/ TEMP9
      D3WDR3=  D3WDR3 +  (BJNA*((-BJNNNN+3.D0*BJNN)/4.D0 ))*VARM**3*VINK
     */ TEMP9
      VINK=.01D0
      IF(M.GE.10) VINK=.1D0
      IF(M.EQ.10) VARM=.05D0
 1000 VARM= VARM+VINK
      D2WDX2 =(D2WDR2*ECOS**2  + DWDR*ESIN**2/RADS)*CONPKP
      D2WDY2 =(D2WDR2*ESIN**2  + DWDR*ECOS**2/RADS)*CONPKP
      D3WDY3  = (D3WDR3*ESIN**3  +  3.D0*D2WDR2*ESIN*ECOS**2/RADS
     *      - 3.D0*DWDR*ESIN*ECOS**2/RADS**2 )*CONPKP
      D3WDXY  = (D3WDR3*ESIN*ECOS**2  + D2WDR2*ESIN*(1.D0-3.D0*ECOS**2)
     */RADS    -DWDR*ESIN*(1.D0-3.D0*ECOS**2)/RADS**2 )*CONPKP
      SHEAR(J)   =  -   D*(D3WDY3  + (2.D0-CONV)*D3WDXY)
 2000 MOMENT(J)=    -   D*( D2WDY2  +CONV*D2wDX2)
C
C        WRITE OUT DATA
C
      WRITE(6,511) (STAR(I),I=1,30)
  511 FORMAT(1H1/1H1 //  30A4)
      WRITE(6,800)    (NAME(I),I=1,18)
      WRITE(6,801)    E1,CONV,HLENGT,CONLP,CONK,BONDFT,CONLB,LOAD,ALENGT
  800 FORMAT(   //15X,' M O M E N T  A N D  S H E A R  F U N C T I O N
```

```
     *A N A L Y S I S   F O R   P U N C H E D   C A R D S' //  20X,'CASE :'
     *,18A4)
  801 FORMAT(  //56X,'PARAMETERS'  //25X,'PAVEMENT :'  //30X,'YOUNG MODU
     *LUS',F10.1,20X,'POISSON|S RATIO',F10.4 / 30X,'THICKNESS',4X,F10.1,
     *20X,'PAVEMENT LENGTH',F10.2 // 25X,'FOUNDATION :'// 30X,'MODULUS K
     *',4X,F10.1,20X,'POISSON|S RATIO    0.5000' / 30X,'THICKNESS',6X,'S
     *EMI-INFINITE',15X,'BONDING FACTER',1X,F10.5   / 30X,'CONSTANT LAMB
     *DA',F8.5      // 25X,'OTHERS :'// 30X,'LOAD',09X,F10.1,20X,'LOAD R
     *ADIUS',4X,F10.2  )
      WRITE(6,830)    Y1,(I,X(I),Y,R(I),THETAN(I),MOMENT(I),SHEAR(I),
     *I=1,NOOFX)
  830 FORMAT(     //// 46X,'AXIS Y TRANSLATION =',F10.4   ////
     *3X,'I',07X,'VALUES OF X',08X,'VALUES OF Y',11X,'RADIUS',14X,'THETA
     *',11X,'MOMENT(X,0)',08X,'SHEAR(X,0)'  //  (2X,I3,6D19.8))
      WRITE(6,16)    (STAR(I),I=1,30)
   16 FORMAT(  /// 30A4)
      IF(JEND.NE.NOOFX)  GO TO 600
      JBEG = 1
  600 WRITE(7,290)   (X(I),MOMENT(I),SHEAR(I),I,I=JBEG,JEND)
      GO TO 9997
  290 FORMAT(3D24.16,I8)
 9998 STOP
      END
```

```
      SUBROUTINE BESJ(X,N,BJ,D,IER)                                     BESJ 420
      BJ=.0                                                             BESJ 440
   31 IF(X-15.)32,32,34                                                 BESJ 510
   32 NTEST=20.+10.*X-X** 2/3                                           BESJ 520
      GO TO 36                                                          BESJ 530
   34 NTEST=90.+X/2.                                                    BESJ 540
   36 IF(N-NTEST)40,38,38                                               BESJ 550
   38 IER=4                                                             BESJ 560
      RETURN                                                            BESJ 570
   40 IER=0                                                             BESJ 580
      N1=N+1                                                            BESJ 590
      BPREV=.0                                                          BESJ 600
      IF(X-5.)50,60,60                                                  BESJ 640
   50 MA=X+6.                                                           BESJ 650
      GO TO 70                                                          BESJ 660
   60 MA=1.4*X+60./X                                                    BESJ 670
   70 MB=N+IFIX(X)/4+2                                                  BESJ 680
      MZERO=MAX0(MA,MB)                                                 BESJ 690
      MMAX=NTEST                                                        BESJ 730
  100 DO 190 M=MZERO,MMAX,3                                             BESJ 740
      FM1=1.0E-28                                                       BESJ 780
      FM=.0                                                             BESJ 790
      ALPHA=.0                                                          BESJ 800
      IF(M-(M/2)*2)120,110,120                                          BESJ 810
  110 JT=-1                                                             BESJ 820
      GO TO 130                                                         BESJ 830
  120 JT=1                                                              BESJ 840
  130 M2=M-2                                                            BESJ 850
      DO 160 K=1,M2                                                     BESJ 860
      MK=M-K                                                            BESJ 870
      BMK=2.*FLOAT(MK)*FM1/X-FM                                         BESJ 880
      FM=FM1                                                            BESJ 890
      FM1=BMK                                                           BESJ 900
      IF(MK-N-1)150,140,150                                             BESJ 910
  140 BJ=BMK                                                            BESJ 920
  150 JT=-JT                                                            BESJ 930
```

```
      S=1+JT                                                            BESJ 940
  160 ALPHA=ALPHA+BMK*S                                                 BESJ 950
      BMK=2.*FM1/X-FM                                                   BESJ 960
      IF(N)180,170,180                                                  BESJ 970
  170 BJ=BMK                                                            BESJ 980
  180 ALPHA=ALPHA+BMK                                                   BESJ 990
      BJ=BJ/ALPHA                                                       BESJ1000
      IF(ABS(BJ-BPREV)-ABS(D*BJ))200,200,190                            BESJ1010
  190 BPREV=BJ                                                          BESJ1020
      IER=3                                                             BESJ1030
  200 RETURN                                                            BESJ1040
      END                                                               BESJ1050
```

```
      TEST CASE FOR MOVING LCAD PROGRAM -- PUNCHED MOMENT
1.0D0                    0.4DC                    200000.0D0
6.5D0                    100.0D0                  6.6D0
200.0D0                  0.0D0
      120 6C.CD0                    0.5D0
  .FALSE.
```

Listing of MAIN Moving Load Program

```
C****
C****     THIS PROGRAM CALCULATES THE 'K1' & 'K2' STRESS INTENSITY
C****          FACTORS FOR MOVING LOADS WHICH ARE DEFINED BY :
C****          K1 = (PIEDOO)**(+.5)*(3+CONV)/(1+CONV)*(1-I)*CONE*CONH*
C****                       LAMBDA**(+1.5)*PZERO
C****          K2 =-(PIEDOO)**(+.5)*(3+CONV)/(1+CONV)*(1-I)*CONE*CONH*
C****                       LAMBDA**(+1.5)*QZERO
C****          WHERE 'I' IS DEFINED AS SQUARE ROOT OF MINUS ONE AND
C****          PZERO  & QZERO ARE CALCULATED ACCORDING TO EQUATIONS
C****          3 & 4 IN THE DOCUMENTATION. IT IS IMPORTANT TO THAT
C****          ANOTHER PROGRAM, GENERATING MOMENTS & SHEARS ON PUNCHED
C****          CARDS, MUST RUN FIRST. THIS OUTPUT SERVES AS INPUT FOR
C****          THE MAINSEFK PROGRAM.
C****
C
C****     ARRAY NAME CONTAINS TEST DATA DESCRIPTION
C****     NOOFX IS TOTAL NUMBER 'X' VALUES
C****     PRISCK IS LOGICAL CONSTANT DETERMINING WHETHER A CHECK IS
C              PERFORMED ON THE CALCULATED FOURIER SOLUTIONS   ---
C              '.TRUE.' INDICATES A CHECK WILL BE PERFORMED
C****     NOOFTX IS THE NUMBER OF POINTS WHERE A CHECK IS DESIRED ON
C              THE FOURIER FIT
C****     XSTART IS THE BEGINNING POSITION OF THE CHECK ON THE FIT
C****     DELXT IS THE DESIRED INCREMENT BETWEEN POSITIONS OF THE CHECK
C              ON THE FIT
C****     ARRAYS X,PCON,QCON ARE CALCULATED X,MOMENT,SHEAR FUNCTIONS
C              OBTAINED FROM PROGRAM 'PUNCH'
C****     BONDFT IS FACTER USED TO CONVERT THE UNBONDED CASE TO A BONDED
C              CASE   ---   USE '1.0D0' FOR THE UNBONDED CASE
C****     CONV IS PAVEMENT'S POSSION'S RATIO
C****     CONE IS PAVEMENT'S YOUNG'S MODULUS
C****     CONH IS PAVEMENT'S THICKNESS
C****     LOAD IS PAVEMENT'S LOAD
C****     CONA IS LOADED AREA'S RADIUS
C****     CONK IS FOUNDATION'S MODULUS K
C****     X1BEG IS BEGINNING VALUE FOR AXIS 'X' TRANSLATION
```

```
C****    X1END IS ENDING VALUE FOR AXIS 'X' TRANSLATION
C****    X1INT IS INCREMENTAL VALUE FOR AXIS 'X' TRANSLATION
C****    K1 IS LOGIAL CONSTANT DETERMINING WHETHER STRESS INTENSITY
C             FACTOR K1 WILL BE CALCULATED   ---    '.TRUE.' INDICATES
C             CALCULATIONS WIL BE MADE
C****    K2 IS LOGIAL CONSTANT DETERMINING WHETHER STRESS INTENSITY
C             FACTOR K2 WILL BE CALCULATED   ---    '.TRUE.' INDICATES
C             CALCULATIONS WIL BE MADE
C****    ZEROM ARE NUMBER OF BEGINNING 'MOMENTS' THAT WILL BE ZEROED
C****    ZEROS ARE NUMBER OF BEGINNING 'SHEARS' THAT WILL BE ZEROED
C****    Y1 IS AXIS Y TRANSLATION
C
      IMPLICIT REAL*8(A-H,O-Z)
      INTEGER    ZEROM,ZEROS,PAGECK,SHRBEG
      LOGICAL K1,K2,PRISCK,MNFLAG,MPFLAG,SNFLAG,SPFLAG,MFLAG,SFLAG,X1CHK
      REAL*4  NAME,STAR,ROOFX1,OUTPU1,OUTPU2,NODATA,NEG,POS
      REAL*8 LOAD
      DIMENSION  PSOL(362),QSOL(362),PCON(1500),QCON(1500),X(1500)
     *,NAME(18),STAR(30),OUTPU1(10),OUTPU2(10),NODATA(10),NEG(10),POS(10
     *),XY(200), CPON(200)
      COMMON  CONV,LOAD,CONA,CONH,CONE,COND,CONVO,DELTAX
     *               ,BONDFT,XMIN,XMAX,CONK,XSTART,DELTXT,X1,Y1
     *,NOOFX,NOOF2X,NOOFTX,NOCFN,NOOFMV,NOOFSN,NOOFSO,NOOFM,NOOFS
      DATA   STAR/30*'****'/,PIEDOO/3.1415962D0/,PRIS/1.D-16/,Y/0.0/
     *,NODATA(1)/'    '/,NODATA(2)/'    '/,NODATA(3)/'NO C'/,NODATA(4)/
     *'ALCU'/,NODATA(5)/'LATI'/,NODATA(6)/'ONS '/,NODATA(7)/'ATTE'/,
     *NODATA(8)/'MPED'/,NODATA(9)/'    '/,NODATA(10)/'    '/,
     *NEG(1)/'X AX'/,NEG(2)/ 'IS T'/,NEG(3)/'RANS'/,NEG(4)/'LATI'/,NEG(5
     *)/'ONAL'/,NEG(6)/' VAL'/,NEG(7)/'UE T'/,NEG(8)/'OO N'/,NEG(9)/'EGA
     *T'/,POS(10)/'IVE '/,
     *POS(1)/'X AX'/,POS(2)/ 'IS T'/,POS(3)/'RANS'/,POS(4)/'LATI'/,POS(5
     *)/'ONAL'/,POS(6)/' VAL'/,POS(7)/'UE T'/,POS(8)/'OO P'/,POS(9)/'OSI
     *T'/,NEG(10)/'IVE '/
 1000 READ(5,510,END=9999)   (NAME(I),I=1,18)
  510 FORMAT(18A4)
C
```

```
C         READ MOMENT AND/OR SHEAR FUNCTION
C
      READ(5,506)NOOFX, CONLP, DELTAX
  506 FORMAT(I10,2D24.16)
      READ(5,507)   PRISCK, NOOFTX, XSTART, DELTXT
  507 FORMAT(L10,I10, 2D24.16)
  210 READ(5,501)       (X(I),PCON(I),QCON(I),I=1,NOOFX)
      NOOF2X=  2*NOOFX
C
C         READ IN CONSTANTS
C
  220 READ(5,501)  BONDFT,CONV,CONE,CONH,LOAD,CONA,CONK
      CONVO=1.DO-CONV
  501 FORMAT(3D24.16)
      NOOFN = 90
      NOOFMV=  4*NOOFN + 2
      NOOFSN=  2*NOOFN
      NOOFSO=  NOOFMV- NOOFSN
      COND=   CONE*CONH**3/(12.DO*(1.DO-CONV**2))
      CONLA = DSQRT(DSQRT(CONK/COND))
      CONLB=CONLA/BONDFT
C
C       READ IN PARAMETERS FOR X1 & Y1
C
      READ(5,501)  X1BEG,X1END,X1INT
      READ(5,505)    K1,K2
  505 FORMAT(2L10)
      X1CHK = .FALSE.
      IF(X1END.LT.X1BEG)   X1INT=  -X1INT
      IF(X1END.EQ.X1BEG)   X1CHK = .TRUE.
      ROOFX1=  X1BEG/DELTAX
      NOOFX1 = IFIX(ROOFX1)
      ROOFX1=  X1INT/DELTAX
      NOOFXI = IFIX(ROOFX1)
      READ(5,503)   ZERCM,ZERCS,Y1
  503 FORMAT(2I10,D24.16)
```

```
      WRITE(6,405) CONLP , PRISCK
  405 FORMAT('1',10X,'CONLP  = ',F24.16,10X,'PRISCK IS',L10)
      WRITE(6,406) ZEROM, ZEROS, Y1
  406 FORMAT( // 15X, 'ZEROM = ',I5,15X,'ZEROS = ',I5,9X,'Y1 = ',F10.4)
      WRITE(6,407) X1BEG, X1END, X1INT
  407 FORMAT( //25X,'X1BEG = ',F10.4,10X,'X1END = ',F10.4,10X,'X1INT = '
     *,F10.4)
      MOMBEG = ZEROM + 1
      SHRBEG = ZEROS + 1
      NOOFS = NOOFX - ZEROS
      NOOFM = NOOFX - ZEROM
      IF(ZEROM.LT.0 .OR. ZEROS.LT.0)  GO TO 3200
      IF(ZEROS.EQ.0)  GO TO 241
      DO 80 I=1,ZEROS
   80 QCON(I)=0.
  241 IF(ZEROM.EQ.0)  GO TO 808
      DO 90 I=1,ZEROM
   90 PCON(I)=0.
      DO 830 I6=1,NOOFX
      K=  NOOF2X + 1 - I6
      X(K)=  -X(I6)
      QCON(K) = QCON(I6)
  830 PCON(K) = PCON(I6)
      WRITE(6,9)      (JI,X(JI),Y,PCON(JI),QCON(JI),JI=1,NOOF2X)
    9 FORMAT(                //  25X,'I',07X,'VALUES OF X',09X,'VALUES OF
     *Y',09X,'MOMENT(X,0)',10X,'SHEAR(X,0)' // (24X,I3,4D20.10))
C
C        WRITE OUT DATA
C
  808 IF(PRISCK)  GO TO 809
      GO TO 3200
  809 WRITE(1,810)   (STAR(I),I=1,30)
 3200 WRITE(6,810)   (STAR(I),I=1,30)
  810 FORMAT(1H1/1H1 //  30A4)
      WRITE(6,800)    (NAME(I),I=1,18)
  800 FORMAT(   //30X,' S T R E S S  I N T E N S I T Y  F A C T O R  A N
```

```
     * A L Y S I S'// 20X,'CASE :',18A4)
      WRITE(6,801)  CONE,CONV,CONH,CONLP,CONK,BONDFT,CONLB,LOAD,CONA
  801 FORMAT(  //56X,'PARAMETERS'  //25X,'PAVEMENT :'  //30X,'YOUNG MODU
     *LUS',F10.1,20X,'POISSON|S RATIO',F10.4 / 30X,'THICKNESS',4X,F10.1,
     *20X,'PAVEMENT LENGTH',F10.2 // 25X,'FOUNDATION :'// 30X,'MODULUS K
     *',4X,F10.1,20X,'POISSON|S RATIO    0.5000' / 30X,'THICKNESS',6X,'S
     *EMI-INFINITE',15X,'BONDING FACTER',1X,F10.5   / 30X,'CONSTANT LAMB
     *DA',F8.5      // 25X,'OTHERS :'// 30X,'LOAD',09X,F10.1,20X,'LOAD R
     *ADIUS',4X,F10.2  )
      WRITE(6,803)
  803 FORMAT(   ///15X,'X1',15X,'Y1',16X,'K1R',18X,'K1I',18X,'K2R',18X,
     *'K2I'  )
      IF(ZEROM.LT.0 .OR. ZEROS.LT.0)  WRITE(6,3201)
 3201 FORMAT(///01X,  '* * CALCULATIONS FOR THIS DATA IMPOSSIBLE AS IMPR
     *OPER NUMERICS ARE SUPPIED FOR MOMENT AND SHEAR "BEGIN" PARAMETERS
     ** *'   //   35X,' CHECK FIRST TWO NUMBERS ON LAST CARD FOR THIS DA
     *TA')
      IF(ZEROM.LT.0 .OR. ZEROS.LT.0)  GO TO 1002
      PAGECK = 0
C
C        OUTPUT CALCULATICN LOOP
C
  100 X1=  NOOFX1*DELTAX
      CALL SOLVE(PSOL,QSOL,PCON,QCON,X,CONLP,K1,K2,PRISCK,NOOFX1,PRIS,
     *PIEDOO,MCMBEG,SHRBEG,MFLAG,SFLAG,MNFLAG,MPFLAG,SNFLAG,SPFLAG)
      IF(MFLAG .AND. SFLAG)  GO TO 304
  401 CALL STREFT(SEFK1R,SEFK1I,SEFK2R,SEFK2I,        PSOL,QSOL,CONLP,
     * K1,K2,PIEDOO,PRIS,CONLB)
  304 IF(K1)   GO TO 300
      DO 301 I=1,10
  301 OUTPU1(I) = NODATA(I)
      GO TO 306
  300 IF(.NOT.(MNFLAG)) GO TC 302
      DO 303 I=1,10
  303 OUTPU1(I) =NEG(I)
      GO TO 306
```

```
302 IF(.NOT.(MPFLAG)) GO TO 306
    DO 305 I=1,10
305 OUTPU1(I) = POS(I)
306 IF(K2)  GO TO 307
    DO 308 I=1,10
308 OUTPU2(I) = NODATA(I)
    GO TO 309
307 IF(.NOT.(SNFLAG)) GO TO 310
    DO 311 I=1,10
311 OUTPU2(I) =NEG(I)
    GO TO 309
310 IF(.NOT. (SPFLAG)) GO TO 309
    DO 313 I=1,10
313 OUTPU2(I) = POS(I)
309 IF((.NOT.(MFLAG)).AND.(.NOT.(SFLAG)))  GO TO 314
    GO TO 315
314 WRITE(6,802)   X1,Y1,SEFK1R,SEFK1I,SEFK2R,SEFK2I
802 FORMAT(/03X,F14.4,5X,F14.4,5X,4D20.10)
    GO TO 402
315 IF(MFLAG.AND.(.NOT.SFLAG))  GO TO 316
    GO TO 317
316 WRITE(6,807)  X1,Y1,(OUTPU1(I),I=1,10),SEFK2R,SEFK2I
807 FORMAT(/03X,F14.4,5X,F14.4,5X,10A4,2D20.10)
    GO TO 402
317 IF(SFLAG.AND. (.NOT.MFLAG))   GO TO 318
    GO TO 319
318 WRITE(6,806)  X1,Y1,SEFK1R,SEFK1I,(OUTPU2(I),I=1,10)
806 FORMAT(/03X,F14.4,5X,F14.4,5X,2D20.10,10A4)
    GO TO 402
319 WRITE(6,820)   X1,Y1,(OUTPU1(I),I=1,10),(OUTPU2(I),I=1,10)
820 FORMAT(/03X,F14.4,5X,F14.4,5X,10A4,10A4)
402 IF(X1CHK)   GO TO 1001
    IF(X1INT.LT.0.)  GO TO 200
    IF(X1.GE.X1END)  GO TO 1001
    GO TO 201
200 IF(X1.LE.X1END)  GO TO 1001
```

```
 201 NOOFX1 = NOOFX1 + NOOFXI
     PAGECK = PAGECK + 1
     IF(PAGECK.EQ.15)  GO TC 3200
     GO TO 100
1001 WRITE(6,811)   (STAR(I),I=1,30)
 811 FORMAT(///   30A4)
     IF(PRISCK)  GO TO 826
     GO TO 1002
 826 WRITE(1,811)   (STAR(I),I=1,30)
1002 GO TO 1000
9999 STOP
     END
```

```
      SUBROUTINE SOLVE(PSOL,QSOL,PCON,QCON,X,CONLP,K1,K2,PRISCK,NOOFX1,
     *PRIS,PIEDOO,MOMBEG,SHRBEG,MFLAG,SFLAG,MNFLAG,MPFLAG,SNFLAG,SPFLAG)
C
C        SUBROUTINE SOLVE CALCULATES FOURIER CONSTANTS MSUBN AND VSUBN
C
      IMPLICIT REAL*8(A-H,O-Z)
      LOGICAL K1,K2,PRISCK,MNFLAG,MPFLAG,SNFLAG,SPFLAG,MFLAG,SFLAG
      REAL*4 MSUBNR, MSUBNI
      REAL*8  LOAD
      INTEGER SHRBEG
      DIMENSION  PSOL(1),QSOL(1),PCON(1),QCON(1),X(1)
      COMMON  CONV,LOAD,CONA,CONH,CONE,COND,CONVO,DELTAX
     *              ,BONDFT,XMIN,XMAX,CONK,XSTART,DELTXT,X1,Y1
     *,NOOFX,NOOF2X,NOOFTX,NOOFN,NOOFMV,NOOFSN,NOOFSO,NOOFM,NOOFS
      MFLAG = .FALSE.
      SFLAG = .FALSE.
      MNFLAG = .FALSE.
      MPFLAG = .FALSE.
      SNFLAG = .FALSE.
      SPFLAG = .FALSE.
      IMOBEG = MOMBEG + NOOFX1
      IMOEND = IMOBEG + 2*NOOFM - 1
      ISRBEG = SHRBEG + NOOFX1
      ISREND = ISRBEG + 2*NOOFS - 1
      IF (IMOBEG .LT.1)  MNFLAG = .TRUE.
      IF(ISRBEG .LT. 1)  SNFLAG = .TRUE.
      IF (IMOEND.GT.NOOF2X) MPFLAG = .TRUE.
      IF(ISREND .GT. NOOF2X)  SPFLAG = .TRUE.
      IF(K1 .AND. ( .NOT. (MNFLAG .OR. MPFLAG)))   GO TO 700
      MFLAG = .TRUE.
      GO TO 701
  700 JBEGN = IMOBEG
      JENDN = IMOEND
  701 IF(K2 .AND. ( .NOT. (SNFLAG .OR. SPFLAG)))   GO TO 702
      SFLAG = .TRUE.
      IF(MFLAG)  GO TO 1000
```

```
      GO TO 703
  702 IF(MFLAG)     GO TO 716
      IF(NOOFS.GE.NOOFM)    JBEGN = ISRBEG
      IF(NOOFS.GE.NOOFM)    JENDN = ISREND
      GO TO 703
  716 JBEGN = ISRBEG
      JENDN = ISREND
  703 DO 150 I=2,NOOFMV,2
      PSOL(I)=0.
      PSOL(I-1)=0.
      QSOL(I)=0.
      QSOL(I-1)=0.
      TSOLE =0.
      TSOLO = 0.
      DO 150 J=JBEGN,JENDN
      JOFFST = J - NOOFX1
  210 ESIN=0.
      ECOS=1.D0
      IF(I.NE.NOOFS0) ECOS= DCOS(-(I-NOOFS0)*PIEDOO*X(J)/(2.D0*CONLP))
      IF(DABS(ECOS).LT.PRIS) ECOS=0.
      IF(MFLAG)    GO TO 160
      PSOL(I-1)=  PSOL(I-1) - PCON(JOFFST)*ECOS*DELTAX/(2.D0*CONLP*COND)
      PSOL (I) = 0.
      TSOLO = TSOLO +PSOL(I-1)
  160 IF(SFLAG)    GO TO 150
      QSOL(I-1)=  QSOL(I-1) - QCON(JOFFST)*ECOS*DELTAX/(2.D0*CONLP*COND)
  150 CONTINUE
C
C        OUTPUT CHECK ON FOURIER FIT
C
      IF(PRISCK)    GO TC 300
      GO TO 1000
  300 IF(X1.EQ.0.) GO TO 301
      GO TO 1000
  301 X111 = XSTART
      WRITE(1,310) X1,Y1
```

```
  310 FORMAT(  1H1  //  20X,'* * * * * SOLVING FOR MOMENT & SHEAR FUNCTI
     *ONS BASED ON CALCULATED FOURIER SOLUTIONS * * * * *'// 31X,'AXIS X
     * TRANSLATION==',F10.4,5X,'AXIS Y TRANSLATION = ',F10.4  ////  20X,
     *'I',17X,'VALUES OF X',16X,'CALCULATED MOMENT',14X,'CALCULATED SHEA
     *R'  //)
      DO 44 I=1,NOOFTX
      CALP = 0.
      CALQ = 0.
      DO 94 J=2,NOOFMV,2
          ESIN=0.
          ECOS=1.D0
      IF(J.NE.NOOFSO) ECOS= DCOS(+(J-NOCFSO)*PIEDOO*X111/(2.D0*CONLP))
      IF(DABS(ECOS).LT.PRIS) ECOS=0.
      ESIN = 0.0
   96 IF(K1)       GO TO 630
      GO TO 640
  630 CALP    = CALP     - COND*(PSOL(J-1)*ECOS )
  640 IF(K2)       GO TO 650
      GO TO 94
  650 CALQ    = CALQ     - COND*(QSOL(J-1)*ECOS )
   94 CONTINUE
                                WRITE(1,812) I, X111,CALP, CALQ
      X111 = X111 + DELTXT
   44 CONTINUE
  812 FORMAT(19X,I3,3(10X,D20.10))
 1000 RETURN
      END
```

```
      SUBROUTINE STREFT(SEFK1R,SEFK1I,SEFK2R,SEFK2I,        PSOL,QSOL,
     *CONLP,K1,K2,PIEDOO,PRIS,CONLB)
C
C        SUBROUTINE STREFT CALCULATES THE PZERO AND QZERO TERMS
C
      IMPLICIT REAL*8(A-H,O-Z)
      REAL*4 RNSTOP
      REAL*8 LOAD
      LOGICAL K1,K2
      DIMENSION    PSOL(1),QSOL(1),
     *          PO1R(100), PO1I(200), PO2R(250), PO2I(250),A(4)
      COMMON  CONV,LOAD,CONA,CONH,CONE,COND,CONVO,DELTAX
     *               ,BONDFT,XMIN,XMAX,CONK,XSTART,DELTXT,X1,Y1
     *,NOOFX,NOOF2X,NOOFTX,NOOFN,NOOFMV,NOOFSN,NOOFSO,NOOFM,NOOFS
      XYZ1 = DSQRT(2.0D0)
      CONPCO=   XYZ1*DSQRT((4.D0-CONVO)*CONVO/XYZ1)/(2.D0*PIEDOO*(4.D0-
     *CONVO)*CONVO*CONLB**2)/2.D0
      CONQCO=   XYZ1*DSQRT((4.D0-CONVO)*CONVO/XYZ1)/(2.D0*PIEDOO*(4.D0-
     *CONVO)*CONVO*CONLB**3)/2.D0
      RNSTOP = CONLP*CONLB/PIEDOO
      NSTOP = IFIX(RNSTOP)
      NOOFSI=  NOOFSN-NSTOP*2
      NISTOP= NSTOP*2 +1
      NOOFS1=  NOOFSO -NSTOP*2 -2
      NLSTOP= NOOFN + NSTOP +1
      NMSTOP = NOOFN - NSTOP
      PORB = 0.0
      POIB = 0.0
      PORA = 0.0
      POIA = 0.0
      QORA = 0.0
      QOIA = 0.0
      QORB = 0.0
      QOIB = 0.0
C
C        LOOP FOR SUMING TERMS IN EQUATIONS 3 & 4 WHICH HAVE 'Z'
```

```
C             DEFINED TO BE NONZERO.
C
      SEFCON=       DSQRT(PIEDOO)* (3.DO+CONV)*CONE*CONH* DSQRT(CONLB)**
     *3/(1.DO+ CONV)
      SEFCON = SEFCON *DSQRT(PIEDOO)
      CST1 = 2.DO*PIEDOO*( 4.DO-CONVO)*CONVO*DSQRT(CONLB**3)*DSQRT(PIEDO
     *O/CONLP)
      CON3 = 1.DO/CST1
      CON3 = CON3/2.DO
      CON4 = CON3*CONLP/PIEDOO
      CONPCO = CONPCO/2.DO
      CONPCB = CONPCO/CONLB
      NSTOP2 = NSTOP + 1
      IM = 2*NOOFN + 2*NSTOP + 2
      DO 68 K = NSTOP2, NOOFN
      IM = IM +2
      AK = K
      PORA = PORA-CON3/DSQRT(AK)*PSOL(IM-1)
      QORA = QORA - CON4/DSQRT(AK**3)*QSOL(IM-1)
   68 CONTINUE
      IM = 2*NOOFN -2*NSTOP + 2
      DO 66 M = NSTOP2, NOOFN
      IM = IM-2
      AM = M
      POIA = POIA-CON3/DSQRT(AM)*PSOL(IM-1)
      QOIA = QOIA - CON4/DSQRT(AM**3)*QSOL(IM-1)
   66 CONTINUE
      NSTOP1 = 2*NSTOP - 1
      IM = 2*NOOFN -2*NSTOP + 2
      DO 69 L = 1, NSTOP1
      IM = IM+2
      PORB = PORB-CONPCO*PSOL(IM-1)
      POIB = POIB-CONPCO*PSOL(IM-1)
      QORB = QORB - CONPCB*QSOL(IM-1)
      QOIB = QORB
   69 CONTINUE
```

```
5000 CONTINUE
     SEFK1R = 1.
     SEFK1I = 1.
     S1RA = SEFCON*PORA+SEFCON*POIA
     S1IA = SEFCON*POIA-SEFCON*PORA
     S1RB = SEFCON*PORB+SEFCON*POIB
     S1IB = SEFCON*POIB-SEFCON*PORB
     PORT = PORA+PORB
     POIT = POIA+POIB
     S1RT = SEFCON*PORT+SEFCON*POIT
     S1IT = SEFCON*POIT-SEFCON*PORT
     S2RA = SEFCON*(QORA - QOIA)
     S2IA = SEFCON*(QORA + QOIA)
     S2RB = SEFCON*(QORB - QOIB)
     S2IB = SEFCON*(QORB + QOIB)
     QORT = QORA + QORB
     QOIT = QOIA + QOIB
     S2RT = SEFCON*(QORT - QOIT)
     S2IT = SEFCON*(QORT + QOIT)
     IF(K1) GO TO 71
     GO TO 72
  71 WRITE(6,67) PORA, POIA, S1RA, S1IA, PORB, POIB, S1RB, S1IB, S1RT,
    2S1IT
  72 IF(K2) GO TO 73
     GO TO 74
  73 WRITE(6,77) QORA, QOIA, S2RA, S2IA, QORB, QOIB, S2RB, S2IB,S2RT,
    2S2IT
  74 CONTINUE
  67 FORMAT( /,10X,'PORA =',E14.6,10X,'POIA =',E14.6,10X,'K1RA =',E14.6
    2,10X,'K1IA =',E14.6,/,10X,'PORB=',E14.6,10X,'POIB =',E14.6,10X,'K1
    3RB =',E14.6,10X,'K1IB =',E14.6,/,30X,'K1RT =',E14.6,15X,'K1IT =',
    4E14.6)
  77 FORMAT( /,10X,'QORA =',E14.6,10X,'QOIA =',E14.6,10X,'K2RA =',E14.6
    2,10X,'K2IA =',E14.6,/,10X,'QORB=',E14.6,10X,'QOIB =',E14.6,10X,'K2
    3RB =',E14.6,10X,'K2IB =',E14.6,/,30X,'K2RT =',E14.6,15X,'K2IT =',
    4E14.6)
```

```
RETURN
END
```

```
   REAL SOIL TEST CASE     E=200,000  H=6.5       16/MAY/73
  .TRUE.          30   -25.0D0                 1.0D0
-0.5975000000000000D+02 -0.4076509754052296D+00  0.0                    1
-0.5925000000000000D+02 -0.2650483611199369D+00  0.0                    2
-0.5875000000000000D+02 -0.1213080731288484D+00  0.0                    3
-0.5825000000000000D+02  0.2145918116692637D-01  0.0                    4
-0.5775000000000000D+02  0.1610817996994242D+00  0.0                    5
-0.5725000000000000D+02  0.2944070127155263D+00  0.0                    6
-0.5675000000000000D+02  0.4178534623755298D+00  0.0                    7
-0.5625000000000000D+02  0.5236798614885330D+00  0.0                    8
-0.5575000000000000D+02  0.6012351460425682D+00  0.0                    9
-0.5525000000000000D+02  0.6581756631036175D+00  0.0                   10
-0.5475000000000000D+02  0.7014549182156922D+00  0.0                   11
-0.5425000000000000D+02  0.7332373883241851D+00  0.0                   12
-0.5375000000000000D+02  0.7557824067178941D+00  0.0                   13
-0.5325000000000000D+02  0.7700794521751296D+00  0.0                   14
-0.5275000000000000D+02  0.7774966776303451D+00  0.0                   15
-0.5225000000000000D+02  0.7786162665682239D+00  0.0                   16
-0.5175000000000000D+02  0.7744260162678614D+00  0.0                   17
-0.5125000000000000D+02  0.7652923429230458D+00  0.0                   18
-0.5075000000000000D+02  0.7520362049983707D+00  0.0                   19
-0.5025000000000000D+02  0.7348908838924502D+00  0.0                   20
-0.4975000000000000D+02  0.7145446654892453D+00  0.0                   21
-0.4925000000000000D+02  0.6911549115212512D+00  0.0                   22
-0.4875000000000000D+02  0.6653311261512743D+00  0.0                   23
-0.4825000000000000D+02  0.6371825280202241D+00  0.0                   24
-0.4775000000000000D+02  0.6072440449940641D+00  0.0                   25
-0.4725000000000000D+02  0.5756043342644487D+00  0.0                   26
-0.4675000000000000D+02  0.5427497901302155D+00  0.0                   27
-0.4625000000000000D+02  0.5087316911350712D+00  0.0                   28
-0.4575000000000000D+02  0.4739896947636000D+00  0.0                   29
-0.4525000000000000D+02  0.4385870373314030D+00  0.0                   30
-0.4475000000000000D+02  0.4029118917213756D+00  0.0                   31
-0.4425000000000000D+02  0.3670133887606224D+00  0.0                   32
-0.4375000000000000D+02  0.3312510537270088D+00  0.0                   33
-0.4325000000000000D+02  0.2956793726846243D+00  0.0                   34
```

-0.4275000000000000D+02	0.2606081923008932D+00	0.0	35
-0.4225000000000000D+02	0.2261104368648819D+00	0.0	36
-0.4175000000000000D+02	0.1924582454302888D+00	0.0	37
-0.4125000000000000D+02	0.1597258633153130D+00	0.0	38
-0.4075000000000000D+02	0.1281524393682495D+00	0.0	39
-0.4025000000000000D+02	0.9783776497157229D-01	0.0	40
-0.3975000000000000D+02	0.6897912149992871D-01	0.0	41
-0.3925000000000000D+02	0.4169455362288597D-01	0.0	42
-0.3875000000000000D+02	0.1614305124012526D-01	0.0	43
-0.3825000000000000D+02	-0.7534820751661426D-02	0.0	44
-0.3775000000000000D+02	-0.2920984784540393D-01	0.0	45
-0.3725000000000000D+02	-0.4872362403656972D-01	0.0	46
-0.3675000000000000D+02	-0.6598780387967954D-01	0.0	47
-0.3625000000000000D+02	-0.8081217497406243D-01	0.0	48
-0.3575000000000000D+02	-0.9313053366848419D-01	0.0	49
-0.3525000000000000D+02	-0.1027410181018618D+00	0.0	50
-0.3475000000000000D+02	-0.1096036621304755D+00	0.0	51
-0.3425000000000000D+02	-0.1134943387413122D+00	0.0	52
-0.3375000000000000D+02	-0.1143926985813328D+00	0.0	53
-0.3325000000000000D+02	-0.1120637404019341D+00	0.0	54
-0.3275000000000000D+02	-0.1064942170566375D+00	0.0	55
-0.3225000000000000D+02	-0.9743497929780498D-01	0.0	56
-0.3175000000000000D+02	-0.8489244978304203D-01	0.0	57
-0.3125000000000000D+02	-0.6859212349403923D-01	0.0	58
-0.3075000000000000D+02	-0.4855327317107537D-01	0.0	59
-0.3025000000000000D+02	-0.2448786771054805D-01	0.0	60
-0.2975000000000000D+02	0.3582579386177398D-02	0.0	61
-0.2925000000000000D+02	0.3593955986701055D-01	0.0	62
-0.2875000000000000D+02	0.7256854669905106D-01	0.0	63
-0.2825000000000000D+02	0.1138243438823563D+00	0.0	64
-0.2775000000000000D+02	0.1596616262590968D+00	0.0	65
-0.2725000000000000D+02	0.2103976456809610D+00	0.0	66
-0.2675000000000000D+02	0.2660369543509656D+00	0.0	67
-0.2625000000000000D+02	0.3269127812671435D+00	0.0	68
-0.2575000000000000D+02	0.3930213137041549D+00	0.0	69
-0.2525000000000000D+02	0.4647011649880083D+00	0.0	70

-0.2475000000000000D+02	0.5420109073048348D+00	0.0	71
-0.2425000000000000D+02	0.6252716562540526D+00	0.0	72
-0.2375000000000000D+02	0.7145873621563820D+00	0.0	73
-0.2325000000000000D+02	0.8102641570608323D+00	0.0	74
-0.2275000000000000D+02	0.9124577641833140D+00	0.0	75
-0.2225000000000000D+02	0.1021473281555034D+01	0.0	76
-0.2175000000000000D+02	0.1137519575355245D+01	0.0	77
-0.2125000000000000D+02	0.1260901734271952D+01	0.0	78
-0.2075000000000000D+02	0.1391886512597280D+01	0.0	79
-0.2025000000000000D+02	0.1530782050606442D+01	0.0	80
-0.1975000000000000D+02	0.1677921699763980D+01	0.0	81
-0.1925000000000000D+02	0.1833625890250640D+01	0.0	82
-0.1875000000000000D+02	0.1998318544234285D+01	0.0	83
-0.1825000000000000D+02	0.2172293811265510D+01	0.0	84
-0.1775000000000000D+02	0.2356083064281766D+01	0.0	85
-0.1725000000000000D+02	0.2549971819352072D+01	0.0	86
-0.1675000000000000D+02	0.2754655216210763D+01	0.0	87
-0.1625000000000000D+02	0.2970419847915533D+01	0.0	88
-0.1575000000000000D+02	0.3198045741515847D+01	0.0	89
-0.1525000000000000D+02	0.3437844468218693D+01	0.0	90
-0.1475000000000000D+02	0.3690751312609209D+01	0.0	91
-0.1425000000000000D+02	0.3957122701235557D+01	0.0	92
-0.1375000000000000D+02	0.4238057579665664D+01	0.0	93
-0.1325000000000000D+02	0.4533932230466761D+01	0.0	94
-0.1275000000000000D+02	0.4846054095843319D+01	0.0	95
-0.1225000000000000D+02	0.5174826310355367D+01	0.0	96
-0.1175000000000000D+02	0.5521799176378260D+01	0.0	97
-0.1125000000000000D+02	0.5887434261091164D+01	0.0	98
-0.1075000000000000D+02	0.6273493122157939D+01	0.0	99
-0.1025000000000000D+02	0.6680445062662737D+01	0.0	100
-0.9750000000000000D+01	0.7110367445125560D+01	0.0	101
-0.9250000000000000D+01	0.7563634055142313D+01	0.0	102
-0.8750000000000000D+01	0.8042603845988292D+01	0.0	103
-0.8250000000000000D+01	0.8547257858349838D+01	0.0	104
-0.7750000000000000D+01	0.9080243315591876D+01	0.0	105
-0.7250000000000000D+01	0.9640117658648709D+01	0.0	106

```
-0.6750000000000000D+01  0.1023036630981858D+02  0.0                    107
-0.6250000000000000D+01  0.1082738710197562D+02  0.0                    108
-0.5750000000000000D+01  0.1138234289813659D+02  0.0                    109
-0.5250000000000000D+01  0.1189074081238208D+02  0.0                    110
-0.4750000000000000D+01  0.1235259315001822D+02  0.0                    111
-0.4250000000000000D+01  0.1276818179086794D+02  0.0                    112
-0.3750000000000000D+01  0.1313737110648288D+02  0.0                    113
-0.3250000000000000D+01  0.1346035041541771D+02  0.0                    114
-0.2750000000000000D+01  0.1373706383049432D+02  0.0                    115
-0.2250000000000000D+01  0.1396763102507103D+02  0.0                    116
-0.1750000000000000D+01  0.1415200973824121D+02  0.0                    117
-0.1250000000000000D+01  0.1429031543790756D+02  0.0                    118
-0.7500000000000000D+00  0.1438243096345005D+02  0.0                    119
-0.2500000000000000D+00  0.1442869013980858D+02  0.0                    120
 1.0D0                   .4D0                    200000.D0
 6.5D0                   100.D0                  6.6D0
  -20.D00                0.0D0                   2.0D0
   .TRUE.    .FALSE.
       60        120   0.D0
```

APPENDIX E

Description and Use of the Program Collocation
Which Calculates the Stress Intensity Factor K
For Finite Cracked Pavements

The program, COLLOCATION, calculates the K1 stress intensity factor for the case of a pavement with a small finite crack. See Figure #1 for an explanation of the system loading procedure. The method chosen to solve the problem is the "boundary collocation of stresses." Particularly, the method uses Williams "Phi" stress function in combination with elasticity theory stress representation.

Theoretically, the stress intensity factor K1 is given by

$$K1 = -\sqrt{2\pi} \cdot d_1$$

where the d_1 term represents the first stress variable in Williams "Phi" stress function. This stress function is given by

$$\Phi = \sum_{n=1}^{N} \left\{ (-1)^{n-1} d_{2n-1} r^{n+\frac{1}{2}} \left[-\cos\left(n-\tfrac{3}{2}\right)\theta + \left(\frac{2n-3}{2n+1}\right)\cos\left(n+\tfrac{1}{2}\right)\theta \right] + (-1)^{n} d_{2n} r^{n} \left[-\cos(n-1)\theta + \cos(n+1)\theta \right] \right\}$$

By using a collocation of stress procedure, the program will solve for the d_i terms. Referring to figure 2, the boundary conditions are as follows

Boundary	Stress Collocation	Type of stress function
A-B	$\sigma_{xy1} = 0$	Williams'
	$\sigma_{xx1} = K\ U_1$	Williams'
B-C	$\sigma_{xy1} = f(x)$	Elasticity Theory
	$\sigma_{yy1} = g(x)$	Elasticity Theory
C-D	$\sigma_{xx1} = 0$	Williams'
	$\sigma_{xy1} = 0$	Williams'
D-E	$\sigma_{xx1} = -P/2a$	Williams'
	$\sigma_{xy1} = 0$	Williams'

The elasticity functions f(x) and g(x) are given as

$$\sigma_{xy1} = f(x) = -\frac{M}{x}\left[x - \frac{d}{2} - c1\right] \cdot \frac{1}{I}$$

$$\sigma_{yy1} = g(x) = \frac{6Q}{d^3}\left[d \cdot c1 + x \cdot d - 2x \cdot c1 - c1^2 - x^2\right]$$

where E_1 represents the pavement's Young's Modulus, ν represents the pavement's Poisson ratio, h represents the pavement's thickness, C1 represents the pavement's crack length, P represents the total system load , 2a represents the width of the loaded area, d represents the pavement's collocation section length, β represents the foundation's rigidity modulus, E_2 represents the foundation's Young's modulus, W represents the pavement's width, and I, M, Q, r, and θ are given as

$$I = d^3/12$$

$$M = \frac{P}{4\beta W} e^{-\beta y}\left(\cos(\beta y) - \sin(\beta y)\right)$$

$$Q = \frac{P}{2W} e^{-\beta y} \cos(\beta y)$$

$$\theta = \tan^{-1}\left(\frac{y}{x}\right)$$

$$r = \sqrt{x^2 + y^2}$$

$$\beta = .689\left[\frac{16 E_1 I}{E_2}\right]^{-.277}$$

To obtain the stresses for which Williams' stress function is defined, we must follow a two-stage derivative procedure of the "Phi" stress function. That is, partial derivatives of the stress function with respect to "r" and "θ" need to be taken initially. Then partial derivatives of these derivatives, with respect to "X" and "Y", need to be taken. The following are the partial derivatives described in the initial step:

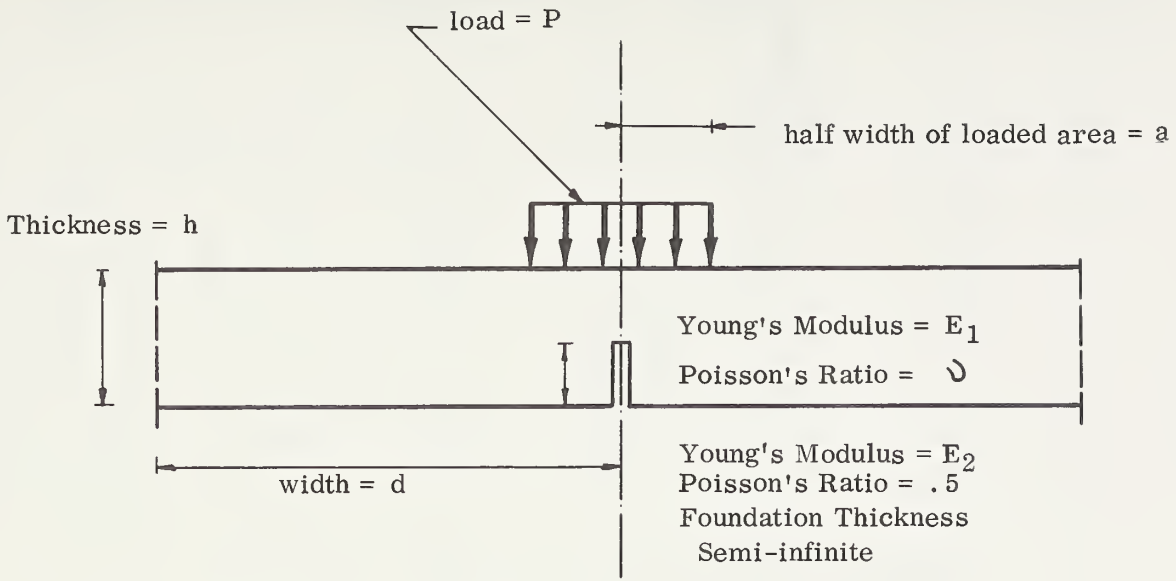

"Collocation" Two-Layered Loading System
Figure 1

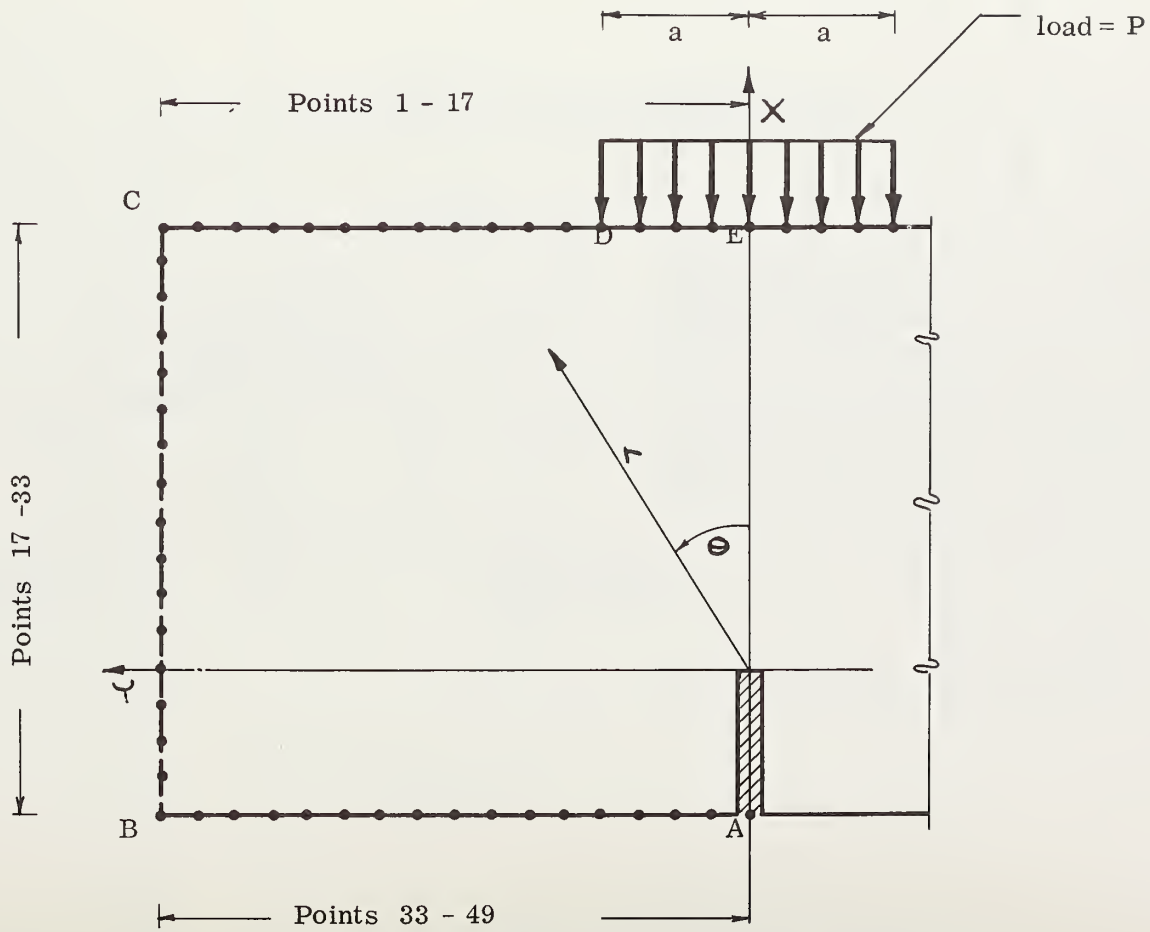

Collocation Grid for the COLLOCATION Program
Figure 2

$$\frac{d\Phi}{dr} = \sum_{n=1}^{NOOFN} \left\{ (-1)^{n-1} d_{2n-1} \left(n+\tfrac{1}{2}\right) r^{\left(n-\frac{1}{2}\right)} \left[-\cos\left(n-\tfrac{3}{2}\right)\theta + \left(\frac{2n-3}{2n+1}\right)\cos\left(n+\tfrac{1}{2}\right)\theta \right] \right.$$

$$\left. + (-1)^{n} d_{2n} (n+1) r^{n} \left[-\cos(n-1)\theta + \cos(n+1)\theta \right] \right\}$$

$$\frac{d\Phi}{d\theta} = \sum_{n=1}^{NOOFN} \left\{ (-1)^{n-1} d_{2n-1} \left(n+\tfrac{1}{2}\right) r^{\left(n-\frac{1}{2}\right)} \left[\left(n-\tfrac{3}{2}\right)\sin\left(n-\tfrac{3}{2}\right)\theta - \left(\frac{2n-3}{2}\right)\sin\left(n+\tfrac{1}{2}\right)\theta \right] \right.$$

$$\left. + (-1)^{n} d_{2n} r^{\left(n+\frac{1}{2}\right)} \left[(n-1)\sin(n-1)\theta - n+1)\sin(n+1)\theta \right] \right\}$$

$$\frac{d^2\Phi}{d\theta\, dr} = \sum_{n=1}^{NOOFN} \left\{ (-1)^{n-1} d_{2n-1} \left(n+\tfrac{1}{2}\right) r^{\left(n-\frac{1}{2}\right)} \left[n-\tfrac{3}{2}\sin\left(n-\tfrac{3}{2}\right)\theta - \left(\frac{2n-3}{2}\right)\sin\left(n+\tfrac{1}{2}\right)\theta \right] \right.$$

$$\left. + (-1)^{n} d_{2n} r^{n} \left[(n-1)\sin(n-1)\theta - (n+1)\sin(n+1)\theta \right] \right\}$$

$$\frac{d^2\Phi}{dr^2} = \sum_{n=1}^{NOOFN} \left\{ (-1)^{n-1} d_{2n-1} \left(n+\tfrac{1}{2}\right)\left(n-\tfrac{1}{2}\right) r^{\left(n-\frac{3}{2}\right)} \left[-\cos\left(n-\tfrac{3}{2}\right)\theta + \left(\frac{2n-3}{2n+1}\right)\cos\left(n+\tfrac{1}{2}\right)\theta \right] \right.$$

$$\left. + (-1)^{n} d_{2n} (n+1)\, n\, r^{(n-1)} \left[-\cos(n-1)\theta + \cos(n+1)\theta \right] \right\}$$

$$\frac{d^2\Phi}{d\theta^2} = \sum_{n=1}^{NOOFN} \left\{ (-1)^{n-1} d_{2n-1} r^{\left(n+\frac{1}{2}\right)} \left[\left(n-\tfrac{3}{2}\right)^2 \cos\left(n-\tfrac{3}{2}\right)\theta - \left(\frac{2n-3}{2}\right)\left(\frac{2n+1}{2}\right)\cos\left(n+\tfrac{1}{2}\right)\theta \right] \right.$$

$$\left. + (-1)^{n} d_{2n} r^{(n+1)} \left[(n-1)^2 \cos(n-1)\theta - (n+1)^2 \cos(n+1)\theta \right] \right\}$$

The parameter NOOFN is a program input and will be discussed later. Now expanding and taking partial derivatives with respect to "X" and "Y", we have

$$\overline{V}_{xx1} = \frac{d^2 \Phi}{dy^2} = \frac{d^2 \Phi}{dr^2} \sin^2\theta + 2 \frac{d^2 \Phi}{d\theta\, dr} \frac{\sin\theta \cos\theta}{r}$$

$$+ \frac{d \Phi}{dr} \cos^2\theta - 2 \frac{d \Phi}{d\theta} \frac{\sin\theta \cos\theta}{r^2} + \frac{d^2 \Phi}{d\theta^2} \frac{\cos^2\theta}{r^2}$$

$$\overline{V}_{yy1} = \frac{d^2 \Phi}{dx^2} = \frac{d^2 \Phi}{dr^2} - 2 \frac{d^2 \Phi}{d\theta\, dr} \frac{\sin\theta \cos\theta}{r}$$

$$+ \frac{d \Phi}{dr} \frac{\sin^2\theta}{r} + 2 \frac{d \Phi}{d\theta} \frac{\sin\theta \cos\theta}{r^2} + \frac{d^2 \Phi}{d\theta^2} \frac{\sin^2\theta}{r^2}$$

$$\overline{V}_{xy1} = -\frac{d^2 \Phi}{dx\, dy} = -\frac{d^2 \Phi}{dr^2} \sin\theta \cos\theta - \frac{d^2 \Phi}{d\theta\, dr} \frac{\cos 2\theta}{r}$$

$$+ \frac{d \Phi}{dr} \frac{\sin\theta \cos\theta}{r} + \frac{d \Phi}{d\theta} \frac{\cos 2\theta}{r^2} + \frac{d^2 \Phi}{d\theta^2} \frac{\sin\theta \cos\theta}{r^2}$$

This concludes the development of the stress functions. However, before we turn to the actual collocation procedures, we must derive one additional function. Notice that one of the boundary conditions along seam A-B is a "stress-displacement" combination. That is,

$$\overline{V}_{xx1} = K\, U_1$$

The U_1 function can be derived from Williams' original "Phi" stress function, and is given by

$$U_1 = U(r,\theta) \cos(\theta) - V(r,\theta) \sin(\theta) + L$$

where $U(r,\theta)$ and $V(r,\theta)$ are displacement functions defined as

$$U(r,\theta) = \frac{1+\nu}{E} \sum_{n=1}^{NOOFN} \Big\{ (-1)^{n-1} d_{2n-1} r^{(n-\frac{1}{2})} \Big[\left(\tfrac{7}{2} - n - 4\nu\right) \cos\left(n - \tfrac{3}{2}\right)\theta$$

$$+ \left(n - \tfrac{3}{2}\right) \cos\left(n + \tfrac{1}{2}\right)\theta \Big] + (-1)^{n} d_{2n} r^{n} \Big[(3 - n - 4\nu) \cos(n+1)\theta$$

$$+ (n+1) \cos(n+1)\theta \Big] \Big\} + L \cos\theta$$

$$V(r,\theta) = \frac{1+\nu}{E} \sum_{n=1}^{NOOFN} \Big\{ (-1)^{n-1} d_{2n-1} r^{(n-\frac{1}{2})} \Big[\left(\tfrac{5}{2} + n - 4\nu\right) \sin\left(n - \tfrac{3}{2}\right)\theta$$

$$- \left(\tfrac{2n-3}{2}\right) \sin\left(n + \tfrac{1}{2}\right) \Big] + (-1)^{n} d_{2n} r^{n} \Big[-(3 + n - 4\nu) \sin(n-1)\theta$$

$$+ (n+1) \sin(n+1)\theta \Big] \Big\} + L \sin\theta$$

K represents the modulus of subgrade reaction, and L is a constant of location.

Since all boundary conditions are now described by mathematical functions, we can turn to the actual collocation procedure. This procedure is a matrix operation which will solve for the d_i terms. In augmental matrix notation, we have

$$\begin{bmatrix} \overline{V}_{xx1} \\ \overline{V}_{xx1} \\ \overline{V}_{xx1} - KU_1 \\ \overline{V}_{yy1} \\ \overline{V}_{xy1} \\ \overline{V}_{xy1} \\ \overline{V}_{xy1} \\ \overline{V}_{xy1} \end{bmatrix} = \begin{bmatrix} -P/2a \\ 0 \\ 0 \\ g(x) \\ 0 \\ 0 \\ f(x) \\ 0 \end{bmatrix} \qquad \begin{array}{c} \underline{\text{Boundary}} \\ D - E \\ C - D \\ A - B \\ B - C \\ D - E \\ C - D \\ B - C \\ A - B \end{array}$$

Now converting the convention matrix notation, we have

$$\begin{bmatrix} C_{1,1} & C_{1,2} & C_{1,3} & \text{----} & C_{1,2*NOOFN+1} \\ C_{2,1} & & & & '' \\ C_{3,1} & & & & '' \\ '' & & & & '' \\ '' & & & & '' \\ C_{NOOFXY,1} & & & & C_{NOOFXY,2*NOOFN+1} \end{bmatrix} * \begin{bmatrix} d_1 \\ d_2 \\ d_3 \\ '' \\ '' \\ d_{2*NOOFN+1} \end{bmatrix} = \begin{bmatrix} a_1 \\ a_2 \\ a_3 \\ '' \\ '' \\ a_{NOOFXY} \end{bmatrix}$$

where the $C_{i,j}$ terms represent the coefficients of the d_i terms and the a_i terms represent the boundary conditions for the particular i^{th} equation. The terms, NOOFN and NOOFXY, indicate respectively the number of Williams' stress functions and the number of equations be used in the program. Because solution convergence could be a problem, it was decided that a "least square" optimalization technique would be employed to solve for the d_i terms. This technique and its computer listing is described in the IBM computer manuel - "The Scientific Subroutine Package" - Subroutines LLSQ and DLLSQ - pp. 160 - 164. By using this method, many more boundary collocations can be used for the same number of Williams' d_i forms. Thus, the only restriction on the size of the matrix is

3) $2 * NOOFN+1 \angle NOOFXY$

With the solution of the d_i terms, the stress intensity factor K1 can of course be calculated. In the program, the variable NOOFXY is calculated in the following manner

NOOFXY = 2 * (NOOFXL + NOOFXU + NOOFXS + NOOFXB) - 4

where NOOFXL, NOOFXU, NOOFXS, and NOOFXB represent respectively the number of collocation positions under the load on the top boundary, outside the load on

the top boundary, on the side boundary, and on the bottom boundary. Now, rewriting equation (3) we have

$$2*NOOFN + 1 \angle 2*(NOOFXL + \cdots\cdots) - 4$$

Simplifing, we have

$$4)\quad NOOFN + 2 \angle NOOFXL + NOOFXU + NOOFXS + NOOFXB$$

The above equation describes the size of the collocation matrix in terms of program inputs.

The program COLLOCATION was formulated into five sections:

1) Reading in system's data

2) Generation of coordinate systems: X-Y and r -θ boundary positions

3) Generation of d_i coefficients

4) Solution of d_i terms by optimaization routine

5) Printed output

Since sections 3, 4, and 5 have been previously explained or are otherwise self-explanatory, they will be despenced with here. To explain sections 1 and 2 and to facilitate better overall understanding, an example will be used.

Suppose we wish to find the stress intensity factors for different crack lengths for a particular system. First we must determine the system's material properties: pavement's Young's modulus, pavement's thickness, foundation's modulus beta, and etc. A list of all material properties appears in Fig. 1. Next, the collocation grid must be designed. Referring to Fig. 2, the parameter d and number of collocation positions per side need to be determined. As a rule, the best results are obtained if collocation grid is a square. Thus, the parameters

h and d should be equal. As for the number of collocations positions, never place them more than a 1/2 inch apart. It is preferable that the spacing between positions be 1/4 to 1/8 inches. With these guide lines in mind, and an asphaltic-concrete system with the following properties,

E_1	-	130,000 psi	a =	.5 inches	
D	-	.5	P =	10 lbs.	W = 1 inch
h	-	2 inches	E_2 =	913 psi	

we might choose d equal to 2 inches and the number of collocating positions per side equal to 17. The system's data will be complete when we specify a crack length and the number of Williams' stress functions. It was noted that the optimal value for NOOFN, the number of Williams' stress functions, varies with the particular system. To obtain this value, a simple sensitivity analysis was conducted. A series of data, all with different values of NOOFN, was inputed to the program (a sample appears in the "dummy data" section of the end of the program listing). The output was obtained (an example appears in charts A-a and A-b), and Figure 3 was plotted. For best results, the optimal value of NOOFN occurs when the curve crests. This would imply that NOOFN should equal 30 for this example. Since NOOFN has now been chosen, we can now run an additional program to obtain the stress intensity factor for any crack length.

To sum up, we recommend that the user follow a two stage procedure to determine the stress intensity factors:

1) Find the material properties for the particular system. Chose a representative value for a crack length. Run a series of data with different values for NOOFN. Develop a graph similar to Fig. A-3. Chose the value of NOOFN where the curve crests.
2) Run an additional program to obtain a stress intensity factor for any crack length.

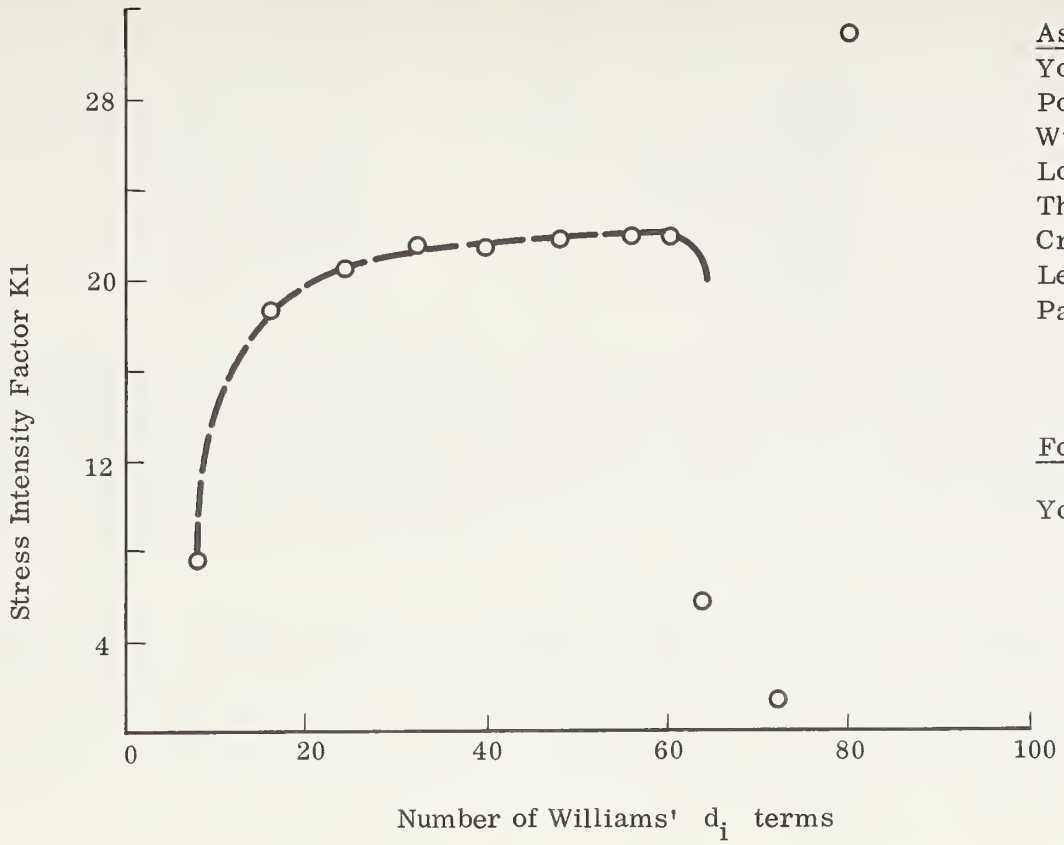

Asphaltic Concrete Pavement	
Young's Modulus	130,000 psi
Poisson's Ratio	.5
Width of loaded area	1. in.
Load	10 lb.
Thickness	2 in.
Crack Length	.5 in.
Length of Pavement	2 in.
Pavement width	1 in.

Foundation	
Young's Modulus	913 psi

Influence of the Number of Williams' d_i terms on the Solution of Stress Intensity Factor K 1

Figure 3

Chart A-a

```
*****************************************************************************************

            S T R E S S   I N T E N S I T Y   F A C T O R   A N A L Y S I S

   CASE :  ASPHALTIC CONCRETE

                                        PARAMETERS

      PAVEMENT :

           YOUNG MODULUS  200000.0                    POISSON'S RATIO     0.5000
           THICKNESS           2.0                    PAVEMENT LENGTH       2.00
           CRACK LENGTH     0.5000                    PAVEMENT WIDTH        2.00

      FOUNDATION :

           YOUNG MODULUS      89.0                    POISSON'S RATIO     0.5000
           THICKNESS      SEMI-INFINITE

      OTHERS :

           LOAD                20.0                   LOADED AREA'S LENGTH  0.5000
           NUMBER OF SOLUTIONS  61


   STRESS INTENSITY FACTOR K1 =        0.5131141334D 02

*****************************************************************************************
```

* * * * * OUTPUT CHECK CN SOLUTICN FIT * * * * *

SUMMARY CF 8CUNDARY REQU1REMENTS

```
EQUATICNS   1 TD   5 SIGMA XX1 DN TDP 8UNDARY -- LDCATIDNS UNDER LDAD
EQUATIONS   6 TO  17 SIGMA XX1 CN TDP 8GUNDARY -- REMAINING LDCATIDNS
EQUATIDNS  18 TD  34 SIGMA XXI CN 8CTTCM 8DUNDARY
EQUATICNS  35 TD  51 SIGMA YY1 DN SIDE 8DUNDARY
EQUATICNS  52 TD  67 SIGMA XY1 DN TDP 8DUNDARY
EQUATIDNS  68 TD  82 SIGMA XY1 CN SIDE 8DUNDARY
EQUATICNS  83 TD  98 SIGMA XY1 ON 8DTTCM 8DUNDARY
EQUATIDN          99 SIGMA XX1 DN X AXIS AT BOTTCM 8DUNDARY
EQUATIDN         100 X AXIS DISPLACEMENT DN X AXIS AT TOP 8DUNDARY
```

EQUATICN ND.	THEDRETICAL VALUE	CALCUATED VALUE	DIFFERENCE
1	-0.1C000C00000000000D 02	-0.9378896561425683D 01	-0.6211034385743175D 00
2	-0.1C0000C00CC00000D 02	-0.1004931505406724D 02	0.4931505406724312D-01
3	-0.100000C0000000000D 02	-0.1103263274620518D 02	0.1032632746205178D 01
4	-0.1CC0C00000000000D 02	-0.1032049013241715D 02	0.3204901324171485D 0C
5	-0.10000C0000CC00C0D 02	-C.7C786291016037 77D 01	-0.2921370898396224D 01
6	0.0	-0.2701672225020780D 01	0.2701672225020780D 01
7	0.0	0.3663803149221075D 00	-0.3663803149221075D 00
8	0.0	0.9177698671261922D 00	-0.9177698671261922D 00
9	0.0	-0.3504838439334356D-03	0.3504838439334356D-03
10	0.0	-0.4766100135598772D 00	0.4766100135598772D 00
11	0.0	0.3141436280787956D-01	-0.3141436280787956D-01
12	0.0	0.4057466564526742D 00	-0.4057466564526742D 00
13	0.0	-0.1851180717392608D-01	0.1851180717392608D-01
14	0.0	-0.2215757086770 5C9D 00	0.2215757086770509D 00
15	0.0	0.2364066926611485D 00	-0.2364066926611485D 00
16	0.0	-0.1728575170363910D-01	0.1728575170363910D-01
17	C.0	0.1116842267128959D-01	-0.1116842267128959D-01
18	0.0	-0.7054229277371498D 00	0.7054229277371498D 00
19	C.0	-0.5778C927935862180 00	0.5778092793586218D 00
20	0.0	-0.9430522599928623D 00	0.9430522599928623D 00
21	0.0	-0.5822391364755475D 00	0.5822391364755475D 00
22	0.0	-0.5951252964150814D 00	0.5951252964150814D 00
23	0.0	-0.7853464588220849D 00	0.7853464588220849D 00
24	0.0	-0.7963C571620873250 00	0.7963057162087325D 00
25	0.0	-0.7814040797583064D 00	0.7814040797583064D 00
26	0.0	-0.6361343174056281D 00	0.6361343174056281D 00
27	0.0	-0.4518649763093755D 00	0.4518649763093755D 00
28	0.0	-0.7042625260334145D 00	0.7042625260334145D 00
29	0.0	-0.1193485461282789D 01	0.1193485461282789D 01
30	0.0	-0.1014619111093135D 01	0.1014619111093135D 01
31	0.0	-0.2425469912756134D 00	0.2425469912756134D 00
32	0.0	-0.2375824783159923D 00	0.2375824783159923D 00
33	0.0	-0.1200337939746977D 01	0.1200337939746977D 01
34	0.0	-0.4976854639087551D-03	0.4976854639087551D-03
35	-0.2700031721025206D 02	-0.2700227577490295D 02	0.1958566508915030-02
36	-0.2362527755857056D 02	-0.2361538338493210D 02	-0.9894174038453939D-02
37	-0.2025023 79C7689C50 02	-0.2024791463137819D 02	-0.2323276310853827D-02
38	-0.1687515825640754D 02	-0.1682421175797299D 02	-0.5098649843455049D-01
39	-0.1350015860C5126C30 02	-0.1361C06784650857D 02	0.1099092413825380D 00
40	-0.1012511895384452D 02	-0.1006289864649199D 02	-0.6222030735253691D-01
41	-0.675007930256301 7D 01	-0.6681490089870693D 01	-0.6858921269232400D-01
42	-0.337503965128 15C8D 01	-0.3488018100252646D 01	0.1129784489711374D 00
43	0.0	-0.2885084756280775D-01	0.2885084756280775D-01
44	0.337503965128 15C80 01	0.3483630361014416D 01	-0.1C859070973290820 00
45	0.675007930256301 7D 01	0.6716659853902687D 01	0.3341944866032919D-01
46	0.1012511895384452D 02	0.1000619695140715D 02	0.1189220024373732D 00
47	0.135001586C512603D 02	0.1355839157777834D 02	-0.5823337265230943D-01
48	0.1687519825640754D 02	0.1692756873252945D 02	-0.5237047612190792D-01
49	0.2025023 79C768905D 02	0.2009597364231848D 02	0.1542642653705641D 00
50	0.2362527755857056D 02	0.2367533908567937D 02	-0.5006152670881646D-01
51	0.2700031721025206D 02	0.2697874149036601D 02	0.2157571990604978D-01
52	0.0	-0.1139239677881505D 00	C.1139239677881505D 00
53	0.0	-0.7540343489682880D-01	0.7540343489682880D-01
54	0.0	0.6850318843796230D-01	-0.6850318843796230D-01
55	0.0	0.1260675152263713D 00	-0.1260675152263713D 00
56	0.0	0.1247662378181525D-01	-0.1247662378181525D-01
57	0.0	-0.1203152732667516D 00	0.1203152732667516D 00
58	0.0	-0.7297253191778570D-01	0.7297253191778570D-01
59	0.0	0.1046052905625758D 00	-0.1046052905625758D 00
60	0.0	0.1360268558460611D 00	-0.1360268558460611D 00
61	0.0	-0.6599915519338850D-01	0.6599915519338850D-01
62	0.0	-0.1596492600545822D 00	0.1596492600545822D 00
63	0.0	0.1019165259722854D 00	-0.1019165259722854D 00
64	0.0	0.1938431 7EE75888CD 00	-0.1938431788798880D 00
65	0.0	-0.2705079600074214D 00	0.2705079600074214D 00
66	0.0	0.1557831762120258D 00	-0.1557831762120258D 00
67	0.0	-0.2928511147547396D-01	0.2928511147547396D-01
68	0.7183181677 67C2500 00	0.8109686758525640D 00	-0.9265050808553910D-01
69	0.1340860579831780D 01	0.1295061525899655D 01	0.4579905393212490D-01
70	0.1867627236194265D 01	0.1907216438827504D 01	-0.3958920263323939D-01
71	0.2298618136854480D 01	0.2371307098345596D 01	-0.7268896149111660D-01
72	0.2633833281812425D 01	0.2637771318025841D 01	-0.3938036213416262D-02
73	0.2873272671068 1C0D 01	0.2886998417446875D 01	-0.1372574637877566D-01
74	0.3016936304621 5C5D 01	0.3048972776973358D 01	-0.3203647235185292D-01
75	0.3064824182472640D 01	0.3110888686905469D 01	-0.4606450443282871D-01
76	0.3016936304621505D 01	0.3C569440831173 05D 01	-0.4000777849579995D-01
77	0.2873272671068 1C00 01	0.2861940189646820D 01	0.1133248142128007D-01
78	0.2633833281812425D 01	0.2652715822415385D 01	-0.1888254060695993D-01
79	0.2298618136854480D 01	0.2389496447549053D 01	-0.9087831069457340D-01
80	0.1867627236194265D 01	0.1855182289011264D 01	0.1244494718300082D-01
81	0.1340860579831780D 01	0.1315289471525634D 01	0.2557110830614539D-01
82	0.7183181677 67C2500 C0	0.8275849684047252D 00	-0.1092668006377002D 00
83	0.0	-0.3839685126132508D-01	0.3839685126132508D-01
84	0.0	0.9534260928014500D-01	-0.9534260928014500D-01
85	0.0	0.3081684865976440D-01	-0.3081684865976440D-01
86	0.0	-0.6923096972559900D-01	0.6923096972559900D-01
87	0.0	-0.4589271624138339D-01	0.4589271624138339D-01
88	0.0	0.2479063522821771D 00	-0.2479063522821771D 00
89	0.0	0.8606153472347990D-01	-0.8606153472347990D-01
90	0.0	-0.2479527812555073D 00	0.2479527812555073D 00
91	C.0	-0.5762963897883410D-01	0.9762963897883410D-01
92	0.0	0.2434579923886931D 00	-0.2434579923886931D 00
93	0.0	0.2565471358836592D 00	-0.2565471358836592D 00
94	0.0	0.6853909067398090D-01	-0.6853909067398090D-01
95	0.0	-0.1572416800046443D 00	0.1572416800046443D 00
96	0.0	-0.4735915335009404D 00	0.4735915335009404D 00
97	0.0	-0.2074130820129810D 00	0.2074130820129810D 00
98	0.0	0.1095221093124245D 01	-0.1095221093124245D 01
99	0.0	-0.1422690446993863D 01	0.1422690446993863D 01
100	UNKNCWN	-0.1738510293752866D-01	

Chart A-b

```
C****
C****     THIS PROGRAM CALCULATES THE 'K1' STRESS INTENSITY FACTER
C****          DEFINED BY:
C****                         K1 = -(2*PIEDOO)**(+.5) * SOL(1)
C****          WHERE SOL(1) IS WILLIAMS' FIRST SOLUTION IN HIS 'PHI'
C****          STRESS FUNCTION. THE SOLUTION IS OBTAINED FROM AN
C****          OPTIMALIZATION LEASE SQUARES PROCESS.
C****
C
C****     ARRAY NAME CONTAINS TEST DATA DESCRIPTION
C****     CONW IS PAVEMENT'S WIDTH
C****     CONH IS PAVEMENT'S THICKNESS
C****     COND IS PAVEMENT'S LENGTH
C****     CONA IS LOADED AREA'S LENGTH
C****     C1 IS PAVEMENT'S CRACK LENGTH
C****     CONP IS PAVEMENT'S LOAD
C****     CONE IS PAVEMENT'S YOUNG'S MODULUS
C****     CONEF IS FOUNDATION'S YOUNG'S MODULUS
C****     CONV IS PAVEMENT'S POSSION'S RATIO
C****     NOOFM IS NUMBER OF WILLIAMS' STRESS FUNCTIONS
C****          OR THE NUMBER OF 'DSUBI' TERMS
C****     NOOFXL IS NUMBER OF BOUNDARY STATIONS ON TOP LAYER UNDER LOAD
C****     NOOFXU IS NUMBER OF BOUNDARY STATIONS ON TOP LAYER OUTSIDE LOAD
C****     NOOFXS IS NUMBER OF BOUNDARY STATIONS ON SIDE LAYER
C****     NOOFXB IS NUMBER OF BOUNDARY STATIONS ON BOTTOM LAYER
C****     PRISCK IS LOGIAL CONSTANT DETERMINING WHETHER AN ACCURACY CHECK
C              IS PERFORMED ON WILLIAMS' SOLUTIONS -- '.TRUE.' INDICATES
C              A CHECK WILL BE MADE
      IMPLICIT REAL*8 (A-H,O-Z)
      LOGICAL  PRISCK,ZEROCK,SOLUCK
      REAL*4   STAR(30),NAME(18),ROOFX
      DIMENSION  X(00050),Y(00050),R(00050),PHI(00050),V9(00200),SOL(010
     *0),COEF(0100,061),COEFCK(006100),CALC(0100),CADD(0100),CON(0100),
     *CONCHK(0100),IPIV(0100)
C****
C****     MAKE SURE ALL ARRAYS ARE DIMENSIONED CORRECT. THE FOLLOWING
C              SHOULD BE ADHERED TO :
C
C              ARRAY          DIMENSIONED AREA
C
C               X          NOOFXL + NOOFXU + NOOFXS + NOOFXB - 2
C               Y          NOOFXL + NOOFXU + NOOFXS + NOOFXB - 2
C               R          NOOFXL + NOOFXU + NOOFXS + NOOFXB - 2
C              PHI         NOOFXL + NOOFXU + NOOFXS + NOOFXB - 2
C              V9          4 * ( NOOFXL + NOOFXU + NOOFXS + NOOFXB ) - 8
C              SOL         2 * NOOFM + 1
C              COEF        2 * ( NOOFXL + NOOFXU + NOOFXS + NOOFXB ) - 2
C                                   BY  2 * NOOFM + 1
C              COEFCK      2 * ( NOOFXL + NOOFXU + NOOFXS + NOOFOB ) - 4
C                                  TIMES  2 * NOOFM + 1
C              CALC        2 * ( NOOFXL + NOOFXU + NOOFXS + NOOFXB ) - 2
C              CADD        2 * ( NOOFXL + NOOFXU + NOOFXS + NOOFXB ) - 2
C              CON         2 * ( NOOFXL + NOOFXU + NOOFXS + NOOFXB ) - 2
C              CONCHK      2 * ( NOOFXL + NOOFXU + NOOFXS + NOOFXB ) - 2
C              IPIV        2 * ( NOOFXL + NOOFXU + NOOFXS + NOOFXB ) - 2
C
```

```
      COMMON  PRIS,CONV,CONE,COR,CORR
      DATA  STAR/30*'****'/
 9000 READ(5,801,END=1001) (NAME(I),I=1,18)
  801 FORMAT(18A4)
      ZEROCK = .TRUE.
      SOLUCK = .TRUE.
C
C     READ IN CONSTANTS
C
      PRIS = 1.0D-14
      READ(5,800)   CONH,COND,C1,CONE,CONEF,CONV,CONW
  800 FORMAT(3D24.16)
      CONI = CONH**3/12.D0
      CONSTT = 16.0D0*CONE*CONI/CONEF
      CONK = 1.288D0*CONEF/(CONSTT**(.108D0))
      CONBTA = 1.508/(CONSTT**(.277D0))
      READ(5,802)    NOOFM,NOOFXU,NOOFXS,NOOFXB,PRISCK
  802 FORMAT(4I10,L10)
      NOOFS = NOOFM*2 + 1
C
C        CALCULATION OF LOAD LENGTH PARAMATERS
C
      READ(5,2100)  NOOFXL,CONA,CONP
 2100 FORMAT(I10,2D24.16)
      IF(C1.EQ.0.0)  ZEROCK = .FALSE.
      IF(C1.EQ.0.0)  PRISCK = .FALSE.
      IF((NOOFM+2).GE.(NOOFXL+NOOFXU+NOOFXS+NOOFXB)) PRISCK=.FALSE.
      IF((NOOFM+2).GE.(NOOFXL+NOOFXU+NOOFXS+NOOFXB)) SOLUCK=.FALSE.
      IF((NOOFM+2).GE.(NOOFXL+NOOFXU+NOOFXS+NOOFXB)) GO TO 8000
      IF(C1.EQ.0.0)  GO TO 8000
      CONP = CONP/CONW
      ROOFX = NOOFXL - 1
      DELXL = CONA/ROOFX
C
C        GENERATION OF X & Y
C
      NOOFTO = NOOFXL + 1
      NOOFXT = NOOFXL + NOOFXU
      NOOFT1 = NOOFXT + 1
      NOOFTS = NOOFXT + NOOFXS - 1
      NOOFT2 = NOOFTS + 1
      NOOFTX = NOOFTS + NOOFXB - 1
      NOOFXX = NOOFXT + NOOFXB
      NOOFY1 = NOOFXX + 1
      NOOFYY = NOOFXX + NOOFXS
      NOOFB1 = NOOFYY + 1
      NOOFC1 = NOOFYY + NOOFXT - 1
      NOOFD1 = NOOFC1 + 1
      NOOFF1 = NOOFC1 + NOOFXS - 2
      NOOFG1 = NOOFF1 + 1
      NOOFXY = NOOFYY + NOOFTX - 2
      NOOFS5 = NOOFXY + 1
      NOOFU5 = NOOFXY + 2
      NOOFR = NOOFU5
      DELXU = (COND - CONA)/NOOFXU
      DELXS = CONH/(NOOFXS - 1)
      DELXB = COND/(NOOFXB - 1)
      Y(1) = 0.
      X(1) = CONH - C1
      DO 803 I=2,NOOFXL
      Y(I) = Y(I- 1) + DELXL
  803 X(I) = X(I-1)
```

```
      Y(NOOFXL) = CONA
      DO 863 I=NOOFT0,NOOFXT
      Y(I) = Y(I- 1) + DELXU
  863 X(I) = X(I-1)
      X(NOOFXT) = CONH - C1
      Y(NOOFXT) = COND
      DO 804 I=NOOFT1,NOOFTS
      Y(I) = Y(I-1)
  804 X(I) = X(I- 1) - DELXS
      Y(NOOFTS) = COND
      X(NOOFTS) = - C1
      DO 805 I=NOOFT2,NOOFTX
      Y(I) = Y(I- 1) - DELXB
  805 X(I) = X(I-1)
      Y(NOOFTX) = 0.
C
C         ZEROING BLANK COEFFICIENTS
C
      DO 22 I=1,NOOFR
      CON(I) =0.
      DO 22 J=1,NOOFS
   22 COEF(I,J) = 0.
C
C         CALCULATION OF POLOR  COORDINATES
C
      DO 5 I=1, NOOFTX
      R(I)=DSQRT(X(I)**2+Y(I)**2)
    5 PHI(I)=DATAN2(Y(I),X(I))
C
C     .CALCULATION OF  SIGMA XX1 COEFFICIENTS
C
      DO 15 I=1,NOOFXX
      K = I
      N = I
      IF(I.GT.NOOFXT) N = I + NOOFXS - 2
      IF(I.EQ.NOOFXX) K = NOOFS5
      IF(I.LE.NOOFXL) CON(K) = -CONP/(2.0D0*CONA)
      Q=1.D0
      DO 15 J=1,NOOFM
      IF(J-(J/2*2)) 80,80,81
   80 COR=1.D0
      GO TO 201
   81 COR=-1.D0
  201 CORR=-COR
      ESIN=  DSIN(PHI(N))
      ECOS=  DCOS(PHI(N))
      IF(DABS(ESIN).LT.PRIS)  ESIN=0.
      IF(DABS(ECOS).LT.PRIS)  ECOS=0.
      CALL STRES1 (Q,PHI(N),D1,D2,D3,D4,D5,R(N))
      COEF(K,2*J-1) =   D1*ESIN*ESIN  +D2*ECOS*ECOS/R(N)  + D3*2.D0*ESIN
     **ECOS/R(N)  +D5*ECOS*ECOS/R(N)**2  -  D4*2.D0*ECOS*ESIN/R(N)**2
      CALL STRES2 (Q,PHI(N),D1,D2,D3,D4,D5,R(N))
      COEF(K,2*J) =     D1*ESIN*ESIN  +D2*ECOS*ECOS/R(N)  + D3*2.D0*ESIN
     **ECOS/R(N)  +D5*ECOS*ECOS/R(N)**2  -  D4*2.D0*ECOS*ESIN/R(N)**2
   15 Q=Q+1.D0
C
C     CALCULATION OF SIGMA YY1 COEFICIENTS
C
      DO 17 I=NOOFY1,NOOFYY
      N = I - NOOFXB - 1
      EE=DEXP(CONBTA*Y(N))
 9788 ECOS=  DCOS(CONBTA*Y(N))
```

```
      ESIN=   DSIN(CONBTA*Y(N))
      IF(DABS(ECOS).LT.PRIS)  ECOS=0.
      IF(DABS(ESIN).LT.PRIS)  ESIN=0.
      CONM=CONP*(ECOS-ESIN)/(EE*4.D0*CONBTA)
   11 CON(I)=-CONM*(X(N)-COND/2.D0+C1)/CONI
      Q=1.D0
      DO 17 J=1,NOOFM
      IF(J-(J/2*2)) 84,84,85
   84 COR=1.D0
      GO TO 203
   85 COR=-1.D0
  203 CORR=-COR
      ESIN=   DSIN(PHI(N))
      ECOS=   DCOS(PHI(N))
      IF(DABS(ESIN).LT.PRIS)  ESIN=0.
      IF(DABS(ECOS).LT.PRIS)  ECOS=0.
      CALL STRES1 (Q,PHI(N),D1,D2,D3,D4,D5,R(N))
      COEF(I,2*J-1) =    D1*ECOS*ECOS  +D2*ESIN*ESIN/R(N)  -2.D0*D3*ESIN*
     *ECOS/R(N)  + 2.D0*D4*ECOS*ESIN/R(N)**2  +  D5*ESIN*ESIN/R(N)**2
      CALL STRES2 (Q,PHI(N),D1,D2,D3,D4,D5,R(N))
      COEF(I,2*J) =      D1*ECOS*ECOS  +D2*ESIN*ESIN/R(N)  -2.D0*D3*ESIN*
     *ECOS/R(N)  + 2.D0*D4*ECOS*ESIN/R(N)**2  +  D5*ESIN*ESIN/R(N)**2
   17 Q=Q+1.D0
C
C     CALCULATION OF SIGMA XY1  COEFFICIENTS
C
      DO 16 I=NOOFB1,NOOFXY
      N = I - NOOFYY +1
      IF(N.LE.NOOFXT .OR. N.GE.NOOFTS) GO TO 550
      EE=DEXP(CONBTA*Y(N))
 9789 ECOS=   DCOS(CONBTA*Y(N))
      IF(DABS(ECOS).LT.PRIS)  ECOS=0.
      CONQ=CONP*ECOS/(EE*2.D0)
   12 CON(I)=6.D0*CONQ/COND**3*(C1*COND+X(N)*COND-2.D0*X(N)*C1-C1**2-X(N
     *)**2)
  550 Q = 1.D0
      DO 16 J=1,NOOFM
      IF(J-(J/2*2)) 82,82,83
   82 COR=1.D0
      GO TO 202
   83 COR=-1.D0
  202 CORR=-COR
      FCOS=   DCOS(2.D0*PHI(N))
      ESIN=   DSIN(PHI(N))
      ECOS=   DCOS(PHI(N))
      IF(DABS(ESIN).LT.PRIS)  ESIN=0.
      IF(DABS(FCOS).LT.PRIS)  FCOS=0.
      IF(DABS(ECOS).LT.PRIS)  ECOS=0.
      CALL STRES1 (Q,PHI(N),D1,D2,D3,D4,D5,R(N))
      COEF(I,2*J-1) =  -D1*ECOS*ESIN   -D3*FCOS/R(N)  +D5*ECOS*ESIN/R(N)
     ***2   +D2*FCOS*ESIN/R(N)  +D4*FCOS/R(N)**2
      CALL STRES2 (Q,PHI(N),D1,D2,D3,D4,D5,R(N))
      COEF(I,2*J) =    -D1*ECOS*ESIN   -D3*FCOS/R(N)  +D5*ECOS*ESIN/R(N)
     ***2   +D2*ECOS*ESIN/R(N)  +D4*FCOS/R(N)**2
   16 Q=Q+1.D0
C
C     CALCULATION OF U AND V DISPLACEMENT COEFFICIENTS
C
      DO 18 I=NOOFXT,NOOFXX
      K = I + 1
      N = I + NOOFXS - 1
      IF(K.LE.NOOFXX)  COEF(K,NOOFS) = -CONK
```

```
      IF(I.EQ.NOOFXX) N = 1
      IF(I.EQ.NOOFXX) COEF(NOOFU5,NOOFS) = 1.0D0
      Q=1.D0
      DO 18 J=1,NOOFM
      IF(J-(J/2*2)) 86,86,87
   86 COR=1.D0
      GO TO 204
   87 COR=-1.D0
  204 CORR=-COR
      ESIN=  DSIN(PHI(N))
      ECOS=  DCOS(PHI(N))
      IF(DABS(ESIN).LT.PRIS)  ESIN=0.
      IF(DABS(ECOS).LT.PRIS)  ECOS=0.
      CALL DISPL1(Q,PHI(N),D1,D2,R(N))
      IF(K.LE.NOOFXX)  COEF(K,2*J-1) = COEF(K,2*J-1) - ( D1*ECOS - D2*ES
     *IN)*CONK
      IF(I.EQ.NOOFXX)  COEF(NOOFU5,2*J-1) = D1*ECOS - D2*ESIN
   19 CALL DISPL2(Q,PHI(N),D1,D2,R(N))
      IF(K.LE.NOOFXX)  COEF(K,2*J) = COEF(K,2*J) - ( D1*ECOS - D2*ESIN)*
     *CONK
      IF(I.EQ.NOOFXX)  COEF(NOOFU5,2*J) = D1*ECOS - D2*ESIN
   18 Q=Q+1.D0
C
C         JUGGLING COEFFICIENTS AND SOLVING FOR SOLUTIONS
C
      DO 828 I=1,NOOFR
      TEMP = COEF(I,NOOFS)
      DO 9174 II=2,NOOFS
      II1 = NOOFS + 1 - JI
 9174 COEF(I,II1 + 1) = COEF(I,II1)
  828 COEF(I,1) = TEMP
      CALL ARRAY1(NOOFXY,NOOFS,NOOFU5,NOOFS,COEFCK,COEF)
      DO 9614 I=1,NOOFXY
 9614 CONCHK(I) = CON(I)
      CALL DLLSQ(COEFCK,CONCHK,NOOFXY,NOOFS,1,SOL,IPIV,1.E-72,IER,V9)
      SEFK1 =-2.506628274631D0*SOL(2)
      CONP = CONP*CONW
C
C         OUTPUT
C
 8000 WRITE(6,810)    (STAR(I),I=1,30)
  810 FORMAT(1H1/1H1 //  30A4)
      WRITE(6,873)     (NAME(I),I=1,18)
  873 FORMAT(    //30X,' S T R E S S  I N T E N S I T Y  F A C T O R  A N
     * A L Y S I S'// 20X,'CASE :',18A4)
      WRITE(6,871) CONF,CONV,CONH,COND,C1,CONW,CONEF,CONP,CONA,NOOFS
  871 FORMAT(  //56X,'PARAMETERS'  //25X,'PAVEMENT :'  //30X,'YOUNG MODU
     *LUS',F10.1,20X,'POISSON|S RATIO',F10.4 / 30X,'THICKNESS',4X,F10.1,
     *20X,'PAVEMENT LENGTH',F10.2  / 30X,'CRACK LENGTH',1X,F10.4,20X,'PA
     *VEMENT WIDTH',1X,F10.2  // 25X,'FOUNDATION :'   //  30X,'YOUNG MOD
     *ULUS'  ,F10.1,20X,'POISSON|S RATIO    0.5000'  / 30X,'THICKNESS',
     *6X,'SEMI-INFINITE'  //  25X,'OTHERS :'  //  30X,'LOAD',09X,F10.1,
     *20X,'LOADED AREA|S LENGTH',F8.4  /  30X,'NUMBER OF SOLUTIONS',I4 )
      IF(SOLUCK)  GO TO 6718
      WRITE(6,6719)
 6719 FORMAT(//  15X,'* * * * * INPUTED VARIABLES DO NOT SATISFY EQUATIO
     *N (4) IN TEXT -- EXECTION WAS TERMINATED * * * * *' )
 6718 IF(ZEROCK)  GO TO 879
      WRITE(6,876)
  876 FORMAT(//  15X,'* * * * * THEORY IS NOT VALID FOR SPECIFIED CRACK
     *LENGTH  --  EXECUTION WAS TERMINATED * * * * *')
      GO TO 877
```

```
  879 IF(IER.EQ.0)GO TO 878
      WRITE(6,90)
   90 FORMAT(///01X'* * * * * SOLUTION PROCEDURE INDICATES MATRIX SEVERE
     *LY ILL-CONDITIONED OR RANK LESS THAN NUMBER OF COLUMNS * * * * *')
  878 WRITE(6,299)  SEEK1
  299 FORMAT(  ///  20X,'STRESS INTENSITY FACTER K1 =',D24.10)
  877 WRITE(6,811)   (STAR(I),I=1,30)
      IF(PRISCK) GO TO 293
      GO TO 9000
  293 WRITE(6,8107)  (STAR(I),I=1,30)
 8107 FORMAT(1H1//  30A4)
      DO 32  I=1, NOOFR
      CALC(I)=0.
      IF(I.EQ.NOOFR)  CALC(I) = SOL(1)
      DO 32  J=2, NOOFS
   32 CALC(I)= CALC(I) + SOL(J)*COEF(I,J)
      DO 5268 I=1, NOOFS5
 5268 CADD(I) = CON(I) - CALC(I)
      WRITE(6,296) NOOFXL,NOOFTO,NOOFXT,NOOFT1,NOOFXX,NOOFY1,NOOFYY,
     *NOOFB1,NOOFC1,NOOFD1,NOOFF1,NOOFG1,NOOFXY,NOOFS5,NOOFU5
  296 FORMAT(  ///  35X ,'* * * * * OUTPUT CHECK ON SOLUTION FIT * * * *
     * *'   ///  43X 'SUMMARY OF BOUNDARY REQUIREMENTS'  //  30X,'EQUATI
     *ONS   1 TO',I4,' SIGMA XX1 ON TOP BOUNDARY -- LOCATIONS UNDER LOAD
     *' /30X, 'EQUATIONS',I4,' TO';I4,' SIGMA XX1 ON TOP BOUNDARY -- REM
     *AINING LOCATIONS'   /   30X,       'EQUATIONS'  ,  I4   ,          '
     * TO',I4,' SIGMA XX1 ON BOTTOM BOUNDARY'  /30X,'EQUATIONS',I4, ' TO
     *',I4,' SIGMA YY1 ON SIDE BOUNDARY'/30X,'EQUATIONS',I4,' TO',I4,' S
     *IGMA XY1 ON TOP BOUNDARY' /30X,'EQUATIONS',I4,' TO',I4,' SIGMA XY1
     * ON SIDE BOUNDARY'/30X,'EQUATIONS',I4,' TO',I4, ' SIGMA XY1 ON BOT
     *TOM BOUNDARY' / 30X, 'EQUATION',8X,I4, ' SIGMA XX1 ON X AXIS AT BO
     *TTOM BOUNDARY'              /30X,'EQUATION',8X,I4,' X AXIS DISPLACEM
     *ENT ON X AXIS AT TOP BOUNDARY'  )
      WRITE(6,297)
  297 FORMAT( // 14X,'EQUATION NO.',13X,'THEORETICAL VALUE',12X,'CALCUAT
     *ED VALUE',15X,'DIFFERENCE'  )
      WRITE(6,291)  (I,CON(I),CALC(I),CADD(I),I=1,NOOFS5)
  291 FORMAT(17X,I3,10X,3D28.16)
      WRITE(6,8261) NOOFU5,CALC(NOOFU5)
 8261 FORMAT(17X,I3,20X,'UNKNOWN',11X,D28.16)
      WRITE(6,811)   (STAR(I),I=1,30)
  811 FORMAT(///   30A4)
      GO TO 9000
 1001 STOP
      END
      SUBROUTINE STRES1 (S,PHEE,D2PDR2,DPDR,D2PDRP,DPDP,D2PDP2,RR)
      IMPLICIT REAL*8 (A-H,O-Z)
      COMMON  PRIS,V1,E1,COR,CORR
      ECOS=  DCOS((S-1.5D0)*PHEE)
      FCOS=  DCOS((S+0.5D0)*PHEE)
      ESIN=  DSIN((S-1.5D0)*PHEE)
      FSIN=  DSIN((S+0.5D0)*PHEE)
      IF(DABS(ESIN).LT.PRIS)  ESIN=0.
      IF(DABS(ECOS).LT.PRIS)  ECOS=0.
      IF(DABS(FCOS).LT.PRIS)  FCOS=0.
      IF(DABS(FSIN).LT.PRIS)  FSIN=0.
      D2PDR2=(  -ECOS +((2.D0*S-3.D0)/(2.D0*S+1.D0))*FCOS)* (S**2-.25D0)
     **RR**(S-1.5D0)*(+1.D0)**(S-1.D0)*CORR
      DPDR=D2PDR2*RR/(S-.5D0)
      D2PDRP=((S-1.5D0)*ESIN -(S-1.5D0)*FSIN)*(S+.5D0)*RR**(S-.5D0)*
     *(+1.D0)**(S-1.D0)*CORR
      DPDP=D2PDRP*RR/(S+.5D0)
      D2PDP2=   ((S-1.5D0)**2*ECOS   -(S-1.5D0)*(S+.5D0)*FCOS)*RR**(S+.5
```

```
*D0)*(+1.D0)**(S-1.D0)*CORR
 RETURN
 END
 SUBROUTINE STRES2 (S,PHEE,D2PDR2,DPDR,D2PDRP,DPDP,D2PDP2,RR)
 IMPLICIT REAL*8 (A-H,O-Z)
 COMMON  PRIS,V1,E1,COR,CORR
 FSIN=  DSIN((S+1.D0)*PHEE)
 ECOS=  DCOS((S-1.D0)*PHEE)
 ESIN=  DSIN((S-1.D0)*PHEE)
 FCOS=  DCOS((S+1.D0)*PHEE)
 IF(DABS(ESIN).LT.PRIS)  ESIN=0.
 IF(DABS(ECOS).LT.PRIS)  ECOS=0.
 IF(DABS(FSIN).LT.PRIS)  FSIN=0.
 IF(DABS(FCOS).LT.PRIS)  FCOS=0.
 D2PDR2=    (-ECOS +FCOS)*(S*S+S)*RR**(S-1.D0)*(+1.D0)**S*COR
 DPDR=D2PDR2*RR/S
 D2PDRP=    ((S-1.D0)*ESIN -(S+1.D0)*FSIN)*(S+1.D0)*RR**S*(+1.D0)**S
**COR
 DPDP=D2PDRP*RR/(S+1.D0)
 D2PDP2=   ((S-1.D0)**2*ECOS  -(S+1.D0)**2*FCOS)*RR**(S+1.D0)*(+1.D0
*)**S*COR
 RETURN
 END
 SUBROUTINE DISPL1(S,PHEE,U,V,RR)
 IMPLICIT REAL*8 (A-H,O-Z)
 COMMON  PRIS,V1,E1,COR,CORR
 ECOS=  DCOS((S-1.5D0)*PHEE)
 FCOS=  DCOS((S+0.5D0)*PHEE)
 FSIN=  DSIN((S+0.5D0)*PHEE)
 ESIN=  DSIN((S-1.5D0)*PHEE)
 IF(DABS(ESIN).LT.PRIS)  ESIN=0.
 IF(DABS(FSIN).LT.PRIS)  FSIN=0.
 IF(DABS(ECOS).LT.PRIS)  ECOS=0.
 IF(DABS(FCOS).LT.PRIS)  FCOS=0.
 V=  ((2.5D0+S-4.D0*V1)*ESIN - (S-1.5D0)*FSIN)*(1.D0+V1)/E1*(+1.D0)
***S*RR**(S-.5D0)*COR
 U=  ((3.5D0-S-4.D0*V1)*ECOS + (S-1.5D0)*FCOS)*(1.D0+V1)/E1*(+1.D0)
***S*RR**(S-.5D0)*COR
 RETURN
 END
 SUBROUTINE DISPL2(S,PHEE,U,V,RR)
 IMPLICIT REAL*8 (A-H,O-Z)
 COMMON  PRIS,V1,E1,COR,CORR
 FSIN=  DSIN((S+1.D0)*PHEE)
 FCOS=  DCOS((S+1.D0)*PHEE)
 ESIN=  DSIN((S-1.D0)*PHEE)
 ECOS=  DCOS((S-1.D0)*PHEE)
 IF(DABS(ESIN).LT.PRIS)  ESIN=0.
 IF(DABS(ECOS).LT.PRIS)  ECOS=0.
 IF(DABS(FCOS).LT.PRIS)  FCOS=0.
 IF(DABS(FSIN).LT.PRIS)  FSIN=0.
 V=  (-(3.D0+S-4.D0*V1)*ESIN +  (S+1.D0)*FSIN)*(1.D0+V1)/E1*(+1.D0)
***S*RR**S*COR
 U=  (+(3.D0-S-4.D0*V1)*ECOS +  (S+1.D0)*FCOS)*(1.D0+V1)/E1*(+1.D0)
***(S+1.D0)*RR**S*CORR
 RETURN
 END
 SUBROUTINE ARRAY1(I,J,N,M,S,D)
 REAL*8 S,D
 DIMENSION  S(1),D(1)
 NI = N - I
 IJ = 0
```

```
      NM = 0
      DO 130 K=1,J
      DO 125 L=1,I
      IJ = IJ + 1
      NM = NM + 1
  125 S(IJ) = D(NM)
  130 NM = NM + NI
      RETURN
      END
      SUBROUTINE DLLSQ(A,B,M,N,L,X,IPIV,EPS,IER,AUX)
      DIMENSION A(1),B(1),X(1),IPIV(1),AUX(1)
      DOUBLE PRECISION A,B,X,AUX,PIV,H,SIG,BETA,TOL
    1 PIV=0.D0
      IEND=0
      DO 4 K=1,N
      IPIV(K)=K
      H=0.D0
      IST=IEND+1
      IEND=IEND+M
      DO 2 I=IST,IEND
    2 H=H+A(I)*A(I)
      AUX(K)=H
      IF(H-PIV)4,4,3
    3 PIV=H
      KPIV=K
    4 CONTINUE
    5 SIG=DSQRT(PIV)
      TOL=SIG*ABS(EPS)
      LM=L*M
      IST=-M
      DO 21 K=1,N
      IST=IST+M+1
      IEND=IST+M-K
      I=KPIV-K
      IF(I)8,8,6
    6 H=AUX(K)
      AUX(K)=AUX(KPIV)
      AUX(KPIV)=H
      ID=I*M
      DO 7 I=IST,IEND
      J=I+ID
      H=A(I)
      A(I)=A(J)
    7 A(J)=H
    8 IF(K-1)11,11,9
    9 SIG=0.D0
      DO 10 I=IST,IEND
   10 SIG=SIG+A(I)*A(I)
      SIG=DSQRT(SIG)
      IF(SIG-TOL)32,32,11
   11 H=A(IST)
      IF(H)12,13,13
   12 SIG=-SIG
   13 IPIV(KPIV)=IPIV(K)
      IPIV(K)=KPIV
      BETA=H+SIG
      A(IST)=BETA
      BETA=1.D0/(SIG*BETA)
      J=N+K
      AUX(J)=-SIG
      IF(K-N)14,19,19
   14 PIV=0.D0
```

```
      ID=0
      JST=K+1
      KPIV=JST
      DO 18 J=JST,N
      ID=ID+M
      H=0.D0
      DO 15 I=IST,IEND
      II=I+ID
   15 H=H+A(I)*A(II)
      H=BETA*H
      DO 16 I=IST,IEND
      II=I+ID
   16 A(II)=A(II)-A(I)*H
      II=IST+ID
      H=AUX(J)-A(II)*A(II)
      AUX(J)=H
      IF(H-PIV)18,18,17
   17 PIV=H
      KPIV=J
   18 CONTINUE
   19 DO 21 J=K,LM,M
      H=0.D0
      IEND=J+M-K
      II=IST
      DO 20 I=J,IEND
      H=H+A(II)*B(I)
   20 II=II+1
      H=BETA*H
      II=IST
      DO 21 I=J,IEND
      B(I)=B(I)-A(II)*H
   21 II=II+1
      IER=0
      I=N
      LN=L*N
      PIV=1.D0/AUX(2*N)
      DO 22 K=N,LN,N
      X(K)=PIV*B(I)
   22 I=I+M
      IF(N-1)26,26,23
   23 JST=(N-1)*M+N
      DO 25 J=2,N
      JST=JST-M-1
      K=N+N+1-J
      PIV=1.D0/AUX(K)
      KST=K-N
      ID=IPIV(KST)-KST
      IST=2-J
      DO 25 K=1,L
      H=B(KST)
      IST=IST+N
      IEND=IST+J-2
      II=JST
      DO 24 I=IST,IEND
      II=II+M
   24 H=H-A(II)*X(I)
      I=IST-1
      II=I+ID
      X(I)=X(II)
      X(II)=PIV*H
   25 KST=KST+M
   26 IST=N+1
```

```
      IEND=0
      DO 29 J=1,L
      IEND=IEND+M
      H=0.D0
      IF(M-N)29,29,27
   27 DO 28 I=IST,IEND
   28 H=H+B(I)*B(I)
      IST=IST+M
   29 AUX(J)=H
      RETURN
   32 IER=K-1
      RETURN
      END
```

DUMMY DATA

```
ASPHALTIC CONCRETE
      2.000D0                    2.000D0                    .5000D0
   200000.0D0                    89.02D0                     .5000D0
     2.0D0
      30        12        17        17   .TRUE.
       5          .500D0                 20.0D0
```

Word	1 - 18
Column	1 - 72
Format	18 A4
Card 1 Title	Alphanumeric Title
Symbol	Name (I), I = 1, 18

18 A 4

Word	1	2	3
Column	1 - 24	25 - 48	49 - 72
Format	D 24.16	D 24.16	D 24.16
Card 2 Material Properties	Pavement's Thickness	Pavement's Length	Pavement's Crack Length
Symbol	CONH	COND	C1

3 D 24.16

Word	1	2	3
Column	1 - 24	25 - 48	49 - 72
Format	D 24.16	D 24.16	D 24.16
Card 3 Additional Material Properties	Pavement's Young's Modulus	Foundation's Young's Modulus	Pavement's Poisson Ratio
Symbol	CONE	CONEF	CONV

2 D 24.16

Word	1
Column	1 - 24
Format	D 24.16
Card 4 Additional Material Properties	Pavement's Width
Symbol	CONW

D 24.16

Word	1	2	3	4	5	
Column	1 - 10	11 - 20	21 - 30	31 - 40	41 - 50	
Format	I 10	I 10	I 10	I 10	I 10	
Card 5 Colloca-tion Const.	Number of William's Stress Functions	Number of Boundary Stations on Top Layer Outside Load	Number of Boundary Stations on Side Layer	Number of Boundary Stations on Bottom Layer	Logical Constant	
Symbol	NOOFM	NOOFXU	NOOFXS	NOOFXB	PRISCK	4 I 10, L 10

Note: Enter "TRUE" for PRISCK if an accuracy check is desired; otherwise leave blank.

Word	1	2	3	
Column	1 - 10	11 - 34	35 - 58	
Format	I 10	D 24.10	D 24.10	
Card 6 Additional Colloca-tion Const.	Number of Boundary Stations on Top Layer Under Load	Pavement's Length of Loaded Area	Total System Load	
Symbol	NOOFXL	CONA	CONP	I10, 2 D 24.10

APPENDIX F
Finite Element Program for

Beam on Elastic Analysis
INPUT INSTRUCTION FOR 2-DIMENSIONAL
FINITE ELEMENT PROGRAM

Card
Type (FORMAT)

1. BEGIN (A6)

A card of this type must preceed each problem set.

2. JOB TITLE (18A4)

This title is printed as a description or identification of the problem.

3. CONTROL INFORMATION (4I5, 3F10.2)

Columns	
1 - 5	Number of nodal points
6 - 10	Number of elements
11 - 15	Number of different materials
16 - 20	Number of boundary pressure cards
21 - 30	Acceleration in X-direction
31 - 40	Acceleration in Y-direction
41 - 50	Reference temperature

4. STRESS INTENSITY FACTOR INFORMATION (8F10.0)

Columns	
1 - 10	X coordinate of crack tip
11 - 20	Y coordinate of crack tip
21 - 30	Radius around crack tip for calculation of stress intensity factors
31 - 40	Concentrated load in pounds
41 - 50	Top layer thickness
51 - 60	Bottom layer thickness
61 - 70	Temperature at top
71 - 80	Temperature at bottom

5. MATERIAL PROPERTIES

One set of material property cards for each material. In each set:

(a) First card (2I5, F10.0)

Columns	
1 - 5	Material identification number
6 - 10	Number of temperature cards (8 max.)
11 - 20	Mass density of the material

(b) Subsequent cards - one for each temperature (4F10.3)

Columns	
1 - 10	Temperature
11 - 20	Elastic modulus
21 - 30	Poisson's Ratio
31 - 40	Coefficients of thermal expansion

6. NODAL POINT INFORMATION (I5, F5.0, 5F10.0)

One card for each nodal point.

Columns	
1 - 5	Nodal point number
6 - 10	Nodal point type - see following explanation
11 - 20	X - ordinate
21 - 30	Y - ordinate
31 - 40	XR
41 - 50	XZ
51 - 60	Temperature

N. P. Types:

0.	XR is specified X load and XZ is specified Y load.
1.	XR is specified X displacement and XZ is specified Y load.
2.	XR is specified X load and XZ is specified Y displacement.
3.	XR is specified X displacement and XZ is specified Y displacement.

7. ELEMENT INFORMATION (6I5)

One card for each element.

Columns	
1 - 5	Number of element
6 - 10	Nodal point I
11 - 15	Nodal point J
16 - 20	Nodal point K
21 - 25	Nodal point L
26 - 30	Material type

The nodal points are the corners of each element and numbered in a counter-clockwise order for a right-handed coordinate system. Triangular elements also have four nodal points with the last two sets equal (K = L).

8. BOUNDARY PRESSURE (2I5, 2F10.0)

One card for each boundary element under normal pressure.

Columns	
1 - 5	Nodal point I
5 - 10	Nodal point J
11 - 20	Normal pressure at I
21 - 30	Normal pressure at J

The boundary element must be on the left as one progresses numerically from I to J. Surface tensile force is input as negative pressure.

9. END (A6)

This card must be at the end of the problem set or after the last set if more than one problem set is to be computed.

PROGRAM GENERATED INPUT

The nodal point cards and element cards must be in numerical sequence. If cards are omitted the program supplies the missing data by: 1) linear interpolation of nodal points and temperatures between the defined values with nodal point type, XR and XZ set equal to zero, and 2) incrementing I, J, K, and L values by one for missing element information with the material type the same as for the last element defined.

NOTE: The finite element method as used in this program assumes linear isotropic elasticity. The mesh of elements as defined in the above instructions is assumed to be of unit thickness. Thus, loads must be the total forces acting on elements of unit thickness.

It also must be noted that the program is dimensioned to handle a maximum of 900 elements and a maximum of 900 nodal points. The greatest difference between nodal points on any element should not exceed 29.

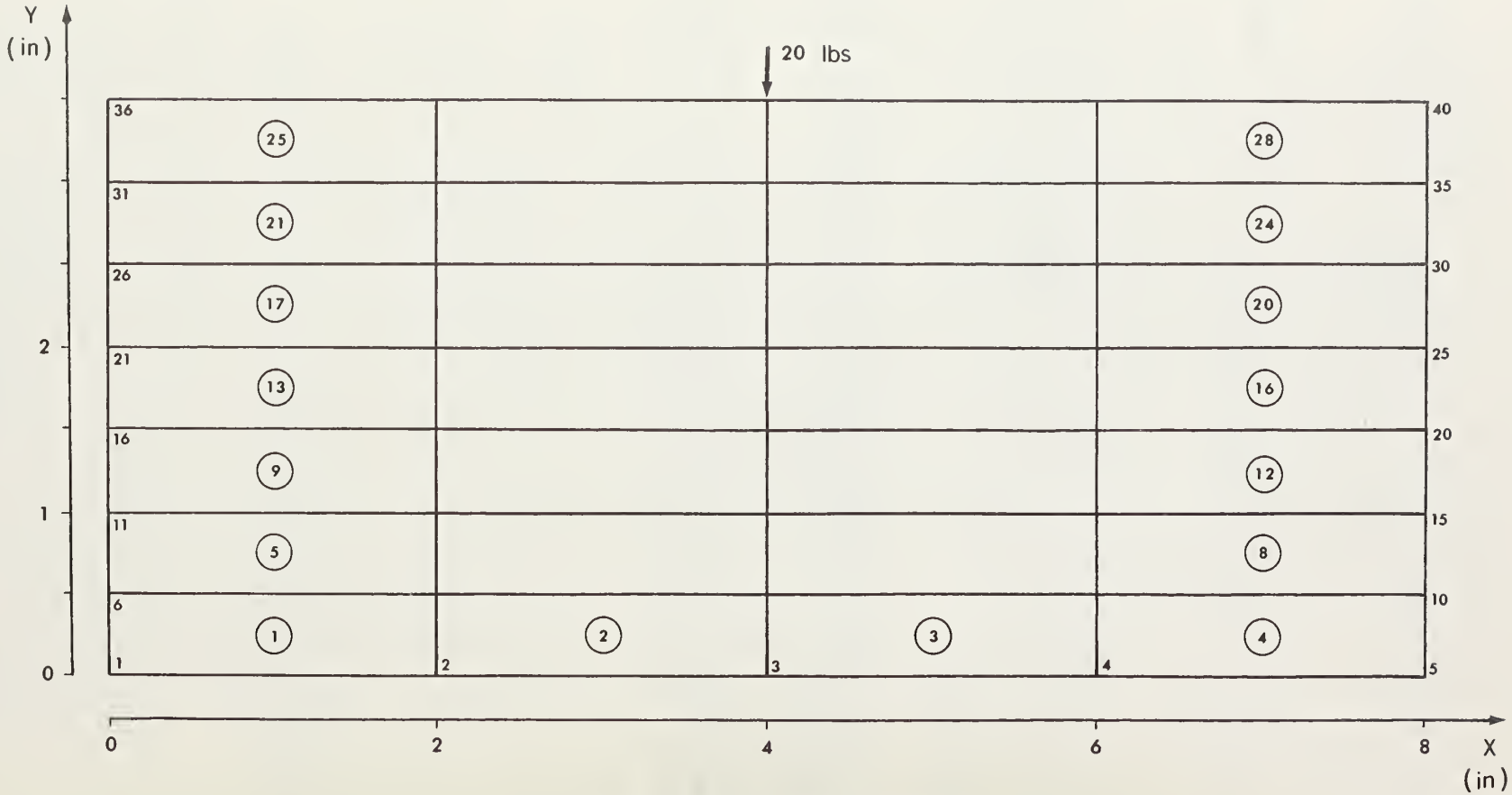

Simple Finite Element Example

Rigidly Supported Beam Loaded at its Center

```
C     ARBITRARY TWO DIMENSIONAL STRUCTURES
C     LINEAR PRESSURE BOUNDARY
      DOUBLE PRECISION S,C,B,A,P,ST,SIG,U,V,CC,BB,CR,AREA,COMM,DU,DV,DL,
     1 DX,DY,XL,RR,CARD1,CARD(2)
      COMMON NUMNP,NUMEL,NUMMAT,NUMPC,ACELR,ACELZ,N,VOL,TEMP,MTYPE,Q,    MAIN0002
     1 HED(18),E(8,4,12),RO(12),NTC(8),R(900),Z(900),UR(900),UZ(900),   MAIN0003
     2 CODE(900),T(900),IBC(200),JBC(200),PR(200,2)                     MAIN0004
      COMMON /ARG/C(3,3),S(10,10),SIG(6),P(8),ST(3,10),RR(5),ZZ(5),
     1LM(4),EE(3),IX(800,5),XC,YC
      COMMON /BANARG/ MBAND,NUMBLK,B(144),A(144,72)
      COMMON /SIFARG/ SIF(200),SSIF(200),THETA(200),DDRC(200),MD(200),
     1                NK,DRC,DXC,DYC
      COMMON /SYSARG/ DDX,DDY,DDR,DDP
      COMMON /SIGN/ STOP
      DATA CARD/'BEGIN ','END   '/
   20 READ(5,999) CARD1
      IF(CARD1.EQ.CARD(1)) GO TO 30
      IF(CARD1.EQ.CARD(2)) STOP
      GO TO 20
   30 READ  (5,1000) HED,NUMNP,NUMEL,NUMMAT,NUMPC,ACELR,ACELZ,Q         MAIN0008
      WRITE (6,2000) HED,NUMNP,NUMEL,NUMMAT,NUMPC,ACELR,ACELZ,Q         MAIN0009
C     ****************************************************************
C     *  INPUT THE FOLLOWING INFORMATIONS:                            *
C     *  1. DDX,DDY = TIP OF CRACK                                    *
C     *  2.     DDR = RADIUS AROUND THE CRACK                         *
C     *  3.     DDP = CONCENTRATED LOAD                               *
C     *  4. HTOP,HBOT = HT.S OF TOP LAYER AND BOTTOM LAYER            *
C     *  5. TTOP,TBOT = TEMP.S AT TOP AND BOTTOM                      *
C     ****************************************************************
      READ(5,2011) DDX,DDY,DDR,DDP,HTOP,HBOT,TTOP,TBOT
      WRITE(6,2012) DDX,DDY,DDR,DDP,HTOP,HBOT,TTOP,TBOT
C     ****************************************************************
   40 DO 50 M=1,NUMMAT                                                  MAIN0010
      READ (5,1001) MTYPE,NTC(MTYPE),RO(MTYPE)                          MAIN0011
      WRITE(6,2001) MTYPE,NTC(MTYPE),RO(MTYPE)                          MAIN0012
      NUMTC=NTC(MTYPE)                                                  MAIN0013
```

```
      READ (5,1002) ((E(I,J,MTYPE),J=1,4),I=1,NUMTC)                    MAIN0014
      WRITE (6,2002) ((E(I,J,MTYPE),J=1,4),I=1,NUMTC)                   MAIN0015
   50 CONTINUE                                                          MAIN0016
      WRITE (6,2003)                                                    MAIN0017
      L=0                                                               MAIN0018
C     ******************************************************************
C     *  ASSUME CONSTANT TEMP. IN THE BOT. LAYER AND LINEAR TEMP.      *
C     *  DIST. IN THE TOP LAYER                                        *
C     ******************************************************************
   60 READ  (5,1003) N,CODE(N),R(N),Z(N),UR(N),UZ(N),T(N)               MAIN0022
      NL=L+1                                                            MAIN0023
      ZX=N-L                                                            MAIN0024
      IF(L.NE.0) GO TO 65
      DR=R(N)/ZX
      DZ=Z(N)/ZX
      GO TO  66
   65 DR=(R(N)-R(L))/ZX
      DZ=(Z(N)-Z(L))/ZX
   66 TOTH=HTOP+HBOT
      T(N)=TTOP+(TBOT-TTOP)*(TOTH-Z(N))/HTOP
      IF(Z(N).LE.HBOT) T(N)=TBOT
   70 L=L+1
      IF(N-L) 100,90,80
   80 CODE(L)=0.0
      IF(L.NE.1) GO TO  85
      R(L)= DR
      Z(L)= DZ
      GO TO 86
   85 R(L)=R(L-1)+DR
      Z(L)=Z(L-1)+DZ
   86 T(L)=TTOP+(TBOT-TTOP)*(TOTH-Z(L))/HTOP
      IF(Z(L).LE.HBOT) T(L)=TBOT
      UR(L)=0.0                                                         MAIN0034
      UZ(L)=0.0                                                         MAIN0035
      GO TO 70                                                          MAIN0036
   90 WRITE (6,2004) (K,CODE(K),R(K),Z(K),UR(K),UZ(K),T(K),K=NL,N)
```

```
      IF(NUMNP-N) 100,110,60                                            MAIN0038
  100 WRITE (6,2005) N                                                  MAIN0039
      GO TO 20
  110 CONTINUE                                                          MAIN0041
      WRITE (6,2006)                                                    MAIN0042
      N=0                                                               MAIN0043
  130 READ (5,1004) M,(IX(M,I),I=1,5)                                   MAIN0044
  140 N=N+1                                                             MAIN0045
      IF (M-N) 170,170,150                                              MAIN0046
  150 IX(N,1)=IX(N-1,1)+1                                               MAIN0047
      IX(N,2)=IX(N-1,2)+1                                               MAIN0048
      IX(N,3)=IX(N-1,3)+1                                               MAIN0049
      IX(N,4)=IX(N-1,4)+1                                               MAIN0050
      IX(N,5)=IX(N-1,5)                                                 MAIN0051
  170 WRITE (6,2007) N,(IX(N,I),I=1,5)
      IF (M-N) 180,180,140                                              MAIN0053
  180 IF (NUMEL-N) 190,190,130                                          MAIN0054
  190 CONTINUE                                                          MAIN0055
      IF (NUMPC) 290,310,290                                            MAIN0056
  290 WRITE (6,2008)                                                    MAIN0057
      DO 300 L=1,NUMPC                                                  MAIN0058
      READ(5,1005) IBC(L),JBC(L),PR(L,1),PR(L,2)                        MAIN0059
  300 WRITE(6,2009) IBC(L),JBC(L),PR(L,1),PR(L,2)                       MAIN0060
  310 CONTINUE                                                          MAIN0061
      J=0                                                               MAIN0062
      DO 340 N=1,NUMEL                                                  MAIN0063
      DO 340 I=1,4                                                      MAIN0064
      DO 325 L=1,4                                                      MAIN0065
      KK=IABS(IX(N,I)-IX(N,L))                                          MAIN0066
      IF (KK-J) 325,325,320                                             MAIN0067
  320 J=KK                                                              MAIN0068
  325 CONTINUE                                                          MAIN0069
  340 CONTINUE                                                          MAIN0070
      MBAND=2*J+2                                                       MAIN0071
  350 CALL STIFF                                                        MAIN0072
      IF(STOP.EQ.1.) GO TO 20
```

```
      CALL BANSOL                                                       MAIN0073
      WRITE (6,2010) (N,B(2*N-1),B(2*N),N=1,NUMNP)                      MAIN0074
      CALL STRESS                                                       MAIN0075
      GO TO 20
  999 FORMAT (A6)
 1000 FORMAT (18A4/4I5,3F10.2)                                          MAIN0077
 1001 FORMAT (2I5,1F10.3)                                               MAIN0078
 1002 FORMAT (4F10.3)                                                   MAIN0079
 1003 FORMAT (I5,F5.1,5F10.4)
 1004 FORMAT (6I5)                                                      MAIN0081
 1005 FORMAT(2I5,2F10.3)                                                MAIN0082
 2000 FORMAT (1H1 18A4/                                                 MAIN0083
     1 30H0 NUMBER OF NODAL POINTS------ I3 /                           MAIN0084
     2 30H0 NUMBER OF ELEMENTS---------- I3 /                           MAIN0085
     3 30H0 NUMBER OF DIFF. MATERIALS--- I3 /                           MAIN0086
     4 30H0 NUMBER OF PRESSURE CARDS---- I3 /                           MAIN0087
     5 30H0 X-ACCELERATION-------------- E12.4/                        MAIN0088
     6 30H0 Y-ACCELERATION-------------- E12.4/                        MAIN0089
     7 30H0 REFERENCE TEMPERATURE------- E12.4)                        MAIN0090
 2001 FORMAT (17H0MATERIAL NUMBER= I3, 30H, NUMBER OF TEMPERATURE CARDS=MAIN0091
     1 I3, 15H, MASS DENSITY= E12.4 )                                   MAIN0092
 2002 FORMAT (15H0  TEMPERATURE 10X 5HE     9X 6HNU     10X 5HALPHA/    MAIN0093
     1(F15.2,3E15.5))                                                   MAIN0094
 2003 FORMAT (108H1NODAL POINT        TYPE  X ORDINATE  Y ORDINATE  X LOMAIN0095
     1AD OR DISPLACEMENT  Y LOAD OR DISPLACEMENT TEMPERATURE )          MAIN0096
 2004 FORMAT (I12,F12.2,2F12.5,2E24.7,F12.3)
 2005 FORMAT (26H0NODAL POINT CARD ERROR N= I5)                         MAIN0098
 2006 FORMAT (49H1ELEMENT NO.      I     J     K     L    MATERIAL  )   MAIN0099
 2007 FORMAT (1I13,4I6,1I12)                                            MAIN0100
 2008 FORMAT(29H0PRESSURE BOUNDARY CONDITIONS/40H     I     J    PRESSURMAIN0101
     1E I    PRESSURE J)                                                MAIN0102
 2009 FORMAT(2I6,2F14.3)                                                MAIN0103
 2010 FORMAT (12H1N.P. NUMBER 18X 2HUX 18X 2HUY / (1I12,2E20.7))        MAIN0104
 2011 FORMAT(8F10.0)
 2012 FORMAT(//' CRACK TIP X                    =',F10.5/
     1         ' CRACK TIP Y                    =',F10.5/
```

```
2          ' RADIUS OF THE CRACK TIP      =',F10.5/
3          ' CONCENTRATED LOAD            =',F10.5/
4          ' HT. OF TOP LAYER             =',F10.5/
5          ' HT. OF BOT.LAYER             =',F10.5/
6          ' TEMP. AT TOP                 =',F10.5/
7          ' TEMP. AT BOT.                =',F10.5/
 END                                                          MAIN0105
```

```
      SUBROUTINE STIFF
C
      DOUBLE PRECISION S,C,B,A,P,ST,SIG,U,V,CC,BB,CR,AREA,COMM,DU,DV,DL,
     1DX,DY,XL,RR
      COMMON NUMNP,NUMEL,NUMMAT,NUMPC,ACELR,ACELZ,N,VOL,TEMP,MTYPE,Q,    STIF0002
     1 HED(18),E(8,4,12),RO(12),NTC(8),R(900),Z(900),UR(900),UZ(900),    STIF0003
     2 CODE(900),T(900),IBC(200),JBC(200),PR(200,2)                      STIF0004
      COMMON /ARG/C(3,3),S(10,10),SIG(6),P(8),ST(3,10),RR(5),ZZ(5),
     1LM(4),EE(3),IX(800,5),XC,YC
      COMMON /BANARG/ MBAND,NUMBLK,B(144),A(144,72)
      COMMON /SIGN/ STOP
      REWIND 2                                                           STIF0008
      NB=36
      ND=2*NB                                                            STIF0010
      ND2=2*ND                                                           STIF0011
      STOP=0.0                                                           STIF0012
      NUMBLK=0                                                           STIF0013
      DO 50 N=1,ND2                                                      STIF0014
      B(N)=0.0                                                           STIF0015
      DO 50 M=1,ND                                                       STIF0016
   50 A(N,M)=0.0                                                         STIF0017
   60 NUMBLK=NUMBLK+1                                                    STIF0018
      NH=NB*(NUMBLK+1)                                                   STIF0019
      NM=NH-NB                                                           STIF0020
      NL=NM-NB+1                                                         STIF0021
      KSHIFT=2*NL-2                                                      STIF0022
      DO 210 N=1,NUMEL                                                   STIF0023
      IF (IX(N,5)) 210,210,65                                            STIF0024
   65 DO 80 I=1,4                                                        STIF0025
      IF (IX(N,I)-NL) 80,70,70                                           STIF0026
   70 IF (IX(N,I)-NM) 90,90,80                                           STIF0027
   80 CONTINUE                                                           STIF0028
      GO TO 210                                                          STIF0029
   90 IF(IX(N,3)-IX(N,2)) 95,85,95
   85 CALL ONED
      IX(N,5)=-IX(N,5)
```

```
      MM=2
      GO TO 130
   95 CALL QUAD
      IX(N,5)=-IX(N,5)                                                  STIF0031
      IF(VOL) 100,100,110                                               STIF0032
  100 WRITE(6,2000) N                                                   STIF0033
      STOP=1.0                                                          STIF0034
  110 MM=4                                                              STIF0035
      IF(IX(N,3)-IX(N,4)) 130,120,130                                   STIF0036
  120 MM=3                                                              STIF0037
  130 DO 140 I=1,MM                                                     STIF0038
  140 LM(I)=2*IX(N,I)-2                                                 STIF0039
      DO 200 I=1,MM                                                     STIF0040
      DO 200 K=1,2                                                      STIF0041
      II=LM(I)+K-KSHIFT                                                 STIF0042
      KK=2*I-2+K                                                        STIF0043
      B(II)=B(II)+P(KK)                                                 STIF0044
      DO 200 J=1,MM                                                     STIF0045
      DO 200 L=1,2                                                      STIF0046
      JJ=LM(J)+L-II+1-KSHIFT                                            STIF0047
      LL=2*J-2+L                                                        STIF0048
      IF(JJ) 200,200,175                                                STIF0049
  175 IF(ND-JJ) 180,195,195                                             STIF0050
  180 WRITE (6,2001) N                                                  STIF0051
      STOP=1.0                                                          STIF0052
      GO TO 210                                                         STIF0053
  195 A(II,JJ)=A(II,JJ)+S(KK,LL)                                        STIF0054
  200 CONTINUE                                                          STIF0055
  210 CONTINUE                                                          STIF0056
      DO 220 N=NL,NM                                                    STIF0057
      IF(N-NUMNP) 215,215,220
  215 K=2*N-KSHIFT
      B(K)=B(K)+UZ(N)                                                   STIF0059
      B(K-1)=B(K-1)+UR(N)
  220 CONTINUE
      IF(NUMPC) 225,310,225                                             STIF0061
```

```
  225 DO 300 L=1,NUMPC                                                  STIF0062
      I=IBC(L)                                                          STIF0063
      J=JBC(L)                                                          STIF0064
      DR=Z(I)-Z(J)                                                      STIF0065
      DZ=R(J)-R(I)                                                      STIF0066
      PP2=(PR(L,2)+PR(L,1))/6.                                          STIF0067
      PP1=PP2+PR(L,1)/6.                                                STIF0068
      PP2=PP2+PR(L,2)/6.                                                STIF0069
      II=2*I-KSHIFT                                                     STIF0070
      JJ=2*J-KSHIFT                                                     STIF0071
      IF(II) 265,265,235                                                STIF0072
  235 IF(II-ND) 240,240,265                                             STIF0073
  240 B(II-1)=B(II-1)+PP1*DR                                            STIF0074
      B(II)=B(II)+PP1*DZ                                                STIF0075
  265 IF(JJ) 300,300,270                                                STIF0076
  270 IF(JJ-ND) 275,275,300                                             STIF0077
  275 B(JJ-1)=B(JJ-1)+PP2*DR                                            STIF0078
      B(JJ)=B(JJ)+PP2*DZ                                                STIF0079
  300 CONTINUE                                                          STIF0080
  310 DO 400 M=NL,NH                                                    STIF0081
      IF (M-NUMNP) 315,315,400                                          STIF0082
  315 U=UR(M)                                                           STIF0083
      N=2*M-1-KSHIFT                                                    STIF0084
      IF (CODE(M)) 390,400,316                                          STIF0085
  316 IF (CODE(M)-1.) 317,370,317                                       STIF0086
  317 IF (CODE(M)-2.) 318,390,318                                       STIF0087
  318 IF (CODE(M)-3.) 390,380,390                                       STIF0088
  370 CALL MODIFY(A,B,ND2,MBAND,N,U)                                    STIF0089
      GO TO 400                                                         STIF0090
  380 CALL MODIFY(A,B,ND2,MBAND,N,U)                                    STIF0091
  390 U=UZ(M)                                                           STIF0092
      N=N+1                                                             STIF0093
      CALL MODIFY(A,B,ND2,MBAND,N,U)                                    STIF0094
  400 CONTINUE                                                          STIF0095
      WRITE (2) (B(N),(A(N,M),M=1,MBAND),N=1,ND)                        STIF0096
      DO 420 N=1,ND                                                     STIF0097
```

```
      K=N+ND                                                            STIF0098
      B(N)=B(K)                                                         STIF0099
      B(K)=0.0                                                          STIF0100
      DO 420 M=1,ND                                                     STIF0101
      A(N,M)=A(K,M)                                                     STIF0102
  420 A(K,M)=0.0                                                        STIF0103
      IF (NM-NUMNP) 60,480,480                                          STIF0104
  480 CONTINUE                                                          STIF0105
  500 RETURN                                                            STIF0108
 2000 FORMAT (26HONEGATIVE AREA ELEMENT NO. I4)                         STIF0109
 2001 FORMAT (29HOBAND WIDTH EXCEEDS ALLOWABLE I4)                      STIF0110
      END                                                               STIF0111
```

```
      SUBROUTINE ONED
C
      DOUBLE PRECISION S,C,B,A,P,ST,SIG,U,V,CC,BB,CR,AREA,COMM,DU,DV,DL,
     1DX,DY,XL,RR
      COMMON NUMNP,NUMEL,NUMMAT,NUMPC,ACELR,ACELZ,N,VOL,TEMP,MTYPE,Q,    MAIN0002
     1 HED(18),E(8,4,12),RO(12),NTC(8),R(900),Z(900),UR(900),UZ(900),    MAIN0003
     2 CODE(900),T(900),IBC(200),JBC(200),PR(200,2)                      MAIN0004
      COMMON /ARG/C(3,3),S(10,10),SIG(6),P(8),ST(3,10),RR(5),ZZ(5),
     1LM(4),EE(3),IX(800,5),XC,YC
      COMMON /BANARG/ MBAND,NUMBLK,B(144),A(144,72)
C
      DO 100 I=1,8
      P(I)=0.0
      DO 100 J=1,8
  100 S(I,J)=0.0
      MTYPE=IX(N,5)
      I=IX(N,1)
      J=IX(N,2)
      DX=R(J)-R(I)
      DY=Z(J)-Z(I)
      XL=DSQRT(DX**2+DY**2)
      COSA=DX/XL
      SINA=DY/XL
      COMM=E(1,2,MTYPE)*E(1,4,MTYPE)/XL
C
      S(1,1)=COSA*COSA*COMM
      S(1,2)=COSA*SINA*COMM
      S(1,3)=-S(1,1)
      S(1,4)=-S(1,2)
      S(2,1)=S(1,2)
      S(2,2)=SINA*SINA*COMM
      S(2,3)=-S(1,2)
      S(2,4)=-S(2,2)
      S(3,1)=S(1,3)
      S(3,2)=S(2,3)
      S(3,3)=S(1,1)
```

```
      S(3,4)=S(1,2)
      S(4,1)=S(1,4)
      S(4,2)=S(2,4)
      S(4,3)=S(3,4)
      S(4,4)=S(2,2)
C
      EP=E(1,3,MTYPE)/E(1,2,MTYPE)
      DX=DX*EP
      DY=DY*EP
      P(1)=S(1,1)*DX+S(1,2)*DY
      P(2)=S(2,1)*DX+S(2,2)*DY
      P(3)=-P(1)
      P(4)=-P(2)
C
      RETURN
C
      END
```

```
      SUBROUTINE QUAD
C
      DOUBLE PRECISION S,C,B,A,P,ST,SIG,U,V,CC,BB,CR,AREA,COMM,DU,DV,DL,
     1DX,DY,XL,RR
      COMMON NUMNP,NUMEL,NUMMAT,NUMPC,ACELR,ACELZ,N,VOL,TEMP,MTYPE,Q,    QUAD0002
     1 HED(18),E(8,4,12),RO(12),NTC(8),R(900),Z(900),UR(900),UZ(900),    QUAD0003
     2 CODE(900),T(900),IBC(200),JBC(200),PR(200,2)                      QUAD0004
      COMMON /ARG/C(3,3),S(10,10),SIG(6),P(8),ST(3,10),RR(5),ZZ(5),
     1LM(4),EE(3),IX(800,5),XC,YC
      COMMON /BANARG/ MBAND,NUMBLK,B(144),A(144,72)
      DIMENSION U(3),V(3)                                                 QUAD0008
      I=IX(N,1)                                                           QUAD0009
      J=IX(N,2)                                                           QUAD0010
      K=IX(N,3)                                                           QUAD0011
      L=IX(N,4)                                                           QUAD0012
      MTYPE=IX(N,5)                                                       QUAD0013
      VOL=0.                                                              QUAD0014
      TEMP=(T(I)+T(J)+T(K)+T(L))/4.0                                      QUAD0015
      RATIO=0.0                                                           QUAD0016
      NUMTC=NTC(MTYPE)                                                    QUAD0017
      IF (NUMTC.EQ.1) GO TO 100                                           QUAD0018
      VOT=TEMP
      EE(1)=100.*(796.6958-11.05089*VOT+0.040377*VOT**2)
      DO 50 M=2,NUMTC                                                     QUAD0019
      IF (E(M,1,MTYPE)-TEMP) 50,60,60                                     QUAD0020
   50 CONTINUE                                                            QUAD0021
   60 DEN=E(M,1,MTYPE)-E(M-1,1,MTYPE)                                     QUAD0022
      IF(DEN) 70,80,70                                                    QUAD0023
   70 RATIO=(TEMP-E(M-1,1,MTYPE))/DEN                                     QUAD0024
   80 DO 90 KK=2,3
   90 EE(KK)=E(M-1,KK+1,MTYPE)+RATIO*(E(M,KK+1,MTYPE)-E(M-1,KK+1,MTYPE))QUAD0026
      GO TO 110                                                           QUAD0027
  100 DO 105 KK=1,3                                                       QUAD0028
  105 EE(KK)=E(1,KK+1,MTYPE)                                              QUAD0029
  110 COMM=EE(1)/(1.-EE(2)**2)                                            QUAD0030
      C(1,1)=COMM                                                         QUAD0031
```

```
      C(1,2)=COMM*EE(2)                                                 QUAD0032
      C(1,3)=0.                                                         QUAD0033
      C(2,1)=C(1,2)                                                     QUAD0034
      C(2,2)=C(1,1)                                                     QUAD0035
      C(2,3)=0.                                                         QUAD0036
      C(3,1)=0.                                                         QUAD0037
      C(3,2)=0.                                                         QUAD0038
      C(3,3)=.5*COMM*(1.-EE(2))                                         QUAD0039
      DO 130 J=1,10                                                     QUAD0040
      DO 120 I=1,3                                                      QUAD0041
  120 ST(I,J)=0.                                                        QUAD0042
      DO 130 I=1,10                                                     QUAD0043
  130 S(I,J)=0.                                                         QUAD0044
      DO 140 I=1,4                                                      QUAD0045
      NPP=IX(N,I)                                                       QUAD0046
      RR(I)=R(NPP)                                                      QUAD0047
  140 ZZ(I)=Z(NPP)                                                      QUAD0048
      IF(IX(N,3)-IX(N,4)) 145,150,145                                   QUAD0058
  145 XC=(RR(1)+RR(2)+RR(3)+RR(4))/4.                                   QUAD0049
      YC=(ZZ(1)+ZZ(2)+ZZ(3)+ZZ(4))/4.                                   QUAD0050
      RR(5)=XC                                                          QUAD0051
      ZZ(5)=YC                                                          QUAD0052
      K=5                                                               QUAD0053
      J=1                                                               QUAD0054
      I=4                                                               QUAD0055
      LM(3)=9                                                           QUAD0056
      NT=4                                                              QUAD0057
      GO TO 160
  150 NT=1                                                              QUAD0059
      LM(3)=5                                                           QUAD0060
      I=1                                                               QUAD0061
      K=3                                                               QUAD0062
      J=2                                                               QUAD0063
      XC=(RR(1)+RR(2)+RR(3))/3.                                         QUAD0064
      YC=(ZZ(1)+ZZ(2)+ZZ(3))/3.                                         QUAD0065
      RR(5)=RR(3)                                                       QUAD0066
```

```
      ZZ(5)=ZZ(3)                                                       QUAD0067
  160 DO 200 NN=1,NT                                                    QUAD0068
      LM(1)=2*I-1                                                       QUAD0069
      LM(2)=2*J-1                                                       QUAD0070
      U(1)=ZZ(J)-ZZ(K)                                                  QUAD0071
      U(2)=ZZ(K)-ZZ(I)                                                  QUAD0072
      U(3)=ZZ(I)-ZZ(J)                                                  QUAD0073
      V(1)=RR(K)-RR(J)                                                  QUAD0074
      V(2)=RR(I)-RR(K)                                                  QUAD0075
      V(3)=RR(J)-RR(I)                                                  QUAD0076
      AREA=(RR(J)*U(2)+RR(I)*U(1)+RR(5)*U(3))/2.                        QUAD0077
      VOL=VOL+AREA                                                      QUAD0078
      COMM=.25/AREA                                                     QUAD0079
      XNT=NT                                                            QUAD0080
      COM=2./XNT                                                        QUAD0081
      COM=COM*COMM                                                      QUAD0082
      DO 180 L=1,3                                                      QUAD0083
      II=LM(L)                                                          QUAD0084
      ST(1,II)=ST(1,II)+U(L)*COM                                        QUAD0085
      ST(2,II+1)=ST(2,II+1)+V(L)*COM                                    QUAD0086
      ST(3,II)=ST(3,II)+V(L)*COM                                        QUAD0087
      ST(3,II+1)=ST(3,II+1)+U(L)*COM                                    QUAD0088
      DO 180 M=1,3                                                      QUAD0089
      JJ=LM(M)                                                          QUAD0090
      S(II,JJ)=S(II,JJ)+(U(L)*C(1,1)*U(M)+V(L)*C(3,3)*V(M))*COMM        QUAD0091
      S(II,JJ+1)=S(II,JJ+1)+(U(L)*C(1,2)*V(M)+V(L)*C(3,3)*U(M))*COMM    QUAD0092
      S(II+1,JJ+1)=S(II+1,JJ+1)+(V(L)*C(1,1)*V(M)+U(L)*C(3,3)*U(M))*COMMQUAD0093
      S(JJ+1,II)=S(II,JJ+1)                                             QUAD0094
  180 CONTINUE                                                          QUAD0095
      I=J                                                               QUAD0096
      J=J+1                                                             QUAD0097
  200 CONTINUE                                                          QUAD0098
      IF(IX(N,3)-IX(N,4)) 220,250,220                                   QUAD0099
  220 DO 240 I=1,2                                                      QUAD0100
      KK=10-I                                                           QUAD0101
      DO 240 K=1,KK                                                     QUAD0102
```

```
      CC=S(KK+1,K)/S(KK+1,KK+1)                                         QUAD0103
      DO 230 J=1,3                                                      QUAD0104
  230 ST(J,K)=ST(J,K)-CC*ST(J,KK+1)                                     QUAD0105
      DO 240 J=1,KK                                                     QUAD0106
  240 S(J,K)=S(J,K)-CC*S(J,KK+1)                                        QUAD0107
  250 CONTINUE                                                          QUAD0108
      DT=TEMP-Q                                                         QUAD0109
      DX=EE(3)*DT                                                       QUAD0110
      DY=EE(3)*DT                                                       QUAD0111
      SIG(1)=-C(1,1)*DX-C(1,2)*DY                                       QUAD0112
      SIG(2)=-C(2,1)*DX-C(2,2)*DY                                       QUAD0113
      SIG(3)=0.                                                         QUAD0114
      DO 520 I=1,8                                                      QUAD0115
      P(I)=0.0                                                          QUAD0116
      DO 510 J=1,3                                                      QUAD0117
  510 P(I)=P(I)-ST(J,I)*SIG(J)                                          QUAD0118
  520 P(I)=P(I)*VOL                                                     QUAD0119
      MM=4                                                              QUAD0120
      IF(IX(N,3).EQ.IX(N,4)) MM=3                                       QUAD0121
      XMM=MM                                                            QUAD0122
      DY=VOL*ACELZ*RO(MTYPE)/XMM                                        QUAD0123
      DX=VOL*ACELR*RO(MTYPE)/XMM                                        QUAD0124
      DO 530 I=1,MM                                                     QUAD0125
      P(2*I)=P(2*I)+DY                                                  QUAD0126
  530 P(2*I-1)=P(2*I-1)+DX                                              QUAD0127
      RETURN                                                            QUAD0128
      END                                                               QUAD0129
```

```
      SUBROUTINE STRESS
C
      DOUBLE PRECISION S,C,B,A,P,ST,SIG,U,V,CC,BB,CR,AREA,COMM,DU,DV,DL,
     1DX,DY,XL,RR
      COMMON NUMNP,NUMEL,NUMMAT,NUMPC,ACELR,ACELZ,N,VOL,TEMP,MTYPE,Q,    STRS0002
     1 HED(18),E(8,4,12),RO(12),NTC(8),R(900),Z(900),UR(900),UZ(900),    STRS0003
     2 CODE(900),T(900),IBC(200),JBC(200),PR(200,2)                      STRS0004
      COMMON /ARG/C(3,3),S(10,10),SIG(6),P(8),ST(3,10),RR(5),ZZ(5),
     1LM(4),EE(3),IX(800,5),XC,YC
      COMMON /BANARG/ MBAND,NUMBLK,B(144),A(144,72)
      COMMON /SIFARG/ SIF(200),SSIF(200),THETA(200),DDRC(200),MD(200),
     1                NK,DRC,DXC,DYC
      COMMON /SYSARG/ DDX,DDY,DDR,DDP
       NK=0
      MPRINT=0                                                            STRS0008
      DO 300 M=1,NUMEL                                                    STRS0009
      N=M                                                                 STRS0010
      IX(N,5)=IABS(IX(N,5))                                               STRS0011
      MTYPE=IX(N,5)                                                       STRS0012
      DO 50 I=1,6
   50 SIG(I)=0.0
      IF(IX(N,3)-IX(N,2)) 90,60,90
   60 I=IX(N,1)
      J=IX(N,2)
      XC=(R(I)+R(J))/2.0
      YC=(Z(I)+Z(J))/2.0
      DX=R(J)-R(I)
      DY=Z(J)-Z(I)
      XL=DSQRT(DX**2+DY**2)
      DU=B(2*J-1)-B(2*I-1)
      DV=B(2*J)-B(2*I)
      DL=DV*DY/XL+DU*DX/XL
      SIG(4)=E(1,4,MTYPE)*DL*E(1,2,MTYPE)/XL
      GO TO 200
   90 CALL QUAD
      MM=4                                                                STRS0014
```

```
      IF(IX(N,3)-IX(N,4)) 170,160,170                                   STRS0015
  160 MM=3                                                              STRS0016
  170 DO 180 I=1,3                                                      STRS0017
      RR(I)=0.                                                          STRS0018
      DO 180 J=1,MM                                                     STRS0019
      II=2*J                                                            STRS0020
      JJ=2*IX(N,J)                                                      STRS0021
  180 RR(I)=RR(I)+ST(I,II)*B(JJ)+ST(I,II-1)*B(JJ-1)                     STRS0022
      DO 190 I=1,3                                                      STRS0023
      DO 190 J=1,3                                                      STRS0024
  190 SIG(I)=SIG(I)+C(I,J)*RR(J)                                        STRS0025
      CC=(SIG(1)+SIG(2))/2.0                                            STRS0026
      BB=(SIG(1)-SIG(2))/2.                                             STRS0027
      CR=DSQRT(BB**2+SIG(3)**2)
      SIG(4)=CC+CR                                                      STRS0029
      SIG(5)=CC-CR                                                      STRS0030
      SIG(6)=0.0                                                        STRS0031
      IF ((BB.EQ.0.0).AND.(SIG(3).EQ.0.0)) GO TO 200                    STRS0032
      SIG(6)=28.648*DATAN2(SIG(3),BB)
  200 IF(MPRINT)  250,220,250                                           STRS0034
  220 WRITE(6,2000)                                                     STRS0035
      MPRINT=50                                                         STRS0036
  250 MPRINT=MPRINT-1                                                   STRS0037
      WRITE (6,2001)  N,XC,YC,(SIG(I),I=1,6)                            STRS0038
      IF(( YC.LT.DDY).OR.( XC.LT.DDX)) GO TO 300
      DXC=XC-DDX
      DYC=YC-DDY
      DRC=SQRT(DXC**2+DYC**2)
      IF(DRC.GT.DDR) GO TO 300
C     ******************************************************************
C     *  CALCULATE STRESS INTENSITY FACTORS                            *
C     ******************************************************************
      NK=NK+1
      MD(NK)=N
      DDRC(NK)=DRC
      SDRC=SQRT(2.*DRC)
```

```
      ANG=ATAN2(DXC,DYC)
      FUN=COS(ANG*0.5)*(1.+SIN(ANG*.5)*SIN(1.5*ANG))
      SIF(NK)=(SIG(1)/FUN)*SDRC*1.772454
      SSIF(NK)=SIF(NK)/DDP
      THETA(NK)=ANG*57.296
  300 CONTINUE                                                          STRS0039
      WRITE(6,2003) NK
      IF(NK.LT. 1 ) GO TO 400
      WRITE(6,2004)
      WRITE(6,2002) (MD(I),THETA(I),DDRC(I),SIF(I),SSIF(I),I=1,NK)
C     ******************************************************************
  400 RETURN
 2000 FORMAT (7H1EL.NO.  7X 1HX  7X 1HY 4X 8HX-STRESS 4X 8HY-STRESS 3X  STRS0041
     1 9HXY-STRESS 2X 10HMAX-STRESS 2X 10HMIN-STRESS 7H  ANGLE )        ST
 2001 FORMAT (I7,2F8.4,1P5E12.4,0P1F7.2)
 2002 FORMAT(I5,4G15.4/)
 2003 FORMAT (/' NUMBER OF ELEMENTS WITHIN THE RADIUS=',I5/)
 2004 FORMAT('  EL.',10X,'ANGLE',9X,'RADIUS',12X,'SIF',6X,'NORM. SIF')
      END                                                               STRS0044
```

```
      SUBROUTINE MODIFY(A,B,NEQ,MBAND,N,U)
C
      DOUBLE PRECISION A,B,U
      DIMENSION A(144,72),B(144)
      DO 250 M=2,MBAND                                          MODI0003
      K=N-M+1                                                   MODI0004
      IF(K) 235,235,230                                         MODI0005
  230 B(K)=B(K)-A(K,M)*U                                        MODI0006
      A(K,M)=0.0                                                MODI0007
  235 K=N+M-1                                                   MODI0008
      IF(NEQ-K) 250,240,240                                     MODI0009
  240 B(K)=B(K)-A(N,M)*U                                        MODI0010
      A(N,M)=0.0                                                MODI0011
  250 CONTINUE                                                  MODI0012
      A(N,1)=1.0                                                MODI0013
      B(N)=U                                                    MODI0014
      RETURN                                                    MODI0015
      END                                                       MODI0016
```

```
      SUBROUTINE BANSOL
C                                                                       BANS0002
      DOUBLE PRECISION A,B,C
      COMMON /BANARG/ MM    ,NUMBLK,B(144),A(144,72)
      NN=72
      NL=NN+1                                                           BANS0004
      NH=NN+NN                                                          BANS0005
      REWIND 1                                                          BANS0006
      REWIND 2                                                          BANS0007
      NB=0                                                              BANS0008
      GO TO 150                                                         BANS0009
  100 NB=NB+1                                                           BANS0010
      DO 125 N=1,NN                                                     BANS0011
      NM=NN+N                                                           BANS0012
      B(N)=B(NM)                                                        BANS0013
      B(NM)=0.0                                                         BANS0014
      DO 125 M=1,MM                                                     BANS0015
      A(N,M)=A(NM,M)                                                    BANS0016
  125 A(NM,M)=0.0                                                       BANS0017
      IF (NUMBLK-NB) 150,200,150                                        BANS0018
  150 READ (2) (B(N),(A(N,M),M=1,MM),N=NL,NH)                           BANS0019
      IF (NB) 200,100,200                                               BANS0020
  200 DO 300 N=1,NN                                                     BANS0021
      IF (A(N,1)) 225,300,225                                           BANS0022
  225 B(N)=B(N)/A(N,1)                                                  BANS0023
      DO 275 L=2,MM                                                     BANS0024
      IF (A(N,L)) 230,275,230                                           BANS0025
  230 C=A(N,L)/A(N,1)                                                   BANS0026
      I=N+L-1                                                           BANS0027
      J=0                                                               BANS0028
      DO 250 K=L,MM                                                     BANS0029
      J=J+1                                                             BANS0030
  250 A(I,J)=A(I,J)-C*A(N,K)                                            BANS0031
      B(I)=B(I)-A(N,L)*B(N)                                             BANS0032
      A(N,L)=C                                                          BANS0033
  275 CONTINUE                                                          BANS0034
```

```
  300 CONTINUE                                                          BANS0035
      IF (NUMBLK-NB) 375,400,375                                        BANS0036
  375 WRITE (1) (B(N),(A(N,M),M=2,MM),N=1,NN)                           BANS0037
      GO TO 100                                                         BANS0038
  400 DO 450 M=1,NN                                                     BANS0039
      N=NN+1-M                                                          BANS0040
      DO 425 K=2,MM                                                     BANS0041
      L=N+K-1                                                           BANS0042
  425 B(N)=B(N)-A(N,K)*B(L)                                             BANS0043
      NM=N+NN                                                           BANS0044
      B(NM)=B(N)                                                        BANS0045
  450 A(NM,NB)=B(N)                                                     BANS0046
      NB=NB-1                                                           BANS0047
      IF (NB) 475,500,475                                               BANS0048
  475 BACKSPACE 1                                                       BANS0049
      READ (1) (B(N),(A(N,M),M=2,MM),N=1,NN)                            BANS0050
      BACKSPACE 1                                                       BANS0051
      GO TO 400                                                         BANS0052
  500 K=0                                                               BANS0053
      DO 600 NB=1,NUMBLK                                                BANS0054
      DO 600 N=1,NN                                                     BANS0055
      NM=N+NN                                                           BANS0056
      K=K+1                                                             BANS0057
  600 B(K)=A(NM,NB)                                                     BANS0058
      RETURN                                                            BANS0059
      END                                                               BANS0060
```

APPENDIX G

c_o Program

Determination of the Starter Flaw from Extrapolation of the Crack Growth Law

```
      DIMENSION HEADIG(7)
      DIMENSION STRFCT(150),CRACK(150),CYCLES(150),STRFCP(150),TEM(150)
   29 READ(5,3,END=9999) NSTFCT,POWER,DELTAC,(STRFCT(I),I=1,NSTFCT)
    3 FORMAT(I2,2F10.6/(16F5.2))
      READ (5,19) NT
   19 FORMAT (I2)
      DO 16 IJK = 1,NT
      READ(5,2)            CONSTA,FCRACK,PLOAD,(HEADIG(I),I=1,7)
    2 FORMAT(E10.2,2F5.2,A3,2X,A4,A4,2X,A4,A1,A4,1X,A3,2X)
      WRITE(6,850)  (HEADIG(I),I=1,7)
  850 FORMAT(1H1/10X,'MIX',05X,'PENETRATION',05X,'DENSITY',05X,'% ASPHAL
     *T',05X,'SAMPLE'// 10X,A3,7X,2A4,7X,A4,A1,8X,A4,9X,A3)
      DO 8 I=1,NSTFCT
      IF(STRFCT(I).EQ.0.0)  STRFCP(I) = 0.0
      IF(STRFCT(I).EQ.0.0)  GO TO 8
      STRFCP(I) = 1./(PLOAD*STRFCT(I))**POWER
      IF(I.EQ.1.OR.I.EQ.2)  GO TO 8
      TEM(I) = (STRFCP(I)+STRFCP(I-1))*DELTAC/2.
    8 CONTINUE
      NMINUS = NSTFCT - 1
  750 FORMAT(20X,'  VALUES OF ONE OVER STRESS INTENSITY FACTORS **4  AND
     * THEIR AREAS  ' /(25X,I3,3X,2E15.5))
      READ(5,1)  NVALUE,(CRACK(I),CYCLES(I),I=1,NVALUE)
    1 FORMAT(I2/(4(F10.6,F10.1)))
      WRITE(6,12)  NVALUE
   12 FORMAT(  //   10X,'VALUES OF C ZERO FOR ',I2,' COMBINATIONS OF FIN
     *AL CRACK LENGTHS' / 27X,'AND ASSOCIATED CYCLE COUNTS' )
      SUMCO = 0.
      K1 = 0
      DO 4 I=1,NVALUE
      CHECK = CYCLES(I)*CONSTA
      JSTOP = (CRACK(I) +DELTAC*.001)/DELTAC
      IF(JSTOP.LE.2)  WRITE(6,280)   CRACK(I),CYCLES(I)
  280 FORMAT(///10X, ' POINTS ',2F12.5,' CAN NOT BE USED -- CRACK LENGTH
     * IS LESS THAN THERE DELTA CRACK LENGTHS')
      IF(JSTOP.LE.2)  GO TO 4
```

```
      SUM = TEM(JSTOP+1)
  200 FORMAT(///,' CHECK = ',E15.4,20X,' JSTOP = ',I5,20X,' SUM = ',E20.
     *8)
      DO 5 J=1,JSTOP
      K = 1 + JSTOP - J
      TEMP = TEM(K)
      IF(K.EQ.2)  WRITE(6,230)   CRACK(I),CYCLES(I)
  230 FORMAT(//' FOR POINTS ',2F12.5,' INTEGRAL DID NOT CLOSE BEFORE STR
     *ESS INTENSITY FACTOR(1) WAS USED -- DATA TO BE IGNORED')
      IF(SUM + TEMP.GE.CHECK) GO TO 9
    5 SUM = SUM + TEMP
    9 X = (STRFCP(K-1)-STRFCP(K))/DELTAC
      CO = DELTAC*(K-1) - (-2.*STRFCP(K) + SQRT(4.*STRFCP(K)**2
     * + 8.*X*(CHECK - SUM)))/(2.*X)
      WRITE(6,10) CO,CRACK(I),CYCLES(I)
      IF(CO.LT.DELTAC)  GO TO 4
      K1 = K1 + 1
      SUMCO = SUMCO + CO
    4 CONTINUE
   10 FORMAT(/05X,' C ZERO = ',F10.6,10X,'FOR POINTS ',2F12.5)
      SUMCO = SUMCO/K1
      WRITE(6,11)  SUMCO
   11 FORMAT(///30X,' AVERAGE C ZERO = ',F10.6)
      TEMP = 0.
      DO 13 J=1,NSTFCT
      IF(SUMCO.EQ.TEMP) JSTART = J
      IF(SUMCO.GT.TEMP.AND.SUMCO.LT.TEMP + DELTAC)  JSTART = J + 1
      IF(FCRACK.EQ.TEMP) JSTOP = J
      IF(FCRACK.GT.TEMP.AND.FCRACK.LT.TEMP + DELTAC)  JSTOP = J
   13 TEMP = TEMP + DELTAC
      X = (STRFCP(JSTOP) - STRFCP(JSTOP+1))/DELTAC
      XINT = (2*STRFCP(JSTOP) -(FCRACK-DELTAC*(JSTOP-1))*X)*
     *(FCRACK-DELTAC*(JSTOP-1))/2.
      X = (STRFCP(JSTART-1) - STRFCP(JSTART))/DELTAC
      XINT = XINT + (STRFCP(JSTART)*2. + (DELTAC*(JSTART-1)-SUMCO)*
     *     X)*(DELTAC*(JSTART-1)-SUMCO)/2.0
```

```
      SUM = 0.
  220 FORMAT(10X,' JSTOP = ',I5,10X,' JSTART = ',I5)
      JSTART = JSTART + 1
      DO 14 J=JSTART,JSTOP
   14 SUM = SUM + TEM(J)
  150 FORMAT(1X,' SUM = ',E20.7,'  FOR I = ',I3,15X,' TEMP = ',E15.8)
      SUM = (SUM + XINT)/CONSTA
      WRITE(6,15)  SUM
   15 FORMAT(  /// 10X,'* * * FAILURE POINT AT ',F10.2,' CYCLES * * * ')
   16 CONTINUE
      GOTO 29
 9999 STOP
      END
```

```
 1
99   3.20    .020
.000 .040 .075 .105 .133 .153 .176 .194 .214 .230 .247 .261 .275 .290 .302 .313
.323 .333 .344 .356 .367 .375 .385 .394 .403 .412 .422 .432 .442 .450 .460 .469
.478 .485 .493 .500 .509 .518 .527 .536 .544 .533 .560 .570 .578 .588 .595 .604
.613 .622 .631 .640 .650 .659 .668 .677 .686 .695 .705 .713 .722 .731 .741 .751
.761 .771 .781 .791 .801 .811 .821 .831 .842 .852 .863 .874 .885 .897 .908 .920
.931 .943 .957 .982 .994 1.0081.0221.0361.0501.0671.0801.0971.1121.1301.1491.166
1.1821.203
 1
+1.900E-111.97 300.0
 8
.6        9600      .8        11000     1.0       11900     1.2       12450
1.4       12850     1.6       13120     1.8       13300     2.0       13400
        END
```

TF 662
.A3 no.
FHWA-RD-73-91

BORROWER

Form DOT F 1720.
FORMERLY FORM DOT

DOT LIBRARY
00054477

FHWA

R&D